Winter 2022

Physiology and Biochemistry of Cold-hardy Table Grapevines

Annasamy S. Chandrakala
University of New Hampshire, Durham

PHYSIOLOGY AND BIOCHEMISTRY OF COLD-HARDY TABLE GRAPEVINES

BY

ANNASAMY S. CHANDRAKALA
Bachelor of Science, University of Madras, India, 1994
Master of Science, University of Madras, India, 1996
Master of Philosophy, Bharathidasan University, India, 2006

THESIS

Submitted to the University of New Hampshire

in Partial Fulfillment of

the Requirements for the Degree of

Master of Science

in

Agricultural Sciences

December 2022

This thesis was examined and approved in partial fulfillment of the requirements for the degree of Master of Science in Agricultural Sciences by:

Thesis Director, Rebecca Sideman, Full Extension Professor, Agriculture, Nutrition and Food Systems

Thesis Co-Director Marta R. M. Lima, Research Assistant Professor, Virginia Tech, School of Plant and Environmental Sciences

Anissa Poleatewich, Assistant Professor, Agriculture, Nutrition and Food Systems

On November 29, 2022

Approval signatures are on file with the University of New Hampshire Graduate School.

ACKNOWLEDGEMENTS

This work was partially funded by the United States Department of Agriculture National Institute of Food and Agriculture Hatch project 1020314 and Northeast Sustainable Agriculture Research and Education graduate student grant GNE21-251.

I am thankful to the University of New Hampshire, Graduate School, and the Department of Agriculture, Nutrition, and Food Systems for accepting me as an international graduate student and granting me opportunity to serve as a Teaching Assistant for three semesters. The teaching assistantship helped me to unlearn, relearn my teaching skills which I had through my previous experiences. The introductory courses, seminar provided by the department and various activities by UNH Global helped me to acclimatize with the University culture.

I would like to thank my co-advisor, Dr. Rebecca Sideman, for her support in completing this degree and continuous input for my betterment throughout this project. I would like to thank her for providing me with the summer support during the last year of this study. I would like to thank my co-advisor, Dr. Marta R. M. Lima for accepting and allowing me to work on this project and sharing her expertise in this field of study. Her constant support in completing this project is much appreciated.

I would also like to express my gratitude toward the members of my thesis committee. Thank you to Dr. Anissa Poleatewich, for your guidance and expertise in plant pathology. I would also like to thank Dr. Rakesh Minocha and Dr. Cheryl Smith for their guidance during the initial stages of this project. Thank you to Dr. Barrett N. Rock for his constant support and

knowledge sharing for the remote sensing work and valued contributions. Thank you to Dr. Subhash Minocha for accepting the SARE project transfer and allowing me to use the tissue culture lab for completing my second objective and all kinds of support. Thank you to Dr. Patricia Stone for her support in processing NMR samples and providing me with the access of AMIX software and results.

I am thankful to Evan Ford and the staff at the Woodman Farm for their help in the maintenance of the vineyard. I am also incredibly grateful for the support of the MacFarlane Greenhouse Manager Luke Hydock and Amber Kittle, who were instrumental in the execution of my greenhouse experiments. Thank you also to my lab mate Palash Mandal for helping in vineyard during my last year data collection, Liza DeGenring and Madeline Hassett for providing me with answers for all kind of questions regarding plant pathology experiments. Finally, thank you to my husband, my sons, and my parents for being the pillar of support in everything I achieve.

TABLE OF CONTENTS

LIST OF TABLES

LIST OF FIGURES

ABSTRACT

PHYSIOLOGY AND BIOCHEMISTRY OF COLD-HARDY TABLE GRAPEVINES

by

Annasamy S. Chandrakala

Grapes are grown worldwide to produce wine, grape juice and are also popular as fresh table grapes or dried raisins. Due to their nutritional value and importance in the multibillion-dollar wine industry, grapes are considered the most commercially important berry crop. Grape production has primarily concentrated on European wine grapes, *Vitis vinifera,* in the dry, hot Mediterranean and Central Asian climates. *V. vinifera* is not cold tolerant enough to endure winter temperatures below -15°C. The introduction of several interspecific hybrids (of both wine and table grape) cultivars in the 20th century and selection of a training system has helped propel the expansion of grapevine cultivation in cooler climates such as the Northeastern US and upper midwestern US states. Training and trellising systems are part of viticultural practices that influence many aspects of grapevine growth and productivity. Especially in cool climates like New Hampshire, choosing an appropriate training system will provide the grapevines with good exposure of leaves and berries to sunlight leading to fruits with improved berry composition and higher levels of sugar accumulation as well as increased concentrations of anthocyanins and phenolic compounds. However, there is limited research on the impact of training systems on cold-hardy table grapevine physiology and biochemistry. To address these knowledge gaps research was conducted at the UNH Woodman Horticultural Research Farm in Durham, NH, where cold-hardy grape varieties are growing on two different training systems. Mars and Canadice grape varieties grown on vertical shoot positioning (VSP) and Munson (M) training systems were used. Grapevine physiology and biochemistry were followed throughout three growing seasons using destructive and non-destructive methods to monitor grapevine health. Additionally, considering the current need for alternative environmentally friendly fungicides, plant material from these cold-hardy grape cultivars was tested for their putative antifungal properties.

The objectives of this study were to: (1) Determine the physiological and biochemical parameters of Canadice and Mars cold-hardy grape varieties growing on vertical shoot positioning (VSP) and Munson training systems, and (2) Investigate the putative antifungal activity of field-collected grapevine leaves and cell suspension cultures obtained from Canadice and Mars grapevines against *Botrytis cinerea.* I hypothesized that the training system would influence the SPAD measurements, spectral indices (normalized difference vegetation index, red edge inflection point, moisture stress index, and phenology index), and gas exchange measurements (intercellular carbon dioxide concentration, stomatal conductance, net photosynthesis, transpiration rate, vapor pressure deficit, and water use efficiency) of Mars and Canadice leaves growing on two different training systems. I also

hypothesized that the training system would have an effect on the amount of leaf photosynthetic pigments, leaf, juice, and skin metabolomes, titratable acidity and soluble solid contents of Canadice and Mars growing on two different training systems (Chapter 2). I hypothesized that field-collected leaves and cell suspension cultures established from Canadice and Mars grape varieties would contain compounds with antifungal activity against *B. cinerea* (Chapter 3).

For objective 1, physiological parameters were measured with SPAD, spectral analysis, and gas exchange analysis on grapevine leaves throughout three growing seasons (2019, 2020, and 2021). Specifically, I determined the SPAD measurements, the spectral indices normalized difference vegetation index (NDVI), red edge inflection point (REIP), moisture stress index (MSI) and phenology index, and gas exchange measurements to determine intercellular carbon dioxide concentration (C_i), stomatal conductance (g_s), vapor pressure deficit (VPD), net photosynthesis (A), transpiration (E), and water use efficiency (WUE). While no differences were found regarding training systems alone, there was a significant interaction of training system with time, suggesting that training system had different effects at different times. For the biochemical parameters, the same leaves that were used to perform SPAD measurements were used to analyze photosynthetic pigments and proton based nuclear magnetic resonance (^{1}H-NMR spectroscopy)-based metabolomics. Consistent with the results of physiological parameters, no differences were found for photosynthetic pigments - chlorophyll *a*, chlorophyll *b*, total chlorophyll, and carotenoids - between training systems, but the training system had different effects at different time points. The leaf metabolites studied using ^{1}H-NMR spectroscopy coupled with multivariate statistical analysis did not distinguish samples based on training systems, but sample separation occurred based on phenological stages. The compounds identified showed variations between flowering, veraison, and harvest. Namely, sucrose gradually increased from flowering to harvest. Additionally, the ^{1}H-NMR spectroscopy-based metabolome of grape juice was investigated in grape berries collected from veraison to harvest. Various kinds of metabolites were identified. Fructose, glucose, alanine, threonine, *myo*-Inositol, and 3-hydroxybutyrate were all shown to increase from veraison to harvest. The amount of fructose and glucose increased over time (between veraison and harvest) and are indicators of berry ripeness. Furthermore, at harvest, grape titratable acidity and total soluble solid content were determined, and berry skin composition was investigated using ultra performance liquid chromatography-mass spectrometry (UPLC-MS) analysis. Distinct sets of metabolites were identified in Mars and Canadice skin samples and were dependent on the training system.

For my objective 2, I investigated the putative antifungal activity of Mars- and Canadice-derived products, specifically field-collected grapevine senescent leaves and cell suspension cultures, against *B. cinerea*. The aim was to gather knowledge that could lead to the development of new botanical fungicides that could be used as an alternative to synthetic fungicides for disease management in vineyards. This approach could contribute to sustainable management practices in the long term. Using grapevine debris (such as canes, wood, and leaves) from *V. vinifera* to suppress *B. cinerea* and other plant pathogens has been successfully demonstrated. However, there is limited research evaluating secondary metabolites with antifungal properties from cold-hardy grapevines. Our results show that

grapevine-derived extracts have antifungal activity *in vitro* and in detached berry experiments when challenged with *B. cinerea*, but the antifungal activity was not translated to *in planta* experiments. The metabolic profiling of senescent leaves and cell suspension cultures of Mars and Canadice identified an array of compounds, including some reported to have antimicrobial properties. Given the list of compounds that have been identified in cold-hardy grapevine-derived products, future work should examine these unique compounds present in the senescent leaves and cell cultures under controlled experimental conditions. While our results indicated that Mars- and Canadice-derived products have antifungal activity, the materials used in this study were crude extracts. Future studies should focus on using finer grapevine-products to test the efficacy against *B. cinerea*, not only *in vitro*, but also using pilot-scale greenhouse trials, and vineyard trials.

CHAPTER 1

INTRODUCTION

1.1 Overview

Grapes are one of the fruit crops grown in greatest volume in the United States (USDA, 2020). The 2020 USDA National Agricultural Statistics Service (NASS) report shows that in 2017 the United States produced an average of 6,771,200 tons, valued at 6.46 million dollars (Kramer et al., 2020; USDA, 2020). New York ranks third in grape production (by volume) after California and Washington. Low winter temperatures are critical environmental factors that limit grapevines' productivity in the Northeastern United States (Goffinet, 2004; Londo et al., 2017). The winter conditions in New England make it challenging to cultivate European wine grapes (*Vitis vinifera*) because they lack the cold tolerance to survive during winter temperatures ranging from -15°C to -20°C (Luby, 1991). The native American species are not grown commercially; they are cold-hardy but have different flavor profiles and traits than table grapes, such as slip skin. Thus, growers cultivate other varieties that have desired flavor profiles that consumers expect in table grapes. Concerns over winter injury have led to the development of cold-hardy hybrid grape varieties (Goffinet, 2004). For many decades, several cold-hardy cultivars have been produced by crossing wild American grape species (e. g. *V. labrusca, V. riparia, V. aestivalis,* and *V. cinerea*) with *V. vinifera*, which enabled grapevine cultivation in colder climates, including New Hampshire (Bradshaw *et al.*, 2018*b*). However, other viticultural practices, such as training systems, can influence aspects of grapevine growth and productivity (Howell et al., 1990; Liu et al., 2015a; Millard, 2005; Morris & Cawthon, 1980; Pool, 2000; Reynolds et al., 2004; Vanden et al., 2013; Wimmer et al., 2018). Growing cold-hardy grapes by following the proper viticultural practices such

as training systems (trellising, vine manipulation, and pruning practices) can overcome distinct types of abiotic and biotic stressors. Fungal pathogens are another challenge for grape production in humid climates. Diseases caused by fungal pathogens affect the grapevines at different phenological stages, which also depend upon distinct environmental conditions (Kassemeyer and Berkelmann-Löhnertz, 2009; Steel *et al.*, 2013). It is imperative to detect and control grapevine diseases at the initial stages with appropriate pest management practices (Moriondo *et al.*, 2005; Romanazzi *et al.*, 2009; Yin *et al.*, 2017). The application of fungicides to control pathogens at different time points of the growing season can lead to resistance development in pathogens (Liu *et al.*, 2016; Alzohairy *et al.*, 2021). It is crucial to find an alternative to chemical fungicides to control pathogens in New Hampshire's viticulture industry (Kulakiotu *et al.*, 2004; Sharma *et al.*, 2009). In this regard, grapevine-derived products such as *calli* culture suspensions, extracts of grapevine debris such as stem, leaves, wood, and other parts of the plant have documented potent antifungal activity (Ribeiro *et al.*, 2015; Singh, 2017; De Bona *et al.*, 2019; Aliaño-gonzález *et al.*, 2020).

1.1.1 Cold-hardy Table Grapevines

Grapevine productivity is affected by cold injury resulting from extremely low temperatures and drastic temperature fluctuations (Karimi, 2020)**.** Winter injury generally occurs during acclimation (the fall and early winter) and de-acclimation (late winter and early spring) phases (Yilmaz *et al.*, 2021). During the winter season, there is a risk that the grapevine buds would freeze and die (Fennell, 2004; Wolf & Cook, 1994). The low temperature (e.g., -23°C for Finger Lakes region) causes water to freeze inside the vines resulting in formation of ice crystals, trunk deformation, and damage to the xylem and phloem tissues (Zabadal et al.,

2007). Additionally, higher bud mortality, significant dehydration of grapevines, bleeding of xylem exudates, and microbial growth results in total loss of the grapevines (Svyantek et al., 2020). The extent of grapevine cold injury depends on the genetic makeup, environment, and cultural practices (Zabadal et al., 2007). New Hampshire, and New England more broadly, has a humid continental climate. The winters are long and cold with heavy snow (most areas receive about 150-320 cm) (NOAA, 2020). The summer months are moderately warm and the grape growing season is short. In the Northeast region rainfall is spread evenly throughout the year, with an average rainfall of 110 cm (NEWA, 2022). By choosing cold-hardy grape cultivars (Khanizadeh *et al.*, 2004; Clark, 2019), winter injury problems can be avoided. Grapevine cold hardiness is the ability of dormant tissues to survive cold temperatures during fall and winter seasons. American wild grapevine cultivars have the ability to withstand temperatures as low as -35°C to -40°C (the north and northeastern parts of US and Canada) depending upon the area (Pierquet and Stushnoff, 1980; Andrews, 1984). The vegetative buds of grapevines survive by preventing the formation of ice crystals inside the tissue by super cooling (water remains liquid at temperatures well below 0°C) mechanism (Londo and Kovaleski, 2019). The supercooling mechanism in cold-hardy grapevines involves the production of hardiness promoting compounds such as abscisic acid, structural and functional proteins related to supercooling, and carbohydrates (Howell, 2000). These compounds produced in different parts of the cold-hardy grapevine tissues make them cold tolerant (Howell, 2000; De Rosa *et al.*, 2021).

In 1919 table grape breeding was initiated in the Eastern United States by the New York State Agricultural Experiment Station (Clark, 2010). *Vitis labrusca* served as the parent for

many table grape cultivars, that is grown in the Northeastern part of the United States (Reisch et al., 2019). *V. labrusca* is the grapevine species that produce berries which have a "fruity and foxy flavor" (referred to as an "American" flavor). Researchers in the Western and Southern parts of the United States also conducted breeding programs. A. B. Stout, of New York Agricultural experimental station, was the first breeder to release the eastern United States 'Stout Seedless' grapes in 1930. The University of Arkansas breeding program begun in 1964 by J.N. Moore, who focused on table grape breeding. The eastern table grapes developed by Stout faced issues such as fungal disease susceptibility, fruit cracking, and winter hardiness limitations (Clark, 2010). Eastern United States table grape breeding program objectives include improved texture, attractive clusters, resistance to cracking, large and seedless berries, and increased disease resistance with improved postharvest handling (Clark, 2010). *Vitis labrusca* characteristics such as winter hardiness, disease resistance and productivity, and *Vitis vinifera* characteristics such as muscat flavor, crispness, better storage capacity, large berry size and seedlessness were used as the main sources for the table grape breeding (Reynolds & Reisch, 2015). Following the subsequent breeding efforts, it led to an increase in the seedlessness quality of the berries. In recent years *Vitis rupestris* and *Vitis cinerea* are being used as a source to achieve the highest possible disease resistance and to minimize fungicide usage (Reynolds & Reisch, 2015). The continued classical breeding methods with molecular breeding by using diversified genetic improvements helped to overcome many limitations and expanded the grape breeding horizon (Reynolds & Reisch, 2015). Various molecular breeding efforts include gene transformation using *Agrobacterium*, gene gun techniques (for example, chitinase-producing gene transfer into *V. vinifera* for disease resistance), and molecular markers for the identification of specific genes that are

responsible for powdery mildew and black rot resistance, and genome mapping is ongoing (VitisGen, 2022). To make table grape breeding more efficient, molecular marker-based maps are being used for the pre-selection of required traits such as disease resistance and seedlessness through a marker-assisted selection process (Lodhi *et al.*, 1995, 1997; Reynolds and Reisch, 2015). Additionally, to assess the similarities and differences among the cultivars; genetic 'fingerprinting' by random amplified polymorphic DNA polymorphisms is being utilized (Ye *et al.*, 1998).

1.1.2 Training Systems

Training is the positioning of grapevine shoots, trunk, and cordons within a trellis framework (White and Hickey, 2020). Trellising is the physical framework and arrangement of end posts, line posts, cross arms, and wires to support the woody and vegetative part of the growing grapevine (White and Hickey, 2020). The combination of trellis (physical framework) and grapevine manipulation (training) is called 'Training system'(White and Hickey, 2020). Training systems can be distilled to four basic combinations: (1) head/spur (2) head/cane (3) cordon/spur (4) cordon/cane. Based on these four combinations there are more than 20 different training systems adapted world-wide to grow grapevines (Pool, 2000; Reynolds and Vanden Heuvel, 2009). Training systems can have an effect on the microclimatic conditions of grapevines which can directly impact their sunlight exposure, temperature, humidity, and other environmental factors (Reynolds *et al.*, 1985; Reynolds and Vanden Heuvel, 2009). Training systems determine the shoot spacing and orientation, thereby controlling the light interception inside the canopy (Howell *et al.*, 1991; Dokoozlian and Kliewer, 1995). The amount of light received by the canopy is a vital factor that influences the quality and yield of grapevines (Smart and Robinson, 1992; Dokoozlian and

Kliewer, 1995). The canopy's light environment is the most critical factor that influences the grape yield and composition (Kliewer & Dokoozlian, 2005; Dokoozlian & Kliewer, 1995), fruit ripening and hardiness of buds and canes (Howell et al., 1991), grapevine volatile compounds, and tolerance to fungal diseases (Kraus et al., 2018; Zahavi & Reuveni, 2012; Zahavi et al., 2001). Researchers have made great progress in understanding how certain viticultural practices such as grapevine's light exposure (Bergqvist et al., 2001; Zoecklein et al., 1998), leaf area to crop ratio (Kliewer and Dokoozlian, 2005), training systems, and shoot density (Reynolds et al., 1996) can affect the grape yield including volatile compounds and sensory response (Reynolds et al., 1994).

Training systems can increase the photosynthetic efficiency of the canopy by increasing the leaf surface area and also increase the light exposure of the grapes (Zoecklein *et al.*, 2008; Reynolds and Vanden Heuvel, 2009). As mentioned earlier, the diversity in training systems has resulted from different vine growing habits, grape varieties, and their yield potential. It also derived from different climatic conditions and environmental factors on vineyard management (Wolf *et al.*, 2003; Zoecklein *et al.*, 2008; Wimmer *et al.*, 2018). Training systems were also found to influence total phenolic compounds, anthocyanins, flavanols, fatty acids and their derivatives (Xu *et al.*, 2015; Vilanova *et al.*, 2017; Liu *et al.*, 2018). Viticulturists adapting diverse training systems can grow grapevines with better disease resistance and reduced disease incidence (Zahavi *et al.*, 2001; Zahavi and Reuveni, 2012; de Bem *et al.*, 2016; Kraus *et al.*, 2018).

Various studies have demonstrated that certain training systems promote the production of phytochemicals, including anthocyanins, flavonoids, carotenoids, and phenolics (Yang and Xiao, 2013; Vilanova *et al.*, 2017; Guerrero *et al.*, 2019). The training systems influence

microclimate conditions, which involve various changes in the canopy due to different environmental conditions that affect the grapevine metabolite contents (Bordelon et al., 2008; Reynolds et al., 2004; Vanden Heuvel et al., 2013). In a two-year study, Ji and Dami, (2008) showed that Traminette grapevines growing on vertical shoot positioning (VSP) with partial exposure of clusters to sunlight had higher monoterpenes compared with grapevines growing on four other training systems (Smart Dyson (SD), Scott Henry (SH), Geneva double curtain (GDC), and High Cordon (HC)). Training systems that were adapted to grow grapevines based on geographical location were believed to increase sunlight penetration, improve yield and berry quality with higher phenolics, antioxidant capacity, and anthocyanins compared to the conventional system (Rahmani et al., 2015). Cluster exposure to sunlight also has an important role on fruit composition with enhanced anthocyanins and other secondary metabolites (Jogaiah et al., 2012).

1.1.3 Grape secondary metabolites with antifungal action

Grapevines are often affected by both biotic and abiotic stresses during the growing season. Biotic stresses include bacteria, fungi, nematodes, and viruses. Fungal pathogens are one of the main biotic stressors that affect grapevines during different stages of growing season which affect the growth and productivity. It is economically challenging to combat grapevine diseases in commercial vineyards (Jones & McManus, 2017). There is an extreme need to detect and control fungal diseases that affect the cold-hardy grapevines in New England from start of the growing season by adopting adequate pest management strategies. Preventing the damage caused by fungal pathogens in grapevines requires the usage of fungicides. Currently, scientists and farmers have many fungicide options to apply to the grapevines during the growing season. For example, there are conventional fungicides such as captan,

mancozeb, sevin, penncozeb to name a few, and organically-approved fungicides such as sulfur-based, copper-based, spray oil, hydrogen peroxide, horticulture grade spray oils and salt-based (Monopotassium phosphate, Potassium bicarbonate, Armicarb and Kaligreen) that are used to manage fungal diseases (Ellis and Erincik, 2008; Ellis and Nita, 2009). However, the long-term usage of fungicides has been causing resistance in the plant pathogens. Some strains of downy mildew causing pathogens have developed resistance to quinone outside inhibitor (QOI, strobilurin) fungicides, which is documented in several United States locations (Colcol & Baudoin, 2016; Wong & Wilcox, 2000). Several studies investigated the powdery mildew resistance towards quinone outside inhibitors by undergoing mutation (G143A) and develop resistance towards multiple chemicals within few years (Ghule et al., 2018; Vielba-Fernández et al., 2020). Fungicide resistance among Black rot and Phomopsis-causing pathogens to fungicides are least known (Miessner *et al.*, 2011; Mostert *et al.*, 2017). Chemical fungicide usage is associated with deleterious effects on the soil environment due to their non-biodegradable nature (Gill and Garg, 2014). It is essential to identify limited usage of current industrial fungicides that can be safer for humans and the environment. Furthermore, consumers' demand for pesticide-free crop production and emphasis on substituting chemical inputs with other agronomic practices that mitigate weed, insect, and disease pressure has directed research towards incorporating new sustainable tools as part of the pest management program (Magnusson and Cranfield, 2005). Natural fungicides with distinct modes of action against plant pathogens could be a better solution (Isaacs et al., 2003). Trying to find alternatives led the scientists to investigate plant secondary metabolites because they are believed to have antifungal activity.

During the last decade, at least 183 phenolic compounds have been identified in the roots, wood, canes, stems, and leaves of the grapevines. The leaves and stems have flavonols (83.43% of total phenolics) and flavan-3-ols (61.63%). Stilbenes such as *trans*-ε-viniferin, *trans*-resveratrol, isohopeaphenol/hopeaphenol, vitisin B, and ampelopsins are primarily accumulated in the wood, followed by the roots, canes, stems and leaves (Souquet *et al.*, 2000; Rayne *et al.*, 2008; Katalinic *et al.*, 2009; Katalinić *et al.*, 2010; Lima *et al.*, 2010; Taware *et al.*, 2010; Çetin *et al.*, 2011; Lago-Vanzela *et al.*, 2011*a*; Lima *et al.*, 2017*a*; Goufo *et al.*, 2020; Loupit *et al.*, 2020). Sixteen individual metabolites identified were associated with disease resistance in grapevine leaves against fungal pathogens (downy mildew, powdery mildew, and fruit rot caused by *Plasmopara viticola, Oidium tukeri,* and *Botrytis cinerea*, respectively) (Batovska et al., 2008). Grapevine leaf extracts were demonstrated to have antifungal activity *in vitro* on the mycelial growth of the pathogens such as *Alternaria solani, Botrytis cinerea, Botrytis fabae, Fusarium oxysporum,* and *Fusarium solani* (El-Khateeb et al., 2013). Several researchers have screened phenolic compounds produced by grapevine leaves antagonistic to *B. cinerea* (Jeandet *et al.*, 1995; Xu *et al.*, 2018*b*; De Bona *et al.*, 2019). Furthermore, some studies demonstrated the use of grapevine extracts for their antifungal properties towards other fungal diseases such as downy mildew, powdery mildew, Phomopsis (Schilder *et al.*, 2002; Billet *et al.*, 2019; El Khawand *et al.*, 2021).

Grapevine debris

Studies show that the grapevine leaves are rich in tannins, flavonoids, procyanidins, organic acids, lipids, enzymes, and vitamins, which can also act as antifungal agents (Felicio et al., 2001; Hebash et al., 2012). These various compounds were also quantitatively evaluated

from grapevine leaves by Monagas et al. (2006). Another study involved the identification of sixteen individual metabolites from grapevine leaves that were associated with disease resistance against fungal pathogens (*Plasmopara viticola, Oidium tukeri*, and *Botrytis cinerea*, which cause downy mildew, powdery mildew, and fruit rot, respectively) (Batovska et al., 2008). Extracts of grapevine debris (including leaves, wood, canes, and other parts of the grapevine) with high amounts of phenolics, alkaloids, and flavonoids also demonstrated antifungal activity (Fernandes et al., 2013a; Schnee et al., 2013; Maia et al., 2019). In theory, the extracts of senescent leaves or pruned canes could be potentially used to treat the grapevine fungal infections rather than, or supplementing, conventional fungicides (Adrian et al., 1996; De Bona et al., 2019; Pavela et al., 2017). The senescent leaves are likely to have more phytochemical compounds than the young leaves, influenced by leaf age and growing season (Bouderias *et al.*, 2020). In early stages grapevine leaves have high chlorophyll, carotenoids and other accessory chemical molecules to produce photosynthates, which have an influence on the berry quality and quantity (Petrie *et al.*, 2000; Debnath *et al.*, 2019). When the leaves enter senescence phase, there is a gradual loss of chlorophyll and accumulation of polyphenols especially, flavanols, flavonoids, and stilbenes; and develop ontogenic resistance against fungal pathogens (Steimetz *et al.*, 2012; Bouderias *et al.*, 2020).

***Calli* culture**

Calli cultures are of cells that grow as unspecialized, unorganized, and continuously dividing. They are produced when explants (pieces of plant tissue) are cultured on an appropriate media containing the right combination of auxin and cytokinin under *in vitro* conditions (Nadeem and Ahmad, 2019). These cells are of two types: embryogenic or non-embryogenic. The embryogenic ones are a small group of competent cells which develop and

lead to a reproducible regeneration of non-zygotic embryos that can produce a complete plant (Ptak *et al.*, 2013). However, non-embryogenic ones are cluster of dedifferentiated cells that are used to synthesize secondary metabolites. In this study non-embryogenic cells are mass-produced and used for investigating the antifungal activity against *Botrytis cinerea.* These *calli* are produced by tissue culture using different grapevine parts such as leaves, shoot apical meristem, lateral meristems, and intercalary meristems. The *calli* are then used to prepare cell suspension cultures (Lima *et al.*, 2012; Lima and Dias, 2012; Lima *et al.*, 2017*a*). The grape phenolic compounds exist in varied concentrations in different plant tissues and using whole plants for their extraction of considerable amounts can be time-consuming and waste plant resources. The cell suspensions (liquid cultures of undifferentiated cells) produced from the *calli* of grapevines with antifungal compounds have the advantage of direct extraction without sacrificing the whole plant (Liswidowati *et al.*, 1991; Donnez *et al.*, 2009) and can be mass-produced in bioreactors (Efferth, 2019).

1.2 Research problem

For many decades, several cold-hardy cultivars have been produced by crossing the wild American grape species (e. g. *V. labrusca, V. riparia, V. aestivalis,* and *V. cinerea*) with the *V. vinifera*, which enabled grapevine cultivation in colder climates, including New Hampshire. However, cold-hardy table grapevine varieties have been less studied than cold-hardy varieties that are used to produce wine. In addition, there is limited research on training systems and their influence on grapevine physiology and biochemistry. To address these knowledge gaps, research was conducted at the UNH Woodman Horticultural Research Farm in Durham, NH, where cold-hardy table grape varieties were grown on two different training

systems. Mars and Canadice grape varieties grown on two training systems, vertical shoot positioning (VSP) and Munson (M), were used as models. Grapevine physiology and biochemistry were followed throughout three growing seasons, paired with disease scouting and diagnostics. The use of a non-destructive method to monitor grapevine health – spectral reflectance – was also tested during this research. Lastly, considering the current need for alternative and environmentally friendly fungicides, plant material and *calli* cultures produced from these cold-hardy grape cultivars were tested for their putative antifungal properties.

1.2.1 Research objectives and hypothesis

Objective 1: To determine the physiological and biochemical parameters of Canadice and Mars cold-hardy grape varieties growing on vertical shoot positioning (VSP) and Munson training systems.

Hypothesis: I hypothesize that the training system influences the SPAD measurements, spectral indices (normalized difference vegetation index, red edge inflection point, moisture stress index, and phenology index), and gas exchange measurements (intercellular carbon dioxide concentration, stomatal conductance, net photosynthesis, transpiration rate, vapor pressure deficit, and water use efficiency) of Mars and Canadice leaves growing on two different training systems. I also hypothesize that the training systems have an effect on the amount of leaf photosynthetic pigments, leaf, juice, and skin metabolomes, titratable acidity and soluble solid contents of Canadice and Mars table grapes (Chapter 2).

Objective 2: To investigate the putative antifungal activity of field-collected grapevine leaves and cell suspension cultures obtained from Canadice and Mars grapevines against *Botrytis cinerea.*

Hypothesis: I hypothesize that field-collected leaves and cell suspension cultures established from Canadice and Mars grape varieties contain compounds that exhibit antifungal activity against *Botrytis cinerea in vitro* (Chapter 3*).*

1.2 Overview of Experimental design and Methodology

In this research, I used two cold-hardy grape cultivars growing on two different training systems to test my hypotheses and meet each of the two research objectives mentioned above. Canadice (red berries) (Pool *et al.*, 1977) and Mars (blue berries) (Moore, 1986) were used as model varieties growing on vertical shoot positioning and Munson training systems in the UNH Woodman horticultural research farm in Durham, NH (lat. 43˚15´N, long. 70°93´W). The soil is Charlton fine sandy loam (coarse loamy, mixed, superactive, mesic Typic Dystrudept (U. S. Department of Agriculture, 2022). The research vineyard was planted in 2015 with eight cultivars trained on VSP and Munson training systems. The vines were fertilized with 0.4 oz of actual N, and weed management accomplished mechanically and through occasional shielded application of glyphosate or paraquat. The pest management is shown in (Table 1) that was recorded for three growing seasons. The temperature, precipitation, and solar irradiation was summarized and presented in (Table 2) for 2019, 2020, and 2021 growing seasons. The vineyard in the Woodman horticultural farm (Fig. 1) originally had 8 varieties of cold-hardy table grape varieties grown on both vertical shoot position (VSP) and Munson training systems and planted in an RCBD (randomized complete block design) with four replicates, with training systems as the main plot, and grape variety

as subplot, with 3 grapevines per subplot (24 vines in each row). The vineyard has a total of 12 rows. Rows 1, 5, 8, and 11 are VSP trained, and rows 2, 6, 9, and 12 are Munson-trained grapevines. The four remaining rows (3, 4, 7, and 11) are planted to a separate experiment with young vines being trained to the Munson system. The data and sample collection for evaluating the physiological and biochemical parameters was done from the south side of each row. For every growing season (June to September), the leaves, berries, and clusters were collected for physiological and biochemical analysis. For both varieties, *in-vitro* studies were conducted in a temperature and humidity-controlled tissue culture growth room and in a greenhouse environment at the University of New Hampshire's Macfarlane Greenhouse. The pruned shoots were collected, propagated, and grown in the greenhouse for further experiments. The explants of the two varieties were collected from the greenhouse and used to produce *calli* cultures and cell suspensions. Their derived extracts were used to test the antifungal activity against *Botrytis cinerea in vitro*.

According to UNH extension reports (Sideman & Hamilton, 2015, 2016, 2019), Canadice and Mars are the two varieties that were highest in yield and showed the highest fungal disease resistance, when compared to the other varieties that are growing in the UNH experimental vineyard. Therefore, these two varieties were used in this study because they had the greatest commercial production for the region and are believed to produce a high amount of disease-suppressing secondary metabolite.

Table 1. Pest management during three growing seasons at the UNH experimental vineyard

Chemical name	Type	2019	2020	2021
Lime sulfur		26 April	4 May	7 May
Penncozeb	Fungicide	24 May, 4 June, 12 June	29 May, 8 June, 18 June, 26 June, 6 July, 31 July	21 May, 28 May, 8 June, 17June
Paraquat	Herbicide	1 May, 16 July	14 Aug	
Captan	Fungicide			30 June, 11 July, 20 July, 30 July, 9 Aug
Sevin (Carbaryl)	Insecticide	25 July	6 July, 16 July	20 July
Kresoxim-methyl	Fungicide	9 July, 7 Aug		20 July
Rampart	Fungicide	18 Aug		
Metrafenone	Fungicide	28 June		
Ziram	Fungicide	28 June		
Zampro	Fungicide			11 July

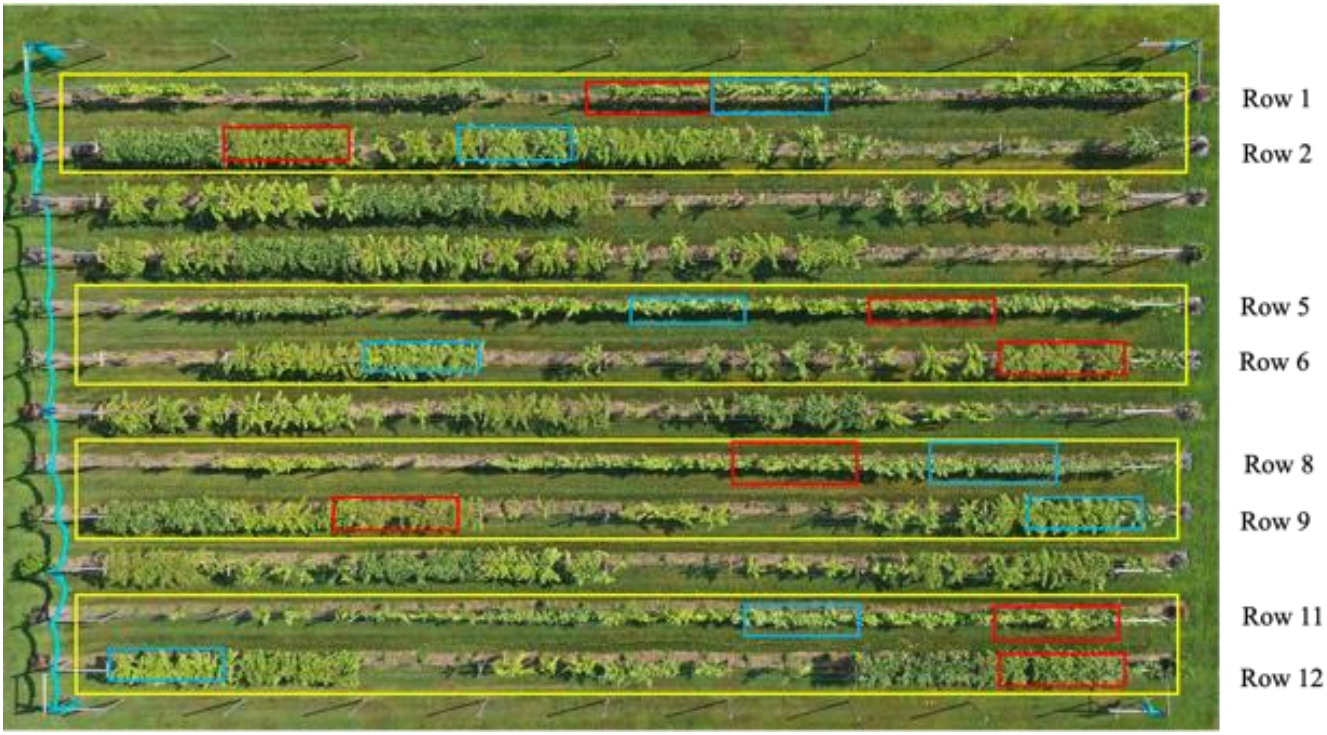

Figure 1. Drone photograph of the vineyard in the Woodman Horticultural Research Farm taken on Aug 1st, 2019. Grapevine rows used in this study are marked as yellow rectangles (Row 1, 5, 8, &11-VSP training system) and (Row 2, 6, 9, &12-Munson training system). Triplicate plants in each row of Canadice and Mars are marked as red and blue rectangles, respectively. Photo credit: Alena Warren, Stafford County Conservation District.

Table 2. Monthly mean temperatures, precipitation, and solar irradiation in Durham, NH throughout the three growing seasons 2019, 2020, and 2021

Month	Mean Temperature (°F)[z]				Precipitation (inches)[z]				Solar radiation (langley)[z]			
	2019	2020	2021	Normal[y]	2019	2020	2021	Normal[y]	2019	2020	2021	Normal[y]
June	63.9	66.3	69.7	65.2	4.97	3.92	0.97	3.96	14875	15661	16640	19162
July	73	73	67.8	70.9	3.69	1.48	12.61	4.02	17393	16317	12167	19091
Aug.	68.6	70.5	71.6	69.3	5.58	1.05	3.28	3.77	14993	14108	12747	17301
Sep.	60.8	62	64.2	61.9	0.24	0.96	4.2	4	10875	11004	9840	13677
Oct.	51.6	50.2	54.8	49.8	2.06	4.5	6.94	4.72	5748	6699	6711	8958
Overall	63.58	64.4	65.62	63.42	16.54	11.91	28	20.47	12777	12758	11621	15638

[z]1 inch = 2.54 cm, (ºF– 32) ÷1.8 = ºC, Langley = 86.04 * KWhr/m2

[y]Normal refers to the 30-year average for 1991–2020, reported for Durham, NH by the (NASA, 2022; NCEI, 2022)

1.3 Aim and thesis outline

This thesis aims to investigate the physiology and biochemistry of two cold-hardy table grapes, Canadice, and Mars growing on two different training systems: vertical shoot positioning (VSP) and Munson. The aim is to determine the choice of the training system that is associated with better physiological and biochemical parameters. There is limited research about cold-hardy table grapes growing on different training systems. My study builds upon the previous research on the influence of training systems on *V. vinifera* varieties and addresses this knowledge gap by determining the effect of two training systems (VSP and Munson) on Canadice and Mars. My research also utilizes previous knowledge on *V. vinifera* grape debris extracts in suppressing disease and expands this knowledge by utilizing the material derived from Mars and Canadice, which may lead to a novel approach to use in vineyard management to control fungal diseases.

This thesis is organized into 4 chapters. Below is a brief description of each chapter.

Chapter 1 (this chapter) includes a general introduction to cold-hardy grapevines, training systems, and grapevine secondary metabolites with antifungal action, providing background

information on the research presented in chapters 2 and 3. The research problem, objectives and aims are also described in this chapter.

Chapter 2 includes a brief introduction of Mars and Canadice, vertical shoot positioning (VSP) and Munson training systems. It also describes the results of physiological methods such as SPAD, hyperspectral indices using an analytical spectral device (ASD), and gas exchange analysis using CIRAS3 PP systems. This chapter also describes the results from the biochemical methods performed such as pigment analysis using UV-Visible spectroscopy; berry skin metabolomics using ultra-performance liquid chromatography-mass spectrometry (UPLC-MS); Leaf and juice metabolomics using H^1 nuclear magnetic resonance spectroscopy (NMR); °BRIX for solid soluble contents of juice samples; Titratable acidity (TA) of juice samples of Canadice and Mars growing on VSP and Munson training systems.

Chapter 3 includes a brief introduction to botrytis rot, its pathogenicity, grapevine's response to pathogen infection; and describes the preparation of extracts from the senescent leaves of Canadice and Mars collected from the vineyard; establishment of Canadice and Mars *calli* and cell suspension cultures. This chapter also describes the results of the *in vitro,* greenhouse detached leaf and detached berry assays performed to investigate the antifungal activity of the grapevine-derived extracts against *Botrytis cinerea*.

Chapter 4 summarizes the overall conclusions of the research and future perspectives.

CHAPTER 2

PHYSIOLOGY AND BIOCHEMISTRY OF MARS AND CANADICE GRAPEVINE VARIETIES

2.1 Introduction

2.1.1 Cold-hardy Table Grapes

Table grape breeding programs have been carried out in response to consumer's demand by performing hybridization techniques to obtain seedless varieties. Worldwide traditional grape production regions utilized *Vitis vinifera* cultivars to cultivate in different parts of the world under different climatic conditions such as dry, hot, Mediterranean and Central Asian climates (Creasy and Creasy, 2009; Bradshaw *et al.*, 2018*a*). However, cultivating *V. vinifera* in Northeastern United States is limited due to cold climate. The *V. vinifera* cultivars lack cold hardiness and are susceptible to a variety of fungal diseases. Therefore phylloxera resistant 'French Hybrids' developed in France and Europe were used for cultivation in colder regions of US but they could not withstand extreme winter conditions in the northern parts of the country due to their lacking of cold-hardy characteristics (Eibach and Töpfer, 2015; Bradshaw *et al.*, 2018*a*). There are several North American grape species such as *V. labrusca, V. riparia, V. rupestris, and V. aestivalis* which are known for cold hardiness and better disease resistance when compared to *V. vinifera* but that have poor fruit quality (Clark, 2019; Moreira and Clark, 2021). Therefore, the grape breeding program in the University of Minnesota experimented with the best protocols to determine the advancement of cold-hardy table grapes development by crossing *V. vinifera* with North American grapes (Luby, 1991). Table grape breeding programs started in the Eastern United States in 1919 by New York Agricultural Experiment Station, and the first seedless table grape 'Stout seedless' was

presented in 1930, followed by ‘Bronx seedless’ in 1937. Later they presented a wide range of grapes with a variety of flavors and appearances. *Vitis labrusca* with a fruity or foxy flavor berry serves as the parent species of many flavorful Northeastern grapes (Reisch, 1993). Two such cold-hardy table grape varieties used in this study are Canadice and Mars.

2.1.1.1 Mars

James N. Moore developed Mars by crossing Island Belle X Arkansas 1339 interspecific (*V. labrusca* and *V. vinifera*) hybrids in 1972 (Moore, 1986; Smiley and Cochran, 2016). Mars are moderately hardy (-23°C to -26°C). However, these varieties are slightly susceptible to anthracnose, black rot, Botrytis bunch rot, crown gall, downy mildew, Phomopsis cane and leaf spot, and powdery mildew (Smiley and Cochran, 2016). Mars has blue berries with thick skin, tight, and very attractive uniform clusters exhibiting high disease resistance towards black rot, downy mildew, powdery mildew, and anthracnose (Sideman and Hamilton, 2015, 2016, 2019).

2.1.1.2 Canadice

Canadice was developed in 1977, by crossing Bath X Himrod interspecific hybrids (*V. labrusca* and *V. vinifera*) at the New York State Agricultural experiment station in Geneva, New York (Pool et al., 1977; Strik, 2011). Although Canadice is winter hardy (-28°C), it is highly susceptible to black rot, moderately susceptible to downy mildew and *Botrytis*, and slightly susceptible to powdery mildew (Hemhill Jr *et al.*, 1992; Hartman and Beale, 2008) . Canadice has red berries with tight, attractive, and uniform clusters exhibiting disease resistance towards black rot, downy mildew, powdery mildew, and anthracnose (Sideman and Hamilton, 2015, 2016, 2019). The clusters are medium-sized, conical with medium-

small round berries. Berries have a thin, friable skin, and are mildly fruity, very sweet and candy-like (Reynolds and Reisch, 2015).

According to UNH extension reports, Mars and Canadice were the cultivars which remained free of symptoms of black rot, downy mildew, powdery mildew, and anthracnose when other varieties such as Reliance, Thomcord, Marquis were affected by fungal diseases (Sideman & Hamilton, 2015, 2016, 2019). Canadice and Mars both consistently produced high yields of marketable fruit and were therefore recommended for commercial production in New Hampshire (Sideman & Hamilton, 2015, 2016, 2019). To successfully utilize the benefits of these cold-hardy grapevines, more information is needed on the physiology and biochemistry of Canadice and Mars

2.1.2 Training systems

In a vineyard, grapevine form defines the spatial distribution of leaves and shoots within a canopy, influencing the sunlight exposure and subsequently the photosynthetic capacity of leaves. Training systems have an impact on the production potential of a vineyard (Smart *et al.*, 1990; Schultz, 1995; Reynolds and Vanden Heuvel, 2009). According to Wimmer *et al.*, (2018) training systems influence the grapevine's size, shape, and canopy architecture which in turn affects fruit composition and productivity. Training systems immediately affect temperature, humidity, and other environmental factors that has impact on the microclimate of the grapevine. It is most important to choose the right grapevine training system that is compatible with the local climate (Liu *et al.*, 2015*a*). There are several of training systems that have been established over the years and selecting the best training system for Northeastern United States is crucial. To answer this question the cold-hardy table grapes

planted in the UNH vineyard were trained to both Vertical Shoot positioning (VSP) and Munson (M) training system.

2.1.2.1 Vertical Shoot Positioning:

VSP training systems (Fig. 2a and b) involve single rows of tall, thin panels of grapevine shoots positioned upwards above the bilateral cordons or canes (Grant, 2019). VSP uses a single support wire approximately 30 inches above the ground, with three pairs of catch wires set at 1-foot intervals above the support wire (Sideman, 2021). It produces a vertical hedge of leaves with a fruiting zone below. Because the shoots are positioned vertically upwards, this training system occupies narrow horizontal spaces, allowing more rows of grapevines to be planted in the same area compared to other training systems. VSP training system can be used in cool regions where the risk of fungal disease is high (Grant, 2019). Additionally, shoots' upward positioning creates a large expanse of leaves, and a large amount of leaf area that is more exposed to sunlight, which promotes the development of fruit clusters and increased bunch weights (Wolf et al., 2003) compared to other non-divided canopies. A study of cultivating grapes on VSP training systems in wet regions demonstrated a low disease incidence and superior berry quality (Liu et al., 2015) compared to single-Guyot and 4-arm Kniffin training systems. The berries growing in the VSP training system had higher concentrations of stable individual, acylated and methoxylated anthocyanins (Liu et al., 2015), and phenolics (Bavougian et al., 2013; Liu et al., 2018) compared to the grapes grown in other training systems such as Single Guyot and 4-arm Kniffin (Liu et al., 2015).

2.1.2.2 Munson training system

The Munson training system (Fig. 3a and b), requires supported cross-arms at each post to support four high wires at about 5-6 feet above the ground, in addition to a single support wire 3 feet above the ground (Sideman, 2021). The canes are trained on two wires, with four canes of each plant trained, two canes to the right and two canes to the left tied along the two central wires (Minnesota Grape Growers Association, 2016; Munson, T. V., 1909).

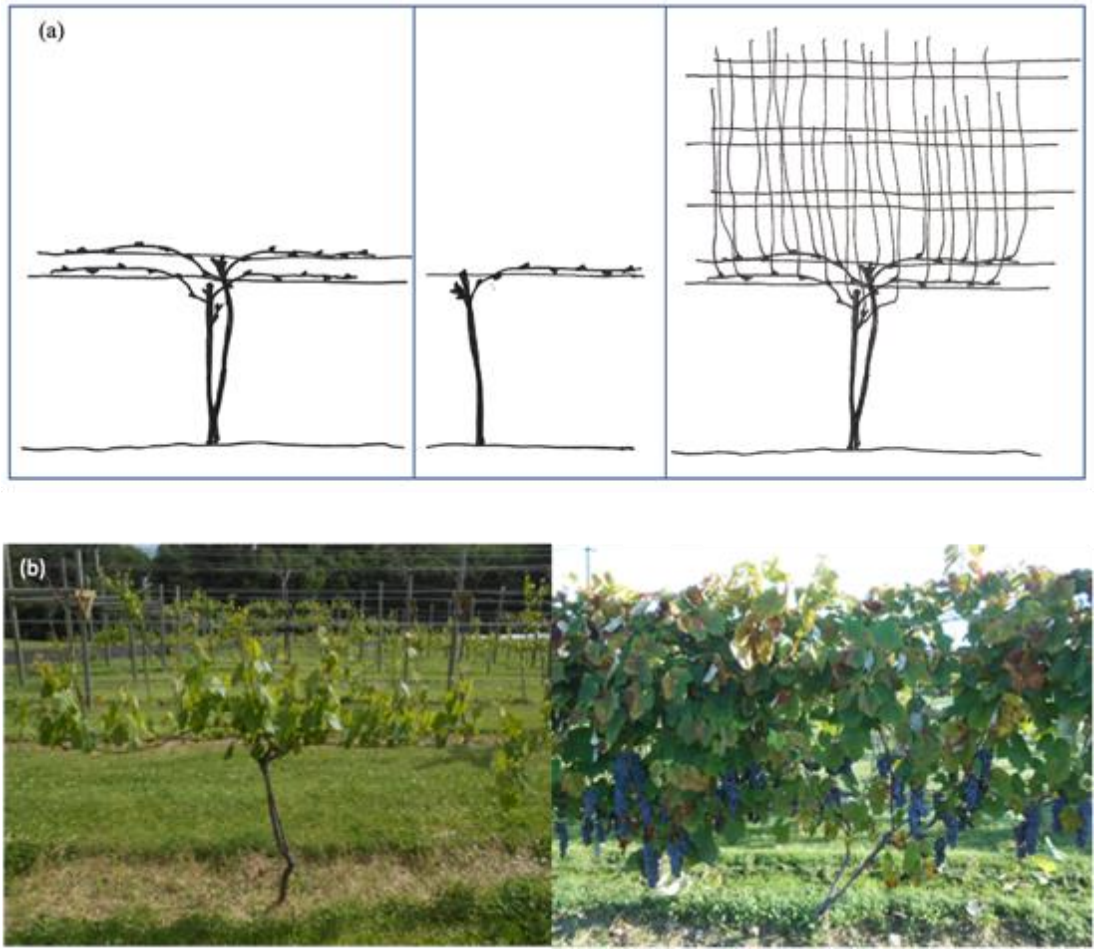

Figure 2. Schematic drawing (a) of the vertical shoot positioning (VSP) training system adapted from (Sideman, 2021), and photos (b) showing VSP training systems during the start (left) and end (right) of the growing season.

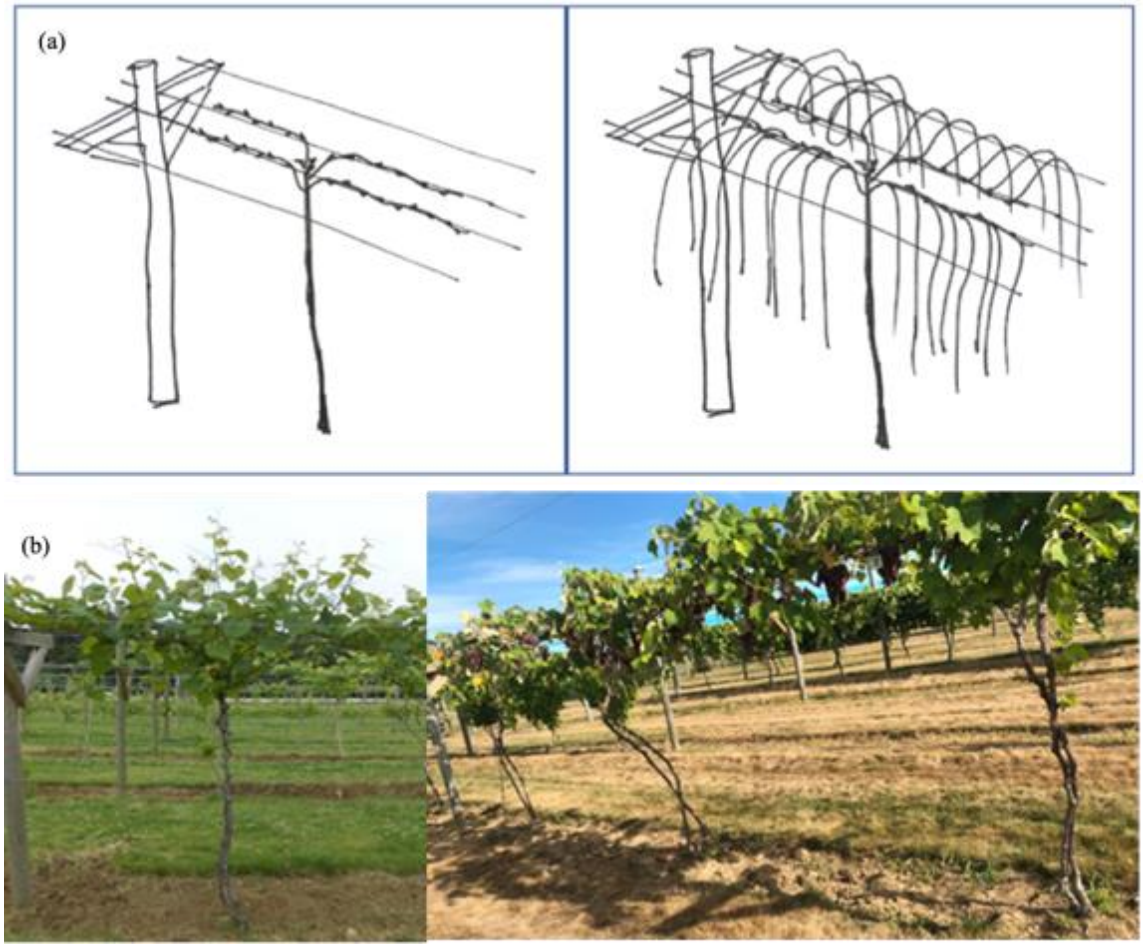

Figure 3. Schematic drawing (a) of the Munson training system adapted from (Sideman, 2021), and photos (b) showing Munson training systems during the start (left) and end (right) of the growing season.

As the grape shoots grow upward to top of the trellis and droop downwards, they bring a curtain of foliage along both sides of each wire, and an open area left between the wires allows excellent penetration of sunlight (Couvillon and Nakayama, 1970). The Munson training system also places the leaves closer to the trellis and cover the clusters from the top, facilitating the fruit's ripening in an uniform pattern (Zabadal *et al.*, 2002). This training system assists in the easy harvesting of clusters by avoiding the shoot entangling and making it easier to pick. The shoot positioning orientation supported by the cross arms supports the grapevine canopy with most of the leaves directed away from the clusters to avoid shading (Zabadal *et al.*, 2002). The single layer of leaves developed at the top of the trellis creates a

microclimate of filtered sunlight for the clusters. Concord vines grown on the Munson training system have been reported to have increased yield, cluster weight, number of clusters per vine, number of berries per cluster, and berry weight when compared to 4-arm Kniffin training system (Couvillon & Nakayama, 1970; Reynolds et al., 2009). Concord grapevines growing on Munson system exhibits a higher fruit yield, soluble solid contents and anthocyanins, and reduced asynchronous fruit maturity compared with 4-arm Kniffin training system (Couvillon & Nakayama, 1970; Reynolds et al., 2009). Similar to VSP and Munson system, the 4-arm Kniffin is a cane pruned system. However, the 4-arm Kniffin is a high training system, similar to Munson, whereas VSP is a low training system. Another study states that Concord vines growing on Munson training system had the highest vine size compared to four other training systems in Chataqua county, New York (Gladwin, 1919). There is limited research on the influence of the training systems on cold-hardy grapevines and even fewer studies concerning cold-hardy table grapes growing on two different training systems (vertical shoot positioning and Munson).

There is still much to learn about the cold-hardy grapevine growth and berry chemistry. The overall aim of this study was to assess physiology and biochemistry of cold-hardy table grapes growing on two different training systems. My specific objective was to characterize the physiological and biochemical parameters of Canadice and Mars cold-hardy grapevine varieties growing on vertical shoot positioning (VSP) and Munson (M) training systems. I hypothesized that the training system would influence the SPAD measurements, spectral indices (normalized difference vegetation index, red edge inflection point, moisture stress index, and phenology index), and gas exchange measurements (intercellular carbon dioxide

concentration, stomatal conductance, net photosynthesis, transpiration rate, vapor pressure deficit, and water use efficiency) of Mars and Canadice leaves growing on two different training systems. I also hypothesized that the training system would have an effect on the amount of leaf photosynthetic pigments, leaf, juice, and skin metabolomes, titratable acidity and soluble solid contents of Canadice and Mars growing on two different training systems.

2.2 Materials and Methods

2.2.1 Plant material and experimental sampling

Canadice and Mars grapevine varieties were grown on vertical shoot positioning (VSP) and Munson (M) training systems at the UNH Woodman horticultural research farm (Durham, NH). Leaves from each variety were sampled weekly from flowering to harvest and fruit were sampled weekly from veraison to harvest, for a total of 12 biological samples per training system and grape variety (4 rows x 3 plants). From each grapevine, the same leaves used for SPAD measurements (Refer to 2.2.2.1) were collected into Ziploc bags (containing a moist paper towel to maintain humidity conditions) and carried to the lab in a cooler. In 2019, the leaves were washed well with deionized water, patted dry using paper towels and then cut into two halves. One half was placed in a 50 mL conical centrifuge tube, flash-frozen in liquid nitrogen, and stored at -80°C until pigment and Nuclear Magnetic Resonance Spectroscopy analysis. The other half was placed back into the Ziploc bag and stored at 4°C until spectral analysis. In 2020 and 2021, the collected leaves were washed with deionized water, patted dry, placed in a 50 mL conical centrifuge tube, flash-frozen in liquid nitrogen, and stored at -80°C until pigment and Nuclear Magnetic Resonance Spectroscopy analysis. From each grapevine, 10 grapes were collected from veraison to harvest, stored in a Ziploc

bag with a moist paper towel and then carried to the lab in a cooler. The berries were washed well with deionized water, grounded using a commercial food blender, homogenized using a handheld homogenizer (Biospec products, OK), centrifuged at 4500 rpm at 4°C for 2 minutes in a cold centrifuge (Sorvall ST8R; Thermo Scientific, MA), and the juice (supernatant) was stored at -80°C until Nuclear Magnetic Resonance Spectroscopy. Additionally, at harvest, four grape clusters were collected from each grapevine.

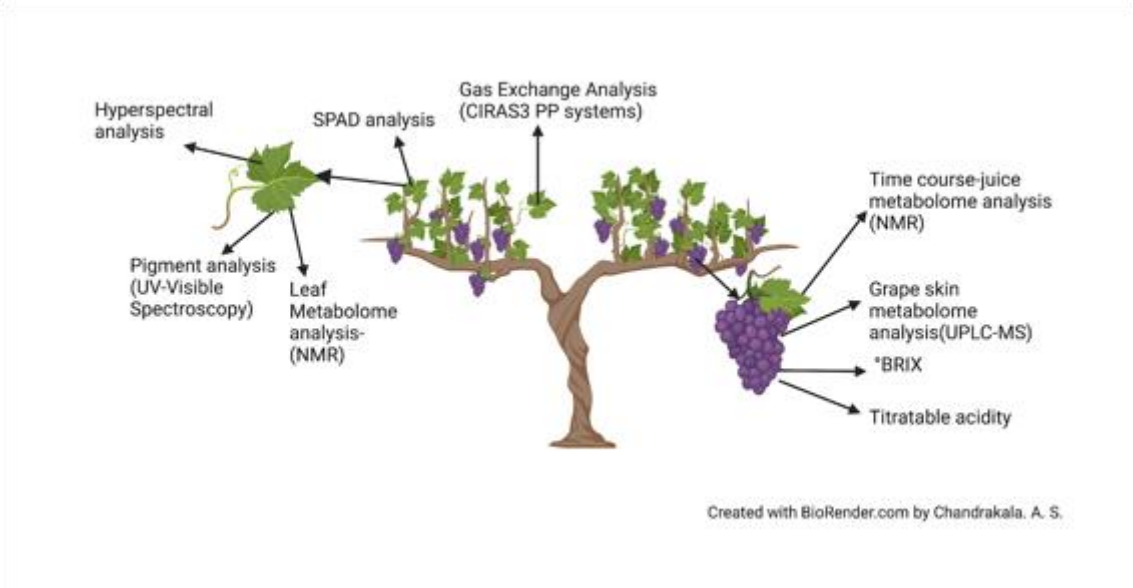

Figure 4. Representative of sampling methodology for physiology and biochemical analysis of the leaves, juice, and berry skin samples collected over three growing seasons (2019, 2020, and 2021).

A set of two grape clusters of each variety were used to collect grape skins. Grapes were squeezed to separate pulp from the skin, and the skins alone were placed in a 50 mL conical centrifuge tube to about 45mL, flash-frozen in liquid nitrogen and stored at -80°C until Liquid Chromatography-Mass Spectrometry analysis. Another set of two clusters were washed well in the deionized water, dried using a paper towel, and then separated as berries. Berries were ground using a commercial food blender and transferred to a 50 mL conical centrifuge tube. The fresh crushed sample was used immediately to determine soluble solids

content, before homogenizing with a hand-held homogenizer, centrifuged at 4°C at 4500 rpm for 2 minutes, and the juice was flash frozen and stored at -20°C until titratable acidity analysis. An illustration showing the sampling strategy is shown in Fig 4.

2.2.2 Physiological methods

2.2.2.1 SPAD measurements

For each grapevine, two healthy leaves that were well exposed to sunlight, one on each side of the plant's trunk, were selected for measurements using a SPAD meter (model 502 Plus, Konica Minolta). A SPAD meter was used to assess the chlorophyll content of grapevine leaves as a nondestructive method. This hand-held equipment measures leaf transmittance at two wavelengths in the red (660 nm approx..) and near infrared, NIR. (940 nm approx.)(Steele *et al.*, 2008; Yang *et al.*, 2021). The selected leaves were located at the 5th or 6th position from the shoot tip to maintain consistency regarding the leaf developmental stage. Three SPAD measurements were taken for each leaf at two lobules and the tip of the leaf, and the average was taken as the value for that leaf. The average of 2 leaves was taken as a biological replicate. Data were measured from three replicate plants for each variety of grapevine.

2.2.2.2 Reflectance measurements

Spectral data were collected only in 2019. The leaf samples stored at 4°C were carried to the reflectance spectrometry laboratory at UNH to collect spectral reflectance data using a Visible Infrared Intelligent Spectrometer (VIRIS GER 2600; Geophysical Environmental Research Corporation, Millbrook, New York). The reflectance measurements were made within 48 hours of collection. Each leaf sample was positioned in a dark background and

analyzed under controlled light conditions. A Halon panel was used as a reference standard prior to starting leaf measurements. A spectralon-coated hemispherical baffle light source of 30 W tungsten and halogen light bulbs was set at a 45^{o} angle 10 cm from the sample throughout the study (Rock *et al.*, 1994). The spectrometer measured reflectance from 350 nm – 2500 nm. From the spectral data, average spectral curves were determined, and four vegetation indices were calculated: 1) red edge inflection point (REIP), 2) normalized difference vegetation index (NDVI), 3) moisture stress index (MSI), and 4) phenology index. The indices were calculated using the formulas mentioned below (Rock et al., 1986, 1988).

REIP = [average first derivative value from 600 to 760nm]

$$\text{NDVI} = \frac{[\text{average } (760 - 900 \text{ nm})] - [\text{average } (630 - 690\text{nm})]}{[\text{average } (760 - 900\text{nm})] + [\text{average}(630 - 690 \text{ nm})]}$$

$$\text{MSI} = \frac{[\text{average } (1550 - 1750 \text{ nm})]}{[\text{average } (760 - 900\text{nm})]}$$

$$\text{Phenology index} = \frac{[\text{average } (1220 - 1260 \text{ nm})]}{[\text{average } (760 - 800\text{nm})]} \text{ or } \frac{\text{NIR 3}}{\text{NIR 1}}$$

2.2.2.3 Gas exchange

Gas exchange measurements were taken on fully exposed leaves on sunny days between 10:30am and 2:00pm following the solar noon calendar, in 2020 and 2021. Measurements were recorded on three leaves of each grapevine, and the average of the three leaves was taken as the value for that biological replicate; measurements were done on 3 replicates (rows) of each training system in 2020, for a total of 9 biological replicates (3 rows x 3 grapevines) and on 4 replicates (rows) of each training system in 2021, for a total of 12 biological replicates (4 rows x 3 grapevines). Leaf gas exchange measurements were made

with a CIRAS-3 photosynthesis system (PP Systems, Amesbury, MA). The leaf cuvette had an 18x25 mm window, and the light was provided by red, green, and blue light-emitting diodes, set for 38% red, 37% green, 25% blue, and 0% white as the closest approximation to sunlight. The CO_2 reference was Exact Reference Air 390 µmol mol^{-1}, H_2O reference fixed at 70% - 80%, depending upon outside environmental humidity. The temperature sensor was IR sensor, leaf area 4.5 cm^2, boundary layer resistance was 0.39 m^2 s mol^{-1}, and stomatal ratio 50%. The gas exchange parameters automatically calculated were intercellular CO_2 concentration (C_i, µmol mol^{-1}), net photosynthesis rate (A, µmol CO_2 m^{-2} s^{-1}), leaf transpiration rate (E, mmol m^{-2} s^{-1}), stomatal conductance (g_s, mol H_2O m^{-2} s^{-1}), vapor pressure deficit (VPD, kPa), and water use efficiency (WUE, µmol (CO_2) $mmol^{-1}$ (H_2O)).

2.2.3 Biochemical methods

2.2.3.1 Photosynthetic pigments

Frozen leaves were ground with a mortar and pestle in the presence of liquid nitrogen. Powdered leaf tissue (approximately 100 mg) was extracted in 10 ml of cold acetone:1 M Tris-HCl (80:20 [vol/vol], pH 8; EMD chemicals, MA; Acros organics, Fisher Scientific, Fair Lawn, NJ) following Sims and Gamon (2002). Samples were incubated at 4°C for 72 h, with shaking using a vortex mixer twice every 24 hours. Absorbance was recorded in a UV-Visible Spectrophotometer (GENESYS 180, Thermo Scientific, MA) at 470, 537, 647, and 663 nm. The amounts of carotenoids, anthocyanins, and chlorophylls *a* and *b* were calculated using the formulas below (Sims and Gamon 2002).

$$\text{Anthocyanin} = 0.08173A_{537} - 0.0069A_{647} - 0.002228A_{663}$$

$$\text{Chla} = 0.01373A_{663} - 0.000897A_{537} - 0.003046A_{647}$$

$$\text{Chlb} = 0.02405A_{647} - 0.004305A_{537} - 0.005507A_{663}$$

$$\text{Carotenoids} = \frac{(\text{A470} - (17.1 \text{ x } (\text{Chla} + \text{Chlb}) - 9.479 \text{ x Anthocyanin}}{119.26}$$

2.2.3.2 Soluble solids content

Soluble solid content was measured on freshly crushed harvest grape samples for three replicates of each grapevine growing on VSP and M separately, using a portable refractometer (Milwaukee MA871, CA).

2.2.3.3 Titratable acidity

Grape juice stored at -20°C was thawed on ice and used for titratable acidity analysis. The titration was conducted using 60 mL of the diluted juice (5 mL juice and 55mL of Milli Q water) against 0.1 M NaOH using an automated titrator (Orion Star T900, Thermo Scientific, MA). Three technical replicates for each grapevine growing on VSP and M were utilized for TA analysis.

2.2.3.4 Proton-Nuclear Magnetic Resonance (^{1}H-NMR) spectroscopy

2.2.3.4.1 Mars and Canadice leaves

The frozen leaf samples were ground using a mortar and pestle in the presence of liquid nitrogen. Freeze-dried leaf samples (90 mg) were extracted in 1300 µL of a buffer made up of 650 µL of methanol-d_4 (Fisher Scientific, Fair Lawn, NJ) plus 650 µL of KH_2PO_4 (Fisher Scientific, Fair Lawn, NJ) buffer (pH 6.0) in D_2O (deuterated water) (Fisher Scientific, Fair Lawn, NJ) containing 0.1% (w/w) trimethyl silane propionic acid sodium salt (Acros

organics, Fisher Scientific, Fair Lawn, NJ) as NMR chemical shift reference (Lima et al., 2010). Samples were vortexed, sonicated for 20 mins, and incubated overnight at 4°C. Supernatant (800 µL) was recovered after centrifugation (14000 rpm, 15 minutes) and stored at 4°C for up to 7 days until NMR analysis. About 600 µL of the extracts were transferred to 5 mm NMR tubes and samples were analyzed by ^{1}H-NMR spectroscopy using conditions already described (Lima et al., 2010).

2.2.3.4.2 Mars and Canadice juice

The frozen juice samples were thawed on ice, re-homogenized, and centrifuged at 4500 rpm at 4°C for 4 minutes. The supernatant was recovered into separate 15 mL centrifuge tubes. For the NMR analysis 630 µL of juice and 70 µL of D_2O (deuterated water) (Fisher Scientific) containing 0.1% (w/w) trimethyl silane propionic acid sodium salt (Acros organics) as ^{1}H-NMR chemical shift reference (Lima et al., 2017). About 600 µL of the extracts were transferred into 5 mm NMR tubes and were analyzed by ^{1}H-NMR spectroscopy using conditions already established (Lima et al., 2017).

2.2.3.5 Ultra-Performance Liquid Chromatography- Mass Spectrometry (UPLC-MS)

The frozen grape skins were lyophilized in a freezer dryer (Labconco, Model 78670, MO) at -55°C for three days and stored at -20°C until being ground to powder. The dried skins were ground to a powder and stored at -20°C until analysis. Approximately 100 mg of each powdered sample were sent to Creative Proteomics (New York, USA) for an untargeted metabolomics analysis using UPLC-MS. At the company, the samples were thawed and transferred to 2 mL tubes, and 80% methanol (Merck) was added. Then samples were ground at 65 kHz for 90 s and vortexed oscillation, followed by sonication for 30 min, at 4°C. All the samples were kept at -20°C for 1 h and centrifuged at 12000 rpm at 4°C for 15 mins. Finally,

200 µL of supernatant and 5 µL of DL-o-Chlorophenylalanine (0.14 mg/mL) were transferred to the vial for LC-MS analysis. At the company separation of metabolites was performed by Acquity UPLC (Waters) combined with Q Exactive MS (Thermo) and screened with ESI-MS. The LC system was comprised of an ACQUITY UPLC HSS T3 (100x2.1mmx1.8µm) with Acquity UPLC (Waters). The mobile phase was composed of solvent A (0.05% formic acid (Merck) and water) and solvent B (acetonitrile (Merck)) with a gradient elution (0-1 mins, 95% A, 1-12 mins, 95%-5% A, 12-13.5 min, 5% A, 13-5-13.6 min, 5%-95% A, 13.6-16 min, 95% A). The flow rate of the mobile phase was 0.3 $mL.min^{-1}$. The column temperature was maintained at 40°C, and the sample manager temperature was set at 4°C. Mass spectrometry parameters for ESI+: heater temperature 300°C; sheath gas flow rate, 45 arb; aux gas flow rate, 15 arb; sweep gas flow rate, 1 arb; spray voltage, 3.0 kV; capillary temperature, 350°C; S-lens RF level, 30%. ESI-: heater temperature 300°C, sheath gas flow rate, 45 arb; aux gas flow rate, 15 arb; sweep gas flow rate, 1 arb; spray voltage 3.2 kV; capillary temperature, 350°C; S-lens RF level, 60% (Liu *et al.*, 2015*b*).

2.2.4 Statistical analysis

Mars and Canadice, as well as growing seasons (2019-2021), were analyzed separately. For SPAD, reflectance, gas exchange, and plant pigment data, the effects along time were analyzed as repeated measures using the MIXED procedure of SAS for repeated measures (v. 9.4; SAS Inst. Inc., Cary, NC). Several autocorrelation structures were investigated based on the Bayesian Information criterion, and the covariance structure with the best fit for each dataset (smallest Bayesian Information Criterion) was used for repeated measures analysis. Time and training system were considered main effects and row was random effect. The

Tukey-Kramer post hoc test was used to separate means when ANOVA determined a significant effect. Significance was considered at $P \leq 0.05$. Data are presented as least square means ± SE.

Untargeted metabolomics data of harvest berry skin samples of both Canadice and Mars growing on two training systems (VSP and Munson) were coupled with multivariate statistical analysis (Principal Component Analysis, PCA, and Partial Least-Squares Discriminant Analysis, PLS-DA) to identify the differentially produced metabolites. For each cultivar, significantly different metabolites between training systems were found using VIP > 1 and t-test ($P < 0.05$). Identified metabolites were subjected to Hierarchical Cluster Analysis.

Processed NMR spectra of grape juice and leaves were imported into Chenomx NMR suite (version 8.5, Chenomx Inc. Alberta, Canada) and data matrices of integrated regions of 0.01 ppm width were generated from whole spectra. Data matrices were center scaled prior to Principal Component Analysis using PRISM (version 9.0, GraphPad, CA). For leaves, spectral signals relevant for sample grouping were identified though analysis of scores and loadings plots. Leaf NMR peak assignment was carried out using the human metabolome database (HMDB, 2022) and literature (Lima *et al.*, 2010). Isolated signals of relevant metabolites were integrated in AMIX (version 4.0, Bruker) in order to compare their amounts between samples. For grape juice, targeted identification of metabolite was carried out using Chenomx. For all compounds with isolated signals, abundance was determined by integrating these isolated spectral regions in AMIX. For both leaves and grape juice, the abundance data were subjected to two-way repeated measures ANOVA using PRISM.

Titratable acidity and soluble solids content data were subjected to Student t-test analysis using PRISM to compare the training system.

2.3 Results

2.3.1 Physiology of Mars and Canadice

2.3.1.1 SPAD analysis of Mars and Canadice leaves growing on Munson and VSP training systems

In 2019, the duration of leaf collection lasted for about eight weeks until veraison, and berry sampling lasted about five weeks. Leaf analysis and leaf collections were discontinued around veraison because of Japanese beetle damage, and no fully healthy leaves were available. The SPAD values (Fig. 5a and b) remained stable (Mars) or showed a trend of increase (Canadice) over the four weeks after flowering and then appeared to decline in both varieties. The decline of SPAD values in July-Aug was associated with a high amount of Japanese beetle damage. However, in Munson training system, SPAD values increased again in late August. For both cultivars there was a significant interaction effect of training system x time (Mars ($P < 0.0001$); Canadice ($P = 0.0032$)) and a significant effect of time ($P < 0.0001$). In the latter part of the growing season, training systems showed greater differences with SPAD values higher in M compared to VSP in both cultivars. The SPAD values were higher for four weeks after flowering then started decreasing in the VSP-trained while increasing in M-trained vines for both cultivars.

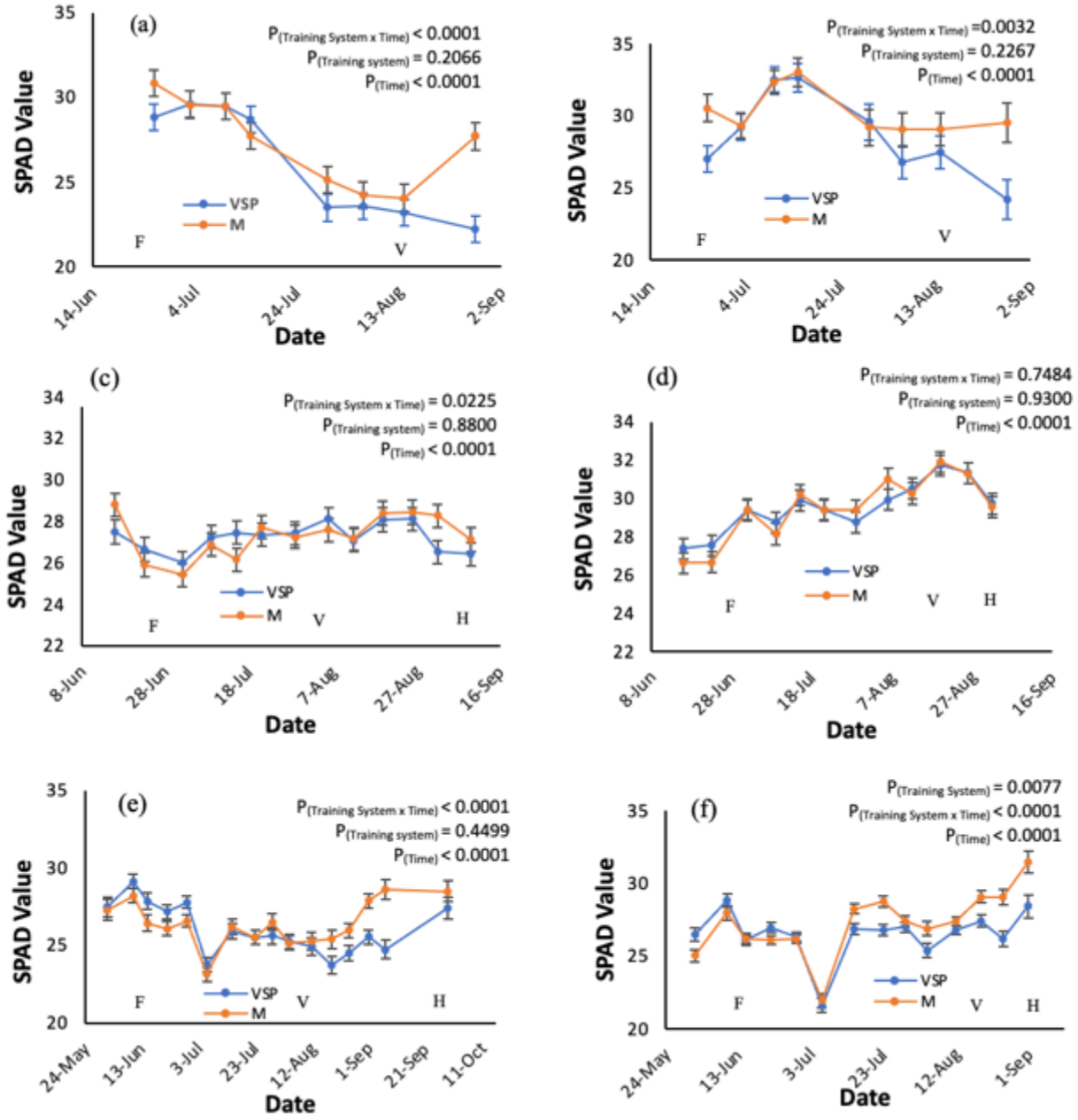

Figure 5. SPAD values of grapevine leaves (a) Mars in 2019, (b) Canadice in 2019, (c) Mars in 2020, (d) Canadice in 2020, (e) Mars in 2021 and (f) Canadice in 2021 growing on vertical shoot positioning (VSP) and Munson (M) training systems. Values shown are mean ± SEM (n=12). Phenological stages are abbreviated as flowering (F), veraison (V), and harvest (H) respectively.

In the 2020 growing season (Fig. 5c and d), the SPAD data collection duration lasted for about 12 weeks for Canadice and 13 weeks for Mars. For Canadice, the SPAD values showed a trend of increasing over the four weeks following flowering and appeared to be

stable in the rest of the growing season, while for Mars SPAD values appeared to vary less than Canadice throughout the entire season. The SPAD readings were not different between the training systems, in both cultivars. For Mars, there was a significant interaction effect of training system x time ($P = 0.0225$); M-trained Mars had slightly higher SPAD values after veraison than the VSP-trained Mars, and there was a significant effect of time ($P < 0.0001$). For Canadice, only time was significant ($P < 0.0001$).

In the 2021 growing season (Fig. 5e and f), the SPAD data collection duration lasted for about 14 weeks for Canadice and 16 weeks for Mars. The SPAD values (in both cultivars) appeared to be stable over four weeks after flowering. Then there was a drastic decline around berry touch on July 6, and then SPAD values once again increased and remained stable in the rest of the growing season. The results show that there was a significant interaction effect of training system x time in both cultivars; M-trained Mars and Canadice had higher SPAD values than VSP-trained ($P < 0.0001$), and this trend continued until harvest. In Mars there was increase in SPAD values from veraison until harvest and in Canadice increase in SPAD values started after berry touch and trend continued until harvest. There was also a significant effect of training system in Canadice ($P = 0.0077$), with M-trained Canadice having higher values than VSP-trained. There was also a significant effect of time ($P < 0.0001$) in both cultivars.

2.3.1.2 Spectral analysis of leaves of Mars and Canadice growing on Munson and VSP training systems

Spectral properties of grapevine vegetation

The reflectance curves of Canadice and Mars (Fig 6) shows the reflectance between 480 and 680 nm, which represents strong chlorophyll absorption. At the same time, reflectance between 520 – 680 nm indicates the unabsorbed green portion of visible light. The reflectance from 750 – 1300 nm, referred to as the near-infrared (NIR) plateau, is an indication of healthy tissue. According to Rock *et al.* (1985, 1986), the sharp rise in the curve between 680 nm and the NIR plateau is referred to as the red edge. According to Horler and Barber (1980); Horler *et al.* (1983), the slope and the red edge position have a direct correlation with leaf chlorophyll concentrations.

The spectral curves generated from the analysis (Fig. 7) were used to calculate different indices related to overall plant health. The indices calculated were red edge inflection point (REIP), normalized difference vegetation index (NDVI), moisture stress index (MSI), and Phenology index (Rock *et al.*, 1985; Hunt and Rock, 1989; Vogelmann *et al.*, 1993; Rock and Lauten, 1996; Karkauskaite *et al.*, 2017; Abdi *et al.*, 2019). REIP is directly correlated with leaf chlorophyll concentrations (Horler et al., 1983; Rock et al., 1988; Vogelmann et al., 1993). NDVI is effective in measuring the chlorophyll content at the leaf level and in assessing the phenological status and primary productivity at the canopy level (Tucker, 1979; Vogelmann *et al.*, 1993). MSI detects the vegetation's leaf water content and water stress during senescence (Hunt & Rock, 1989 and Rocket al., 1985). The phenology index helps to detect the water stress level and maturation index of the plant at the leaf level (Rock and Lauten, 1996).

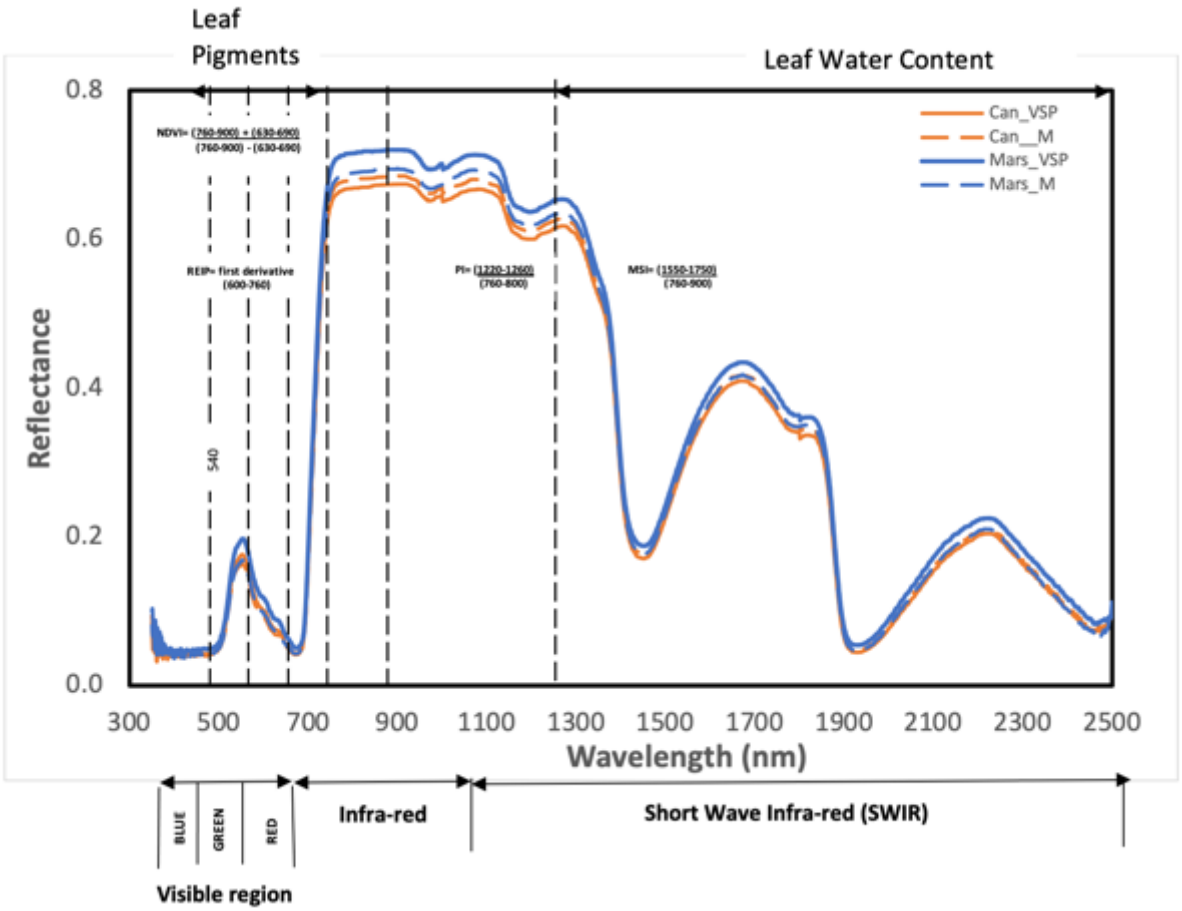

Figure 6. Vegetative reflectance curve of Canadice and Mars growing on two different training systems (VSP and Munson) acquired using the Analytical Spectral device (ASD). Leaf pigments, cell structure and leaf water content bands are indicated. Normalized reflectance of averages of spectral curves of Canadice growing on vertical shoot positioning (orange) and Munson (blue) training systems are represented between 350-2500 nm.

The results (Fig. 8a-d) show that REIP and NDVI initially remain stable and then tend to decrease over time until veraison in both cultivars. However, in the Munson training system, NDVI and REIP values increased again near the end of the growing season. In Canadice, there was a significant interaction effect of training system x time on REIP; M-trained Canadice had higher REIP from four weeks after flowering than VSP-trained Canadice ($P = 0.0007$). There was a significant effect of time on REIP ($P < 0.0001$) in both cultivars.

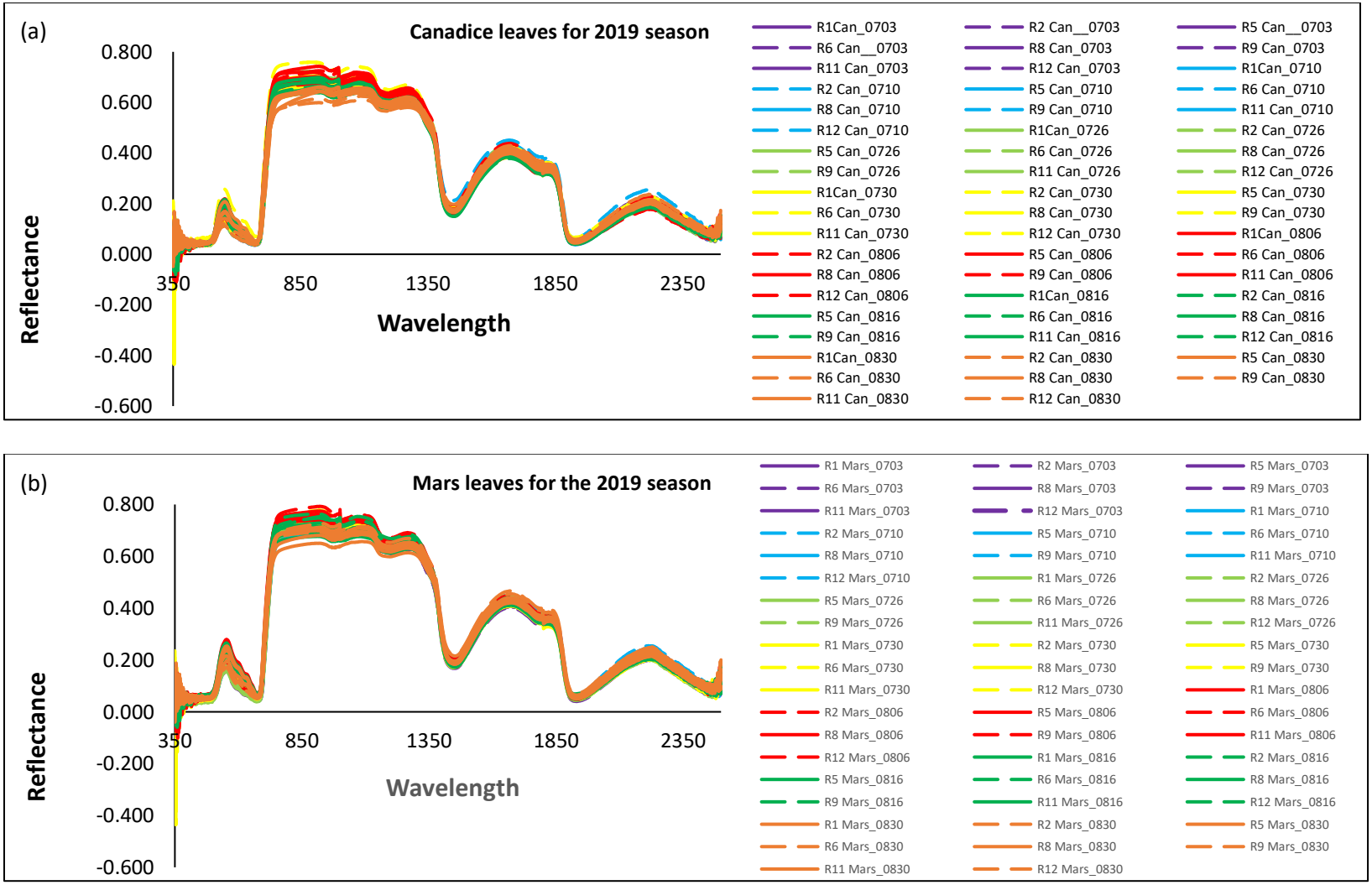

Figure 7. Spectral curves obtained from the analytical spectral device (ASD) of Canadice and Mars and leaves collected in each vineyard row (R1-R12), growing on vertical shoot positioning (full lines) and Munson (dashed lines) training systems, from July 3rd to Aug 30th, 2019

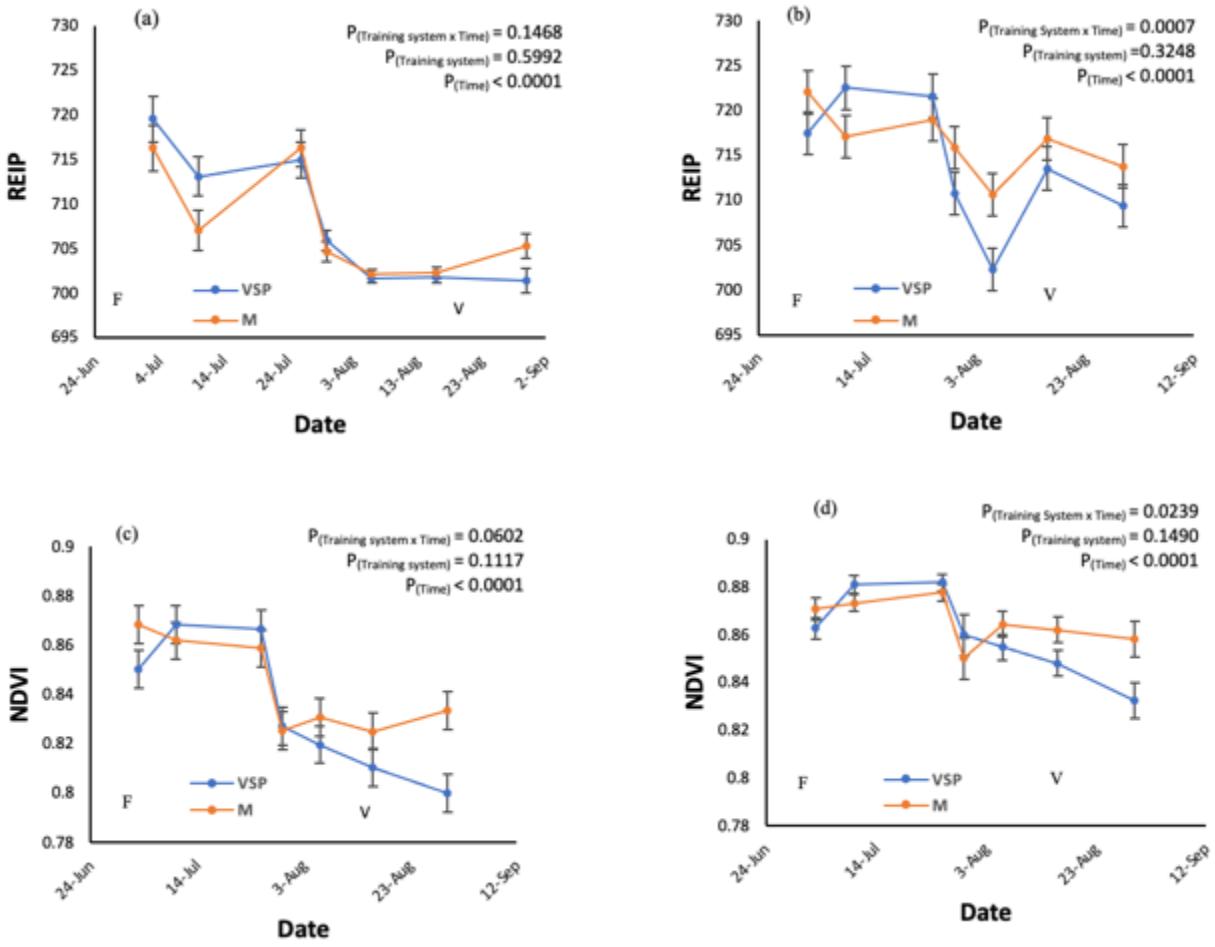

Figure 8. Vegetative indices of grapevine leaves. Red edge inflection point (REIP) of (a) Mars and (b) Canadice. Normalized difference vegetation index (NDVI) of (c) Mars and (d) Canadice. Values shown are mean ±SEM (n=12). Phenological stages are abbreviated as flowering (F), veraison (V), and harvest (H) respectively.

In Canadice, there was a significant interaction effect of training system x time on NDVI; M-trained Canadice had higher NDVI from four weeks after flowering than VSP-trained Canadice ($P = 0.0239$). There was a significant effect of time ($P < 0.0001$) in both cultivars.

The results (Fig. 9a-d) show that MSI and phenology remained stable for 5 weeks after flowering and then tend to increase over time while approaching the end of the growing season in both cultivars.

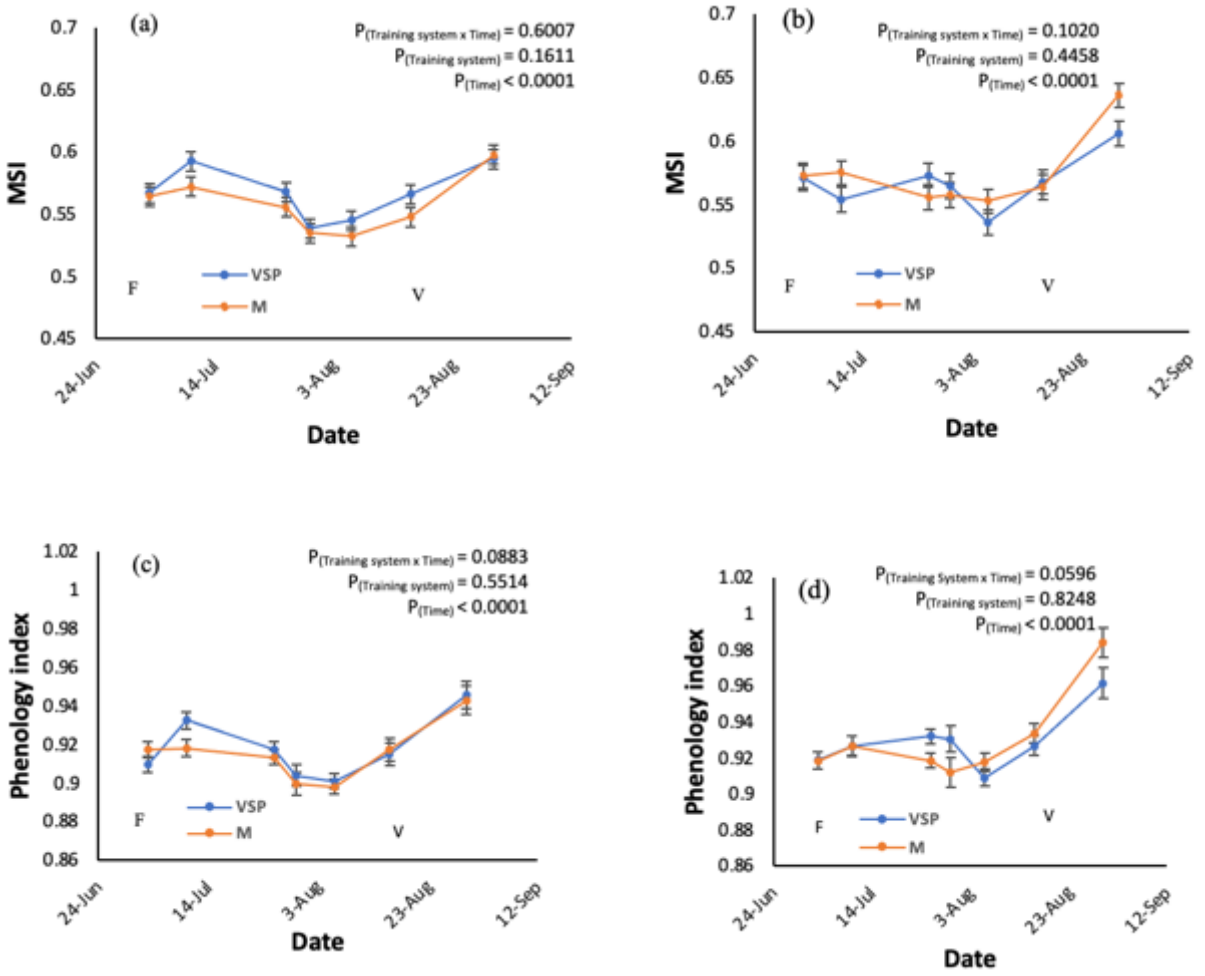

Figure 9. Vegetative indices of grapevine leaves. Moisture stress index (MSI) of (a) Mars and (b) Canadice. Phenology index of (c) Mars and (d) Canadice growing on vertical shoot positioning (VSP) and Munson (M) training systems. Values shown are mean ± SEM (n=12). Phenological stages are abbreviated as flowering (F), veraison (V), and harvest (H) respectively.

MSI provides an accurate indication of leaf water content in vegetation; as the water content decreases, the MSI values increase and approach 1.0, which is the indication of the highest amount of water stress (Hunt and Rock, 1989). The increase in MSI values indicates the vegetation's water stress during senescence. For both Canadice and Mars, there was a significant effect of time on MSI ($P < 0.0001$). The phenology index is the indication of water stress and, additionally, the maturation index of the vegetation (Rock and Lauten, 1996). An increase in phenology index describes the reduction in the photosynthetic efficiency of the vegetation and vines approaching senescence at the end of the growing

season. In both Canadice and Mars, there was a significant effect of time on phenology index ($P < 0.0001$).

2.3.1.3 Gas exchange analysis of Mars and Canadice Leaves growing on Munson and VSP training systems.

Gas exchange measurements were conducted on Mars and Canadice during the 2020 and 2021 growing seasons. In the 2020 growing season, the duration of gas exchange data collection lasted for about 7 weeks for Mars and 6 weeks for Canadice. In the 2021 growing season, the gas exchange data collection lasted for about 13 weeks for Mars and 11 weeks for Canadice.

In Mars, the intercellular CO_2 concentration (C_i) (Fig. 10a and c) significantly decreased over time in 2020 ($P < 0.0001$). In the 2021 growing season there were effects of time ($P < 0.0001$), and training system ($P = 0.0390$), with VSP-trained Mars showing higher Ci four weeks after flowering until harvest. For Canadice, the intercellular CO_2 concentration (C_i) **(**Fig**.** 10b and d**)** in the 2020 growing season had a significant interaction effect of training system x time ($P = 0.0360$), with higher Ci on VSP overtime compared with M. A significant effect of time ($P < 0.0001$) was also noted. In the 2021 growing season, there was a significant interaction effect of training system x time ($P = 0.0119$), with VSP showing higher Ci than M four weeks after flowering until veraison and there was a significant effect of time ($P < 0.0001$).

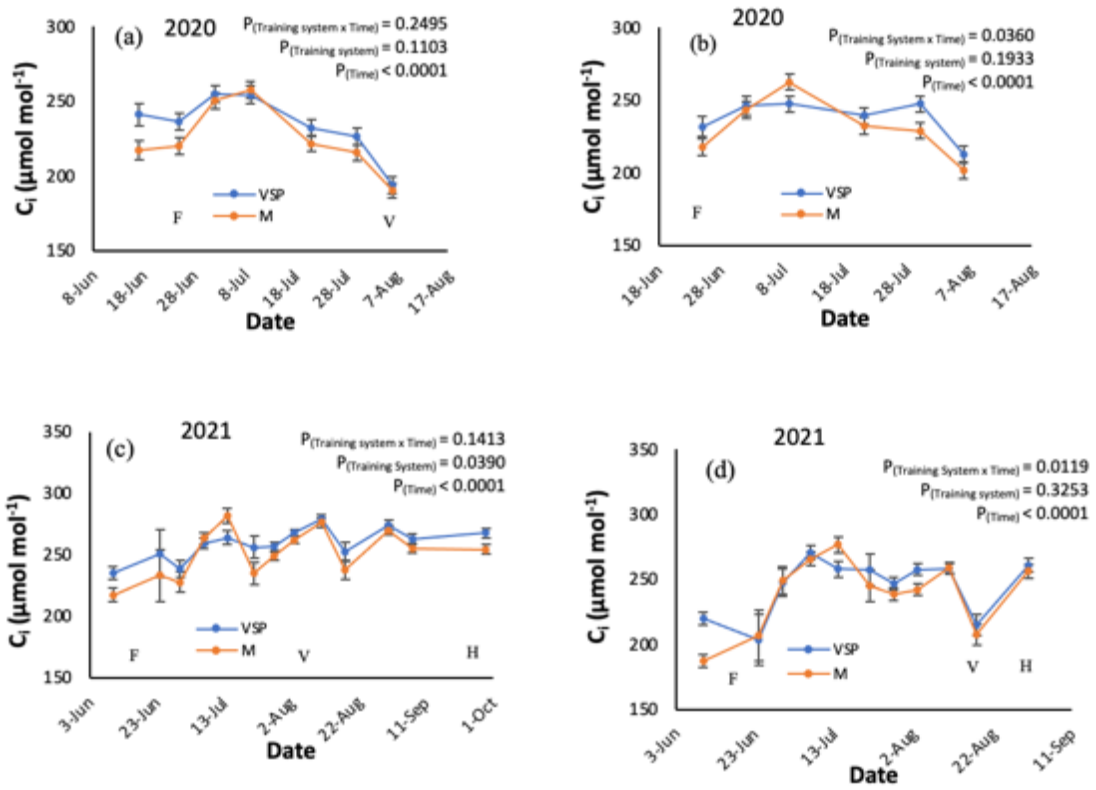

Figure 10. Intercellular CO_2 concentration (Ci, µmol mol-1) in 2020 (a) Mars (b) Canadice and in 2021 (c) Mars (d) Canadice**.** Values are shown are mean ± SEM (n=9 in 2020, n=12 in 2021). Phenological stages are abbreviated as flowering (F), veraison (V), and harvest (H) respectively.

For Mars, the stomatal conductance (g_s) (Fig. 11a and c) in the 2020 growing season had a significant interaction effect of training system x time (P = 0.0043); VSP-trained Mars had much higher g_s than M-trained Mars from flowering until veraison. The effects of training system (P = 0.0132), and time (P < 0.0001), were also significant. In the 2021 growing season, a significant interaction effect of training system x time (P = 0.0003); VSP-trained Mars had higher g_s than M-trained Mars from veraison until harvest, as well as a significant effect of time (P < 0.0001). In Canadice, the g_s **(**Fig. 11b and d) during the 2020 growing season, there was a significant effect of training system (P = 0.0334), VSP-trained Canadice had higher g_s than M-trained Canadice but not for entire time point from flowering to veraison and a significant effect of time (P < 0.0001). In the 2021 growing season, there was

a significant interaction effect of training system x time; M-trained Canadice had higher g_s than the VSP-trained Canadice (P = 0.0018) from three weeks after flowering until harvest on some dates, but not over the entire time period and a significant effect of time (P < 0.0001).

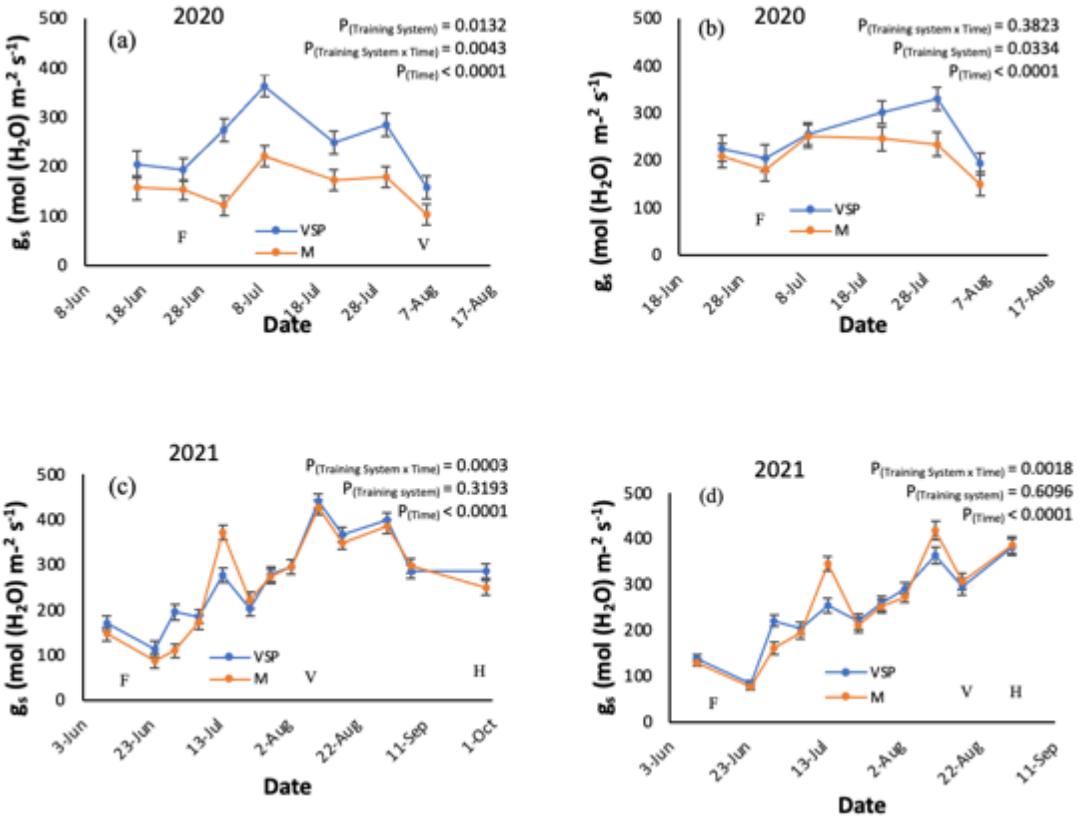

Figure 11. Stomatal conductance (gs) in 2020 (a) Mars (b) Canadice and in 2021 (c) Mars (d) Canadice. Values are shown are mean ± SEM (n=9 in 2020, n=12 in 2021). Phenological stages are abbreviated as flowering (F), veraison (V), and harvest (H) respectively.

For vapor pressure deficit (VPD) in Mars, (Fig. 12a and c) for the 2020 growing season, there was a significant effect of training system (P = 0.0449), with Munson showing higher values than VSP from flowering until veraison and a significant effect of time (P < 0.0001), with VPD showing a slight increase from Jul 8 towards harvest. In the 2021 growing season, there was only a significant effect of time (P < 0.0001), but this year VPD decreased towards harvest in both training systems. In Canadice, VPD **(**Fig. 12b and d**)** during 2020 growing

season had a significant interaction effect of training system x time (P = 0.0414) with M-trained Canadice showing higher VPD from flowering until harvest than VSP-trained Canadice and there was a significant effect of time (P < 0.0001). In the 2021 growing season, there was only a significant effect of time (P < 0.0001).

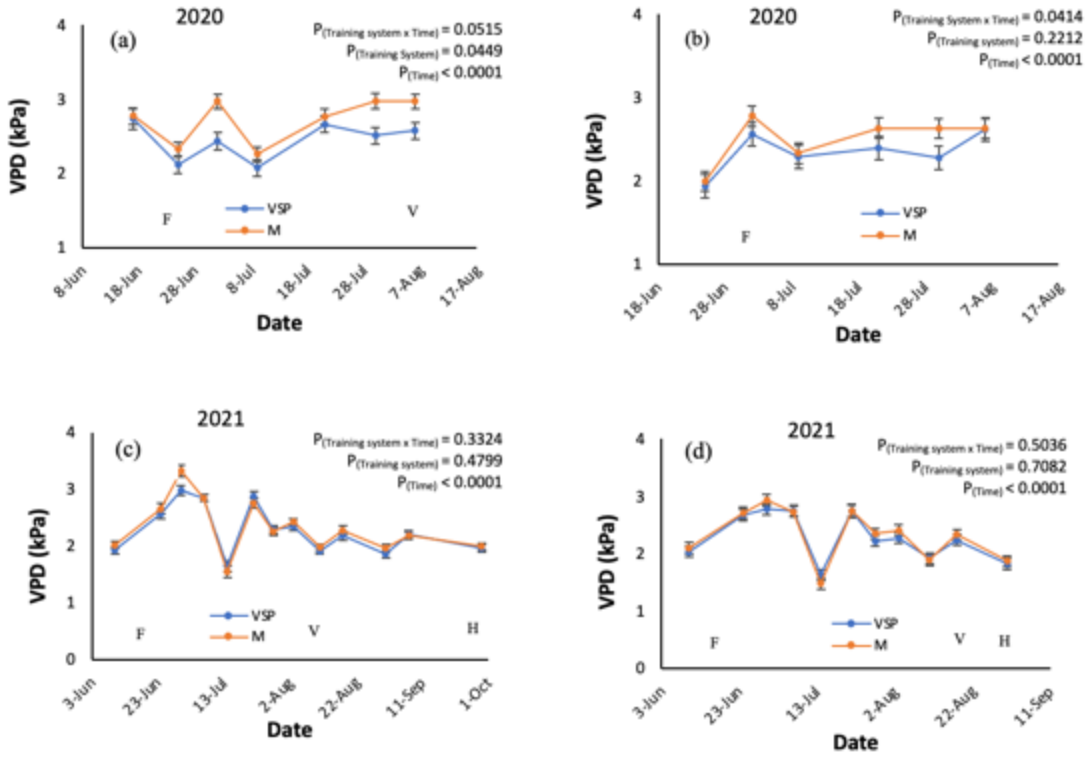

Figure 12. Vapor pressure deficit (VPD) in 2020 (a) Mars (b) Canadice and in 2021 (c) Mars (d) Canadice. Values are shown are mean ± SEM (n=9 in 2020, n=12 in 2021). Phenological stages are abbreviated as flowering (F), veraison (V), and harvest (H) respectively.

In Mars net photosynthetic rate (A) **(**Fig 13a and c) during the 2020 growing season, had a significant interaction effect of training system x time (P = 0.0016); VSP-trained Mars had much higher A than M-trained Mars with 'A' increasing from flowering until veraison. There was also a significant effect of training system (P = 0.0258), and time (P < 0.0001). In the 2021 growing season, there was a significant interaction effect of training system x time (P = 0.0205); M-trained Mars had higher A than the VSP-trained Mars from four weeks after

flowering until harvest. A significant effect of time ($P < 0.0001$) was also noticed. In Canadice, **A (**Fig. 13b and d**)** in the 2020 growing season, had a significant effect of time ($P < 0.0001$). In the 2021 growing season, there was a significant interaction effect of training system x time ($P = 0.0105$); M-trained Canadice had the higher A than VSP-trained Canadice from four weeks after flowering until harvest, and a significant effect of time ($P < 0.0001$).

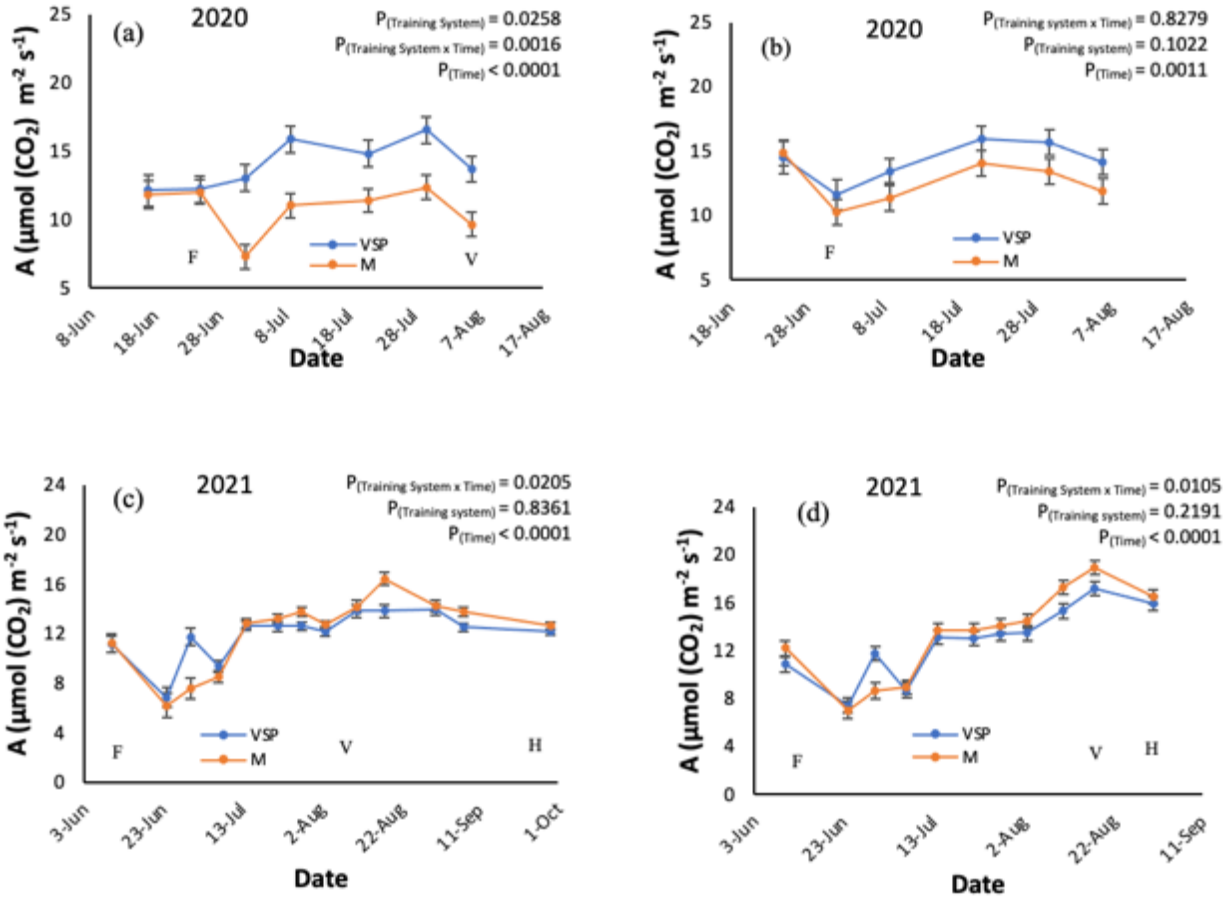

Figure 13. Net photosynthetic rate (A) in 2020 (a) Mars (b) Canadice and in 2021 (c) Mars (d) Canadice. Values are shown are mean ±SEM (n=9 in 2020, n=12 in 2021). Phenological stages are abbreviated as flowering (F), veraison (V), and harvest (H) respectively.

In Mars, transpiration (E) **(**Fig. 14a and c) during the 2020 growing season; had a significant interaction effect of training system x time; ($P = 0.0002$), with VSP-trained Mars showing much higher E than M-trained Mars from flowering until veraison. A significant effect of

training system (P = 0.0090), and a significant effect of time (P < 0.0001), were also noticed. In the 2021 growing season, there was a significant interaction effect of training system x time (P < 0.0001), with VSP showing higher E than M four weeks after flowering until harvest and a significant effect time (P < 0.0001). In Canadice, E **(**Fig 14b and d**)** during the 2020 growing season, we observed a significant effect time (P = 0.0006). In the 2021 growing season, there was a significant interaction effect of training system x time (P = 0.0165); M-trained Canadice had higher E than the M-trained Canadice from veraison until harvest, and a significant effect of time (P < 0.0001).

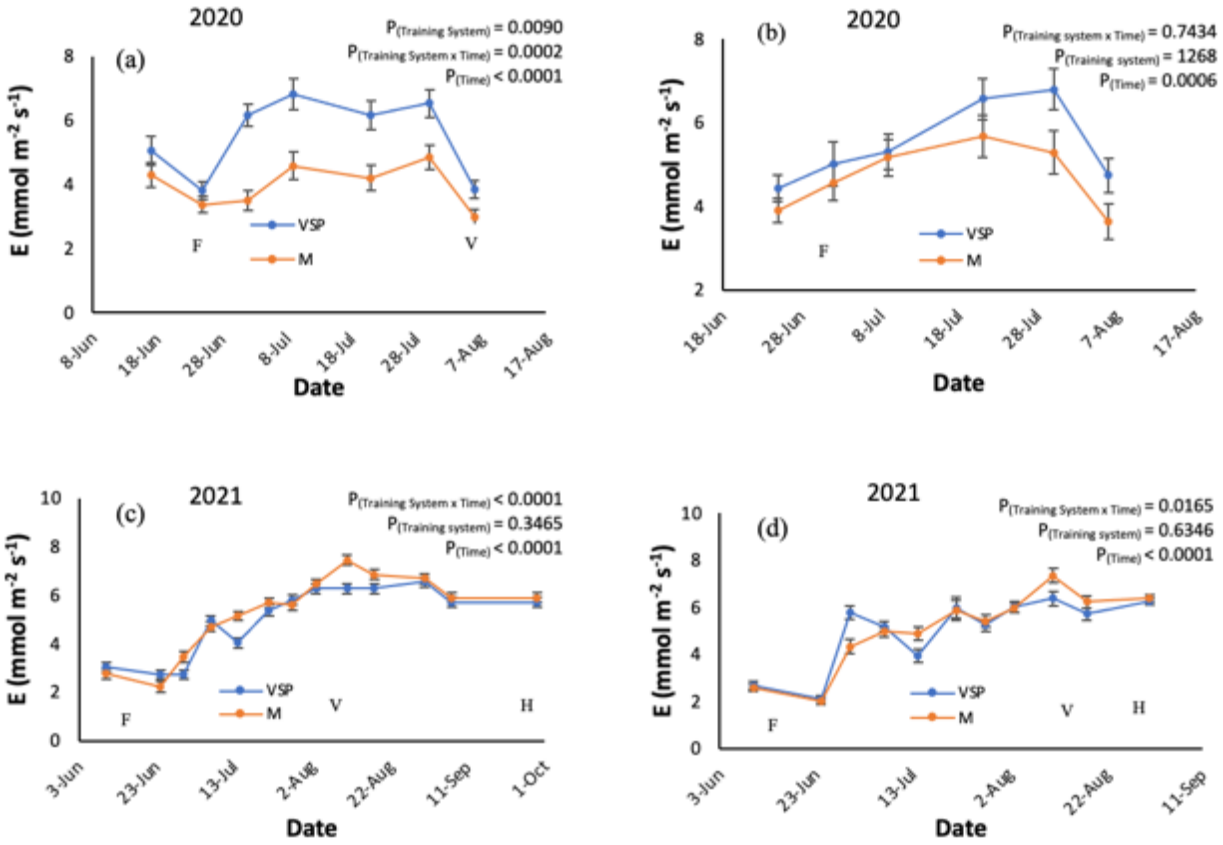

Figure 14. Transpiration (E) in 2020 (a) Mars (b) Canadice and in 2021 (c) Mars (d) Canadice. Values are shown are mean ± SEM (n=9 in 2020, n=12 in 2021). Phenological stages are abbreviated as Flowering (F), Veraison (V), and Harvest (H) respectively.

In Mars water use efficiency (WUE) **(**Fig. 15a and c**)** in 2020 growing season had a significant effect of time (P < 0.0001). In the 2021 growing season, there was a significant

interaction effect of training system x time (P = 0.0081) with M-trained Mars showing higher WUE than VSP from veraison until harvest, and a significant effect of time (P < 0.0001). In Canadice WUE **(**Fig 15b and d**)** during the 2020 and 2021 growing seasons had a significant effect of time (P < 0.0001).

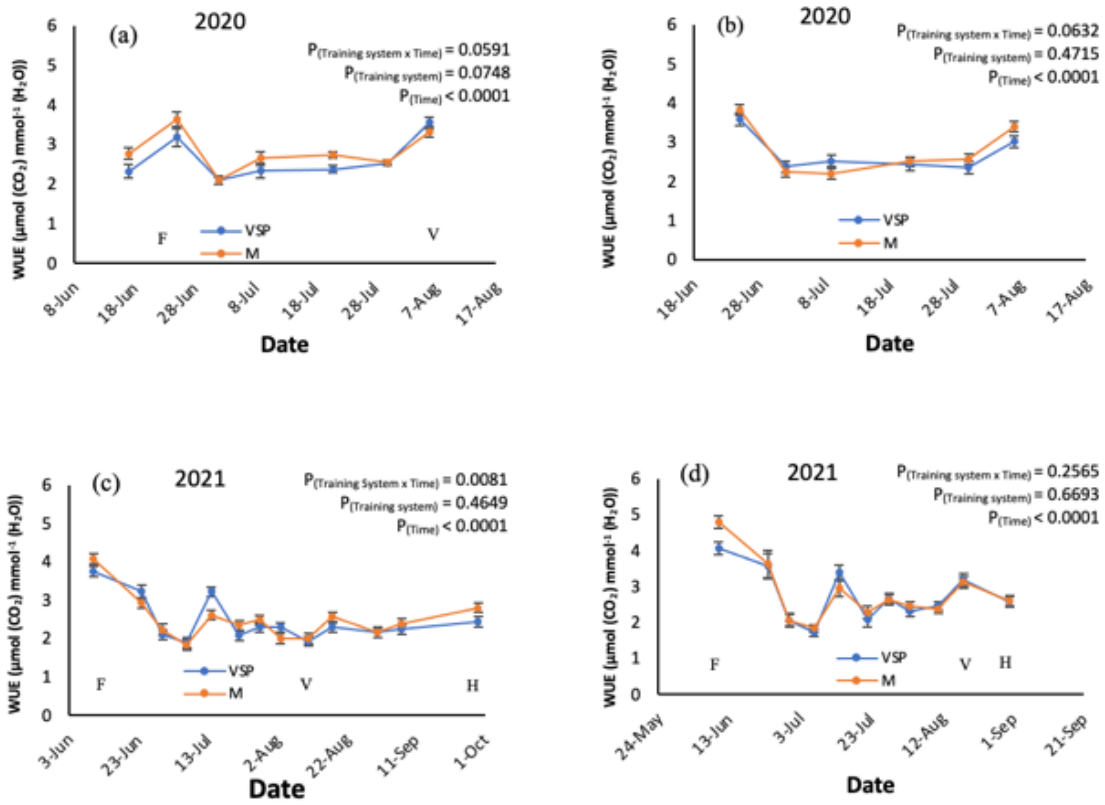

Figure 15. Water use efficiency (WUE) in 2020 (a) Mars (b) Canadice and in 2021 (c) Mars (d) Canadice. Values are shown are mean ± SEM (n=9 in 2020, n=12 in 2021). Phenological stages are abbreviated as flowering (F), veraison (V), and harvest (H) respectively.

2.3.2 Biochemistry of Mars and Canadice

2.3.2.1 Leaf Pigment analysis of Mars and Canadice growing on VSP and Munson training systems

Leaf chlorophyll *a*, chlorophyll *b*, carotenoids, and total chlorophyll were quantified for both cultivars growing on both training systems. In 2019, the amount of these pigments showed a trend of decreasing along the growing season but tended to increase during the two weeks leading to harvest (Fig. 16 a-h)

The 2019 results show that there was a significant interaction effect of training system x time in both grape cultivars with Munson showing higher values at the end of the growing season, on chlorophyll *a* (Fig.16a and b; Mars $P = 0.0120$, Canadice $P = 0.009$), chlorophyll *b* (Fig. 16c and d; Mars $P = 0.0023$, Canadice $P = 0.0028$), and total chlorophyll (Fig. 16e and f; Mars $P = 0.0090$, Canadice $P = 0.0014$). A significant effect of time on chlorophyll *a* (Fig. 16a and b; Mars $P < 0.0001$, Canadice $P < 0.0001$), chlorophyll *b* (Fig 15c and d; Mars $P < 0.0001$, Canadice $P < 0.0001$), and total chlorophyll (Fig. 16e and f; Mars $P < 0.0001$, Canadice $P < 0.0001$) was also detected. For carotenoids there was a significant interaction effect of training system x time in Canadice with M-trained Canadice having higher carotenoids than M-trained Canadice two weeks after flowering until rest of the growing season (Fig.16h; $P = 0.0217$), and a significant effect of time was also detected (Fig. 16h; $P < 0.0001$), while in Mars only a significant effect of time (Fig. 16g; Mars $P < 0.0001$) was found.

During the 2020 growing season, due to COVID restrictions on research settings, leaf sampling was done only at two time points (veraison and harvest). The 2020 growing season pigment analysis results (Fig 17a-h) show that there was a significant effect of time on chlorophyll *a* (Fig. 17a; $P = 0.0025$), chlorophyll *b* (Fig. 17c; $P = 0.0449$), total chlorophylls (Fig. 17e; $P = 0.0056$), and carotenoids (Fig. 17g; $P < 0.0001$), but only on Mars. No differences in photosynthetic pigments were found between Canadice leaves collected at veraison and harvest (Fig. 17b, d, f, and h).

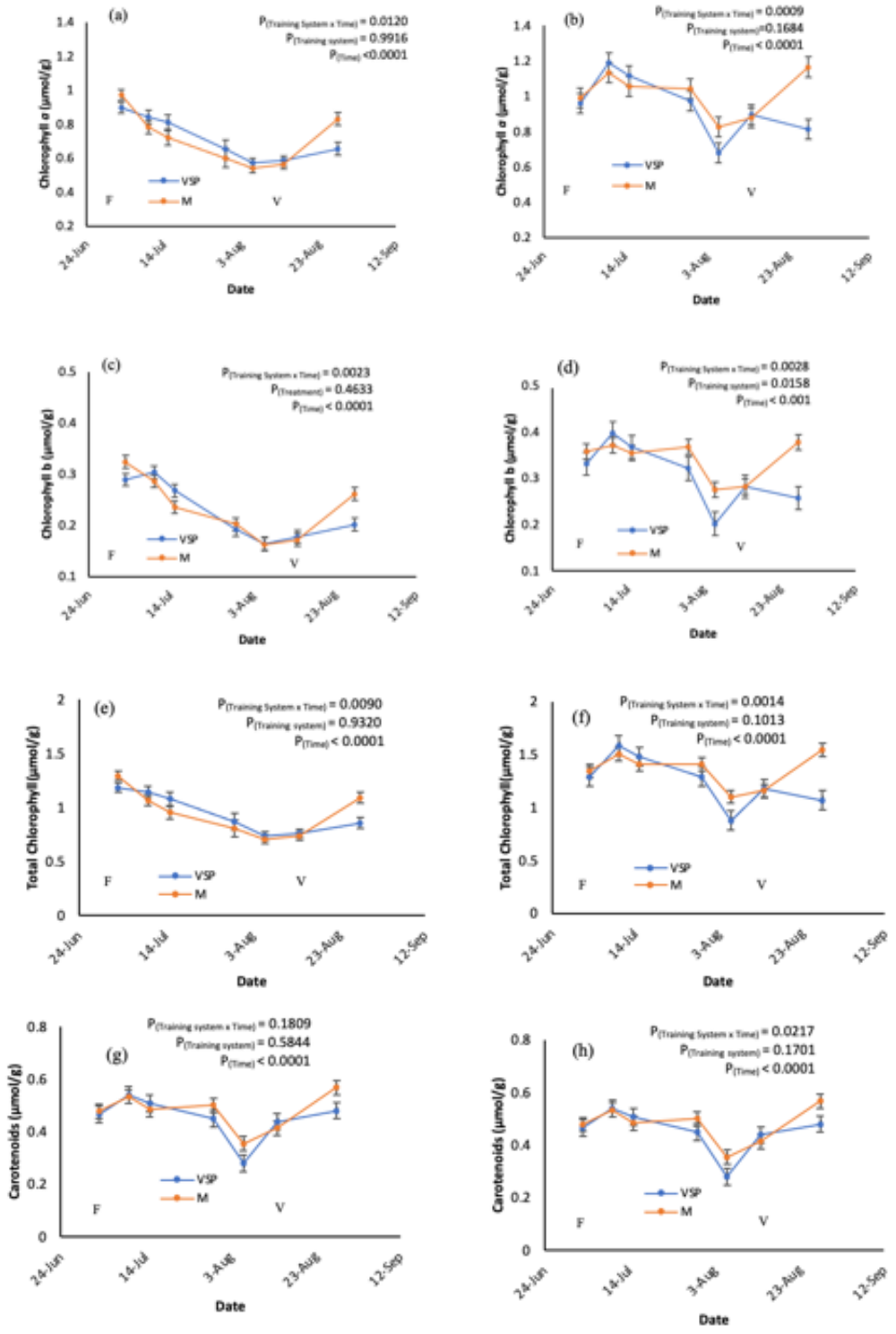

Figure 16. Photosynthetic pigment concentration of Mars and Canadice leaves growing on vertical shoot positioning or Munson training systems in 2019. Chlorophyll a (a) Mars and (b) Canadice. Chlorophyll b (c) Mars and (d) Canadice. Total Chlorophyll (e) Mars and (f) Canadice. Carotenoids (g) Mars and (h) Canadice. Values shown are mean ± SEM (n=12). Two-way repeated measures ANOVA with Tukey's multiple comparison ($p<0.05$). Phenological stages are labelled as flowering (F), veraison (V), and harvest (H).

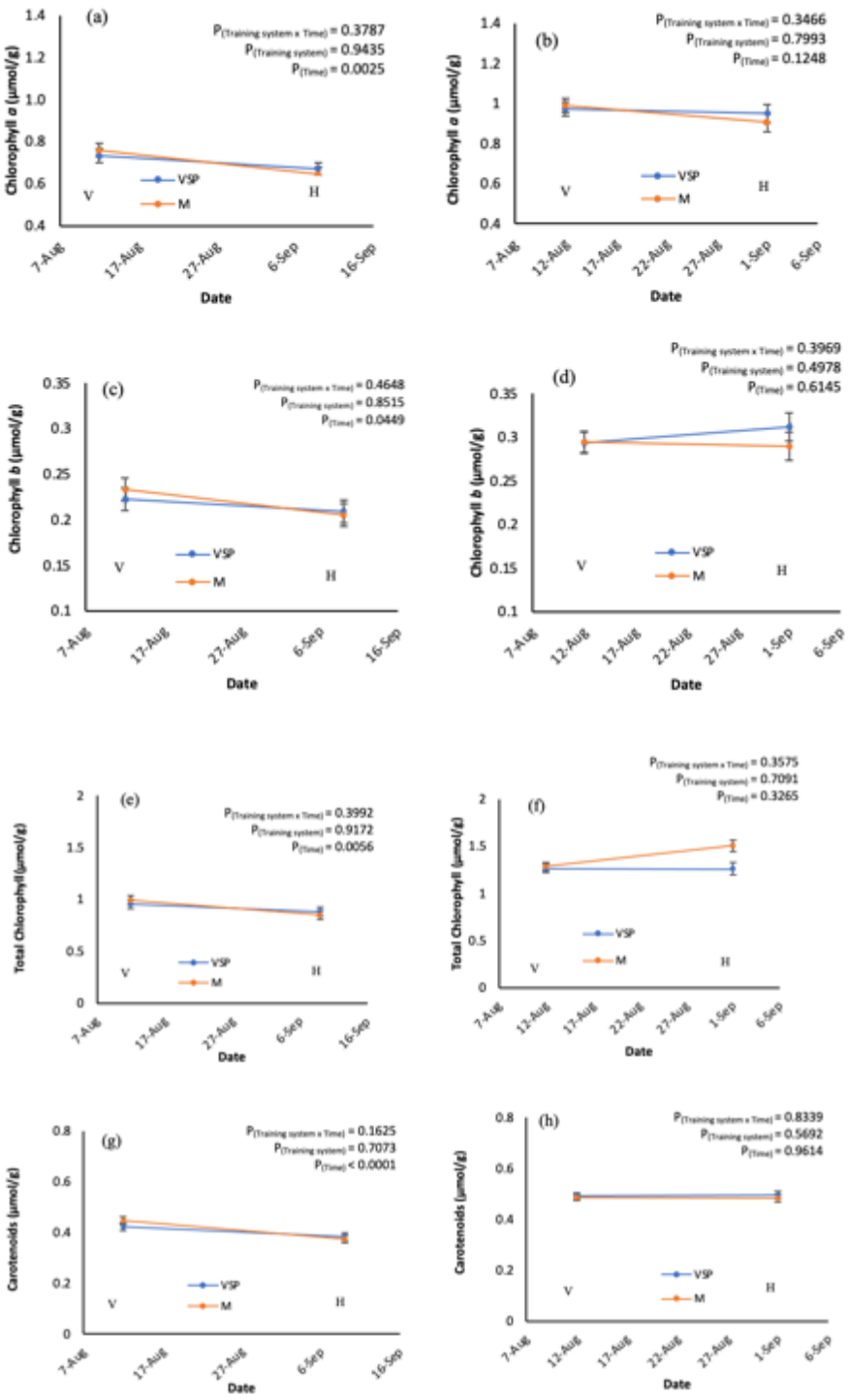

Figure 17. Photosynthetic pigment concentration of Mars and Canadice leaves growing vertical shoot positioning or Munson training systems in 2020**.** Chlorophyll a (a) Mars and (b) Canadice. Chlorophyll b (c) Mars and (d) Canadice. Total Chlorophyll (e) Mars and (f) Canadice. Carotenoids (g) Mars and (h) Canadice. Values shown are mean ± SEM (n=12). Two-way repeated measures ANOVA with Tukey's multiple comparison ($p<0.05$). Phenological stages are labelled as flowering (F), veraison (V), and harvest (H).

The 2021 results show (Fig. 18a-h) that there was a significant interaction effect of training system x time interaction on chlorophyll *a;* M-trained Mars had higher chlorophyll *a* than VSP-trained Mars from veraison until harvest, and M-trained Canadice had higher chlorophyll *a* four weeks after flowering until harvest than VSP-trained Canadice (Fig. 18a and b; Mars $P < 0.0001$, Canadice $P < 0.0001$). There was a significant interaction effect of training system x time on chlorophyll *b*; M-trained Mars had a higher chlorophyll *b* than VSP-trained Mars from veraison until harvest and M-trained Canadice had a higher chlorophyll *b* than VSP-trained Canadice from veraison until harvest (Fig. 18c and d; Mars $P < 0.0001$, Canadice $P=0.0185$). A significant effect of time on chlorophyll *a* (Fig. 18a and b; Mars $P < 0.0001$, Canadice $P < 0.0001$), and chlorophyll *b* (Fig. 18c and d; Mars $P < 0.0001$, Canadice $P < 0.0001$) was also found. For total chlorophylls there was a significant interaction effect of training system x time in Mars; M-trained Mars had higher total chlorophyll than VSP-trained Mars from veraison until harvest (Fig.18e; $P < 0.0001$), but in Canadice only a significant effect of time was found (Fig. 18f; $P < 0.0001$). There was a significant effect of time on carotenoids both in Mars and Canadice was detected (Fig. 18g and h; $P < 0.0001$). Overall, chlorophylls varied little during the growing season, and tended to start decreasing 2-3 weeks before harvest. For both Mars and Canadice, the chlorophylls were higher in the Munson training system during the last part of the growing season. The carotenoids tended to increase after berry touch (July 7) for about six weeks and appear to decrease thereafter until harvest in both cultivars.

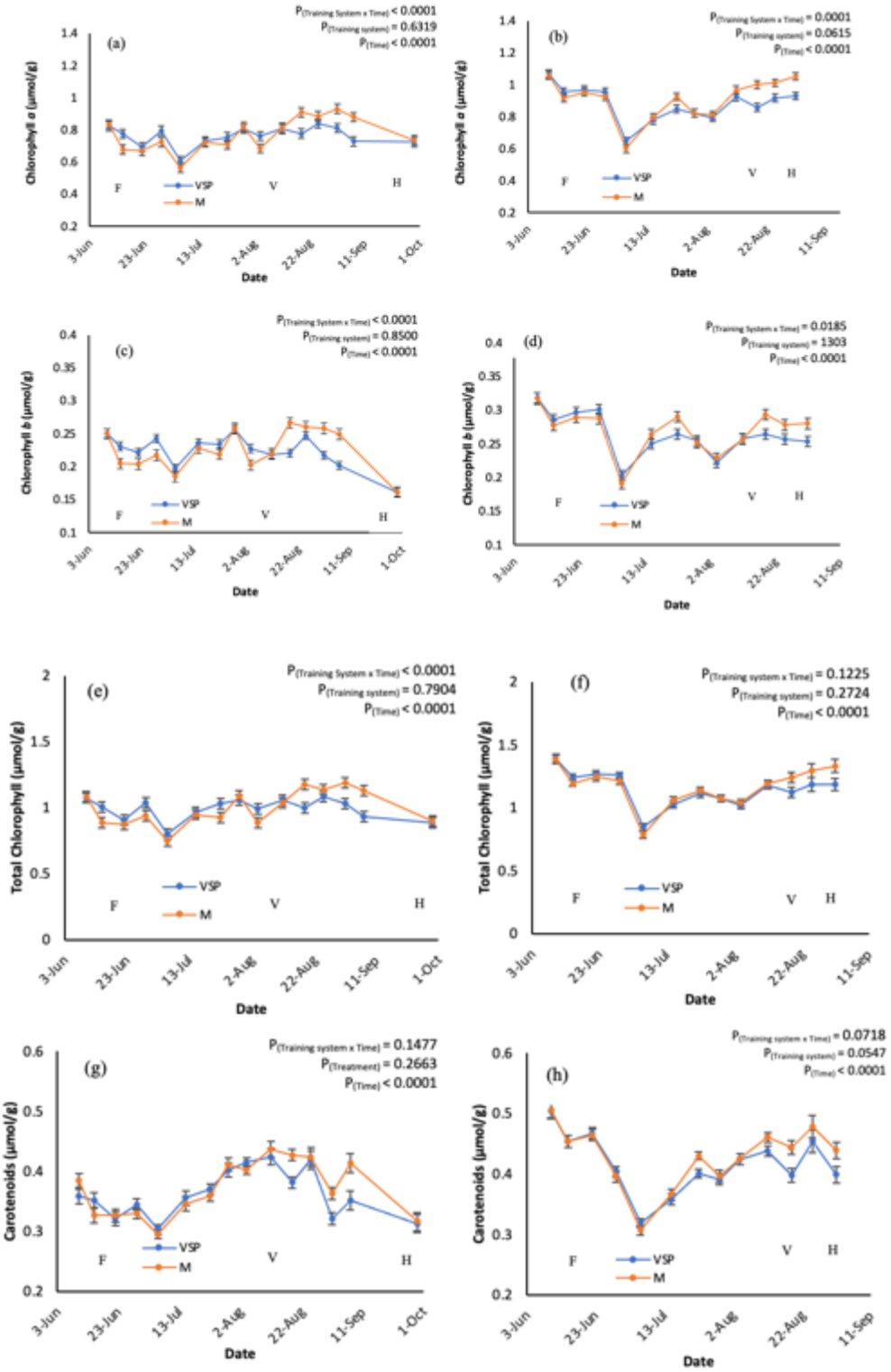

Figure 18. Photosynthetic pigment concentration of Mars and Canadice leaves growing on vertical shoot positioning or Munson training systems in 2021. Chlorophyll a (a) Mars and (b) Canadice. Chlorophyll b (c) Mars and (d) Canadice. Total Chlorophyll (e) Mars and (f) Canadice. Carotenoids (g) Mars and (h) Canadice. Values shown are mean ± SEM (n=12). Two-way repeated measures ANOVA with Tukey's multiple comparison ($p < 0.05$). Phenological stages are labelled as flowering (F), veraison (V), and harvest (H).

2.3.2.2 Leaf metabolomic analysis of Mars and Canadice growing on VSP and Munson training systems

Representative ^{1}H-NMR spectra of Mars and Canadice leaf extracts (0.0-10.0 ppm) recorded for leaves growing on VSP or M training systems at flowering, veraison and harvest are shown in Figures 19-21. The spectra of Mars and Canadice leaf extracts growing on VSP and M training systems were visually very similar.

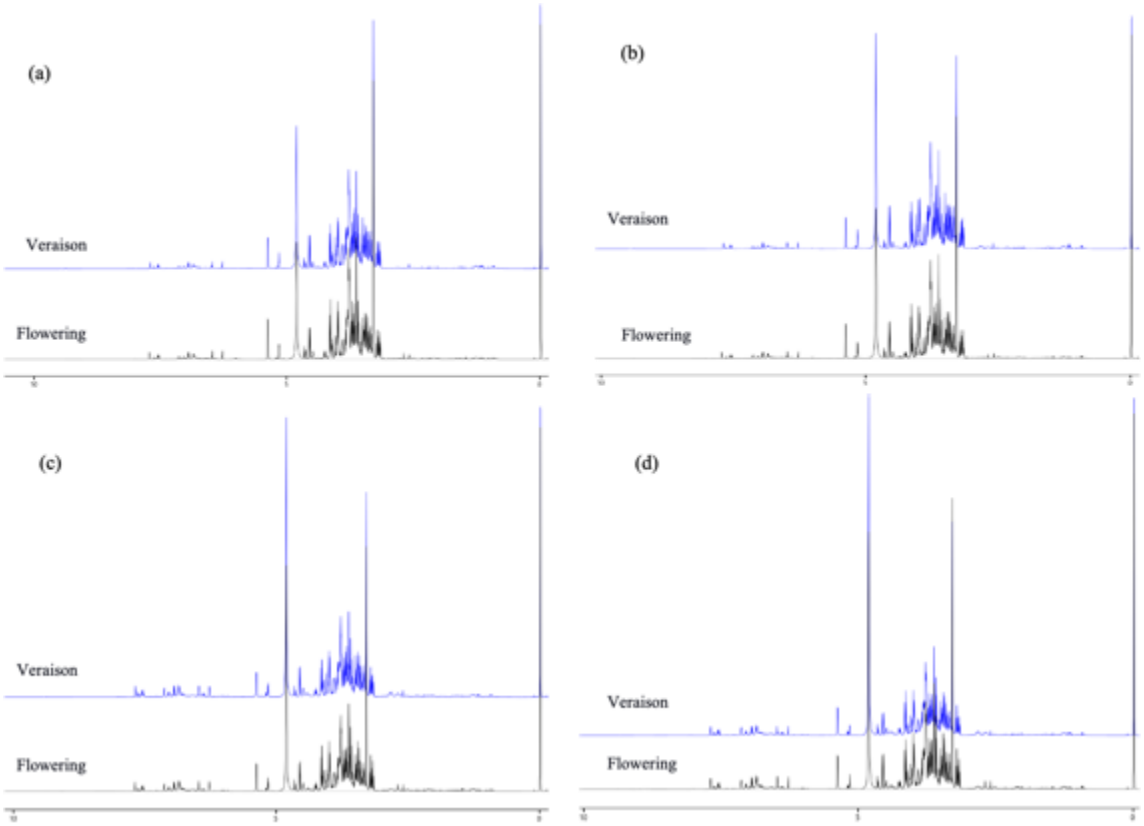

Figure 19. Typical 1D ^{1}H-NMR spectra of grapevine leaf extracts (0.0–10.0 ppm) in 2019 at two different time points (flowering (black) and veraison (blue)). Canadice leaves growing on (a) VSP training system (b) M training system. Mars leaves growing on (c) VSP training system (d) M training system.

The representation of spectra enlargements of aliphatic (0.5-3.2 ppm), sugar (3.2-6.0 ppm), and aromatic regions (6.0-8.0 ppm) for Canadice and Mars growing to VSP and M training systems are shown in Figures 22-25. The expansions of the lower intensity aliphatic (0.5-3.2 ppm), and aromatic (6.0-8.0 ppm) regions have better visible spectral profiles in (Fig. 22-25

b and c. The grapevine leaf extracts major signals were identified and are listed in Table 3. In the sugar region, signals arise from sucrose and many unassigned peaks.

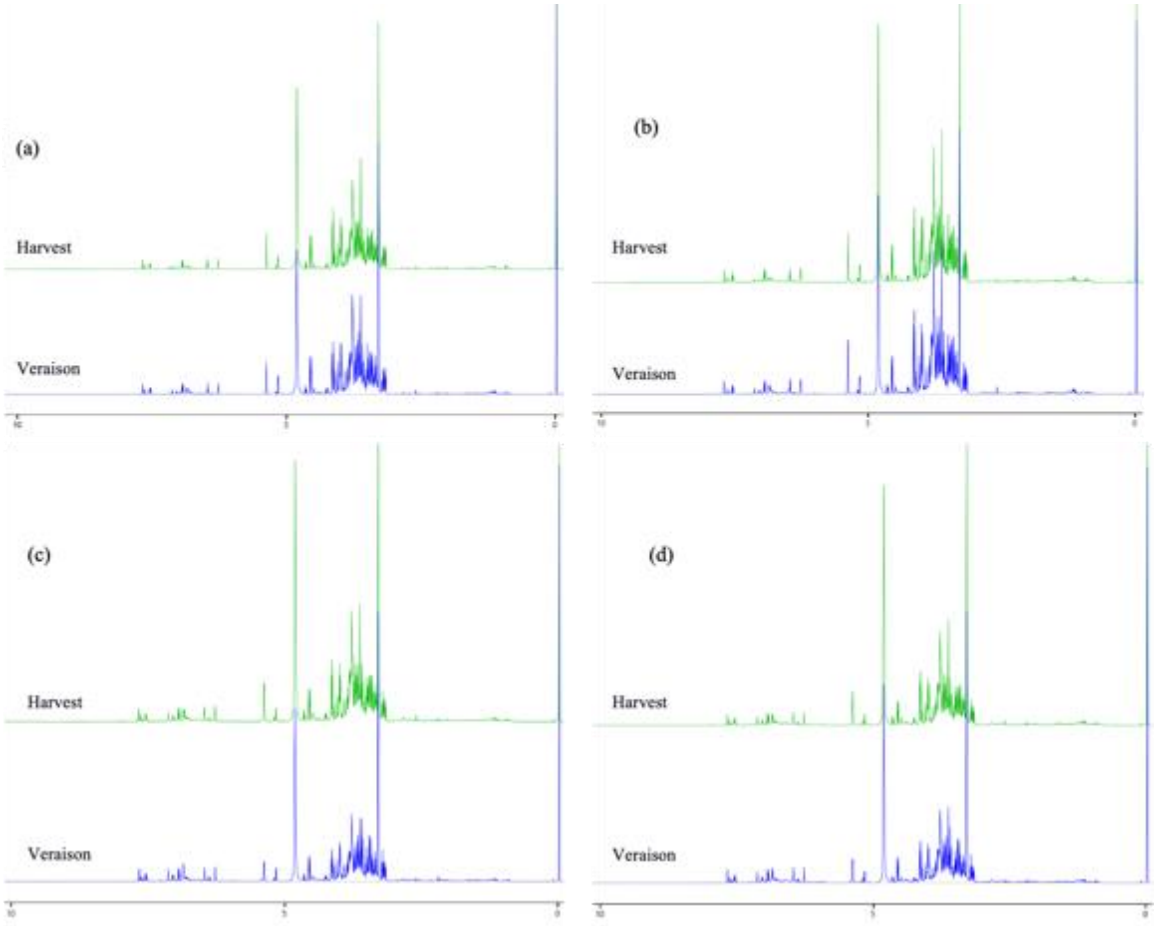

Figure 20. Typical 1D ^{1}H-NMR spectra of grapevine leaf extracts (0.0–10.0 ppm) in 2020 at two different time points (veraison (blue) and harvest(green)). Canadice leaves growing on (a) VSP training system (b) M training system. Mars leaves growing on (c) VSP training system (d) M training system.

For 2019 season, PCA was applied to 1D ^{1}H-NMR spectra of Mars and Canadice leaves growing on VSP and M training systems to investigate differences between the metabolic profiles of both grape varieties between training systems statistically and to detect the main peaks responsible for those differences. A scores scatter plot of the first two PCs obtained considering the whole ^{1}H-NMR spectra (0.5-8.5 ppm) is shown in Figs. 26a and c and shows clear separation of phenological stages along PC1 and PC2 for both grape varieties, but there was no separation based on training systems.

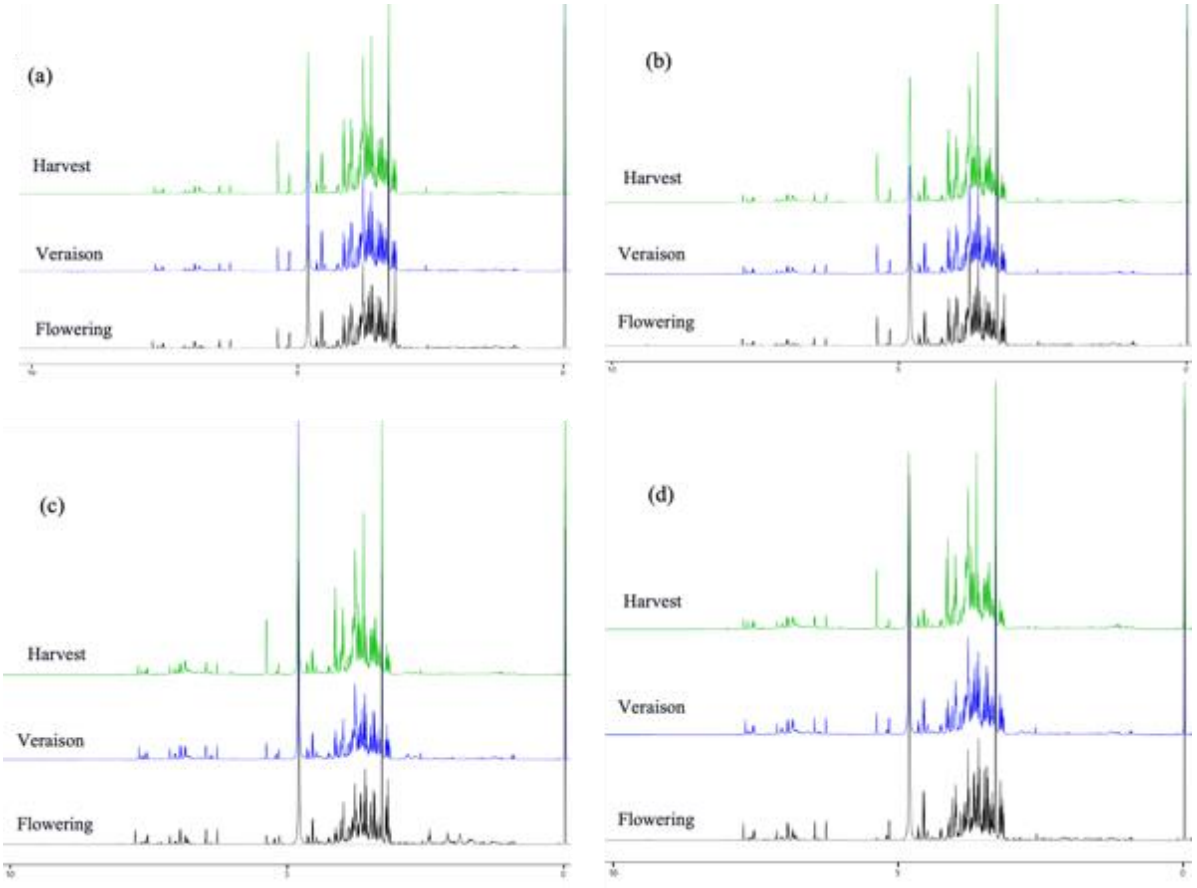

Figure 21. Typical 1D ^{1}H NMR spectra of grapevine leaf extracts (0.0–10.0 ppm) in **2021** three different time points (flowering (black), veraison (blue), and harvest (green)). Mars leaves growing on (a) VSP training system (b) M training system. Canadice leaves growing on (c) VSP training system (d) M training system.

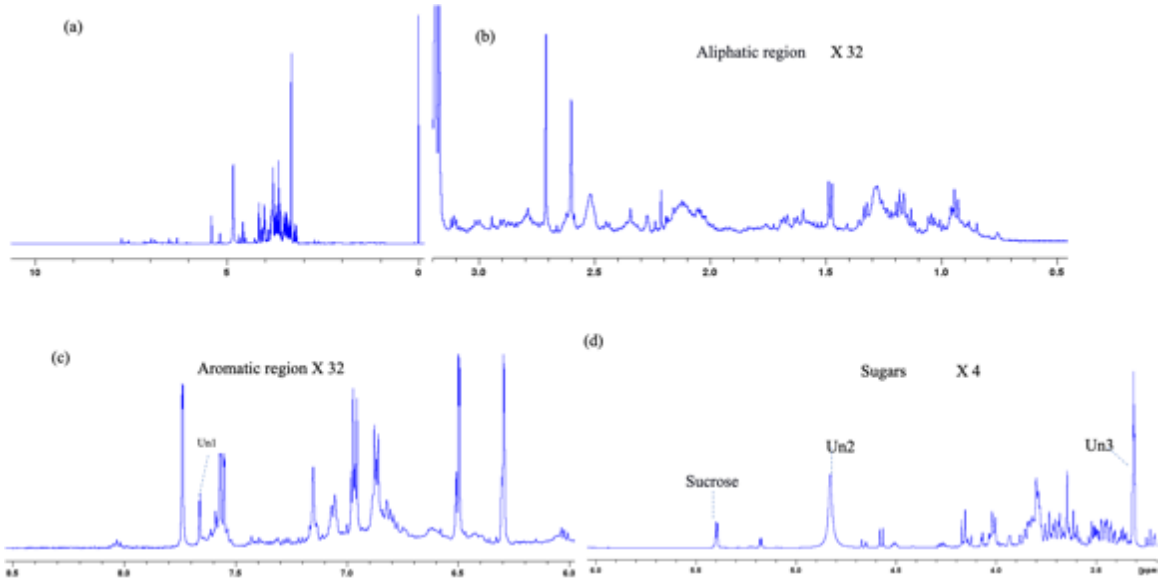

Figure 22. Typical ^{1}H NMR spectra of Canadice leaf extract growing on VSP training system, (a) full spectrum with enlargements of the (b) aliphatic (0.5–3.2 ppm x 32), (c) aromatic (6.0–8.5 ppm x 32), and (d) sugars (3.2-6.0 ppm x 4) regions.

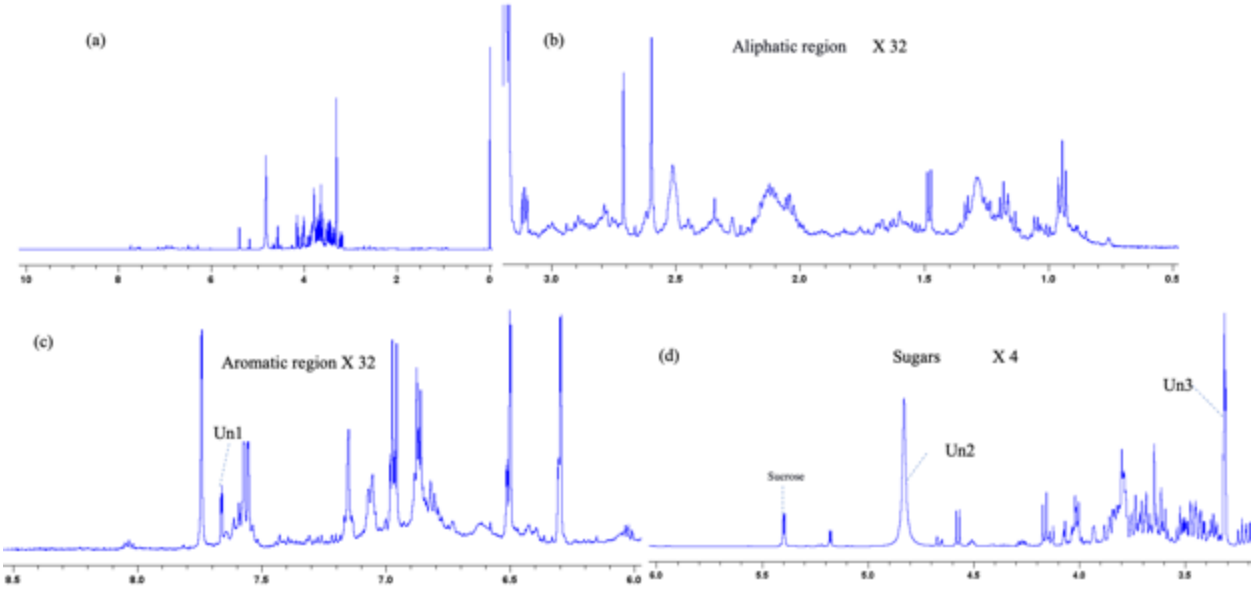

Figure 23. Typical 1D ^{1}H-NMR spectra of Canadice leaf extract growing on (a) M training system, with enlargements of the (b) aliphatic (0.5–3.2 ppm x32) regions, (c) aromatic (6.0–8.0 ppm x4), and (d) sugars (3.2-6.0 x32 ppm).

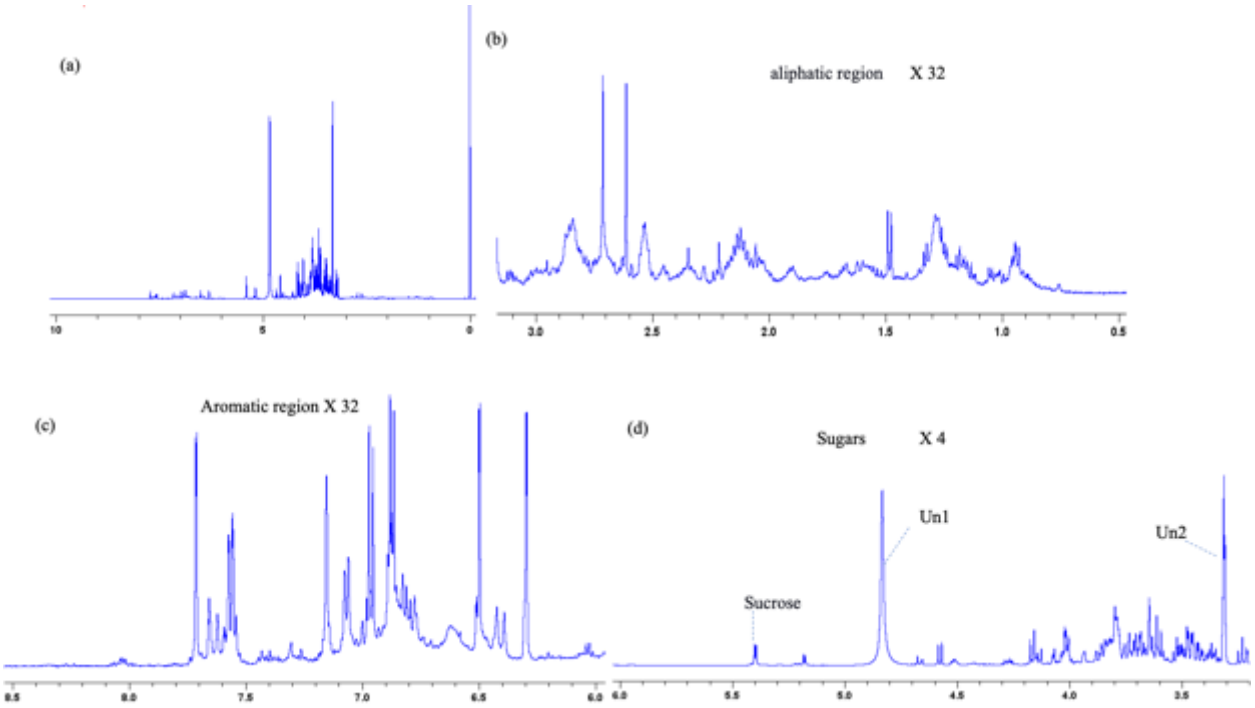

Figure 24. Typical 1D ^{1}H NMR spectra of Mars leaf extract growing on (a) VSP training system, with enlargements of the (b) aliphatic (0.5–3.2 ppm X32) regions, (c) aromatic (6.0–8.0 ppm X32), and (d) sugars (3.2-6.0 ppm X4).

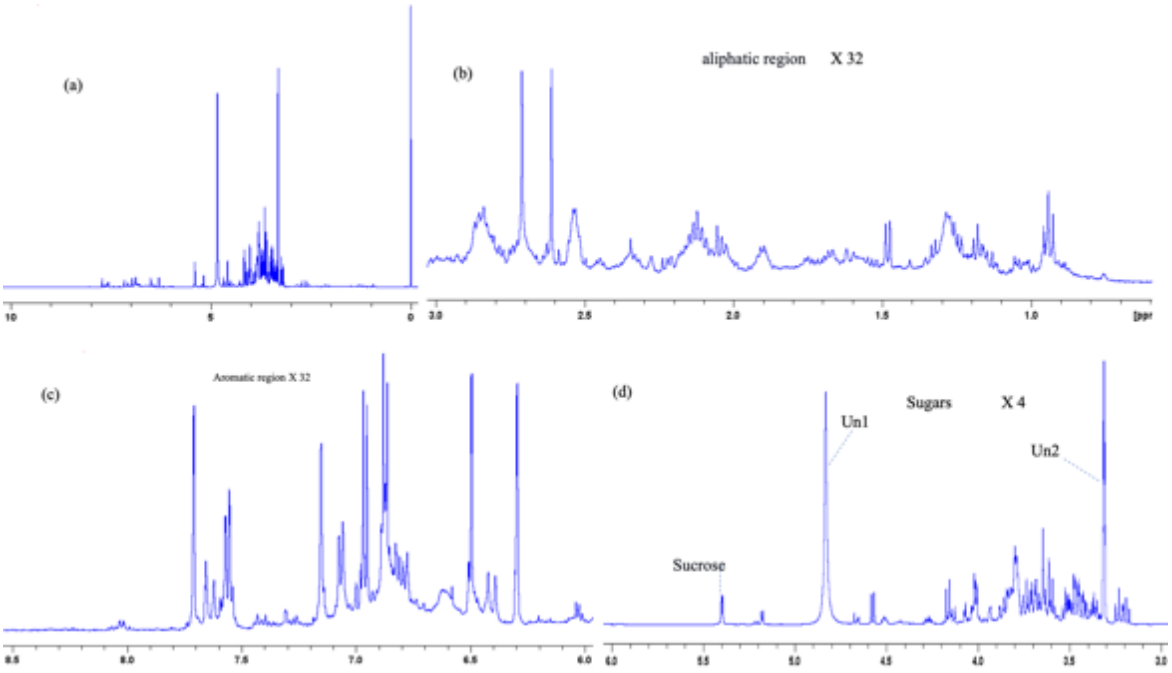

Figure 25. Typical 1D ^{1}H-NMR spectra of Mars leaf extract growing on (a) M training system, with enlargements of the (b) aliphatic (0.5–3.0 ppm X32) regions, (c) aromatic (6.0–8.0 ppm X32), and (d) sugars (3.0-6.0 ppm X4).

Table 3. Metabolites identified in ^{1}H-NMR spectra of Canadice and Mars leaves growing on vertical shoot positioning or Munson training systems during three growing seasons (2019, 2020, and 2021).

Assignment	δ_{Hppm} (Multiplicity/J Hz)[b]
Sucrose	3.5(m), 3.6(m), 3.7(m), 3.8 (m), 3.9(m), 4.0(m), 4.2(dd), **5.4**(dd/3.9)
Unknown 1	7.75(s)
Unknown 2	4.815 (s)
Unknown 3	3.33(t)

[b] Chemical shifts of spin systems in bold refer to the isolated signals used for integration. Spin multiplicity designations: s = singlet, d = doublet, t = triplet, dd = doublet of doublets, td = triplet of doublets, and m = complex multiplet

The metabolites contributing to the separation of phenological stages along PC1 and PC2 can be distinguished in the loadings plot, (Fig. 26b and d) together with visual inspection of the spectra. The loadings plot shows visible discriminating signals lie in the sugar region, showing sucrose and three unassigned compounds.

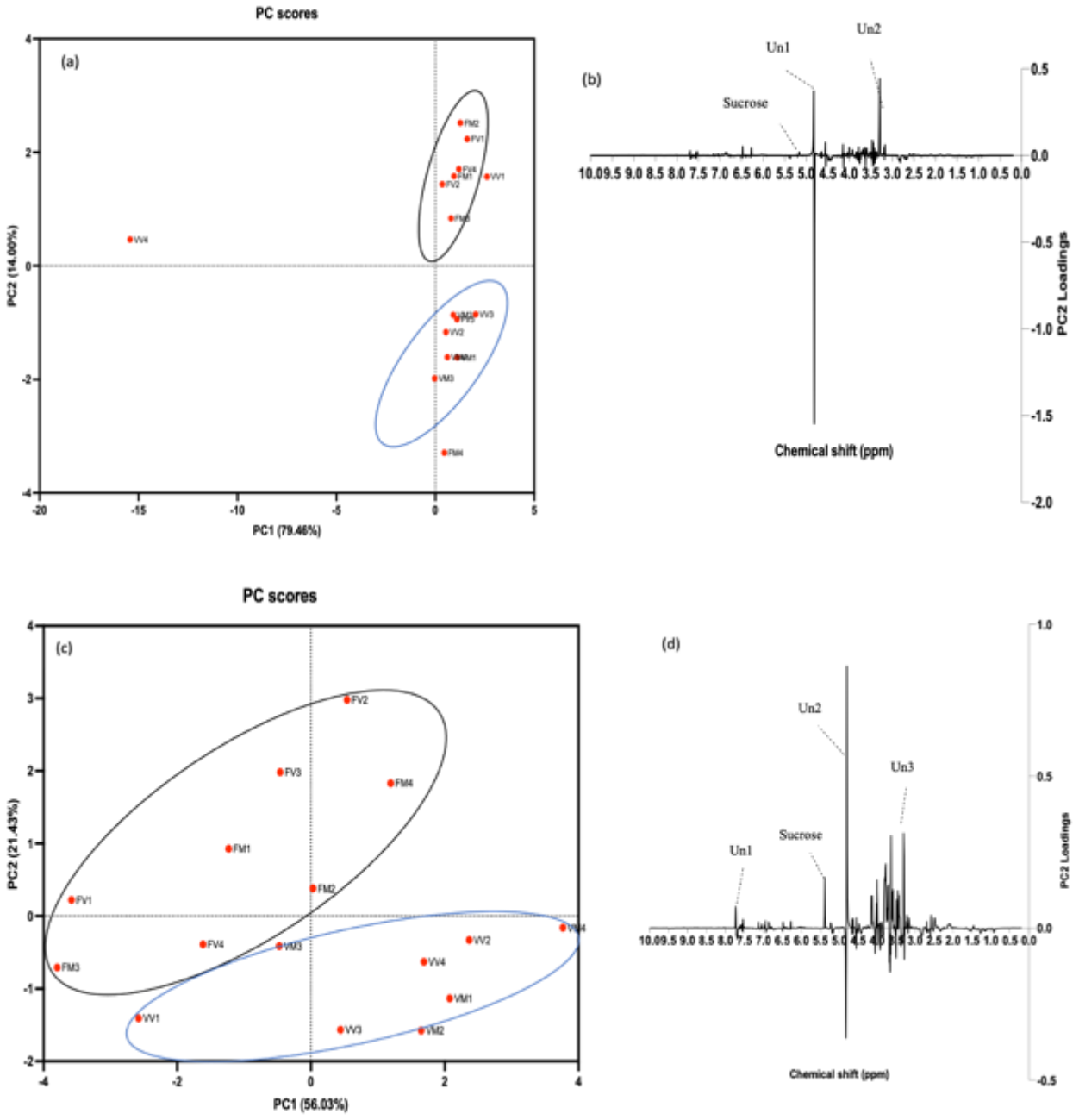

Figure 26. PCA scores scatter plot and loadings plot obtained considering the whole spectra of grapevine leaf extracts collected at flowering and veraison in 2019, (a) Mars scatter plot (b) Mars PC2 loadings plot (c) Canadice scatter plot (d) Canadice PC2 loadings plot. Flowering samples (FV 1-4 from VSP; FM 1-4 from M) and veraison samples (VV 1-4 from VSP; VM 1-4 from M).

The reason behind is the samples position in a given direction in the scores plot is determined by the metabolites lying the same direction in the loadings plot. In this study during the 2019 growing season both flowering samples lay towards positive PC2 values and veraison leaves

lay towards negative PC2 values in score plot in both Mars and Canadice grown on VSP and M training systems. There was one outlier in Mars and Canadice veraison samples, respectively.

During the 2020 growing season, PCA was applied to the 1D ^{1}H-NMR spectra of Mars and Canadice leaves growing on VSP and M training systems to investigate differences between the metabolic profiles of both grape varieties between training systems. A scores scatter plot of the first two PCs obtained considering the whole ^{1}H-NMR spectra (0.5-8.5 ppm) is shown in the (Fig. 27a and c) and shows clear separation of phenological stages along PC1 and PC2 for both grape varieties. Again, there was no separation between training systems. The veraison samples lay towards positive PC1 values and harvest samples lay towards negative PC1 values in the scores plot in both grapevine varieties growing in VSP and M training systems. The metabolites contributing to the separation of phenological stages along PC1 and PC2 can be distinguished in the loadings plot, (Fig. 27b and d) together with visual inspection of the spectra. The loadings plot shows visible discriminating signals lie in the sugar region, showing sucrose and two unassigned compounds. There was one outlier in Mars and Canadice veraison and harvest samples, respectively.

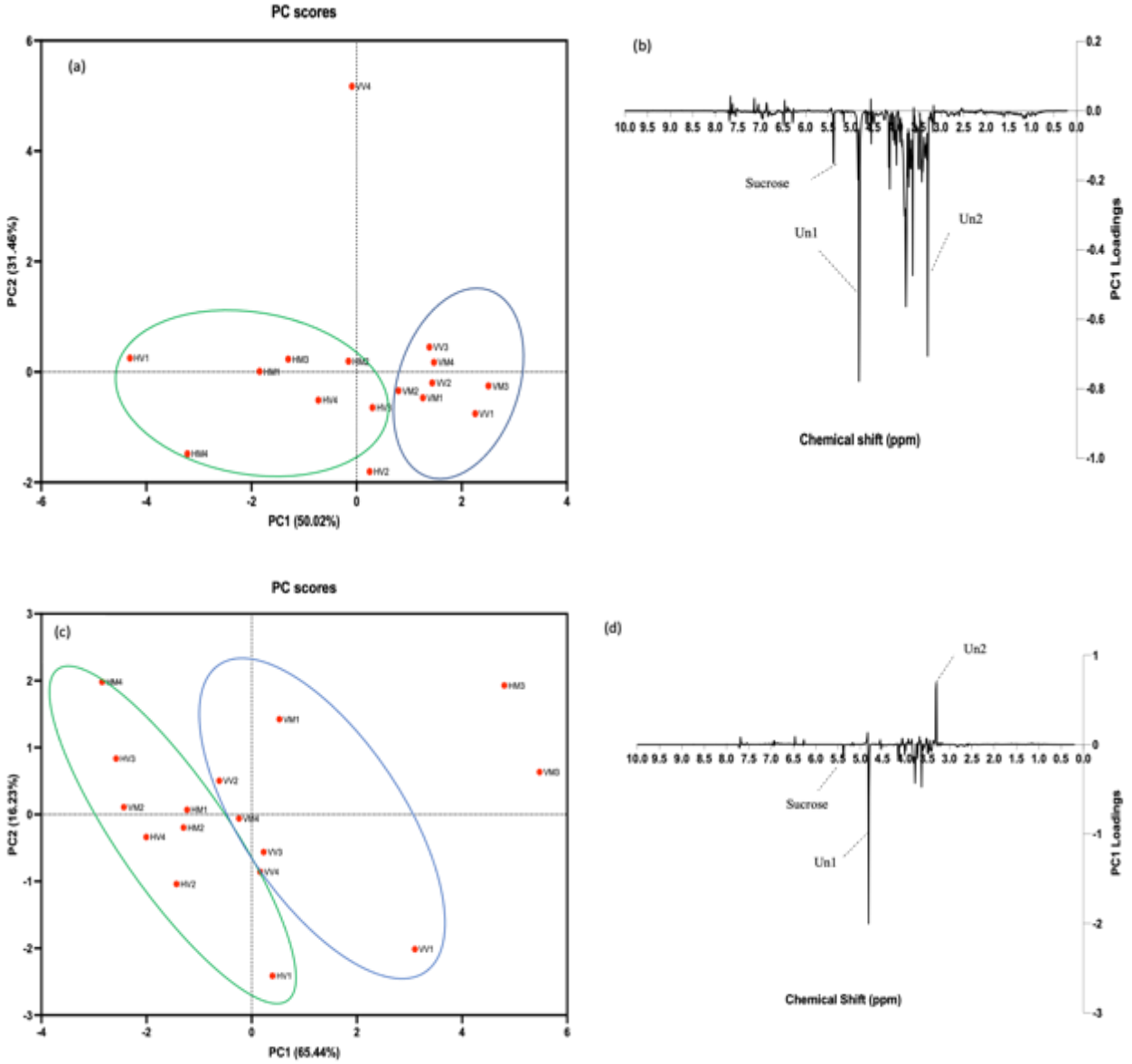

Figure 27. PCA scores scatter plot and loadings plot obtained considering the whole spectra of grapevine leaf extracts collected at verasion and harvest in 2020**,** (a) Mars scatter plot (b) Mars PC1 loadings plot (c) Canadice scatter plot (d) Canadice PC1 loadings plot. Veraison samples (VV 1-4 from VSP; VM 1-4 from M) and harvest samples (HV 1-4 from VSP; HM 1-4 from M).

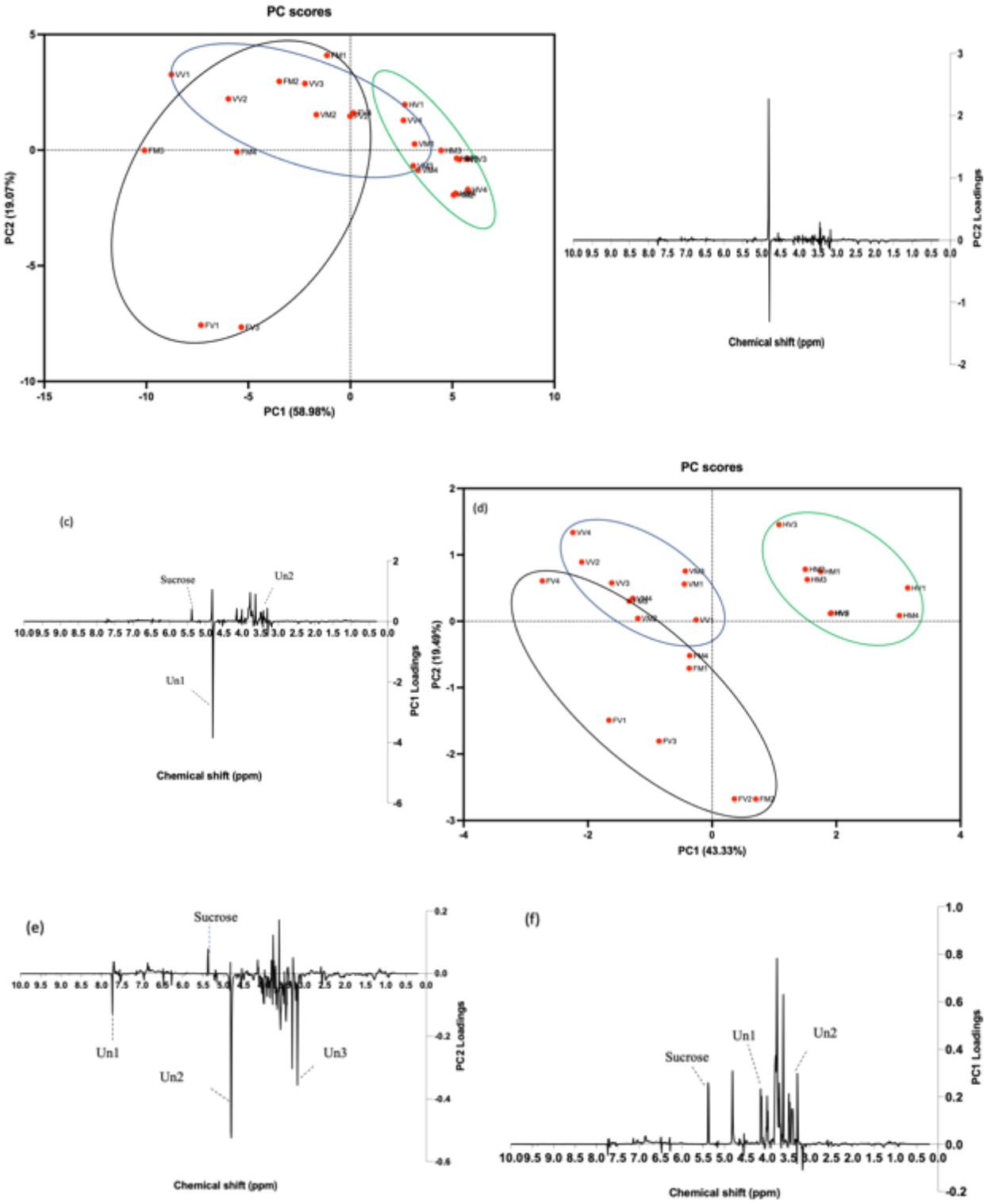

Figure 28. PCA scores scatter plot and loadings plot of phenological stages of grapevine leaf extracts collected during flowering, verasion and harvest in 2021, (a) Mars scatter plot (b) Mars PC2 loadings plot (c) Mars PC1 loadings plot (d) Canadice scatter plot (e) Canadice PC2 loadings plot (f) Canadice PC1 loadings plot. Flowering samples (FV 1-4 from VSP; FM 1-4 from M), veraison samples (VV 1-4 from VSP; VM 1-4 from M) and harvest samples (HV 1-4 from VSP; HM 1-4 from M).

During the 2021 growing season, PCA was applied to the 1D ^{1}H-NMR spectra of Mars and Canadice leaves growing on VSP and M training systems to investigate differences between the metabolic profiles of both grape varieties between training systems. A scores scatter plot of the first two PCs obtained considering the whole ^{1}H-NMR spectra (0.5-8.5 ppm) is shown in the (Fig. 28a and d) and shows clear separation of phenological stages along PC1 and PC2 for both grape varieties.

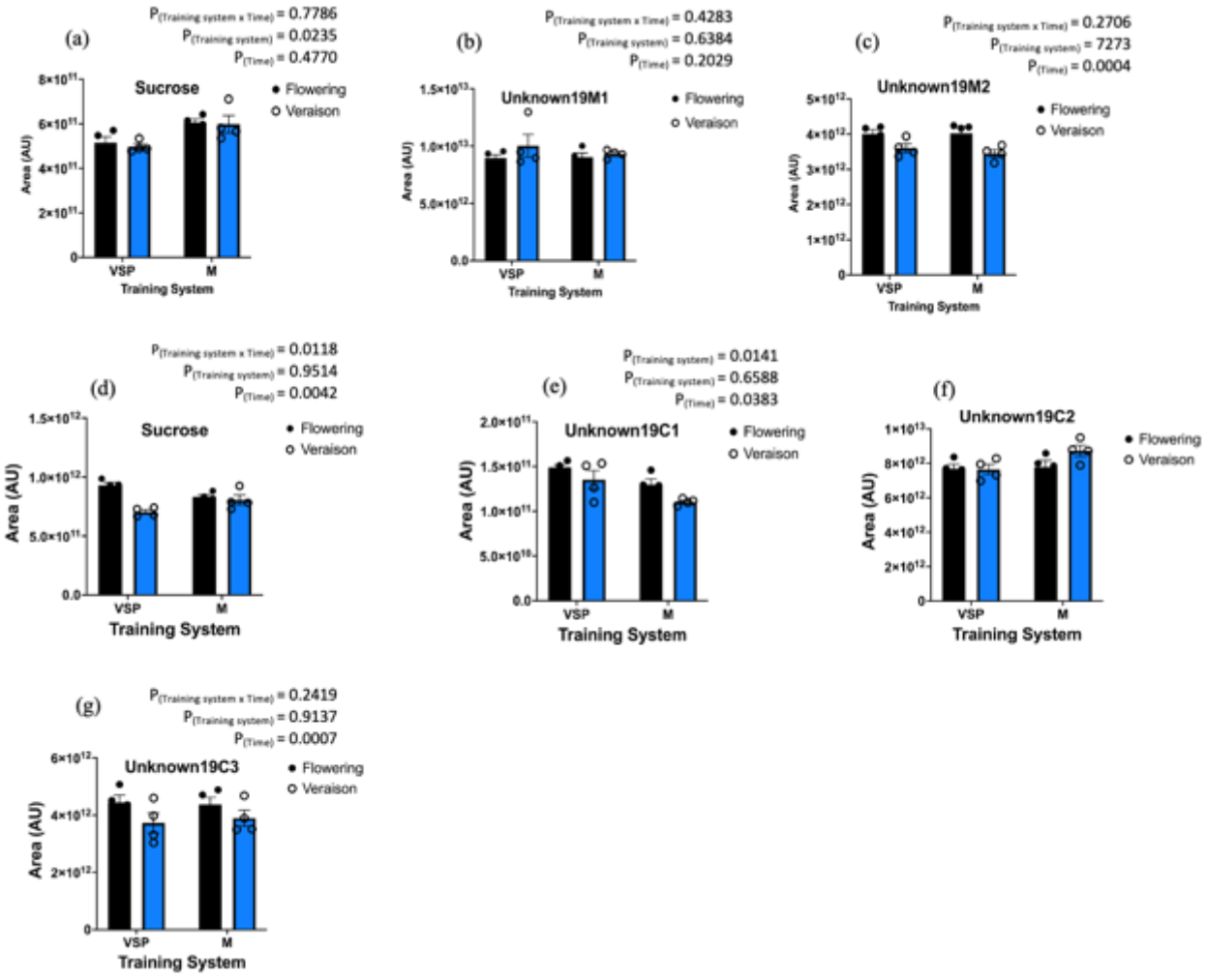

Figure 29. Bar graphs of metabolite concentrations in grapevine leaves during the 2019 growing season. Mars leaves (a) sucrose (b) unknown 1 (c) unknown 2; Canadice leaves (d) sucrose (e) unknown 1 (f) unknown 2 (g) unknown 3. Metabolites shown based on training systems during different phenological stages (flowering (black bar) and veraison (blue bar)). Bars show mean ± SEM; individual datapoints are also shown (two-way repeated measures ANOVA with Tukey's multiple comparison, $P<0.05$)

The veraison samples lay towards positive PC1 values and harvest samples lay towards negative PC1 values in the scores plot in both grapevine varieties growing in VSP and M training systems. There was no separation based on training systems. The flowering and verasion samples lay towards negative PC1 values and harvest samples towards positive PC2 values. Thus, the corresponding PC2 and PC1 loadings plot (Fig. 28b, c, e, and f) shows that the visibly discriminating signals lie mainly in the sugar region, showing sucrose and three unassigned compounds in both grapevine varieties. In Mars there was an overlap between flowering and veraison samples, with harvest samples being separated. In Canadice, all three phenological stages were clearly separated.

Metabolite changes in grapevine leaves: The signals highlighted by PCA analysis in grapevine leaves were integrated using AMIX software. The average amount of each discriminant metabolite detected in 2019, 2020 and 2021 is presented in Figs. 29, 30 and 31, respectively. In total 4 metabolites were identified including sucrose and three unknown compounds. During the 2019 season, in Mars there was a significant effect of training system on sucrose ($P = 0.0235$); (Fig. 29a), having higher sucrose in Munson training system compared to VSP during both flowering and veraison. There was a significant effect of time on unknown metabolite 2 ($P = 0.0004$) (Fig. 29c). In Canadice there was a significant interaction effect of training system x time on sucrose ($P = 0.0118$); VSP-trained Canadice had higher sucrose than M-trained Canadice during flowering and higher sucrose in M-trained Canadice than VSP-trained Canadice during veraison (Fig. 29d). There was a significant effect of training system on unknown metabolite 1 ($P =0.0141$) (Fig. 29e), with higher amounts in VSP compared to M in Canadice during both flowering and veraison.

There was also a significant effect of time on sucrose (P = 0.0042), unknown metabolite 1 (P = 0.0383), and unknown metabolite 3 (P = 0.0007).

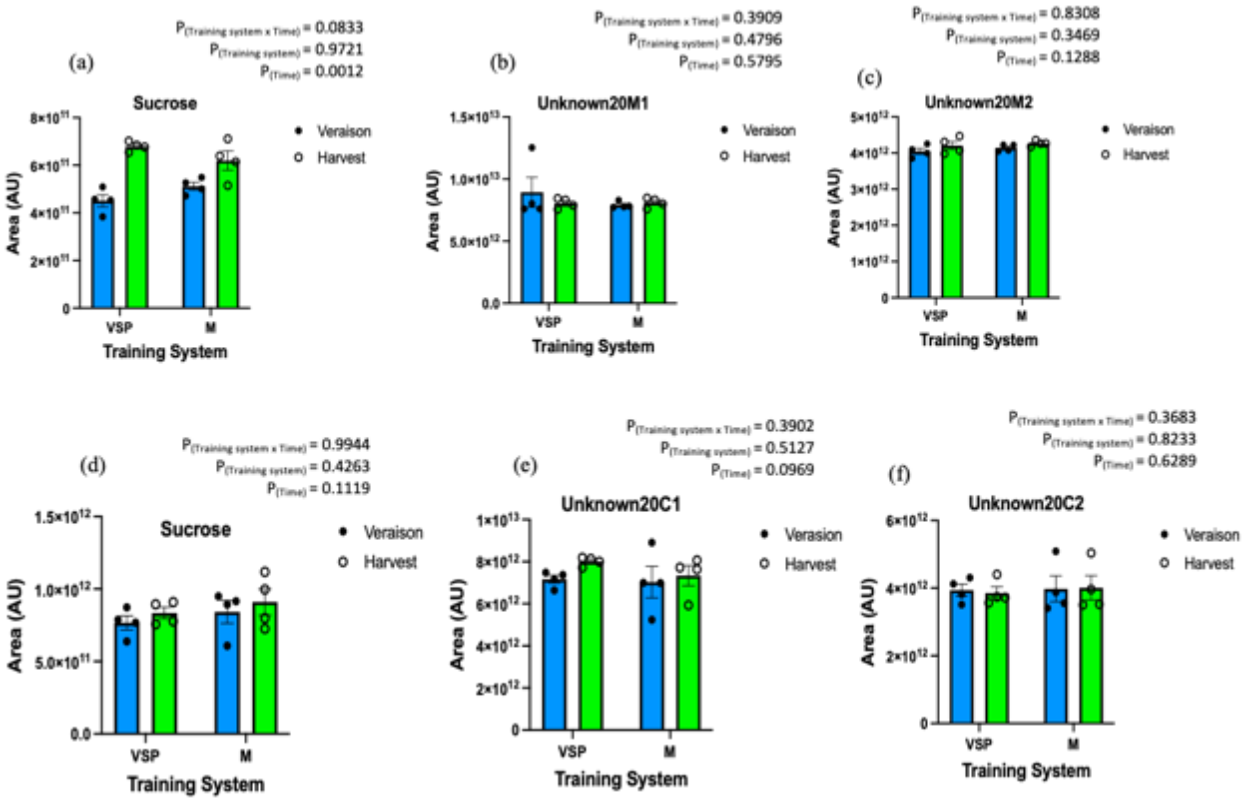

Figure 30. Metabolites amounts in grapevine leaves during the 2020 growing season. Mars leaves (a) sucrose (b) unknown 1 (c) unknown 2; Canadice leaves (d) sucrose (e) unknown 1 (f) unknown 2. Metabolites are shown based on training systems during different phenological stages (veraison (blue bar) and harvest (green bar)). Bars shown mean ± SEM; individual datapoints are also shown (two-way repeated measures ANOVA with Tukey's multiple comparison, *P<0.05).*

During the 2020 season, in Mars there was a significant effect of time on sucrose (P = 0.0012) (Fig. 30a). The sucrose was higher in harvest samples compared to veraison samples.

During the 2021 season, in Mars there was a significant interaction effect of training system x time on unknown metabolite 1 (P = 0.0086); VSP-trained Mars had higher unknown metabolite 1 during veraison than M-trained Mars and M-trained Mars had higher unknown 1 than VSP-trained Mars during flowering (Fig. 31b). There was a significant effect of training

system on unknown metabolite 2 (P = 0.0208) (Fig.31c), with higher amounts in M compared to VSP during all three timepoints.

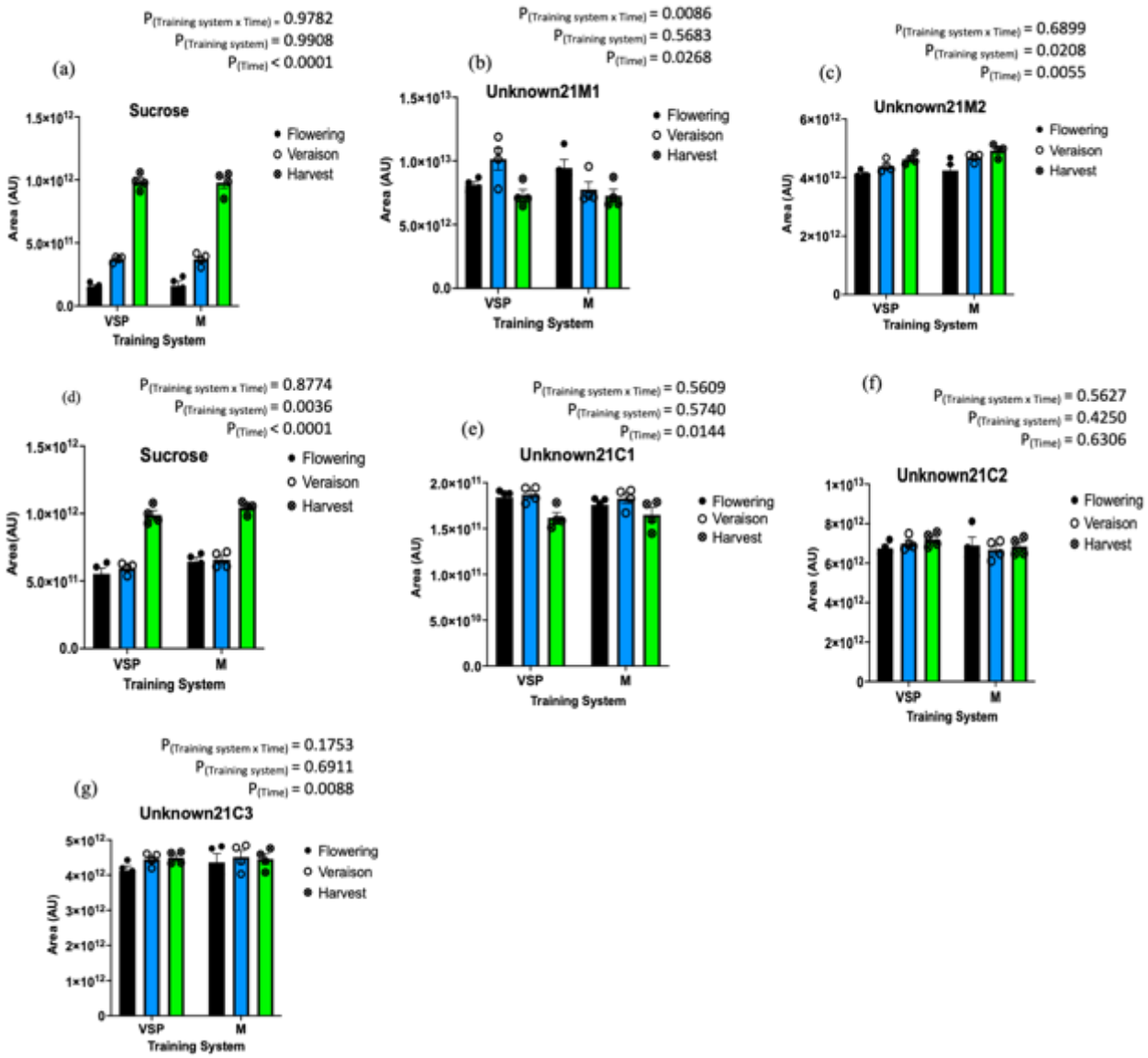

Figure 31. Metabolites amounts in grapevine leaves during the 2021 growing season. Mars leaves (a) sucrose (b) unknown 1 (c) unknown 2; Canadice leaves (d) sucrose (f) unknown 1 (g) unknown 2 (d) unknown 3. Metabolites are shown based on training systems during different phenological stages (flowering (black bar), veraison (blue bar), and harvest (green bar)). Bars show mean ± SEM; individual data points are also shown (two-way repeated measures ANOVA with Tukey's multiple comparison, P<0.05.

There was also a significant effect of time on sucrose (P < 0.0001), unknown metabolites 1 (P = 0.0268) and 2 (P = 0.0055) (Fig. 31a, b, and c). In Canadice there was a significant

effect of training system on sucrose (P = 0.0036) (Fig. 31d), with a higher amount in M compared to VSP in the harvest samples.There was a significant effect of time on sucrose (P < 0.0001), unknown metabolites 1 (P = 0.0144) and 3 (P = 0.0088) (Fig. 31d, e, and g). The sucrose showed a gradual increase from flowering, veraison and harvest, being highest in harvest samples in both grapevine varieties (Fig. 31a and d).

2.3.2.3 Grape juice metabolomic analysis of Mars and Canadice growing on VSP and Munson training systems

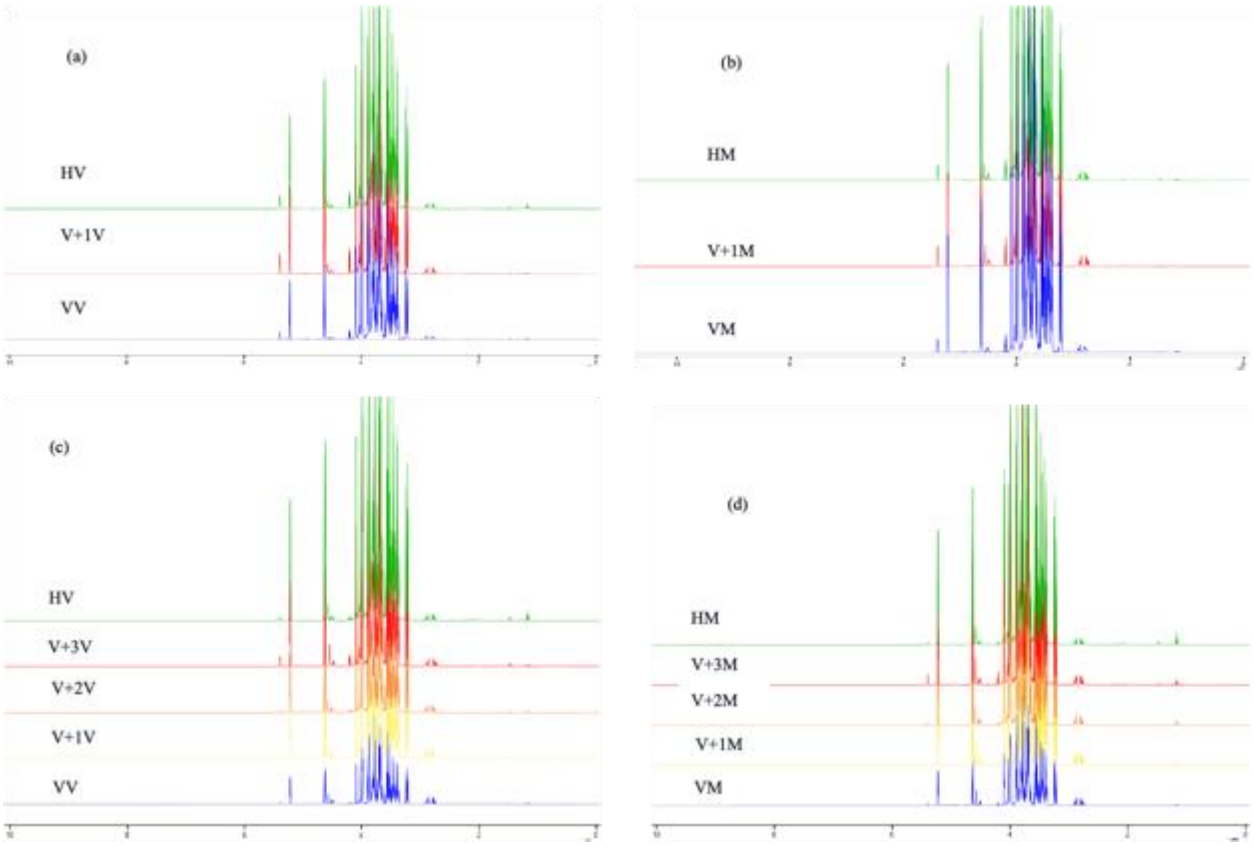

Figure 32. Typical 1D ^{1}H-NMR spectra of grape juice time course in 2019 showing different timepoints from version to harvest between training systems. (a) Canadice growing on VSP training system (veraison (VV), veraison week 2 (V+1V), and harvest (HV); (b) Canadice growing on M training system (veraison (VM), veraison week 2 (V+1M), and harvest (HM); (c) Mars growing on VSP training system (veraison (VV), veraison week 2 (V+1V), version week 3 (V+2V), veraison week 4 (V+3V),and harvest (HV); (d) Mars growing on M training system (veraison (VM), veraison week 2 (V+1M), version week 3 (V+2M), veraison week 4 (V+3M),and harvest (HM).

Representative ^{1}H-NMR spectra of Mars and Canadice grape juice from grapes collected from veraison to harvest are shown in (Figure. 32 and 33a-d). The spectra of Mars and Canadice juice from grapes growing on VSP and M training systems were visually very similar.

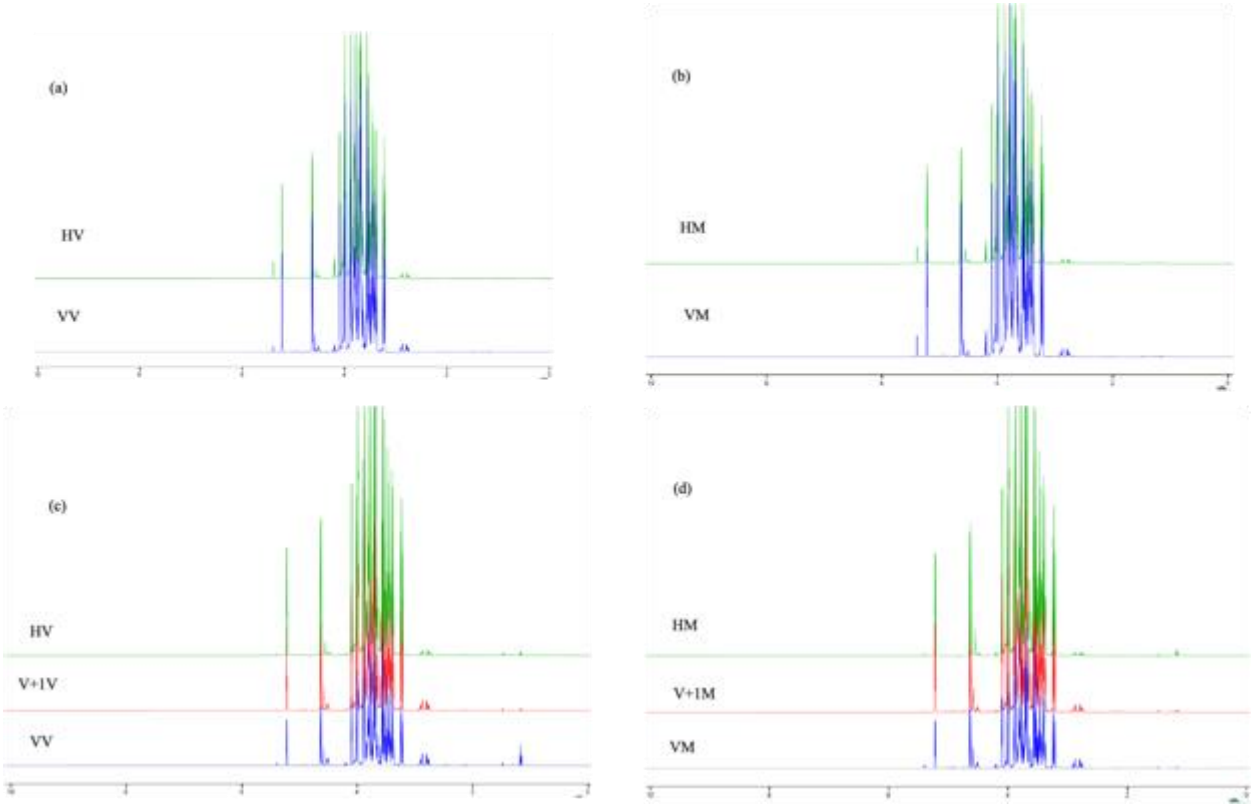

Figure 33. Typical 1D ^{1}H-NMR spectra of grape juice time course in 2020 showing different time points from veraison to harvest. (a) Canadice s growing on VSP training system (veraison (VV) and harvest (HV); (b) Canadice growing on M training system (veraison (VM) and harvest (HM); (c) Mars growing on VSP training system (veraison (VV), veraison week 2 (V+1V), and harvest (HV); (d) Mars growing on M training system (veraison (VM), veraison week 2 (V+1M), and harvest (HM).

The spectral profile expanded the aliphatic (0.5-3.2 ppm), sugars (3.2-6.0 ppm), and aromatic (6.0-8.0 ppm) regions (Fig 34 and 35a-d). The expansions of the lower intensity aliphatic (0.5-3.2 ppm) regions have better visible spectral profiles in (Fig. 34b and d; 35b and d). The major signals in the spectra of grapevine juice were identified and are listed in Table 4. In total 22 metabolites were identified, including amino acids (alanine, arginine, asparagine,

aspartate, glutamate, glutamine, histidine, isoleucine, leucine, phenylalanine, proline, threonine, tyrosine, and valine), sugars (glucose, fructose, and sucrose), salt or ester form of keto acids (levulinate), alcohol (ethanol), and other small molecules (3-hydroxybutyrate, 4-aminobutyrate [GABA], and *myo*-inositol) as well as signals arising from polyphenols.

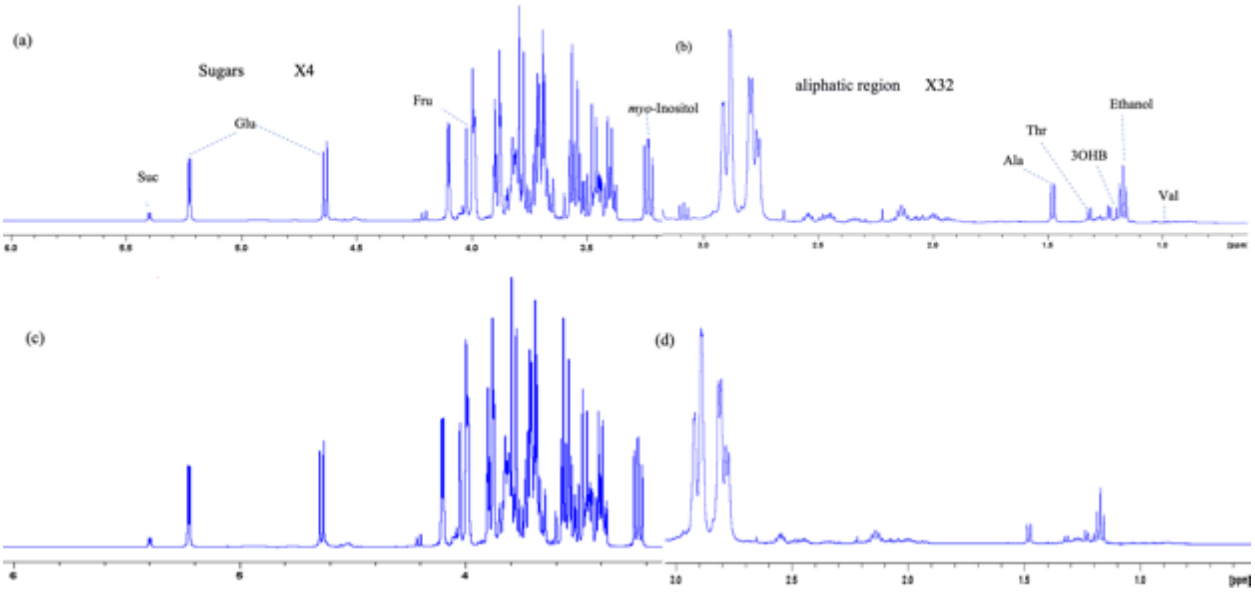

Figure 34. Typical ^{1}H NMR spectra of grape juice**,** with enlargements of the sugar (3.2-6.0 ppm) and aliphatic (0.5–3.2 ppm) regions. Canadice growing on VSP training system (a) Sugars (3.2-6.0 ppm) (b) aliphatic (0.5-3.2 ppm) regions. Canadice growing on M training system (c) sugar (3.2-6.0 ppm) and (d) aliphatic (0.5-3.2 ppm) regions.

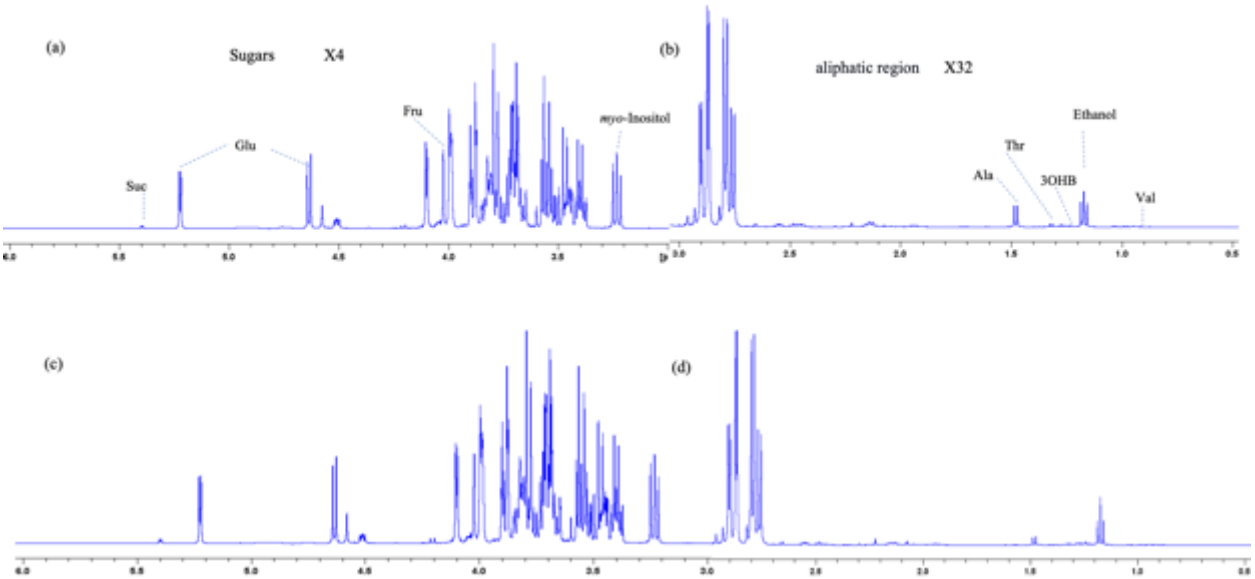

Figure 35. Typical ^{1}H NMR spectra of grape juice, with enlargements of the sugar (3.2-6.0 ppm) and aliphatic (0.5–3.2 ppm) regions. Mars growing on VSP training system (a) Sugars (3.2-6.0 ppm) (b) aliphatic (0.5-3.2 ppm) regions. Mars growing on M training system (c) sugar (3.2-6.0 ppm) and (d) aliphatic (0.5-3.2 ppm) regions.

Table 4. Metabolites observed in proton nuclear magnetic resonance spectra of Canadice and Mars grapevine juice.

Assignment	**$\delta_{H\ ppm}$[b] (Multiplicity/J Hz)**
3-Hydroxybutyrate	**1.23** (d/6.4), 2.47 (m), 4.20 (td)
4-Aminobutyrate	1.92 (m), 2.42 (t), 3.04 (dt)
Alanine	**1.48** (d/7.2), 3.78 (q)
Arginine	1.64 (m), 1.72 (m), 1.91 (m), 3.24 (t), 3.77 (t)
Asparagine	2.78 (dd), 2.90 (dd), 3.99 (dd), 6.90 (br)
Aspartate	2.75 (dd), 2.85 (dd), 3.93 (dd)
Ethanol	**1.17** (t/7.1), 3.65 (q)
Fructose	3.55 (d), 3.58 (m), 3.68 (m), 3.69 (d), 3.72 (d), 3.79 (m), 3.81 (m), 3.89 (m), 3.99 (m), 4.01 (m), **4.10** (d)
Glucose	3.23 (dd), 3.40 (m), 3.46 (m), 3.48 (t), 3.53 (dd), 3.71 (t), 3.72 (dd), 3.74 (m), 3.83 (m), 3.89 (dd), 4.64 (d), **5.23**(d/3.7)
Glutamate	2.08 (m), 2.13 (m), 2.47 (m), 2.5 (m), 3.78 (t)
Glutamine	2.14 (m), 2.43 (m), 2.47 (m), 3.78 (t), 6.89 (s)
Histidine	3.33 (dd), 3.36 (t), 4.03 (t), 7.39 (s), 8.66 (s)
Isoleucine	0.91 (t), 0.98 (d), 1.25 (m), 1.46 (m), 1.97 (m), 3.67 (d)
Leucine	**0.95** (m), 0.96 (m), 1.70 (m), 3.74 (m)
Levulinate	2.22 (s), 2.54 (t), 2.84 (t)
myo-Inositol	3.12 (dd), 3.28 (dd), 4.00 (t), 7.32 (d), 7.36 (m), 7.42 (m)
Phenylalanine	3.1(m), 3.3(m), 4.0(m), 7.4(m)
Proline	2.01 (m), 2.06 (m), 2.35 (m), 3.33 (m), 3.41 (m), 4.13 (dd)
Sucrose	3.46, (t), 3.55 (dd), 3.67 (s), 3.75 (t), 3.80 (m), 3.82 (m), 3.88 (m), 4.04 (t), 4.21 (d), **5.40** (d/3.9)
Threonine	**1.32** (d/6.6), 3.58 (d), 4.25 (m)
Tyrosine	3.03 (dd), 3.20 (dd), 3.94 (t), 6.89 (d), 7.18 (d)
Valine	**0.98** (dd/7.1), 1.03 (d), 2.26 (m), 3.61 (d)

[b] Chemical shifts of spin systems in bold refer to the isolated signals used to integrate spectra. Spin multiplicity designations: s = singlet, d = doublet, t = triplet, dd = doublet of doublets, td = triplet of doublets, br = broad, and m = multiplet.

PCA was applied to ^{1}H-NMR spectra of Mars and Canadice juice samples from grapes growing on VSP and M training systems in order to investigate differences between the metabolic profiles of time course of both grape varieties and to detect main peaks responsible for those differences. A scores scatter plot of the first two PCs obtained considering the whole ^{1}H-NMR spectra (0.0-10.0 ppm) is shown in the (Fig. 36 and 37a and c) and shows clear separation of phenological stages along PC1 and PC2 for Mars and Canadice in 2019

and 2020 growing seasons. But there was no separation based on training systems was noticed.

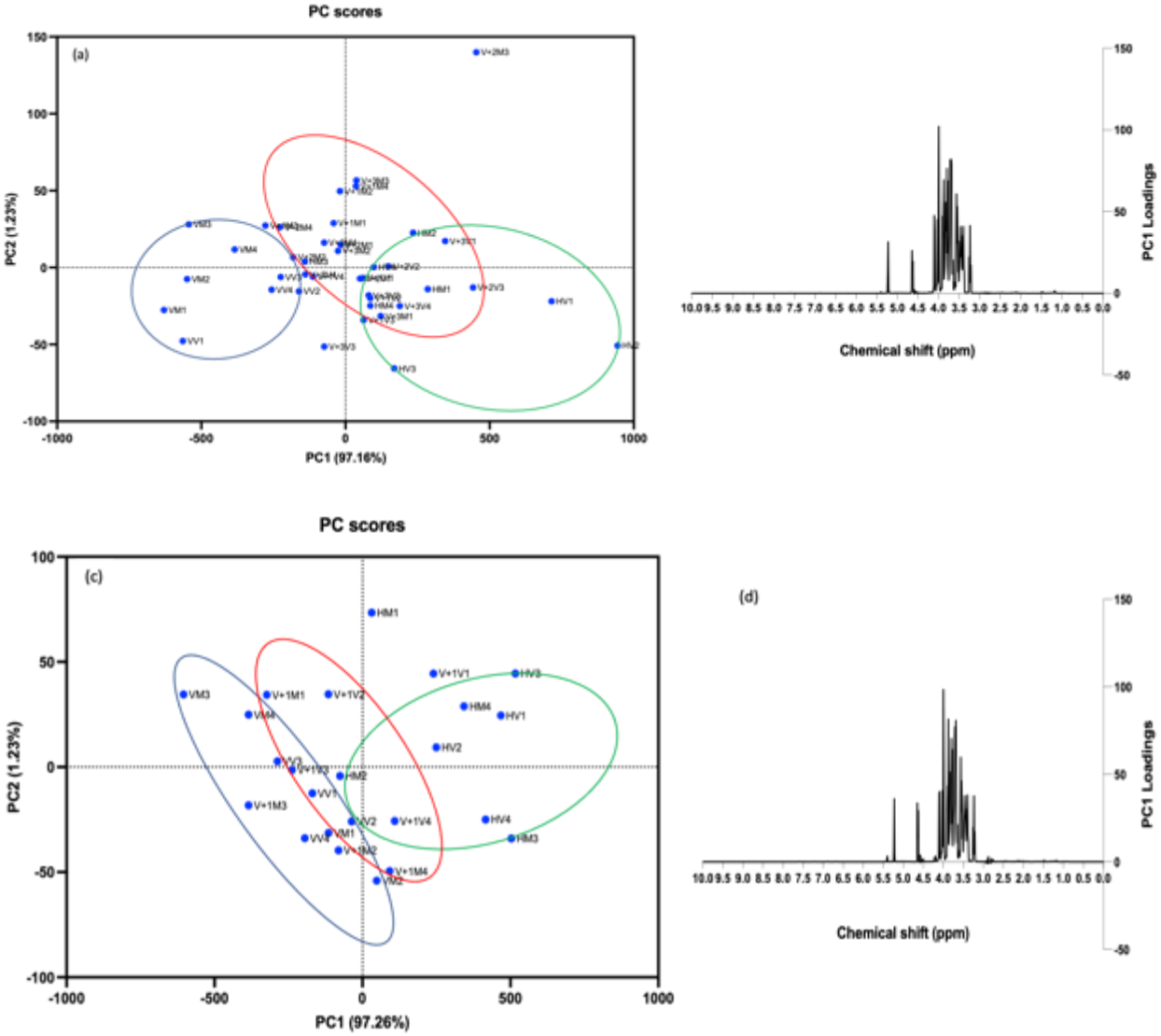

Figure 36. PCA scores scatter plot and loadings plot of grape juice from veraison to harvest in 2019 considering the whole spectra. (a) Mars scores scatter plot (b) Mars PC1 loadings plot (c) Canadice scores scatter plot (d) Canadice PC1 loadings plot. Labels for Canadice samples growing on VSP training system (veraison (VV), veraison week 2 (V+1V), and harvest (HV); growing on M training system (veraison (VM), veraison week 2 (V+1M), and harvest (HM); Mars samples growing on VSP training system (veraison (VV), veraison week 2 (V+1V), version week 3 (V+2V), veraison week 4 (V+3V),and harvest (HV); growing on M training system (veraison (VM), veraison week 2 (V+1M), version week 3 (V+2M), veraison week 4 (V+3M),and harvest (HM).

The metabolites contributing to the separation of phenological stages along PC1 and PC2 can be distinguished in the loadings plot, (Fig. 36 and 37b and d) together with visual inspection

of the spectra. The reason behind is the samples position in each direction in the scores plot is determined by the metabolites lying the same direction in the loadings plot.

During the 2019 and 2020 growing season, in Mars and Canadice, time course samples lay towards negative PC1 values and harvest samples lay towards positive PC1 values in the scores plot without any difference between training systems (Fig. 36a and c, 37a). However, in 2020 season the Canadice, veraison samples lay towards negative PC2 values and harvest samples lay towards positive PC2 values without any difference between training systems (Fig. 37c). Thus, the corresponding PC1and PC2 loadings plots (Fig. 36 & 37b and d) shows that the visibly discriminating signals lie mainly in the sugar region, indicating an increase of sugars in grape juice at harvest compared to juice of grapes collected earlier in the season. In Mars there was clear separation of veraison samples but overlap between the following week of veraison and harvest samples. An outlier of two second week veraison samples was also noticed (Fig. 36a). In Canadice there was an overlap between veraison and first week after version samples, also an overlap between after first week veraison and harvest samples. There was one outlier from after week 1 verasion and harvest samples, respectively (Fig. 36c). In Mars there was a clear separation between veraison and harvest samples. The after week veraison samples overlaps with veraison and harvest samples with one outlier from veraison and harvest samples, respectively (Fig.37a). In Canadice there was a clear separation between veraison and harvest samples. An outlier of harvest samples was noticed (Fig. 37c).

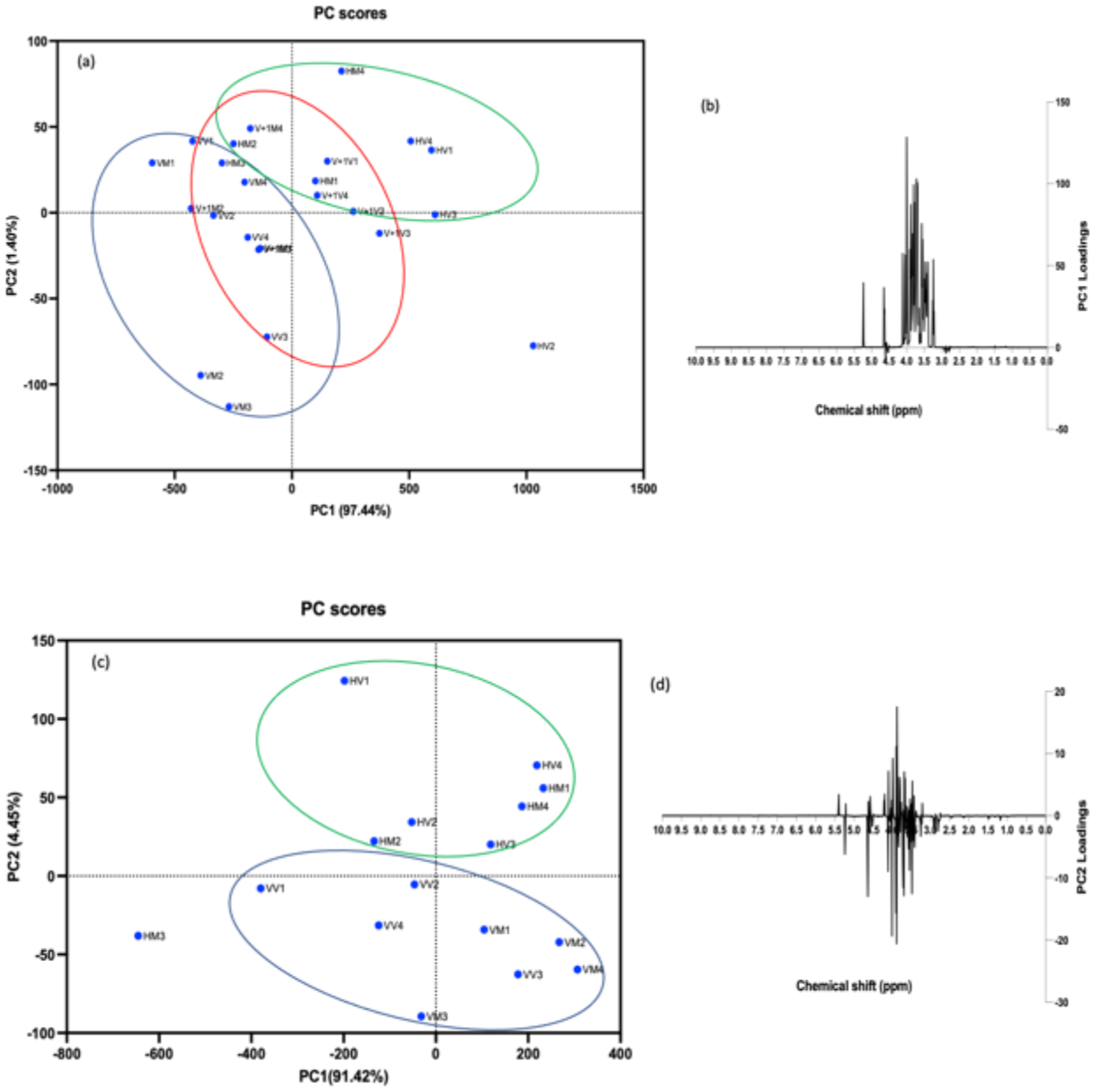

Figure 37. PCA scores scatter plot and loadings plot of time course; veraison to harvest and separation based on training systems; vertical shoot positioning (VSP) and Munson ((M) training systems in 2020 growing season obtained considering the whole spectra (juice from ten berries per plant). (a) Mars scores scatter plot (b) Mars PC1 loadings plot (c) Canadice scores scatter plot (d) Canadice PC2 loadings plot. Labels for time course Canadice samples growing on VSP training system (veraison (VV) and harvest (HV); growing on M training system (veraison (VM) and harvest (HM); for Mars growing on VSP training system (veraison (VV), veraison week 2 (V+1V), and harvest (HV); growing on M training system (veraison (VM), veraison week 2 (V+1M), and harvest (HM).

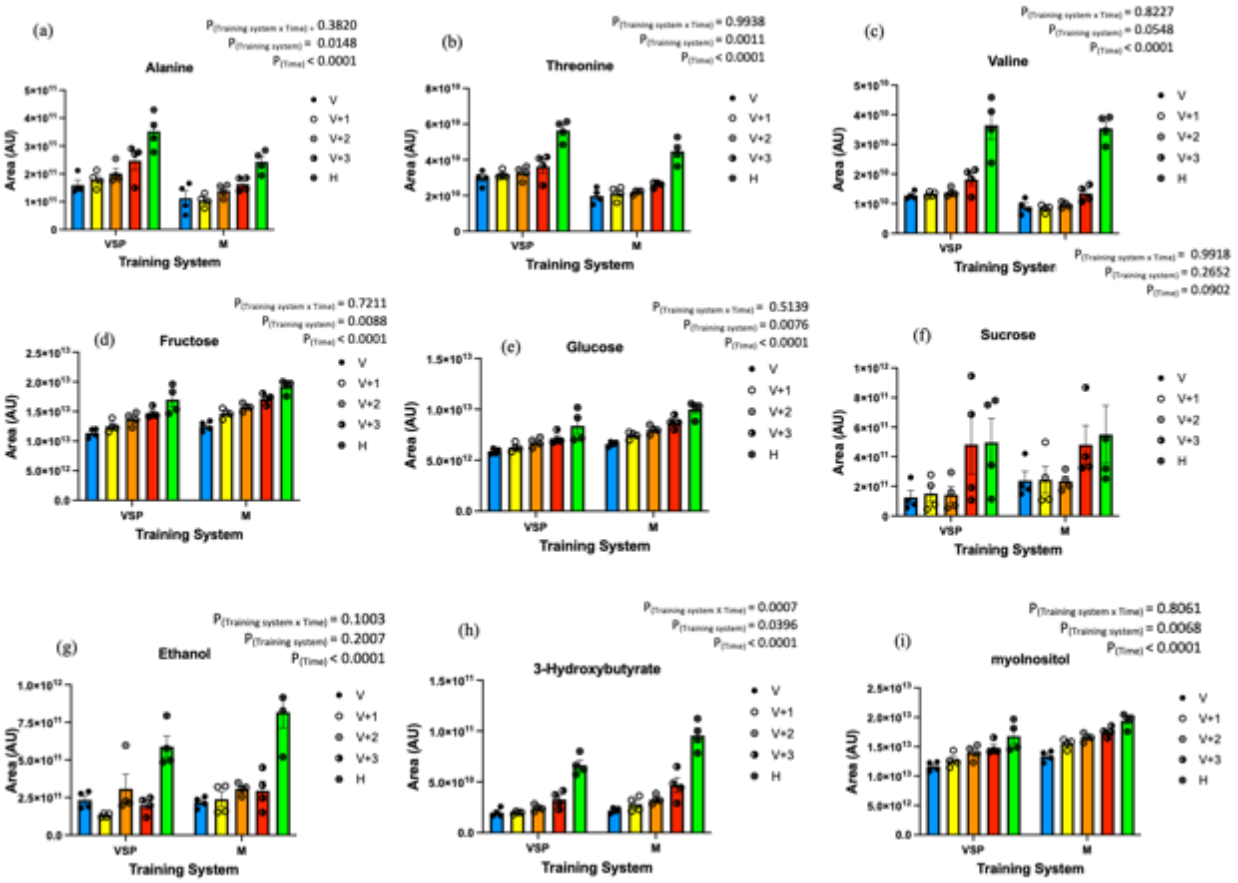

Figure 38. Metabolite amounts in Mars grapevine time course (veraison to harvest) during 2019 growing season. Metabolites shown based on training systems during time course (veraison to harvest). (a) alanine (b) threonine (c) valine (d) fructose (e) glucose (f) sucrose (g) ethanol (h) 3-hydroxybutyrate (i) *myo*-inositol. Bars shown mean ± SEM; individual datapoints are also shown (two-way repeated measures ANOVA with Tukey's multiple comparison, $P<0.05$). Blue bars represent veraison samples, green bars represent harvest samples and yellow, orange, and red bars represent subsequent week veraison samples.

Metabolite changes in grape juice: All the compounds identified in grape juice with isolated signals visible in the spectra were integrated, and areas used as an indication of compound amount in the samples. The average amount of each metabolite is presented in Figures 38-41. Overall, the results indicate that there was an increase in the amount of most metabolites in Mars and Canadice during the time course from veraison to harvest in 2019 (Fig. 38 and 39a-i). During the 2019 growing season in Mars, there was a significant interaction effect of training system x time on 3-hydroxybutyrate ($P = 0.0007$); M-trained Mars had higher 3-hydroxybutyrate than VSP-trained Mars in the harvest samples (Fig. 38h).

There was a significant effect of training system on alanine (P = 0.0148), threonine (P = 0.0011), glucose (P = 0.0088), fructose (P = 0.0076), 3-hydroxybutyrate (P = 0.0396) and *myo*-inositol (P = 0.0068) (Fig. 38a, b, d, e and i). Alanine and threonine levels were higher in VSP compared to M. Fructose, glucose, 3-hydroxybutyrate, and *myo*-Inositol levels were higher in M compared to VSP. There was a significant effect of time on all metabolites (P < 0.0001) except on sucrose. In Canadice, there was a significant interaction effect of training system x time on ethanol; VSP-trained Canadice had higher ethanol than M-trained Canadice at harvest (Fig 39g). There was a significant effect of training system in alanine (P = 0.0365) (Fig. 39a), with alanine being higher in VSP compared to M. There was also a significant effect of time on alanine (P = 0.0009), threonine (P = 0.0007), valine (P < 0.0001), fructose (P < 0.0001), glucose (P < 0.0001), ethanol (P = 0.0014), 3-hyrdoxybutyrate (P < 0.0001) and *myo*-inositol (P < 0.0001) (Fig. 38a, b, c, d, e, g, h, and i) in Canadice. All the above metabolites were higher in the harvest samples compared to veraison and the following week after veraison samples.

During the 2020 growing season, most of the metabolites increased during the time course (Fig. 40 and 41a-i). In Mars, there was a significant interaction effect of training system x time in fructose (P = 0.0018), glucose (P = 0.0023), and *myo*-inositol (P = 0.0071); VSP-trained Mars had higher fructose, glucose, and *myo*-inositol than VSP-trained Mars with gradual increase from veraison to harvest; (Fig. 40d, e, and i). There was a significant effect of training system on alanine (P = 0.0030), threonine (P= 0.0014), and valine (P= 0.0010) (Fig. 40a, b, and c), with all three metabolites being higher in VSP compared to M. There was also a significant effect of time on glucose, fructose, 3-hydroxybutyrate, and *myo*-

inositol (P < 0.0001) (Fig. 40d, e, h, and i). All four metabolites were higher in harvest samples when compared to the veraison and the following week after veraison samples. In Canadice, there was a significant effect of time on fructose (P= 0.0018), glucose (P = 0.0007), ethanol (P = 0.0093), 3-hydroxybutyrate (P = 0.0056), and *myo*-inositol (P = 0.0045) (Fig. 41d, e, g, h, and i). All the metabolites were higher in harvest samples compared to the veraison samples, except ethanol which was higher in veraison samples compared to harvest samples.

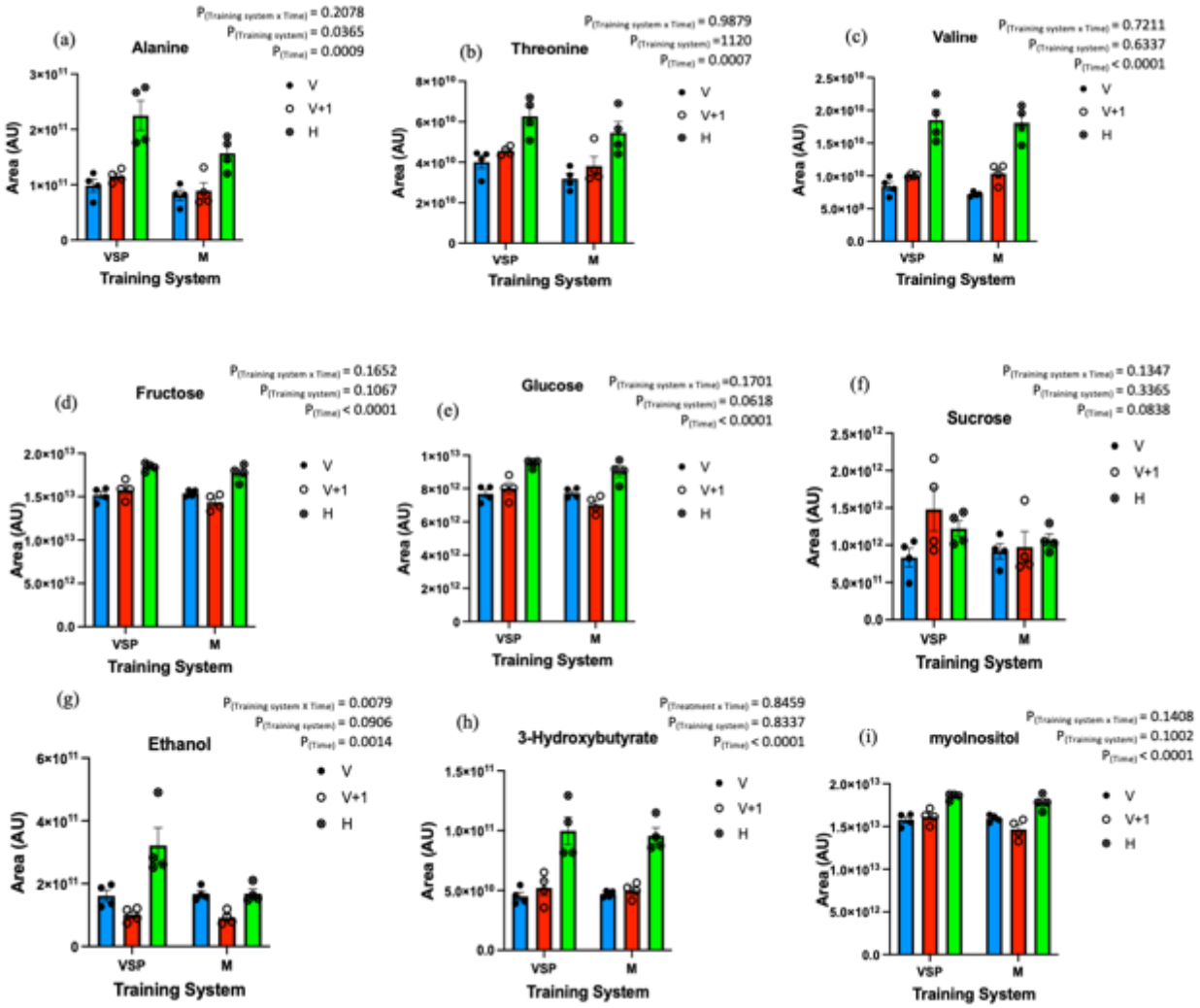

Figure 39. Metabolite amounts in Canadice grapevine time course (veraison to harvest) during 2019 growing season. Metabolites shown based on training systems during time course (veraison to harvest). (a) alanine (b) threonine (c) valine (d) fructose (e) glucose (f) sucrose (g) ethanol (h) 3-hydroxybutyrate (i) *myo*-inositol. Bar show mean ± SEM; individual data points are also shown (two-way repeated measures ANOVA with Tukey's multiple comparison, P<0.05). Blue bars represent veraison samples, green bars represent harvest samples, red bar represent subsequent week veraison samples.

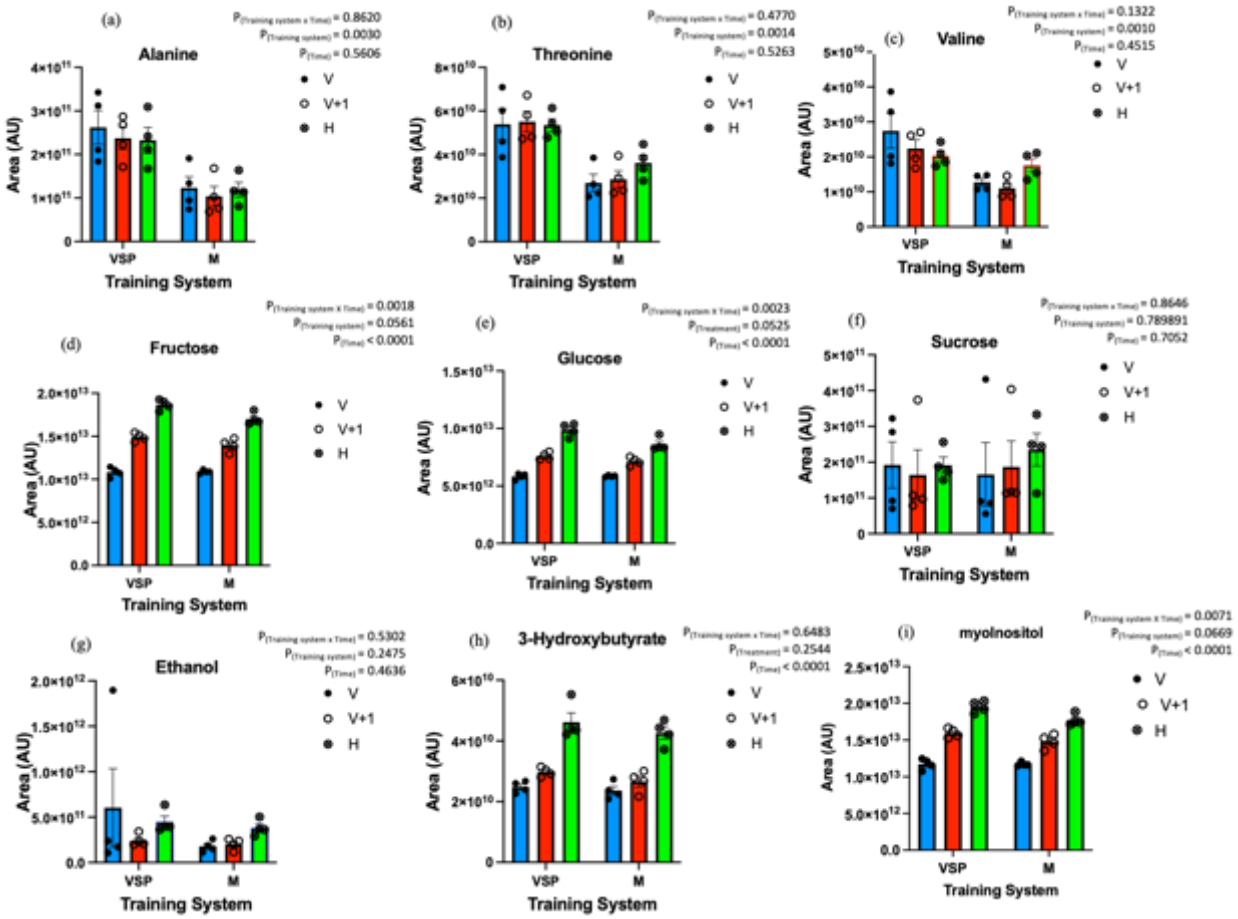

Figure 40. Metabolite amounts in Mars grapevine time course (veraison to harvest) during 2020 growing season. Metabolites shown based on training systems during time course (veraison to harvest). (a) alanine (b) threonine (c) valine (d) fructose (e) glucose (f) sucrose (g) ethanol (h) 3-hydroxybutyrate (i) *myo*-inositol. Bars show mean ± SEM; individual points are also shown (two-way repeated measures ANOVA with Tukey's multiple comparison, $P<0.05$). Blue bars represent veraison samples, green bars represent harvest samples, and red bar represent subsequent week veraison samples.

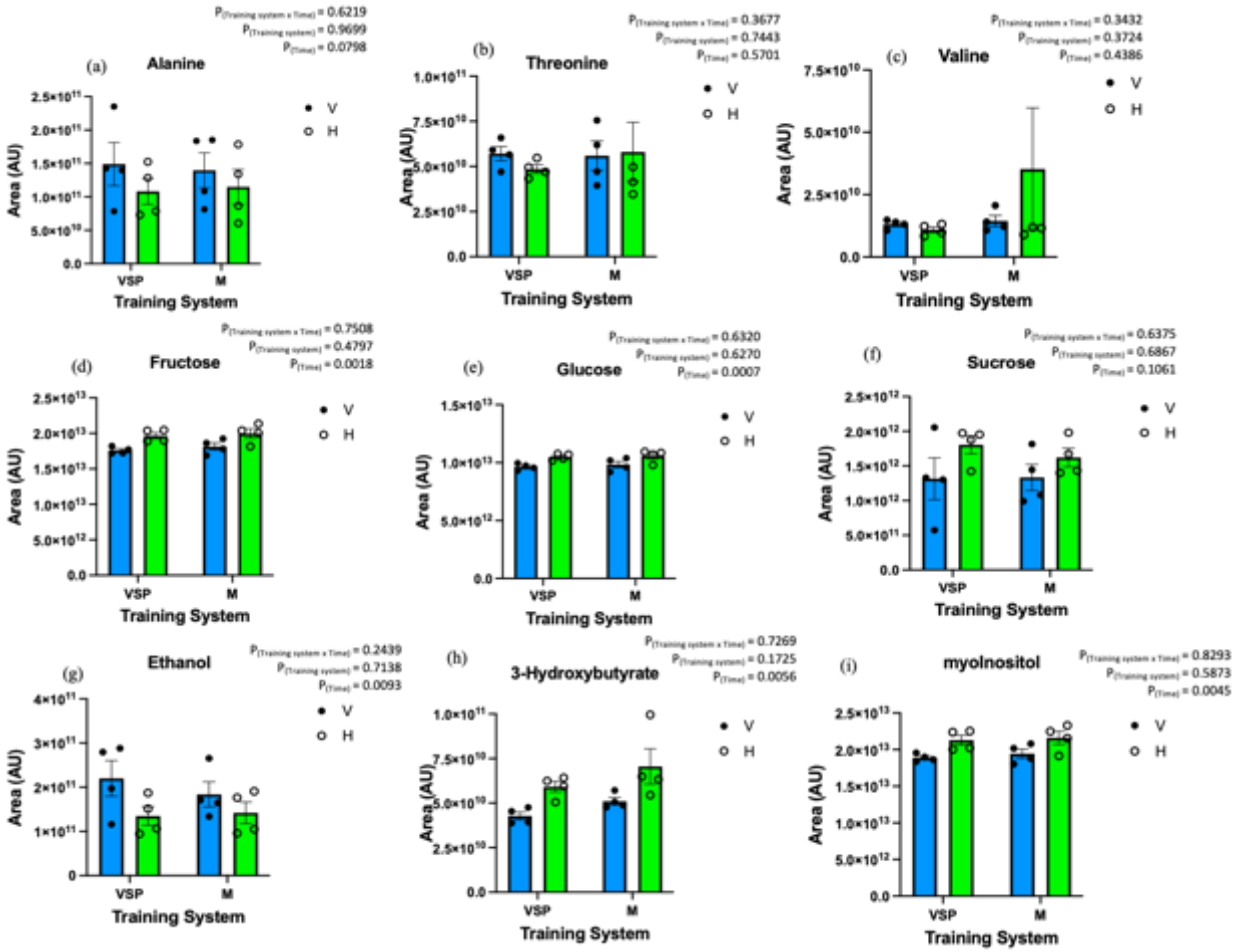

Figure 41. Metabolite amounts in Canadice grapevine time course (veraison to harvest) during 2020 growing season**.** Metabolites shown based on training systems during time course (veraison to harvest). (a) alanine (b) threonine (c) valine (d) fructose (e) glucose (f) sucrose (g) ethanol (h) 3-hydroxybutyrate (i) *myo*-inositol. Bars show mean ± SEM; individual datapoints are also shown (two-way repeated measures ANOVA with Tukey's multiple comparison, P<0.05). Blue bars represent version samples and green bars represent harvest samples.

2.3.2.4 Titratable acidity of Mars and Canadice growing on Munson and VSP training systems

At harvest, titratable acidity for Mars and Canadice was measured for 2019, 2020 and 2021 growing seasons (Fig. 42a and b). In Mars there was a significant effect of the training system on titratable acidity during the 2020 season (P = 0.0061), whereas there was no significant effect of training during the 2019 and 2021 growing seasons. In contrast, training

systems had no significant effect on titratable acidity for Canadice during all three growing seasons.

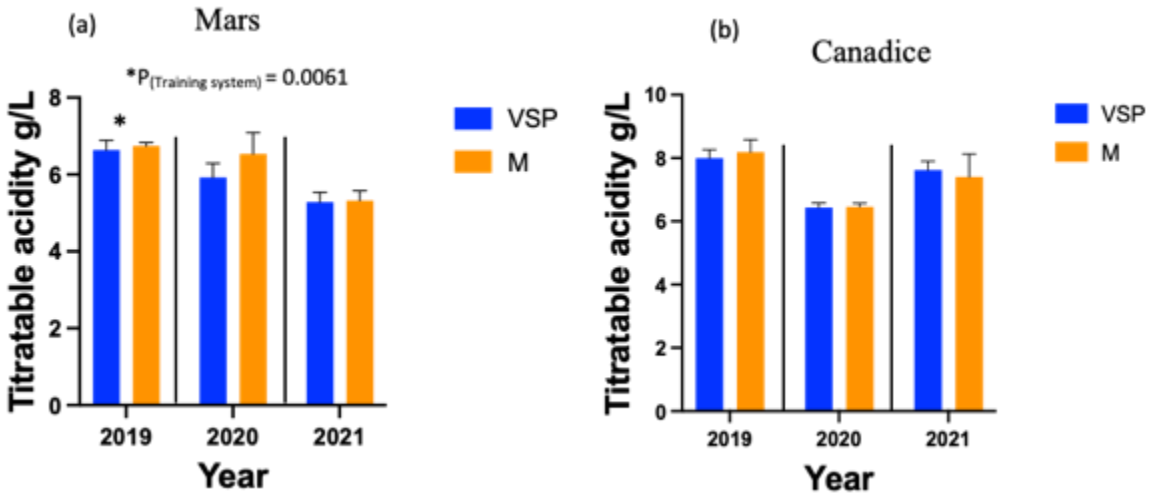

Figure 42. Titratable acidity at harvest were separately analyzed during 2019, 2020, 2021 seasons for grapes growing on vertical shoot positing or Munson training systems (a) Mars and (b) Canadice. Values shown are mean ± SEM (n=12) (t-test ($P < 0.05$). * represents the significant training system.

2.3.2.5 Total soluble solid content of Mars and Canadice growing on Munson and VSP training systems

At harvest, total soluble solids contents were measured for Mars and Canadice for 2019, 2020, and 2021 growing seasons (Fig. 43a and b). In Mars, there was a significant effect of the training system on total soluble solid contents during the 2019 growing season ($P < 0.0001$). In contrast, the training system had no significant effect on the total soluble solid contents during the 2020 and 2021 growing seasons. In Canadice, there was a significant effect of the training system on the total soluble solid contents during the 2021 growing season ($P = 0.014$). In contrast, there was no significant effect of the training system on total soluble solids during the 2019 and 2020 seasons.

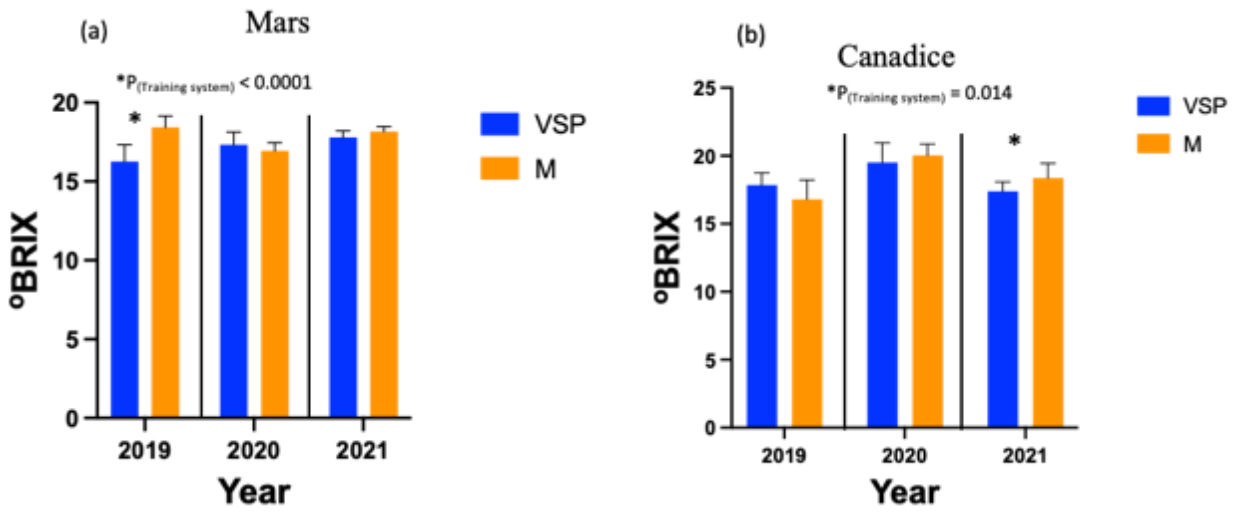

Figure 43. Total soluble solid contents at harvest were separately analyzed during 2019, 2020, 2021 seasons for grapes growing on vertical shoot positing or Munson training systems (a) Mars and (b) Canadice. Values shown are mean ± SEM (n=12) (t-test ($P<0.05$). * represents the significant training system.

2.3.2.6 Berry skin metabolome analysis of Mars and Canadice growing on Munson and VSP training systems

Typical chromatograms resulting from UPLC-MS analysis of methanolic extracts of Canadice and Mars skin samples are shown in Fig. 44. There were no obvious differences that could be visually observed between grape varieties and the training systems the grapevines are growing on. Thus, the UPLC-MS data were subjected to multivariate statistical analysis using PCA and PLS-DA to identify the potential biomarkers due to different training system.

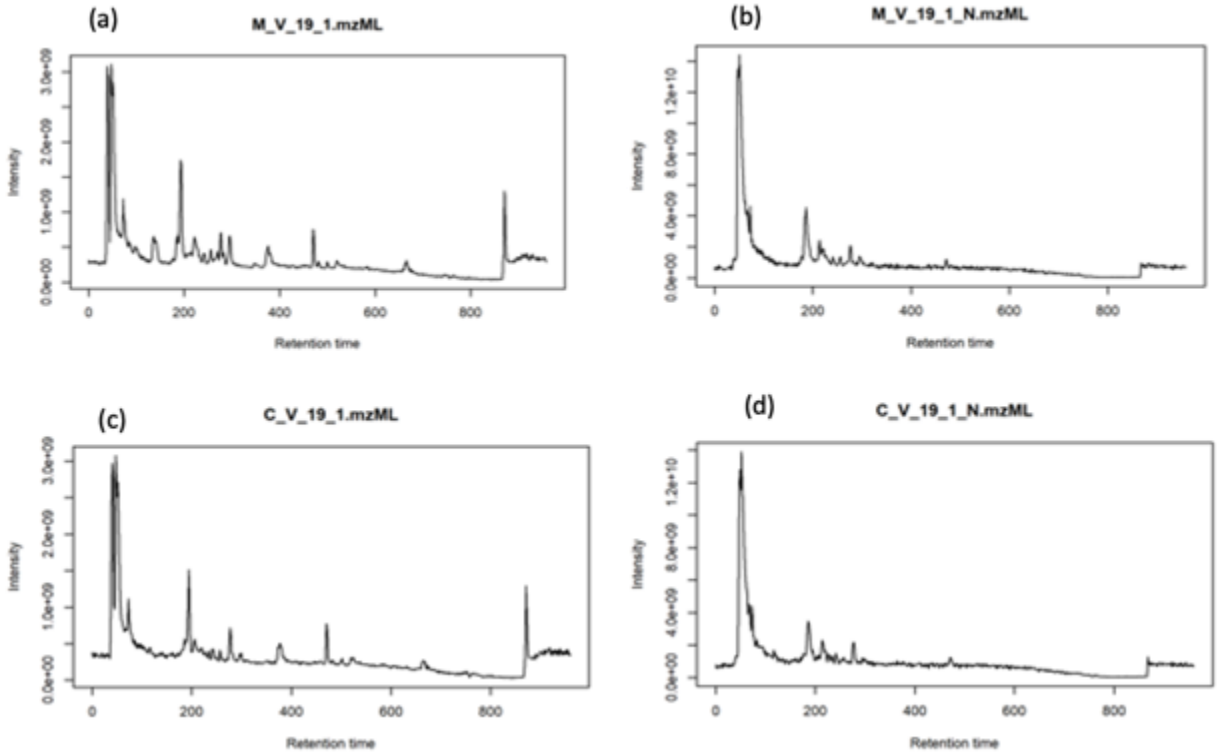

Figure 44. Representative of base peak intensity chromatograms of the (a) Mars skin sample for UPLC-MS positive ions mode; (b) Mars skin sample UPLC-MS for negative ions mode; (c) Canadice skin sample for UPLC-MS positive ions monde; (d) Canadice skin sample for UPLC-MS positive ions mode.

Principal components (PC) 1 and 2 were the best discriminating PCs, cumulatively accounting for 48.9% of total variance for Mars UPLC-MS positive ions mode and 47.5% for Mars UPLC-MS negative ions mode. The scores scatter plot resulting from the combination of these two PCs clearly showed the separation between training system (Fig. 45a and c). The VSP training system compounds grouped towards more positive values of PC2 while Munson training system compounds grouped towards negative values of PC2.

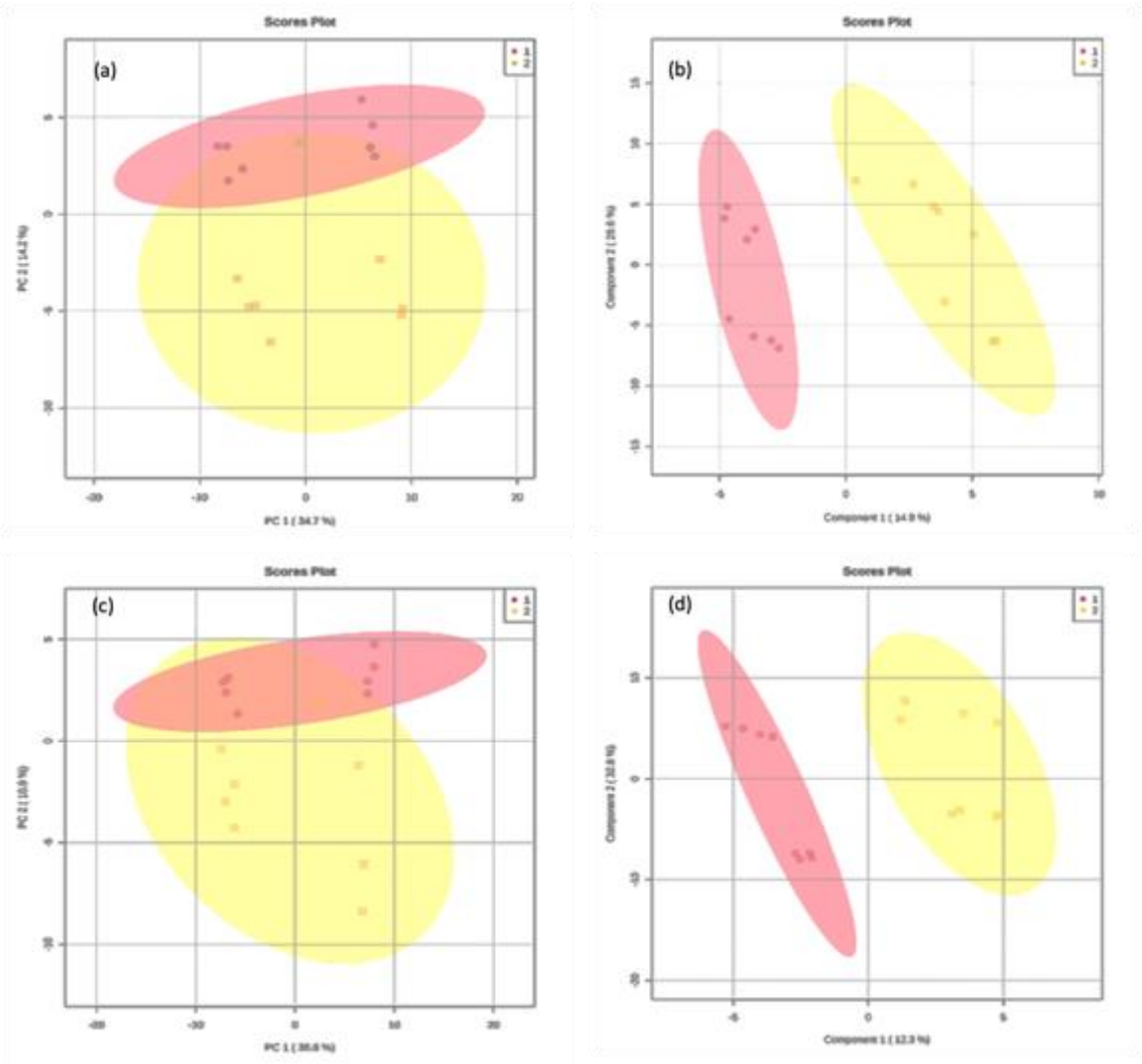

Figure 45. Mars skin metabolome separation based on training systems: VSP (red) and M (yellow**).** (a) PCA scores scatter plot for UPLC-MS negative ions mode; (b) PLS-DA scores scatter plot for UPLC-MS negative ions mode; (c) PCA scores scatter plot for UPLC-MS positive ions monde; (d) PLS-DA scores scatter plot for UPLC-MS positive ions mode.

Similarly, principal components (PC) 1 and 2 were the best discriminating PCs, cumulatively accounting for 48.7% for Canadice UPLC-MS positive ions mode, and 50.3% for Canadice UPLC-MS negative ions mode. For Canadice, PCA did not separate compounds between training system (VSP and M) and the groups mostly overlap. The scores scatter plot resulting from the combination of these two PCs clearly showed the separation between training system (Fig. 46a and c). PLS-DA was also performed as supervised method based on training

systems. Components 1 and 2 were the best for discriminating the compounds based on training systems, cumulatively accounting for 44.5% of total variance for Mars UPLC-MS positive ions mode and 45.1% for Mars UPLC-MS negative ions mode. The scores scatter plot resulting from the combination of these two components clearly showed the separation between training system (Fig 45b and d). The VSP training system compounds grouped towards more negative values of component 1 while Munson training system compounds grouped towards positive values of component 1. Similarly, components 1 and 2 were the best for discriminating the compounds based on training systems, cumulatively accounting for 41.9% for Canadice UPLC-MS positive ions mode, and 45.5% for Canadice UPLC-MS negative ions mode. The VSP training system compounds grouped towards more negative values of component 1 while Munson training system compounds grouped towards positive values of component 1. The scores scatter plot resulting from the combination of these two components clearly showed the separation between training system (Fig. 46b and d). For each grape variety, significantly different metabolites between training systems were found using VIP > 1 and t-test ($P < 0.05$). Identified metabolites were subjected to Hierarchical Cluster Analysis. The results show that there was a significant effect of training system on skin metabolic profile in both cultivars (Fig. 47a-c).

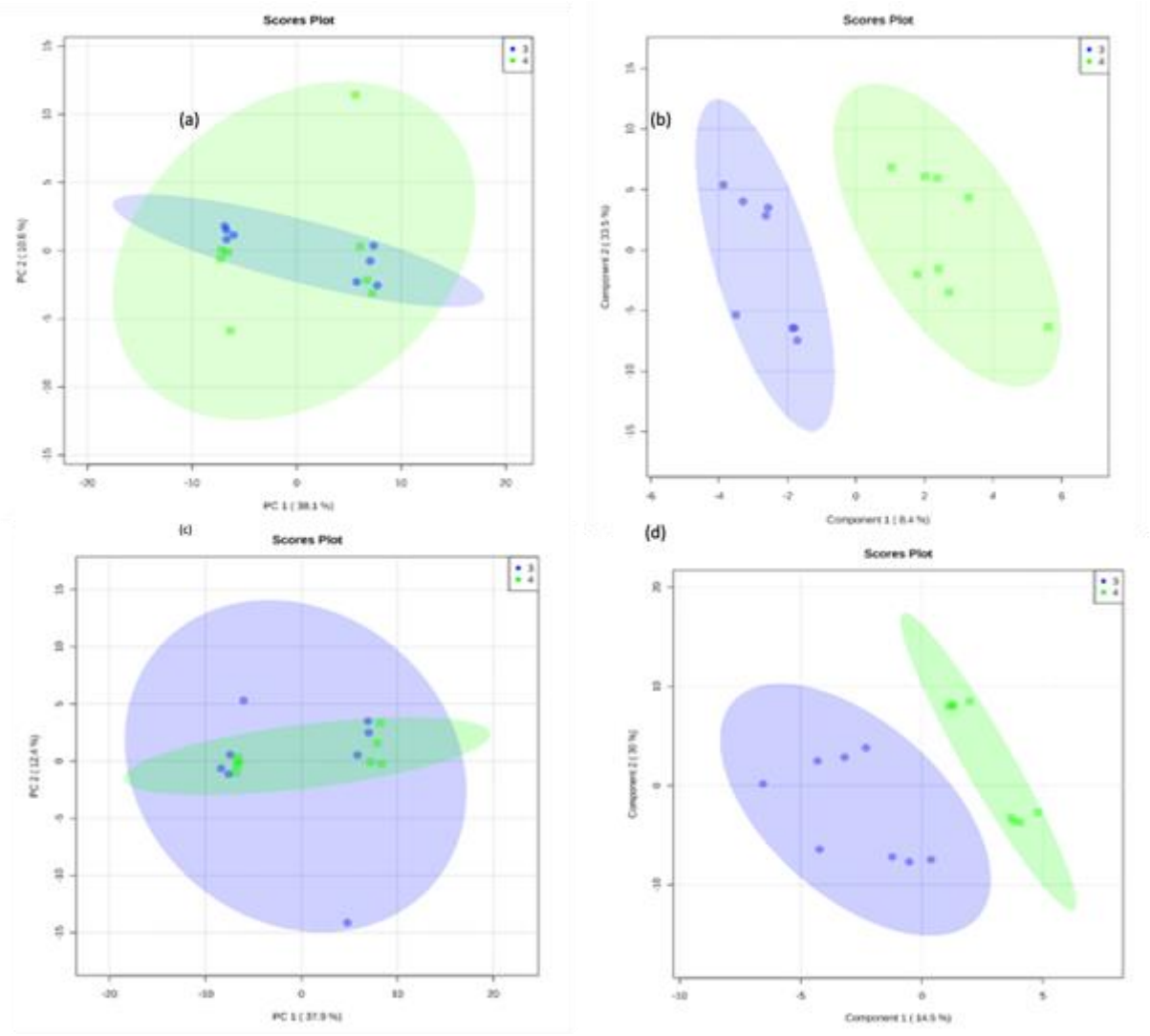

Figure 46. Canadice skin metabolome separation based on training systems: VSP (blue) and M (green). (a) PCA scores scatter plot for UPLC-MS negative ions mode; (b) PLS-DA scores scatter plot for UPLC-MS negative ions mode; (c) PCA scores scatter plot for UPLC-MS positive ions mode; (d) PLS-DA scores scatter plot for UPLC-MS positive ions mode.

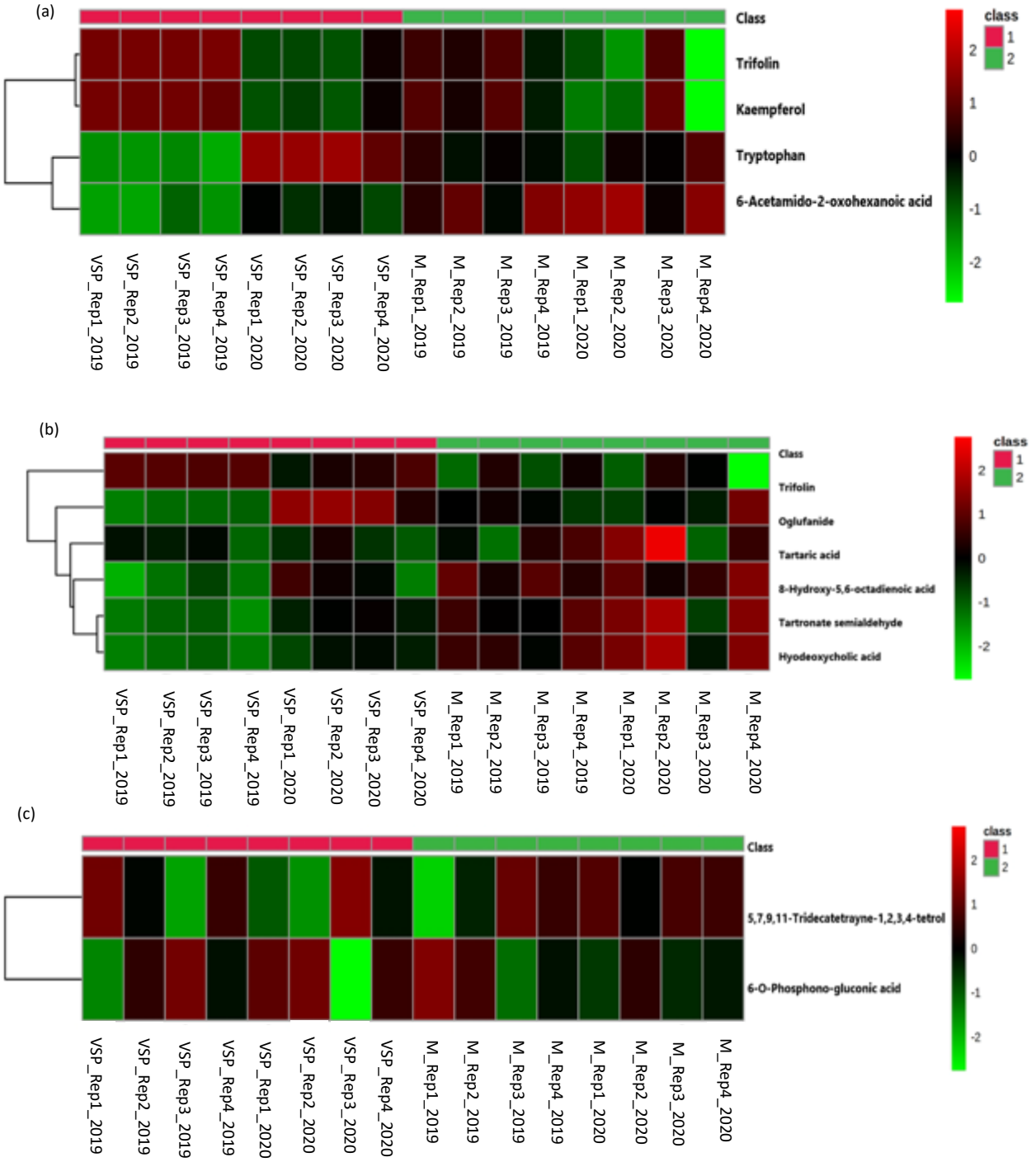

Figure 47. Hierarchical cluster analysis of significantly different metabolites showing increase (red) or decrease (green) in two different training systems - vertical shoot positioning (Class 1, red) and Munson (Class 2, green). (a)Mars skin, generated from UPLC-MS positive ions mode (b) Mars skin generated from UPLC-MS negative ions mode (c) Canadice grape skin, generated from UPLC-MS positive ions mode.

To further evaluate if there could be any differences found in individual compounds, and not just in total metabolomes, the major metabolites present in the skin samples were identified

for both grape varieties growing on VSP and M training systems. For Mars, among the eight identified metabolites, five were found to be significantly higher when grapes were grown using the VSP training system. For Canadice, three metabolites were identified and found to be significantly higher in M training system compared to VSP training system. Mars grape skin compounds significantly different between training systems both in positive and negative ions mode are shown in Fig. 47a, and 47b and listed in Table 5. Canadice skin compounds significantly different between training systems on positive ions mode are shown in Fig. 47c and listed in Table 6. There were no significantly different compounds on negative ions mode for Canadice identified.

Table 5. UPLC-MS data of the major identified compounds in Mars skin samples growing on two different training systems.

Compound	**Relative Abundance (AU)**		**P Value**
	VSP	**M**	
Trifolin	798.4	253	0.007
Kaempferol	503	161.9	0.014
Tryptophan	18	8.09	0.022
Oglufanide	13	4.4	0.023
Unidentified	1.25	0.568	0.013
Tartronate semialdehyde	28925	65942	0.018
6-Aceamido-2-oxohexanoic acid	4.6	14	0.009
8-Hydroxy-5,6-octadienoic acid	16	43	0.011

Table 6. UPLC-MS data of the major identified compounds in Canadice skin samples growing on two different training systems.

Compound	**Relative Abundance (AU)**		**P Value**
	VSP	**M**	
5,7,9,1-Tridecatetrayne-1,2,3,4-tetrol	10	26	0.049
6-O-Phosphogluconic acid	4.8	12	0.003
N-acetylvaline	14.34	31.73	0.046

2.4 Discussion

In this study, training systems had influence on the physiological and biochemical parameters, but our data does not allow us to infer which one is the best. Most of the parameters were significantly different based on time and the results varied between variety and year to year. Traditional methods used for chlorophyll estimation using spectrophotometric measurements are destructive and time consuming. In this work, both nondestructive and destructive methods were used to compare the accuracy of chlorophyll content of grapevine leaves over three growing seasons. Leaf metabolomics, titratable acidity and total soluble solid contents were analyzed over three growing seasons. Photosynthetic parameters, berry skin, and juice metabolomics were also estimated over two growing seasons. This is the first study to characterize the physiological and biochemical parameters of cold-hardy table grapevines growing on two different training systems.

2.4.1 SPAD readings and leaf pigment analysis of Mars and Canadice growing on Munson and VSP training systems.

Several authors (Reyes *et al.*, 2006; Steele *et al.*, 2008; Ru *et al.*, 2020) described that SPAD-502 is a reliable tool for the estimation of chlorophyll content in leaves of plants under different environmental conditions. According to Uddling *et al.*, (2007) there was a strong linear relationship between leaf chlorophyll content and SPAD measurements taken on birch, wheat and potato leaflets. In our study comparing SPAD values of two grape varieties growing on two different training systems, we found that they were mostly similar in both training systems. Similar results were reported in a study that compared SPAD data of two table grape varieties (‘Autumn King’ and ‘Scarlet Royal’) growing on two different training systems, and the SPAD values did not show significant difference between two training

systems in either variety (El-kereamy and Kurtural, 2022). In our study, there was an effect of training system over time on the SPAD values of both grape varieties. The effect could have been enhanced by modifying the method used to perform leaf sampling in Munson system. In VSP system the leaves grow vertically to the soil and adaxial surface of the leaves exposed to sunlight at different angles (Sanchez-Rodriguez and Spósito, 2020). In the Munson system the leaves on the top shoots grow horizontal to the soil and the leaves on the hanging shoots grow vertical to the soil. The leaves that were sampled in this study remained vertical to the soil in both VSP and Munson system, though Munson was an overhead trellis, the leaves grow vertical to the soil in the hanging shoots of Munson system.

Leaf chlorophylls are essential to convert the light energy to chemical energy and directly related to the photosynthetic efficiency and primary productivity of the vines (Casanova-Gascón *et al.*, 2018). The use of SPAD demonstrated to provide an immediate assessment of the status of grapevine leaf greenness; the coefficient of SPAD values and chlorophyll content were highest at flowering, lowest at harvest, and decreasing at veraison, recorded lowest during harvest (Porro *et al.*, 2001). However, SPAD readings performed on cv. Cabernet Sauvignon to estimate the total N content showed lower precision, with no relationship between SPAD values and grape yield (Brunetto *et al.*, 2012; Taskos *et al.*, 2015). Yamada and Fujimura (1991) observed that choosing the right wavelength with large absorption coefficient for chlorophyll increases the accuracy in chlorophyll meters (using 652 nm in SPAD and CCM (chlorophyll content meter)); resulting in higher accuracy while measuring in leaves with low chlorophyll content and lower accuracy while measuring in leaves with high chlorophyll content. The leaf chlorophyll contents are directly correlated with SPAD meter values (Vijay *et al.*, 2017).

In our study, the possible influence of training systems on photosynthetic pigment concentration in cultivars Mars and Canadice was studied. While researchers have studied the effect of phenological stages on photosynthetic pigments, there is no information on the effect of training systems on photosynthetic pigments. Leaves are the primary photosynthetic organs and chlorophyll is the main player in photosynthesis. It is important to quantify these pigments to understand the grapevine productivity during the biological annual cycle to understand the variations that occurs to the photosynthetic apparatus due to stress or an indicator of senescence (Filimon *et al.*, 2016). The changes in the photosynthetic capacity caused by stressors will affect the overall productivity of the growing season. Training systems play a key role in controlling the grapevine leaf exposure to sunlight and perform photosynthesis with the help of chlorophylls and accessory pigments such as carotenoids (Zoecklein *et al.*, 2008; Zhang *et al.*, 2016).

There is a pattern of increase in pigment concentration in leaves from flowering to harvest noticed in our study with both Mars and Canadice. However, there was a difference between growing seasons, in 2020 there was a decrease of chlorophylls from veraison to harvest (Fig. 16) and in 2021 chlorophylls were mostly stable and started decreasing only from two weeks before harvest (Fig. 17). This trend was not similar to the previous research reported in *V. vinifera,* that the leaves at flowering stage have a low photosynthetic activity, and concentration of assimilatory pigments gradually increase with biological growth, and continue to accumulate until veraison (Lovisolo *et al.*, 1996; Filimon *et al.*, 2014; Keller, 2015). This pattern was also confirmed in the study performed by Filimon *et al.*, (2016). Carotenoids in Mars and Canadice increased until veraison and then decrease until senescence in 2020, which is also confirmed by the study performed using *V. vinifera* table

grape cultivars Cetatuia and Milcov (Filimon *et al.*, 2016). However, the pattern of carotenoids fluctuated more in 2021 growing season. There are reports that states that degradation of carotenoids occurs after 30 days from the start of chlorophyll breakdown and the leaf starts appearing yellow while approaching senescence (Bertamini and Nedunchezhian, 2001, 2005).

2.4.2 Spectral indices of Mars and Canadice growing on Munson and VSP training systems.

Hyperspectral analysis is a remote sensing technique that allows for rapid, non-destructive analysis. It is used in forests and various agricultural fields to detect the overall plant health and early detection of stresses. Hyperspectral analysis allows researchers to distinguish and identify the vegetation's unique spectral signatures when subjected to various types of biotic and abiotic stresses (Rock et al., 1986). The importance and advantage of remote sensing techniques in identifying different types of fungal diseases before affecting a significant part of the plant (Oerke et al., 2016; Pantazi et al., 2019; Rumpf et al., 2010; Blanchfield et al., 2006) can play an essential role in preventing the economic loss in commercial vineyards. As the leaves in the grapevines expand, mature, and senesce, various physiological and morphological changes will affect their spectral properties (Usha and Singh, 2013).

In our one-year study, SPAD values, NDVI, and REIP followed a similar trend during the sampling time in 2019, with significant difference between training systems. All three data (SPAD, NDVI, and REIP) measures the chlorophyll content of leaves. The vegetative indices NDVI and REIP followed the same trend as chlorophylls *a* and *b* in both grapevine varieties (presented in section 2.3.2). The spectral indices initially remained stable and then tended to

decrease over time until veraison, which is likely related to the reduction in net photosynthesis and growth. The decrease in REIP, NDVI, and photosynthetic pigments indicate that the leaves' total chlorophyll content and primary productivity decrease when approaching the end of the growing season (Debnath *et al.*, 2019, 2021). However, there is an interaction of training system and time, and following veraison, photosynthetic pigment levels, NDVI and REIP tended to increase, but only in the Munson training system. The moisture stress index (MSI) indicates the leaf water content and phenology index is the NIR3/1 ratio, an indicator of the degree of foliage development during the growing season, but it also indicates the leaf water content (Lauten and Rock, 1992). According to Rock and Lauten (1996), phenology index was used to monitor the maturation index of the vegetation. In this study, the phenology index and MSI values increased shortly before veraison in both grape varieties and training systems, reaching a higher value after veraison. This trend of increase indicates increased water stress and maturation index with the approach to the end of the growing season and senescence (Rock *et al.*, 1988; Rock and Lauten, 1996). Previous studies for REIP, MSI, and phenology index were mostly performed in trees and forests, this study builds on that research.

2.4.3 Gas exchange parameters of Mars and Canadice growing on Munson and VSP training systems.

In our research, gas exchange parameters of both grape varieties growing on VSP and Munson training systems showed a gradual decline when the grapevines approached leaf senescence at the end of the growing season. According to Salvi *et al.*, (2021) there will be a low rate of photosynthesis and transpiration recorded when there is lower rainfall, which correlates with the values recorded in this study during the 2020 growing season. The

precipitation and temperature recorded for 2020 growing season is shown in Table 2 with two other growing seasons (2019 and 2021). According to Salvi *et al.* (2021), the gas exchange parameters such as net photosynthesis (A) and transpiration (E) observed a downward trend in VSP and SHW training systems with a progressing phenological status of grapevine leaf. The gas exchange results of our study was also supported by another study evaluating cv. Niagara Rosada growing on overhead, VSP and lyre training systems that did not demonstrate much difference in terms of gas exchange parameters due to growth in similar environmental conditions and water availability (Norberto *et al.*, 2009). Similarly, in our research VSP and Munson training systems did not show difference on gas exchange parameters in both in cultivars. In another study, *V. vinifera* cv. Syrah growing on VSP and Geneva double curtain (GDC) training systems showed no difference in the assimilation rate during the two growing seasons (Favero *et al.*, 2010). In contrast, *V. vinifera* cv. Erbaluce trained on VSP had a lower assimilation rate than the vines trained on the overhead training system (Novello *et al.*, 2001). Similarly, a 26% reduction in the rate of photosynthesis was reported for *V. vinifera* cv. Sangiovese growing in VSP training system compared to the traditionally trained vines (Poni *et al.*, 2006). Another study demonstrated that position of the leaf also affects the gas exchange parameters such as assimilation, stomatal conductance and transpiration in Pinot Noir, with younger leaves showing a higher transpiration and water use efficiency than the leaves opposite to the cluster (Candolfi-Vasconcelos *et al.*, 1994).

In a study using *V. labrusca* cv. Niagara Rosada growing on VSP and overhead training system, there were no differences with the photosynthetic rate (A), transpiration (E) and stomatal conductance (g_s) regardless of the growing season evaluated (Sanchez-Rodriguez

and Spósito, 2020). The horizontal positioning and hanging pattern of shoots on the Munson system and the vertical positioning on the VSP system cause the adaxial surface of the leaves to be exposed to sunlight at different angles. Despite these different growth patterns, in our study training systems did not influence the measurements of gas exchange parameters, such as intercellular CO_2 concentration (C_i), stomatal conductance (g_s), assimilation (A), transpiration (E), vapor pressure deficit (VPD), and water use efficiency (WUE) at various vine phenological stages, for both Canadice and Mars during the 2021 growing season. However, there were slightly higher values recorded for stomatal conductance, assimilation and transpiration for the vines growing on VSP compared with the Munson system during the 2020 growing season in Mars and Canadice until veraison. This was similar to the results of Koblet et al. (1996), who demonstrated a significant effect of training system, with gas exchange 27% lower in high trained vines than the low trained vines early in the season, but not later in the season.

The gas exchange parameters intercellular carbon dioxide concentration and stomatal conductance were similar for both training systems and were stable for three weeks after flowering and then started to decline for both grape varieties in 2020 season. However, the g_s values were higher for VSP-trained vines in both grape varieties. In 2021 there was an increase from flowering, with a sudden decline during berry touch, increased until veraison and then decreased approaching harvest. These results were in contrast to the study performed on *V. vinifera* cv. Tempranillo cordon-trained and head-trained exhibiting similar carbon dioxide assimilation rate and stomatal conductance during the flowering and green berry stage, while higher in head-trained vines during veraison and harvest than the cordon-

trained ones (Baigorri *et al.*, 2001). According to Ru *et al.* (2020), the leaf transpiration (E) ability of grapevines changes during different stages of growth, resulting in a decline in leaf temperature with the same vapor pressure deficit (VPD). Stomatal conductance (g_s) is closely related to the water stress index, and higher water stress leads to the closure of leaf stomata and a reduction in the transpiration rate (E) (Ru *et al.*, 2020). In our study vines approaching harvest, due to water stress the stomatal conductance decreased, and water use efficiency increased during both 2020 and 2021 growing seasons in both grapevine varieties regardless of training systems.

2.4.4 Leaf metabolomes of Mars and Canadice growing on Munson and VSP training systems.

^{1}H-NMR spectroscopy is a tool extensively used for metabolite identification of grapevine leaves (Ali *et al.*, 2009, 2012; Lima *et al.*, 2010; Gougeon *et al.*, 2019; Alves Filho *et al.*, 2022). Principal component analysis (PCA) provides a method to differentiate between leaf samples collected at different phenological stages; the sample groups were visualized as scores plots, while the loading plots offered clue on the nature of sample separation (Lima *et al.*, 2010). In our study the metabolite profile was different between cultivars and their phenophases (different phenological stages) but were not different between training systems (VSP and M). The discriminant compounds detected were sucrose in both Mars and Canadice across all three growing seasons. There were two unidentified compounds in the sugar region in both cultivars, and one more unidentified compound in the aromatic region only in Canadice, especially from the flowering samples (2019 and 2021). The PC loadings plots indicated the varying compounds in each region of the spectrum, which play a key role in the distinction between different phenological stages, but no distinction between training

systems was noticed. Sucrose is the main form of sugar transported in plants and gets converted to glucose and fructose, and in our study, sucrose was the only metabolite that was identified in grapevine leaves in both cultivars. Three more unknown compounds were identified. Due to lack of freely-available databases, the metabolites that were detected by PCA were only tentatively identified based on the literature. The results show that there was a gradual increase of sucrose from flowering, a decrease during veraison and once again increase during the harvest stage in the 2021 growing season. However, the 2019 and 2020 growing seasons leaf spectra represent only two phenological stages. The changes in sucrose content at different phenological stages confirms with the previous study that quantifies sucrose in leaves of Canadice and few more cultivars that sucrose being less during flowering, and a significant increase while the vines are approaching harvest (Wu *et al.*, 2011). In another study the leaves of *V. vinifera* cultivar Riesling had trend of increase of sucrose from start to end of the growing season during two growing seasons (Ren *et al.*, 2022). In Mars in 2019, and in Canadice in 2021, there were significantly higher amounts of sucrose in M training system compared with the VSP.

2.4.5 Grape juice metabolomics of Mars and Canadice growing on Munson and VSP training systems.

^{1}H-NMR spectroscopy an extensively used tool for metabolite identification of grape juice (Ali *et al.*, 2009, 2012; Lima *et al.*, 2010; Gougeon *et al.*, 2019; Alves Filho *et al.*, 2022). Principal component analysis (PCA) was able to differentiate the samples of time course study between veraison and harvest; the sample groups were visualized in scores plots, while the loading plots offered clue on the nature of sample separation (Lima *et al.*, 2017*b*). Using

^{1}H-NMR spectroscopy, we were able to identify, in a single analysis, 22 metabolites belonging to several chemical classes, including amino acids, sugars, salt or ester forms of keto acids, alcohols, and other small molecules (Table 2). This analytical technique has several advantages such as the fast sample preparation and the possibility of high-throughput screening and has proven to be a great technique for grape metabolomic profiling (Ali *et al.*, 2011*a*,*b*, 2012). The grape berry undergoes three phases during its growth: stage 1 and 3 are characterized with rapid growth due to increased cell division and expansion (Coombe *et al.*, 1992). In stage 1, malate, tartrate, tannins, and hydroxycinnamates are produced and reach maximum concentration 60 days after flowering (Possner and Kliewer, 1985). Stage 2 is a lag period which occurs 7 – 10 weeks after flowering. The transition from stage 2 to stage 3 occurs within 24 h, which is veraison (Coombe *et al.*, 1992). In our results the changes in the sugar content with the gradual increase of glucose and fructose from veraison to harvest are shown in Fig. 37-40. These results are in agreement with the previous research reported that 20 days after veraison glucose and fructose concentration increases (Findlay *et al.*, 1987). Sugar concentration is the indicator for the assessment of ripeness and decision of harvesting time, usually confirmed by ^{o}BRIX values. This is in an agreement with the study performed on three Portuguese cultivars that showed an increase in berry size, color development (anthocyanin accumulation in red and blue grapes), and sweetness (glucose and fructose) (Ali *et al.*, 2011*a*). Stage 3 starts with ripening (from veraison to harvest) and involves fruit undergoing dramatic morphological changes. Our research shows an increase in glucose and fructose with a visual color change from veraison to harvest and decrease in sucrose levels, and it is reported that between veraison and harvest sucrose is exported from the source (leaf) and imported to berries (Findlay *et al.*, 1987). Our study also agrees with the previous

findings of sucrose being lower, while glucose and fructose become higher in the stages between veraison and harvest (Ali *et al.*, 2011*b*). Our data is consistent with the previous study where there was an increase of alanine and inositol between veraison and harvest (Ali *et al.*, 2012). The study reports that alanine and inositol are involved in grapevine resistance and concentrations increase when vine is under stress (Ali *et al.*, 2012). The production and accumulation of inositol results in the synthesis of stress metabolites rapidly and the higher amounts of inositol in Mars and Canadice confirms their resistant traits. Mars and Canadice have reduced susceptibility to various types of fungal diseases during five seasons study conducted in UNH vineyard (Sideman and Hamilton, 2015, 2016, 2019). Inositol is actively involved in signal transduction and, when accumulated, facilitates the plant resistance to quickly respond to pathogen attacks (Hamzehzarghani *et al.*, 2005).

2.4.6 Titratable acidity of Mars and Canadice growing on Munson and VSP training systems.

Titratable acidity (TA) of Canadice ranged at harvest from 6.43 to 8.19 in different growing seasons, which was similar to Isabel (*V. labrusca)* grapes (Tecchio *et al.*, 2020). TA for Mars ranged from 5.28 to 6.74, (more acidic than Canadice), which was similar to Bordo (*V. labrusca)* grapes (Tecchio *et al.*, 2020). Canadice and Mars are interspecific hybrids of *V. labrusca* and *V. vinifera* (Pool *et al.*, 1977; Moore, 1986). Temperature and incidence of solar radiation are the factors that majorly influence organic acid degradation due to increased respiration, resulting in decreased TA (Etienne *et al.*, 2013). In another study, the training systems Hudson River Umbrella and Umbrella Kniffin, which had the highest fruit exposure to sun light, resulted in berries with low TA and malate along with highest pH and tartrate. The vines trained with a mid-wire cordon had the second highest TA and lowest

BRIX (Reynolds *et al.*, 1985). On the other hand, a four-year study with two white grapes and two red grapes growing on three different training systems (Geneva Double Curtain , single wire, and bilateral cordon system) had no significant effect of training systems on TA of any of the four cultivars (Morris *et al.*, 1984). Similarly, in our study VSP is a type of bilateral cordon and M a type of overhead training, and the results were not consistent but showed a significant influence of training system on TA only in Mars during one of the growing seasons.

2.4.7 Total soluble solids content of Mars and Canadice growing on Munson and VSP training systems.

In our study, BRIX or TSS of Mars and Canadice was not influenced by training system consistently. There was a significant difference on TSS between training systems in Mars during 2019 and in Canadice during 2021. According to Costa *et al.*, (2021), the TSS values of 'BRS Cora' (a hybrid of *V. labrusca)* was higher in VSP and lyre training system during one growing season but no significant difference between training systems whereas, TSS was higher in the berries growing on the overhead training system during another growing season. In our study, M training system is a type of overhead training and BRIX values were higher, though not significantly different from VSP (Costa *et al.*, 2021). Training systems influence the grapevines' response to climatic factors due to differences in their canopy structure, affecting the photo assimilate synthesis (Martínez-Lüscher *et al.*, 2016). In our study during 2020 the weather was drier and grapes produced had a higher BRIX compared to the other growing seasons. Growing seasons with higher temperatures and high incidence of solar radiation will significantly impact the rate of photosynthesis and sugar accumulation, which would certainly reflect on the total soluble solid contents (Greer and Weedon, 2012).

Therefore, it is vital to adopt a suitable training system for better exposure of grape clusters to sunlight and producing berries with highly accumulated sugars (Martínez-Lüscher *et al.*, 2016).

2.4.8 Berry skin metabolomes of Mars and Canadice growing on Munson and VSP training systems.

UPLC-MS coupled with PCA and PLS-DA was used to evaluate differences between the metabolome profile of Canadice and Mars fruit from vines growing on VSP and M training systems during two growing seasons (2019 and 2020). The application of PCA and PLS-DA to UPLC-MS data revealed a difference between the compounds present in the skin samples, clearly segregating VSP and M training systems in both cultivars. The ability of this approach, allying the metabolite analysis with multivariate statistics to discriminate between training systems serves as a better diagnostic method to understand how each training system influences berry skin metabolites. Our results show a marked increase of certain metabolites in the VSP training system. Mars grape skin compounds that were significantly different between training systems are shown in (Fig. 46a and b) and listed in Table 3. Tryptophan, kaempferol, trifolin, and Oglufanide, found to be higher in skins of Mars grown on VSP, are part of the phenylpropanoid pathway which are involved in pathogen resistance mechanism (Li *et al.*, 2005; Lago-Vanzela *et al.*, 2011*b*; Zhang *et al.*, 2020). Flavonoids are the phenolic compounds that are most abundant in grapevines (Ali *et al.*, 2010; Khan *et al.*, 2019; Nascimento *et al.*, 2019). The grapevines that are more exposed to solar radiation was shown to induce the accumulation of compounds such as quercetin, kaempferol, and myricetin-3-glucosides in both berry skin and pulp (Spayd *et al.*, 2002; Pereira *et al.*, 2006; Mattivi *et al.*, 2006). This was consistent with the results in our study where berries exposed to more

sunlight in the VSP training system due to the cluster positioning produced significant phenolic compounds.

6-Acetamido-2-oxohexanoic acid, a compound produced in the lysine catabolic pathway, and 8-Hydroxy-5,6-octadienoic acid, a polyunsaturated fatty acid, were found to be higher in Mars grape skin grown on M training system; these compounds are reported to increase during the maturation stage (Slegers *et al.*, 2015). The M training system provides uniform ripening of the berry clusters due to the canopy architecture and the presence of above compounds in higher amounts at harvest confirms that their occurrence during maturation stage. Tartronate semialdehyde, also found to be higher Mars growing in M training system, is involved in the glyoxylate cycle and has been reported to be associated with berry development and cell division (Burbidge *et al.*, 2021).

Canadice grape skin compounds significantly different between training systems are shown in Fig. 46c and listed in Table 4. The compounds 5,7,9,1-Tridecatetrayne-1,2,3,4-tetrol, a long chain fatty alcohol, and 6-O-Phosphogluconic acid, an intermediate of pentose phosphate pathway linked to NADP reduction (Burbidge *et al.*, 2021) are involved in antioxidant synthesis in grapes. N-acetyl valine, is involved in phenolic compound synthetic pathway and provide berries with high antioxidant properties (Hildebrandt *et al.*, 2015). All three compounds are present in higher amounts in grape skins under the M training system.

2.5 Conclusion

The SPAD values vary significantly between training systems over time in Canadice and Mars. The spectral analysis that was performed using the same leaves collected in the 2019 growing season also showed similar results. The present work highlights the importance of

non-destructive methods such as SPAD and spectral measurements to measure chlorophyll and the results were confirmed by pairing with the wet lab analysis of chlorophyll. In future, leaf sampling can be done from the top of the trellis in the M training system to see if there are significant differences among the training systems.

In our study, the leaf pigments did vary significantly between training systems, whereas they varied differently with time in both Mars and Canadice. The pigment concentrations (chl *a*, chl *b*) highly relate with the spectral measurements NDVI and REIP performed during the 2019 growing season. The gradual decrease in the photosynthetic pigment concentration is likely related to the reduction in net photosynthesis and growth response. The photosynthetic pigments followed the same trend in 2020 and 2021, with no significant variation between training systems in both cultivars.

In our study, spectral indices were not significantly different between training systems, whereas they varied significantly with time in both grapevine varieties. The present work highlights the importance of spectral indices (NDVI, REIP, and MSI) for monitoring physiological processes (pigment status and foliar moisture) occurring at the leaf level. In the future, proximal sensing should be performed in the field at the canopy level to assess the degree of variability that occurs from year to year. Proximal sensing is used in wine grape vineyards to manage the site-specific variabilities of grapevine physiology to ensure high quality fruit production. In a study it was reported that temporal proximal sensing is possible to assess vine water status, primary metabolism, berry secondary metabolism and yield (Yu *et al.*, 2021).

In our study for both cultivars, gas exchange parameters (intercellular carbon dioxide concentration, stomatal conductance, vapor pressure deficit, net photosynthetic rate, transpiration rate, and water use efficiency) were influenced by training system over time. The parameters stomatal conductance, vapor pressure deficit, net photosynthetic rate, and transpiration rate showed visible differences according to training systems from flowering to harvest only for the cv. Mars for the year 2020. But the trend did not follow in 2021 season with not much difference between training systems.

With the NMR-based metabolic profiling approach for leaves, we traced the metabolic responses of Mars and Canadice cultivars growing on VSP and training systems during flowering, veraison, and harvest phenophases. Canadice differed from Mars with respect to the metabolite concentrations, and most metabolites increased in concentration as the grapevines approached harvest. Further, NMR as an analytical approach proved to be effective in discriminating the metabolomic profiles of cold-hardy cultivars Mars and Canadice growing on different training systems. Furthermore, studies such as transcriptomic and proteomic profiling might confirm the changes in metabolites during phenophases and the differences between training systems.

NMR profiling of berry juice collected from veraison to harvest on a weekly basis showed that most of the metabolites increased in concentration in both Mars and Canadice as the grapevines approached harvest, with no separation based on training systems. The increase in the concentration of sugars while approaching harvest is an indication of healthy development of berries. A two-year time course study also confirmed there was a significant

effect of the training system on some of the metabolites in both cultivars and that a few of the metabolites varied over time. Further study with transcriptomic and proteomic analysis may reveal additional details about the changes in metabolites between training systems.

The titratable acidity (TA) showed no consistent effect of the training system on the TA in either cultivar, but there was a significant effect of training system on TA for Mars in one growing season. During harvest TA decreases and the sugar level increases naturally which represents ripeness. The results of the total soluble content of Mars and Canadice did not show any significant effect of the training system on ^{o}BRIX values overall. There was, however, a significant effect of the training system on ^{o}BRIX in Mars for one growing season and in Canadice during other growing seasons. Moreover, there were no consistent results showing the significant effect of the training system in both cultivars. Further studies could confirm the change in sugar and TA content as the berries are approaching harvest. However, ^{o}BRIX and TA can be performed weekly from veraison through harvest to determine whether training systems impacts timing of maturity, or the maximum TA and ^{o}BRIX levels attained.

According to the results of UPLC-MS data, we propose that the differentially produced compounds in the berry skins of Mars and Canadice growing on two different training systems are associated with the cluster microclimate imposed by the different training systems. VSP has large expanse of leaves and clusters that grow outside the canopy and are well exposed to sunlight. Whereas, in M the shoots grow over the top of the trellis, providing shade to the clusters. In future, study can be performed to identify and quantify compounds present in berry skins that are present in sun-exposed and shaded regions. Moreover, the

investigation can be performed to correlate by characterizing the compounds produced in berries collected from sun-exposed and shaded regions with the amount of shade and light received by the clusters collected from the grapevines growing in both training systems. This type of research can unravel the compounds produced in sun-exposed and shaded berries. It is possible that the compounds related to grape maturation were higher in the M training system and in this training system the canopy architecture places the leaves over the clusters so that there is uniform distribution of sunlight leading to uniform ripening when compared to VSP.

Overall, the result of this study suggests that training system has an impact on many physiological and biochemical parameters but not all, and these in turn have an effect on the various aspects of plant health and berry chemistry. Based on these primary results there is an indication that training system influences various parameters in cold-hardy grapevines. For many parameters in several seasons, Munson-trained grapevines had higher photosynthetic activity than VSP-trained vines, especially during the latter part of the growing season. This could partially account for observations that the Munson system produces higher yields (Sideman and Hamilton, 2016, 2019). However, there is evidence that Munson system produces higher yields and can be recommended to the grapevine growers to enhance grapevine productivity and berry metabolomes (Sideman and Hamilton, 2016, 2019). The UNH extension research also reports that Mars and Canadice are good for commercial production in New Hampshire (Sideman and Hamilton, 2016, 2019).

CHAPTER 3

ANTIFUNGAL ACTIVITY OF COLD-HARDY TABLE GRAPEVINE-DERIVED PRODUCTS AGAINST BOTRYTIS CINEREA

3.1 Introduction

3.1.1 Botrytis rot or Gray mold

Botrytis cinerea (Pers.:Fr), the causal agent of botrytis bunch rot or gray mold, is one of the most destructive grapevine diseases worldwide (Sharma *et al.*, 2009; Ky *et al.*, 2012; Steel *et al.*, 2013). Botrytis consists of ~35 necrotrophic species, some having a vast range (*B. cinerea* and *B. pseudocinerea*), impacting ~1400 different plant species (Kassemeyer and Berkelmann-Loehnertz, 2009). Most economically important crops are affected by *B. cinerea* and this fungus is the major contributor to food waste and a threat to global food security (Williamson *et al.*, 2007; Romanazzi *et al.*, 2016). Botrytis can grow on succulent plant tissue (young and green), ripened fruit, or dead tissues (Elad *et al.*, 2016). When any green part of the grapevine is affected by *B. cinerea,* it can affect the berry quality and productivity (Davies *et al.*, 2021; Rienth *et al.*, 2021). Gray mold disease is a massive concern in post-harvest storage of fruits and vegetables, leading to substantial economic loss and food security (Williamson *et al.*, 2007; Romanazzi and Feliziani, 2014). In viticulture, Botrytis can cause reduced fruit and wine quality, a significant concern for the wineries (Steel *et al.*, 2013) and affect table grape sales in grocery stores (Cappellini *et al.*, 1986). By contrast, under specific climatic conditions that include moist nights, foggy mornings, and dry days infection of *B. cinerea* is limited to outermost layers of epidermis (Ribéreau-Gayon *et al.*, 1980), leading to dehydration of berries with increased sugar concentration and accumulation of specific aromatic compounds leading to improved grape quality. This type of infection

results in ‘noble rot’ and berries with noble rot are utilized to produce sweet, smooth, full-bodied wines, the so-called ‘botrytized wines’ (Vannini and Chilosi, 2013). However, the bunch rot caused by *Botrytis* is a significant problem for grapevines in the Northeastern U.S. because the growing seasons are warm and humid, and summer rains favor disease development (Hazelrigg and Kingsley-Richards, 2017). Gray mold, caused by the fungus *Botrytis cinerea*, is one of the most destructive diseases of grapes in vineyards, where warm, moist conditions can cause severe infections and devastating crop losses to the viticulturists (Avenot *et al.*, 2020; DeLong *et al.*, 2020).

3.1.2 *Botrytis cinerea* and its pathogenicity

B. cinerea overwinters as sclerotia on the surface of or inside different plant parts and then releases its spores in the spring during a rainy period (Kassemeyer and Berkelmann-Loehnertz, 2009). The sclerotia and mycelium (vegetative structure) produce conidia (spores). Conidia get disseminated by rain and wind onto the healthy tissue (Williamson *et al.*, 2007; Elad *et al.*, 2016). Fruit infections start near late bloom, and the fungus spreads rapidly through the cluster through berry-to-berry contact (Kassemeyer and Berkelmann-Loehnertz, 2009; Moyer and Grove, 2011; Romanazzi and Feliziani, 2014). Severe losses occur due to *Botrytis* during the post-veraison/preharvest period (Romanazzi and Feliziani, 2014). Grape growers rely on multiple fungicide applications throughout the growing season to manage fungal diseases, including botrytis (Moyer and Grove, 2011). The development of multiple-fungicide resistance (the ability to survive when exposed to a chemical) by *B. cinerea* is of significant concern (Northover, 1986; Liu *et al.*, 2016; Fan *et al.*, 2017). Several fungicides, such as benomyl and iprodione alone or mixed with captan, have already lost

their effectiveness (Northover, 1986; Avenot *et al.*, 2020). Thus, alternative practices incorporating sanitation, fungicides, canopy management, breeding resistant cultivars, and other IPM strategies are critical to managing *Botrytis* infection.

3.1.3 Grapevine's response to fungal infection

In grapevines, synthesis of stress metabolites, primarily phytoalexins, is initiated in response to plant pathogens like *Botrytis cinerea* (Bavaresco et al., 1997; Jeandet et al., 1995;) and *Plasmopara viticola* (Langcake and Pryce, 1976; Langcake, 1981; Dercks and Creasy, 1989) or stress due to UV irradiation (Langcake and Pryce, 1977; Creasy and Coffee, 1988; Jeandet *et al.*, 1991). Grapevines respond to fungal infections by producing more phenolics, flavonoids, and anthocyanins to protect themselves (Batovska et al., 2008; Lima et al., 2017a; Lima et al., 2017b). *V. vinifera* and *V. riparia* leaves, when infected with *B. cinerea,* produced phytoalexins such as resveratrol, α-viniferin, and ε-viniferin, and demonstrated disease resistance towards the pathogen (Langcake, 1981). However, *V. riparia* leaves produced more phytoalexins compared to *V. vinifera* leaves (Langcake, 1981). Detached *Vitis* leaves infected with *B. cinerea* demonstrated the production of resveratrol and p-hydroxy stilbenes around the lesion area (Langcake and Pryce, 1977). Resveratrol, a major stilbene produced as a response to grapevine's infection with *B. cinerea*, also demonstrated an inhibitory effect on the radial growth of *B. cinerea* mycelia *in vitro* (Hoos and Blaich, 1990). Adrian *et al.* (1997) determined the biological activity of resveratrol against the germination of *B. cinerea;* as the concentration of resveratrol increased, the percentage of germination of the fungus decreased. A time course study of resveratrol production in the leaves and berries of *V. vinifera* and *V. labrusca,* demonstrated that the latter had more

accumulation of phenolic compounds for the same developmental stages (Jeandet *et al.*, 1991). Grape berries inoculated with *B. cinerea* produced antifungal compounds in different concentrations depending upon grapevine varieties, with resistant varieties producing higher concentration and accumulation around the infected area than the susceptible varieties (Bavaresco *et al.*, 1997).

This chapter focuses on the antifungal activity of grapevine-derived products against *B. cinerea* infection in grapevines, by testing the antifungal activity of extracts of senescent leaves and cell suspension cultures from the grape cultivars Mars and Canadice. I hypothesized that field-collected leaves and cell suspension cultures established from Canadice and Mars grape varieties would contain compounds with antifungal activity against *Botrytis cinerea*.

3.2 Materials and Methods

3.2.1 Plant material

3.2.1.1 Mars and Canadice *calli* and cell suspension cultures

Solid cultures of undifferentiated cells (*calli*) were established from the leaves, leaf meristems, and cambium of Canadice and Mars grapevine explants obtained from green-house grown plants. Grapevine shoots were collected from the vineyard in the month of October and subjected to acclimation by keeping them at 4°C for four weeks and then cut into 2 buds each. The shoot cuttings were dipped in the rooting hormone Hormodin (OHP, Inc., Morrisville, NC) and placed in the cone shaped plastic containers with pre-moistened 1:1 perlite: vermiculite (Whittermore Co Inc., Lawrence, MA) mixture to initiate rooting.

The shoots were maintained in a misting chamber at 22°C with 65% relative humidity and mist settings-125µmol/hrs accumulation trigger, 2 pulses mist at 0.2 min duration with10 seconds delay between pulses with tap water. Once bud break occurred and two to three leaves and root growth were visible, the plants were removed from the mist and fertilized with 17-4-17 100 mgL^{-1} N (Jack's Professional LX, JR Peters Inc. Allentown, PA). When the plants were accustomed to no misting conditions, they were transferred into pots with potting media. The pots were maintained in the greenhouse set to 21°C day/18°C night, 65% relative humidity with 4 minutes of irrigation pulses and a 10-minute pause between 1000 pulses daily. Plants were fertilized with 17-4-17 at 150 mgL^{-1} N (Jack's Professional LX, JR Peters Inc. Allentown, PA) at each irrigation. Once the plants developed 10 leaves, the leaves and shoots were pruned and carried to the lab using a lab cooler. The leaves and shoots were sanitized using 10% hypochlorite solution (commercial bleach) and washed well with autoclaved deionized water three to four times. Then leaves were cut into small pieces using a sterilized scalpel. The leaf meristem was excised underneath the petiole. The cut leaf pieces, cambium and leaf meristems were separately cultured in Murashige and Skoog media (Research Products International, IL) with sucrose (30 %; Fisher Scientific, Fair Lawn, NJ), agar (0.8 %; Gold Biotechnology, Inc., MO), plant growth hormones benzylaminopurine (0.2 mg/L; Phyto Tech Lab, Lenexa, KS) and indole acetic acid (1.0 mg/L; Sigma Aldrich, MO), and casein hydrolysate (250 mg/L; Sigma Aldrich, MO). These tissue culture plates took about 4 weeks to produce *calli*, as shown in Fig. 48 and 49. The cultures were maintained on a solid Murashige and Skoog media and grown at 25±1°C, with 16 h light/8 h dark photoperiod illuminated with fluorescent light bulbs.

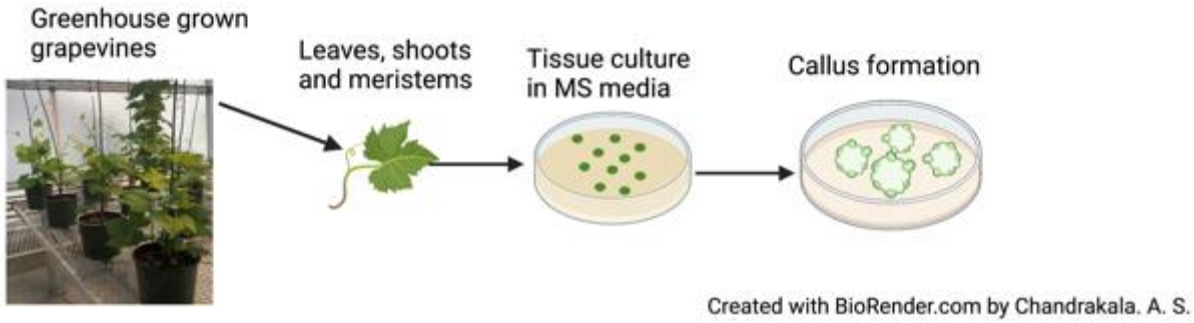

Figure 48. *Calli* culture establishment using grapevine leaves, cambium and leaf meristem in Murashige and Skoog media.

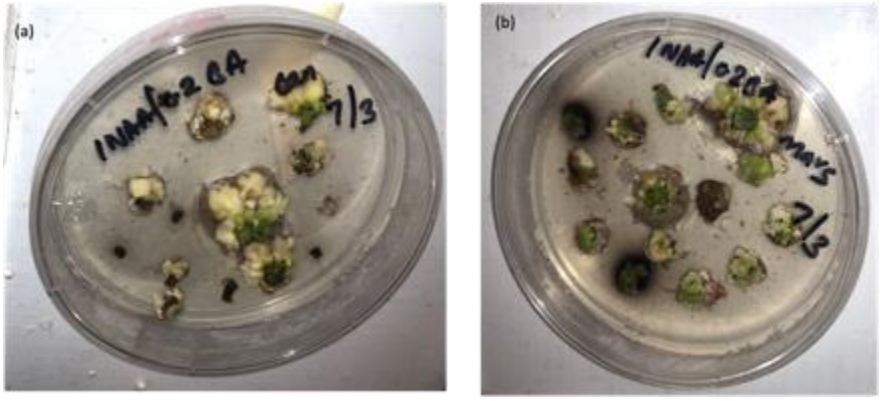

Figure 49. *Calli* in Murashige and Skoog media. (a) Canadice (b) Mars

Calli were routinely sub-cultured in 4-week intervals to maintain the cell lines (Lima *et al.*, 2012; Lima and Dias, 2012). The *calli* cultures were used to establish liquid cultures of undifferentiated cells (cell suspension cultures) using liquid Murashige and Skoog media with sucrose (30 %), casein hydrolysate (250 mg/L) and the plant growth hormones benzylaminopurine (0.2 mg/L) and indole acetic acid (1.0 mg/L)). The cell suspension cultures were initiated by transferring chopped 3 weeks-old *calli* into about 125 mL Erlenmeyer flasks containing 50 mL of liquid media. The cell cultures were maintained at 25±1°C, with 16 h light/8 h dark photoperiod illuminated with fluorescent light bulbs with constant shaking at 100 rpm. Subculturing occurred every 2 weeks by transferring 10 mL of

14 days-old cell suspension culture into the fresh medium, as shown in Fig 50. After 5-7 subcultures, a homogenous suspension culture was obtained and was used for antifungal experiments.

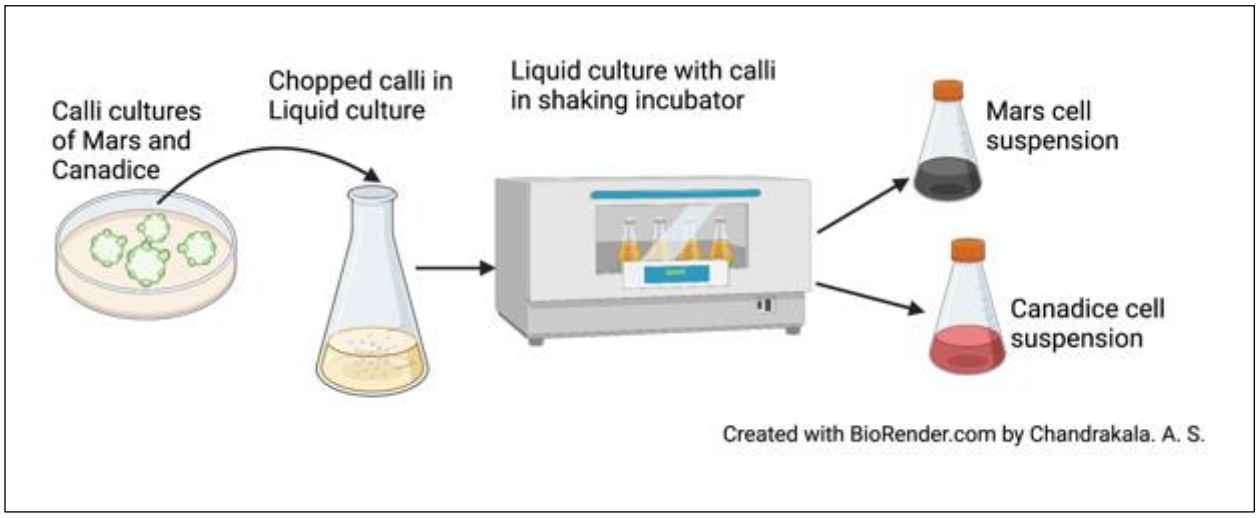

Figure 50. Cell suspension culture establishment using the *calli* in liquid Murashige and Skoog media.

3.2.1.2 Mars and Canadice senescent leaves

Mars and Canadice senescent leaves were collected from the vineyard, and their extracts were used to test their antifungal properties. The leaves were collected, brought to the lab, washed with deionized water, patted dry, placed in conical centrifuge tubes and flash-frozen in liquid nitrogen and stored at -80°C. The frozen leaves were ground using liquid nitrogen, and about 50 g of leaf tissue (Mars and Canadice separately) were boiled in 100 mL of water for 20 minutes. The resulting extract was filter sterilized using 0.45 µm corning bottle top vacuum filters (Sigma Aldrich, MA) and used to test the antifungal activity *in vitro* (Fernandes *et al.*, 2013; Maia *et al.*, 2019). Similarly, leaf extracts were prepared for both Mars and Canadice in 70% methanol and 80% ethanol, respectively (50 g leaves in 100 mL

of 70% methanol and 50 g leaves in 100 mL of 80% ethanol). Sterile water, 70% methanol and 80% ethanol served as control treatments.

3.2.2 Plant material metabolomic profiling

Mars and Canadice cell suspension cultures (50 mL) were centrifuged in a conical centrifuge tube (4500 rpm, 4°C, 5 minutes), and the pellets were retained. The pellet was then lyophilized in a freeze dryer (LabConco, AK). Mars and Canadice leaves were collected and placed in Ziploc bags in a lab cooler, washed well with deionized water, patted dry, placed in a conical centrifuge tube and flash-frozen in liquid nitrogen immediately upon harvest and stored at -80°C. The frozen leaves were ground and then lyophilized in a freeze dryer (LabConco, AK). About 100 mg of freeze-dried Mars and Canadice cell suspensions and leaf samples were sent to the Roy J. Carver Biotechnology Center (University of Illinois) to perform metabolic profiling using liquid chromatography-mass spectrometry (LC-MS). The analysis were done by using approximately 50 mg of each sample soaking in 1 mL of acetonitrile:isopropanol:water (3:3:2) for 1 hour, homogenized on bead mill 4 (Thermo, Germering, Germany), centrifuged at 20000 rpm for 10 min. 100 µL of supernatant were collected in a separate microfuge and spiked with internal standard (4-Chloro-DL-phenylalanine) and 20 µL was injected into the LC/MS system. The Dionex Ultimate 3000 series HPLC system (Thermo, Germering, Germany) with a degasser, an autosampler and a binary pump. The LC separation was performed on a Phenomenex Kinetex C18 column (4.6 x 100 mm, 2.6 µm) with mobile phase A (H_2O with 0.1% formic acid) and mobile phase B (acetonitrile with 0.1% formic acid). The flow rate was 0.25 mL/min. The linear gradient was as follows: 0-3 min, 100% A; 20-30 min, 0% A; 31-36 min, 100% A. The autosampler was set to 15°C. Mass spectra was acquired under both positive (sheath gas flow rate:45; aux gas

flow rate:11; sweep gas flow rate:2; spray voltage: 3.5 kV; capillary temp: 250°C; Aux gas heater: 415°C) and gas flow rate: 11; sweep gas flow rate: 2; spray voltage: 3.5 kV; capillary temp: 250°C; Aux gas heater temp: 415°C) and negative electrospray ionization (sheath gas flow rate: 45; aux gas flow rate: 11; sweep gas flow rate:2; spray voltage: -2.5 kV; capillary temp: 250°C; Aux gas heater temp: 415°C). The full scan mass spectrum resolution was set to 70,000 with scan range of m/z 67 ~ m/z 1,000, and AGC target was 1E6 with a maximum injection time of 200 ms. LC-MS data was further analyzed with Thermo Compound Discoverer software (v. 2.1 SPI) for chromatographic alignment and compound/feature identification/quantification. The workflow is Untargeted Metabolomics with Statistics Detect Unknowns with ID Using Online Databases (HMDB, 2022; KEGG, 2022). The following settings were used in Select Spectra: minimum precursor mass (65 Da) and maximum precursor mass (5,000 Da); in Align Retention Time: Maximum shift (1 min) and Mass tolerance (5 ppm); in Detect unknown compounds: Mass tolerance (5 ppm), Intensity tolerance (30%), S/N (3), and Minimum peak intensity (1000000) (Elolimy *et al.*, 2019).

3.2.3 Fungal Culture

3.2.3.1 *Botrytis cinerea* culture and maintenance

To produce fresh fungal culture, a *B. cinerea* isolated from infected petunia (kindly donated by Dr. Poleatewich's lab, UNH) was cultured on fresh potato dextrose agar (PDA) (Hardy diagnostics, Santa Maria, CA). Moreover, to check if the *B. cinerea* could also infect grapevine parts, I tested by inoculating grapevine detached leaves of Mars and Canadice and store-bought grapes (variety unknown) and after confirmation of infection the isolates were sub-cultured and used for all the antifungal experiments. Thirty-six grams of PDA in one liter

of deionized water was autoclaved and poured into the microbiological Petri plates. The fungus was sub-cultured in the PDA media, and fungal plates were incubated for 5 days at room temperature in the dark. Then the plates were exposed to 14 h darkness/12 h light at 21°C for 6 days to induce sporulation. The cultured plates were stored at room temperature in the dark until inoculum preparation.

3.2.3.2 Preparation of inoculum

To obtain spore suspension, the culture plate was flooded with 10 mL of sterile Sabouraud Maltose Broth (SMB) containing 0.1% Tween 80 (VWR, Randor, PA). Conidia were dislodged using a sterile FisherBrand cell spreader (Fisher Scientific, Hampton, NH). Then the resulting suspension was filtered through 4 layers of sterile cheesecloth (De Bona *et al.*, 2019). Spore concentrations were determined with a hemocytometer (Hausser Scientific, Horsham, PA) and adjusted to $5x10^5$ spores mL^{-1} using sterile double deionized water.

3.2.4 Antifungal activity assays

3.2.4.1 *In vitro* plate assays

PDA amended with leaf extract (2.5 mL in 100mLPDA) or cell suspension (5 mL in 100 mL PDA) was poured into Petri plates having two compartments (I plates) (Fig. 51 and 52). Each assay consisted of 10 plates and was repeated three times for each grape variety. The plates were challenged with fungal inoculum to test antifungal activity. One-half of the I plate was inoculated by spraying a spore suspension of $5x10^5$ conidia per mL to runoff. The non-inoculated half was sprayed with sterile water, as a negative control. Then the plates were placed in the dark (25±2°C). The mycelial growth of *B. cinerea* was assessed two, three,

five, and seven days after inoculation by measuring the growth of fungus vertically and horizontally across the lesion (D1 and D2 as diameters) and the growth area was calculated using the formula $Area = \pi[\frac{D1}{2} * \frac{D2}{2}]$ (Hendricks *et al.*, 2017). The area of the mycelial growth was expressed as the area of fungal growth (AFG). The plates were evaluated for disease incidence on day 7, using the formula: disease incidence = (the number of spores/the total area of the plate) x 100%. The conidia were dislodged using sterile water, the resulting suspension was filtered through 4 layers cheese cloth and the spores were counted using hemocytometer. The design of experiment followed a complete randomized design.

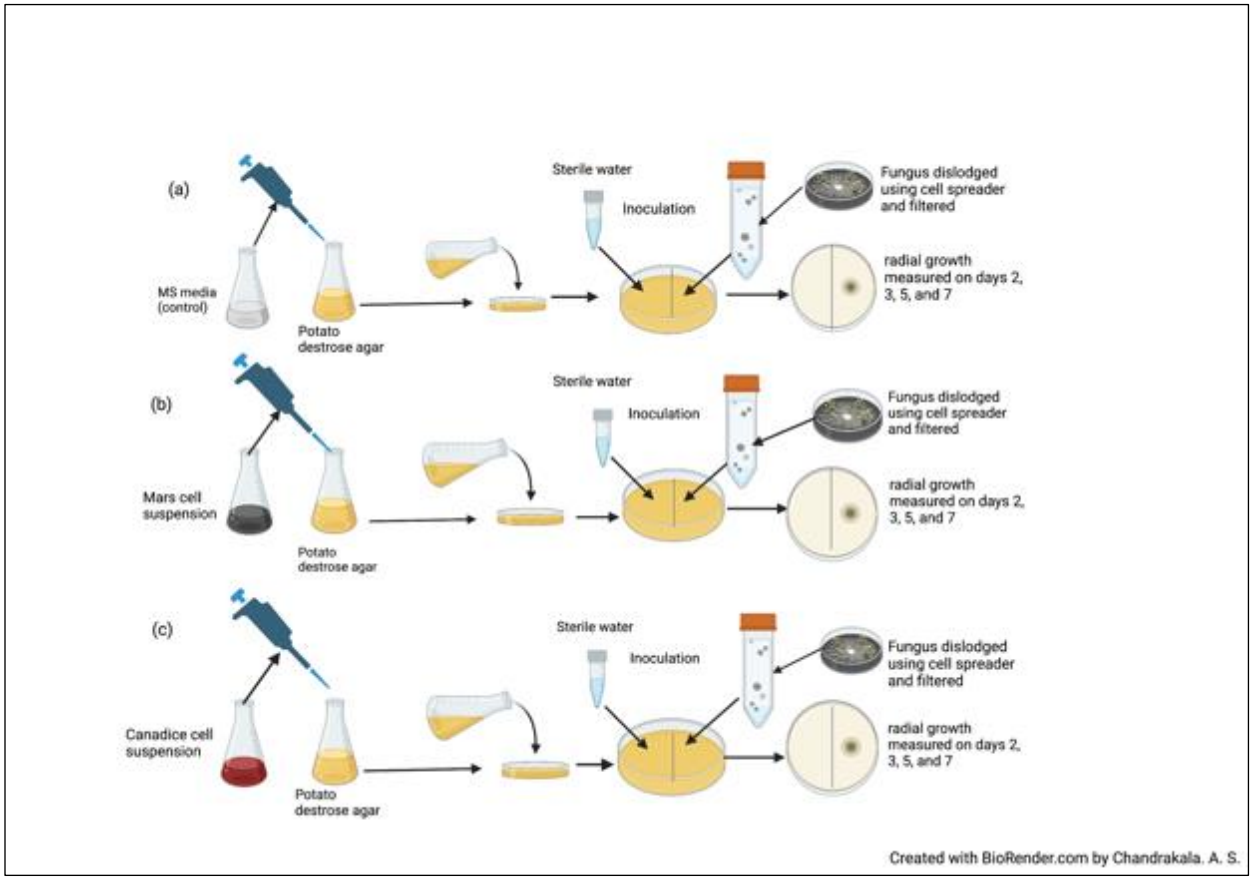

Figure 51. Assay diagram of the antifungal activity cell suspension cultures (a) control (b) Mars and (c) Canadice against *B. cinerea.*

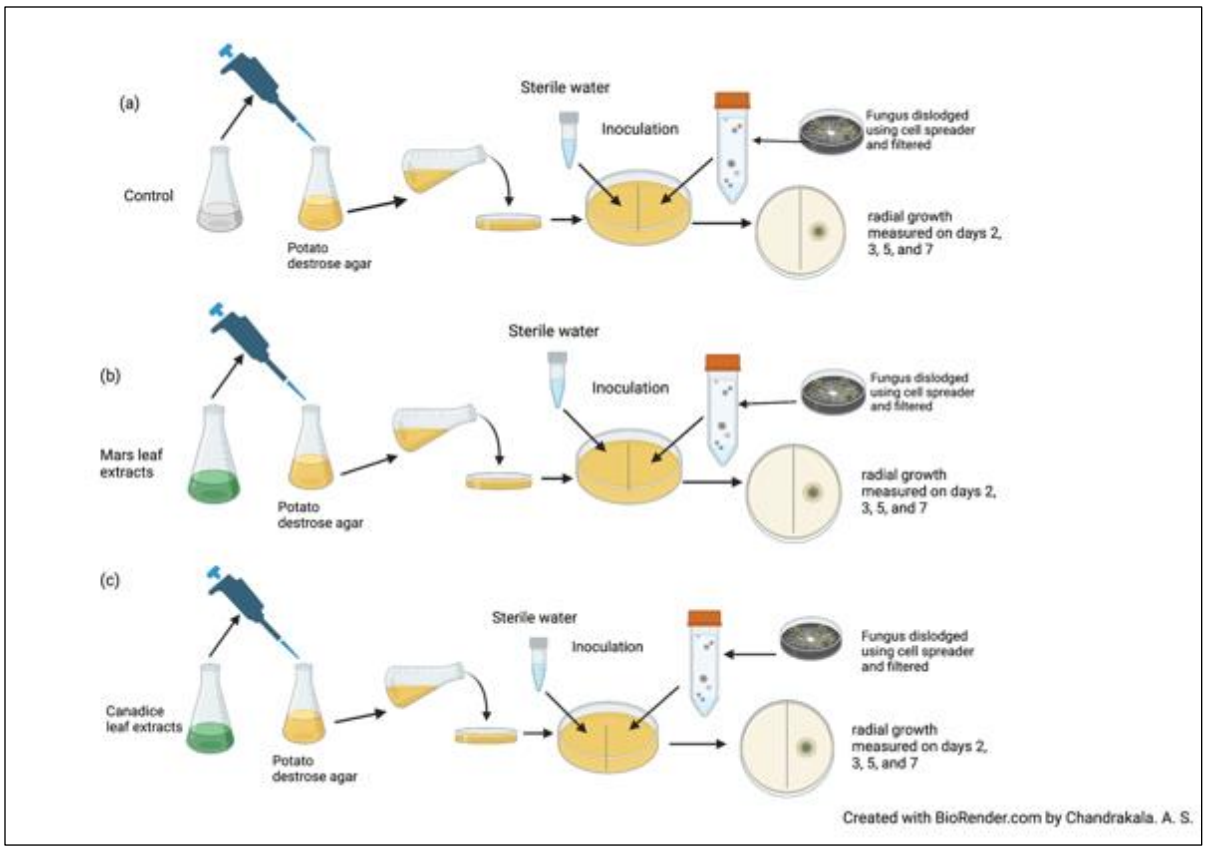

Figure 52. Assay diagram of the antifungal activity of senescent leaf extracts (a) Control (b) Mars and (c) Canadice against *B. cinerea.*

3.2.4.2 Detached leaf assay

Mars leaves were collected from greenhouse-grown grapevines and brought to the lab using a lab cooler. The leaves were sprayed with 500 µL of Mars ethanolic extract, water control, and ethanol control. Ten leaves were sprayed per treatment, and the experiment was repeated twice. The treated leaves were placed in Petri dishes with water agar media. Then leaves were inoculated with a 10 µL of 5 x 10^5 spores mL^{-1} suspension of *B. cinerea.* After inoculation, the Petri dishes were incubated in the dark. Lesions were counted in each leaf, and disease severity was calculated using the number of lesions formed from the number of leaves infected.

3.2.4.3 Detached grape berry assays

Store brought table grapes (variety unknown) were treated with Mars and Canadice leaf extracts (water, ethanolic and methanolic extracts). Another assay was conducted using Mars grapes treated with cell suspension cultures (control, Mars, and Canadice cell suspension extracts). Table grape berries were sprayed with 1 mL of leaf extract solutions (500 mg/mL) and 1 mL of cell suspension culture. The appropriate water, ethanol, methanol, or MS media controls was used. After being air-dried at room temperature for 30 minutes, each berry was inoculated with 10 µL of $5x10^5$ conidia per mL of *B. cinerea* to runoff. All the berries were placed in plastic containers and kept at 22 °C in the dark for 7 days. Disease incidence was calculated by counting the percentage of infected berries on day 4 and day 7, and rot lesion diameter was measured on day 4 and day 7. Rot % = number of rotten berries/10 berries (which is number of total berries per treatment). The rot lesion diameter was calculated from the mycelial growth of *B. cinerea*, that was assessed by measuring vertically and horizontally across the lesion (D1 and D2 as diameters) and the area of the fungal growth was calculated using the following formula $Area = \pi \left[\frac{D1}{2} * \frac{D2}{2}\right]$ (Hendricks *et al.*, 2017). The area of the mycelial growth was calculated both 4- and 7-days post-inoculation and expressed as the area of the fungal growth (AFG). The design of experiment followed a complete randomized design. The experiment was repeated twice with four replicates, consisting of 10 berries per treatment (Xu *et al.*, 2018*b*).

3.2.4.4 Greenhouse assays

Grape leaf ethanolic extracts were sprayed on the greenhouse-grown grapevine plants at concentration (500 mg/mL) until runoff. Sterile distilled water and 80% ethanol were used as

a control. Eight replicates were used for each treatment, as represented in Fig. 53. The experiment was repeated twice. Three leaves from each plant were challenged by spraying a $5x10^5$ *B. cinerea* conidia per mL to runoff using the inoculum described above (Langcake, 1981*b*; El-Khateeb *et al.*, 2013; De Bona *et al.*, 2019; De Bona *et al.*, 2020). After inoculation, the leaves were covered using Ziploc bags and maintained at 18°C and 65% relative humidity in the greenhouse. Two, three, five-, and seven-days post-inoculation, the plants were evaluated for disease incidence (Fig. 64). Disease incidence = (the number of lesions/three leaves) x 100%.

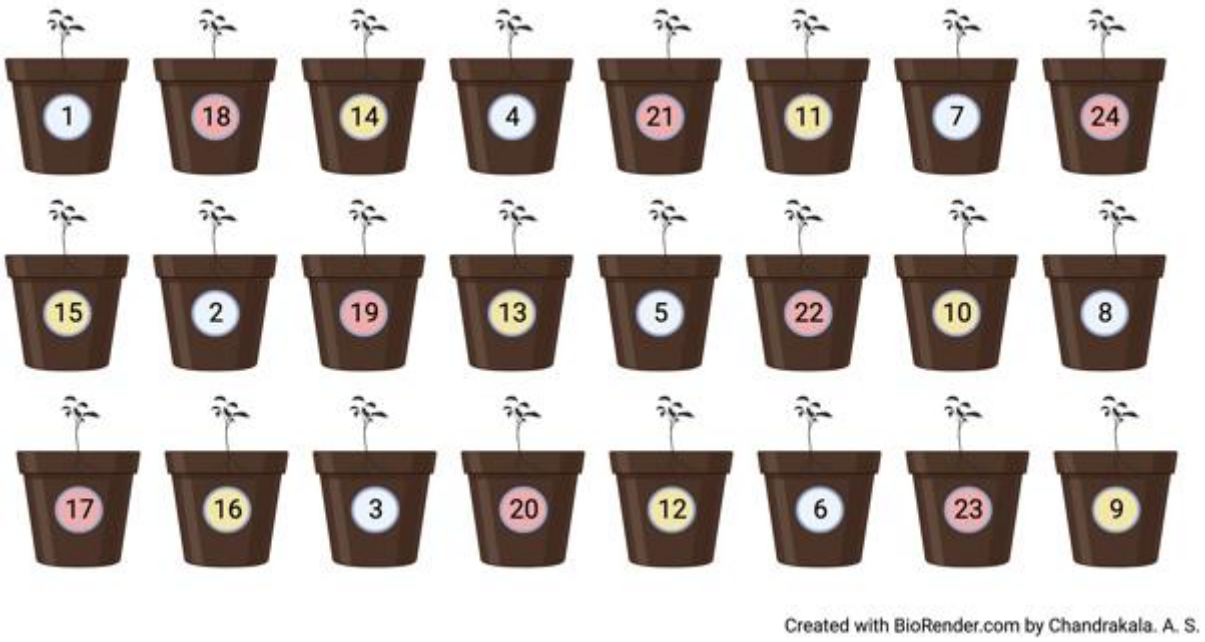

Figure 53. Greenhouse assay diagram: Antifungal assay set up in greenhouse in a complete randomized design**.** Pots numbered 1-8 in white color circles were treated with water control, pots numbered 9-16 in yellow color circles were treated with ethanol control, and pots numbered 17-24 in pink color circles were treated with Canadice ethanolic leaf extract. After treatment, plants were challenged with *B. cinerea*. There were 8 pots per treatment.

3.2.5 Statistical analysis

Data analysis was performed using PRISM 9.0 version (Graphpad, CA). Data for Petri dish, *in planta*, and berry experiments were analyzed using a two-way analysis of variance (two-

way ANOVA). The results showed significant interaction of treatment x time effect on area of fungal growth. Then the simple effects were performed by one-way ANOVA for each day (day 2, 3, 5, and 7 separately) and Tukey's multiple comparison to identify differences among the treatments and to determine the treated extract having the lower AFG of *B. cinerea*. One-way ANOVA was performed to analyze the spore count generated from the plate assays (for both leaf extracts and cell suspension cultures) and detached leaf assay. Tukey's multiple comparison procedure was used to identify differences among the treatments and thus determine the extract with greatest antifungal activity against *B. cinerea*. The metabolic profiling for each grape variety, and the fold difference of identified compounds present in leaf and cell suspension culture were calculated. Fold difference is the measure of change in the identified compound between leaf and cell suspension culture and vice versa. The top 10 compounds higher in leaves compared to cell cultures and the 10 compounds higher in cell cultures compared to leaves, respectively, were identified.

3.3 Results

3.3.1 *In vitro* antifungal activity of cell suspension cultures against *Botrytis cinerea*

For cell suspension cultures, due to significant interaction effect of treatment and time ($P < 0.0001$) (Fig 54), the diameter of fungal growth was increasing with time (from day 2 to 7) and was different between the I-plates treated with suspension culture and control. Mars and Canadice cell suspension culture treated plates had smaller AFG when compared to control after challenging with *B. cinerea*. Then simple effects were analyzed for each day separately between treatments. For day 2, I-plates treated with both Mars and Canadice cell suspension culture had significantly lower AFG of *B. cinerea* compared to the control ($P < 0.0001$). The

Mars cell suspension had significantly lower AFG of *B. cinerea* compared to Canadice cell suspension (P = 0.0002). For both day 3 and day 5, Mars and Canadice cell suspension treated I-plates had significantly lower AFG of *B. cinerea* compared to control (P < 0.0001) and those treated with Mars cell suspension had significantly lower AFG than Canadice cell suspension (P = 0.0035; P < 0.0001 respectively). On day 7, Mars and Canadice cell suspension treated I plates still had a significantly lower AFG of *B. cinerea* compared to control (P < 0.0001; P = 0.0073, respectively). There was no significant effect of Mars cell suspension on AFG of *B. cinerea* compared to Canadice cell suspension.

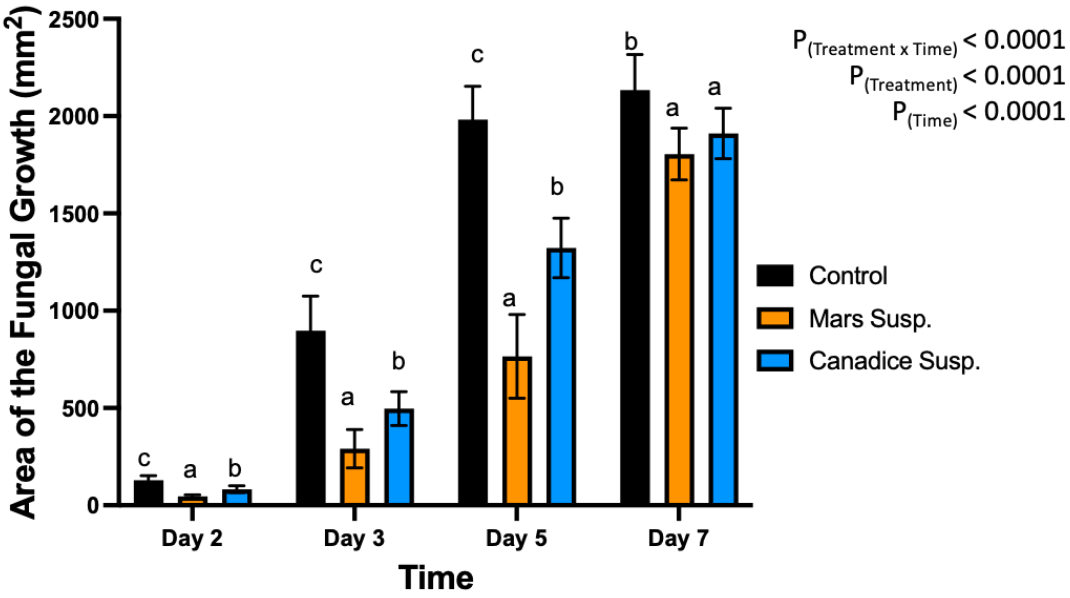

Figure 54. Bar graphs represent the antifungal activity of Mars and Canadice cell suspension cultures on area of the fungal growth (AFG) of *B. cinerea* on days 2, 3, 5, and 7 *in vitro*. Bars show mean ± SE; (n=10). Given significant interaction effect of treatment and time (P < 0.0001) simple effects ANOVAs and Tukey multiple comparison, P < 0.05 were performed separately for each day; different letters indicate significant differences. Black bars (control), orange bars (Mars suspension) and blue bar (Canadice suspension) respectively.

Cell suspension culture treated I-plates not only had lower area of fungal growth, but also had lower number of spores when compared to control. I-plates treated with Mars and Canadice cell suspension culture had significantly lower number of spores of *B. cinerea* compared to the control (Fig. 55; P < 0.0001). Furthermore, those treated with Mars cell

suspension had significantly fewer spores of *B. cinerea* than those treated with Canadice cell suspension culture (Fig. 55; P = 0.0002).

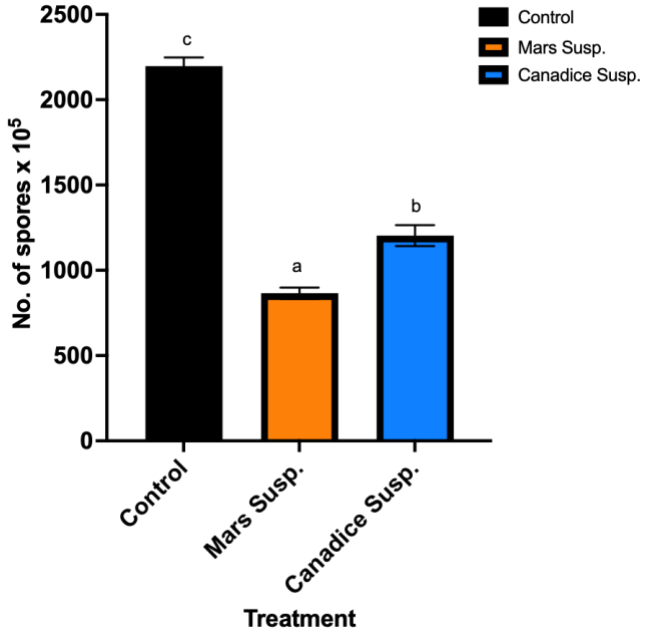

Figure 55. Bar graphs represent the number of spores produced on day 7 of the effect of antifungal activity of cell suspensions on the growth of *B. cinerea in vitro*. Values shown are mean ±SE (n=10). Control (black bar), Mars (orange bar), and Canadice (blue bar). (one-way ANOVA, Tukey multiple comparison, P < 0.05). Different letters indicate significant differences.

3.3.2 *In vitro* antifungal activity of field-collected leaf extracts against *Botrytis cinerea*

The *in vitro* assay using I plates treated with different extracts of senescent leaves were tested against the activity of *B. cinerea.* Overall, the Mars leaf ethanolic and methanolic extracts treated I-plates had the lower growth when compared to all the other treatments. The main effects and simple effects were analyzed to compare treatments for each day separately.

For senescent leaf water extracts, there was a significant interaction effect of treatment x time (P =0.0015). Mars and Canadice leaf water extract treated plates had smaller AFG when compared to water control after challenging with *B. cinerea*. Then the simple effects were analyzed for each day separately to compare treatments (Fig 56). For day 2, I-plates treated with Mars leaf water extract had significantly lower AFG of *B. cinerea* compared to water

control (P = 0.0049) and Canadice leaf extract (P = 0.0019), which did not differ significantly. For day 3 Mars and Canadice leaf extracts had significantly lower AFG of *B. cinerea* compared to the water control (P = 0.0077). There was no significant different AFG between Canadice and Mars leaf water extracts. On both day 5 and 7, Mars leaf water extract had significantly lower AFG of *B. cinerea* compared to water control (P < 0.0001) but was only significantly different from Canadice leaf water extract on day 7 (P = 0.0007). Water control and Canadice leaf water extract did not differ significantly on these days.

For senescent leaf ethanolic extracts, there was a significant interaction effect of treatment x time (P < 0.0001). Mars and Canadice leaf ethanolic extract treated plates had smaller AFG when compared to ethanol control after challenging with *B. cinerea*. Then simple effects were analyzed separately for each day between treatments (Fig 57). On day 2, I-plates treated with Mars and Canadice leaf ethanolic extract had significantly lower AFG of *B. cinerea* compared to the ethanol control (P < 0.0001), but the ethanolic extracts were not different from each other. On days 3 and 5, Mars and Canadice leaf ethanolic extracts had a significantly lower AFG of *B. cinerea* compared to ethanol control (P < 0.0001). Mars leaf ethanolic extracts had significantly lower AFG of *B. cinerea* compared to Canadice leaf ethanolic extracts (P = 0.0003; P < 0.0001 respectively). For day 7, Mars and Canadice leaf ethanolic extract had significantly lower AFG of *B. cinerea* compared to ethanol control (P < 0.0001) but were not significantly different from each other.

For senescent leaf methanolic extracts, there was a significant interaction effect of treatment x time (P < 0.0001). Overall, Mars and Canadice leaf ethanolic extract treated plates had smaller AFG when compared to methanol control after challenging with *B. cinerea*. The data

were then analyzed for each day separately for simple effects (Fig 58). For day 2, I-plates treated with Mars and Canadice leaf methanolic extract had significantly lower AFG of *B. cinerea* compared to the methanol control ($P < 0.0001$), but two extracts did not differ from one another. On day 3, both Mars and Canadice leaf ethanolic extracts had a significantly lower AFG of *B. cinerea* compared to methanol control ($P < 0.0001$), and Mars leaf methanolic extracts had a significantly lower AFG of *B. cinerea* compared to Canadice leaf methanolic extract ($P < 0.0001$). For day 5, Mars leaf methanolic extracts had a significantly lower AFG of *B. cinerea* compared to methanol control ($P < 0.0001$), and Canadice leaf methanolic extract ($P < 0.0001$). There was no significant effect of Canadice leaf methanolic extracts on AFG of *B. cinerea* compared to methanol control. For day 7, Mars leaf methanolic extract had a significantly lower AFG of *B. cinerea* compared to control and Canadice leaf methanolic extract ($P < 0.0001$). Canadice leaf methanolic extract had a significantly lower AFG of *B. cinerea* compared to methanol control ($P = 0.0340$).

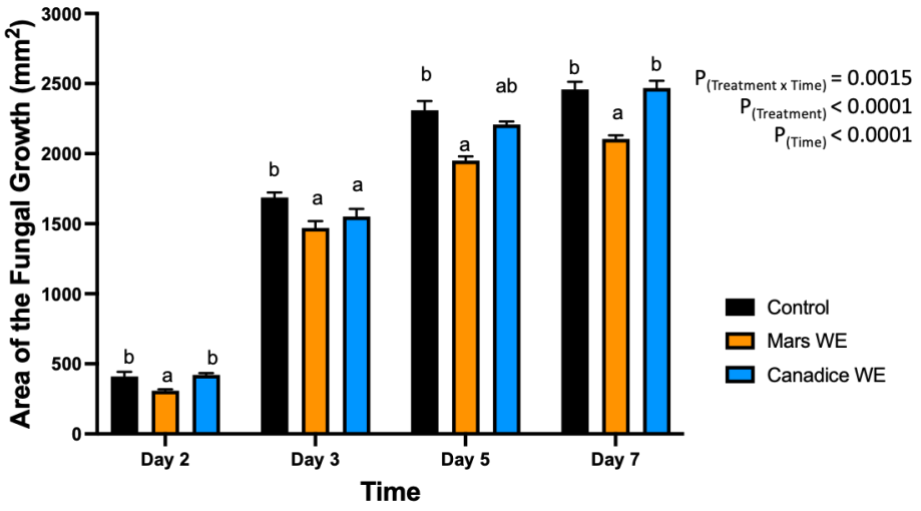

Figure 56. Bar graphs represent the antifungal activity of water extracts of Mars and Canadice leaf on area of the fungal growth (AFG) of *B. cinerea* on days 2, 3, 5, and 7 *in vitro*. Bars show mean ± SE; (n=10). Given significant interaction effect of treatment and time ($P = 0.0015$) simple effects ANOVAs and Tukey multiple comparison, $P < 0.05$ were performed separately for each day; different letters indicate significant differences. Black bars (water control), orange bars (Mars water extract (Mars WE)) and blue bar (Canadice water extract Canadice (WE)) respectively.

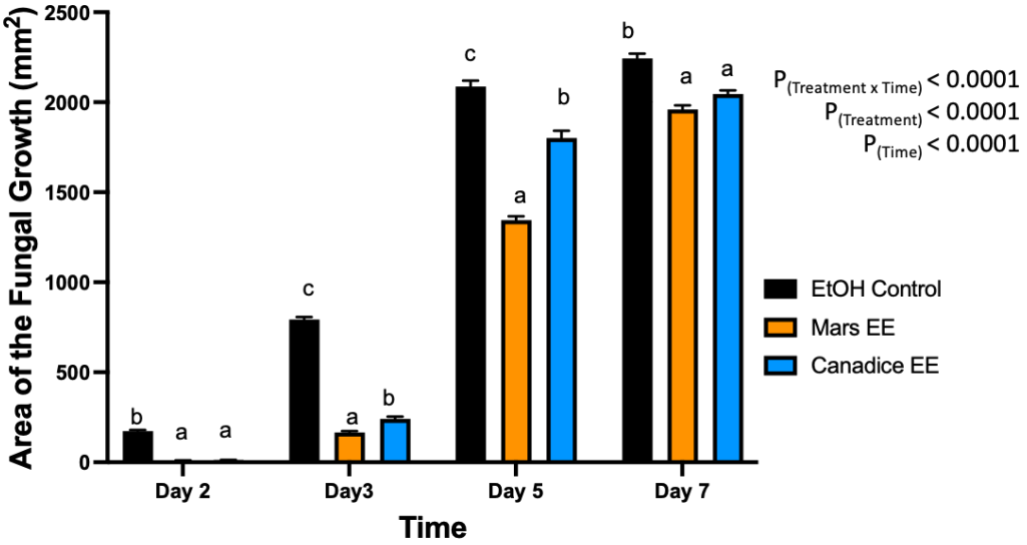

Figure 57. Bar graphs represent the antifungal activity of ethanolic extracts of Mars and Canadice leaves on area of the fungal growth (AFG) of *B. cinerea* on days 2, 3, 5, and 7 *in vitro*. Bars show mean ± SE; (n=10). Given significant interaction effect of treatment and time ($P < 0.0001$) simple effects ANOVAs and Tukey multiple comparison, $P < 0.05$ were performed separately for each day; different letters indicate significant differences. Black bars (ethanol control (EtOH), orange bars (Mars ethanolic extract (Mars EE)) and blue bar (Canadice ethanolic extract (Canadice EE)) respectively.

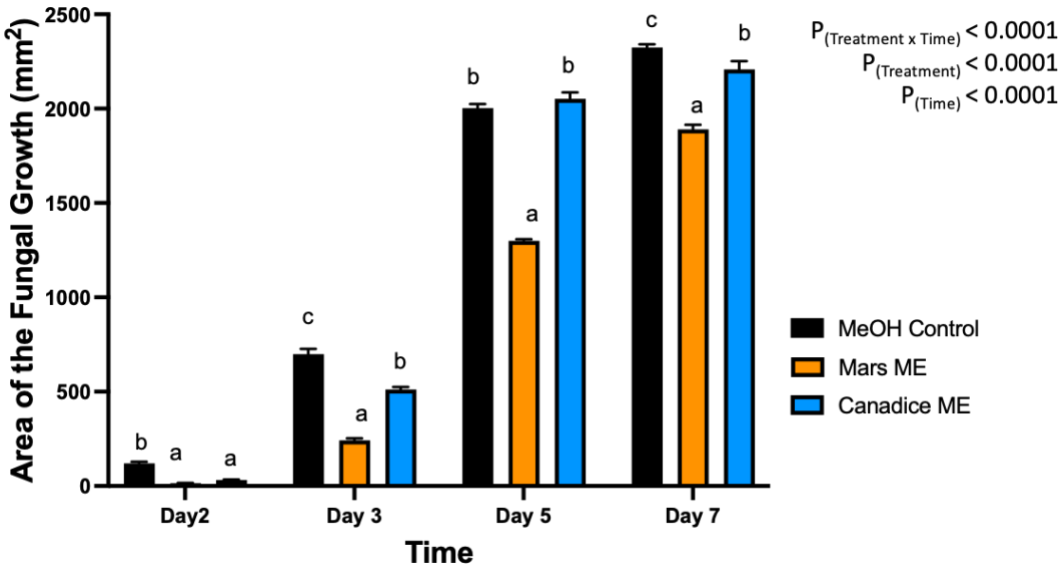

Figure 58. Bar graphs represent the antifungal activity of methanolic extracts of Mars and Canadice leaves on area of the fungal growth (AFG) of *B. cinerea* on days 2, 3, 5, and 7 *in vitro*. Bars show mean ± SE; (n=10). Given significant interaction effect of treatment and time ($P < 0.0001$) simple effects ANOVAs and Tukey multiple comparison, $P < 0.05$ were performed separately for each day; different letters indicate significant differences. Black bars (methanol control (MeOH)), orange bars (Mars methanolic extract (Mars ME)) and blue bar (Canadice methanolic extract Canadice (ME)) respectively.

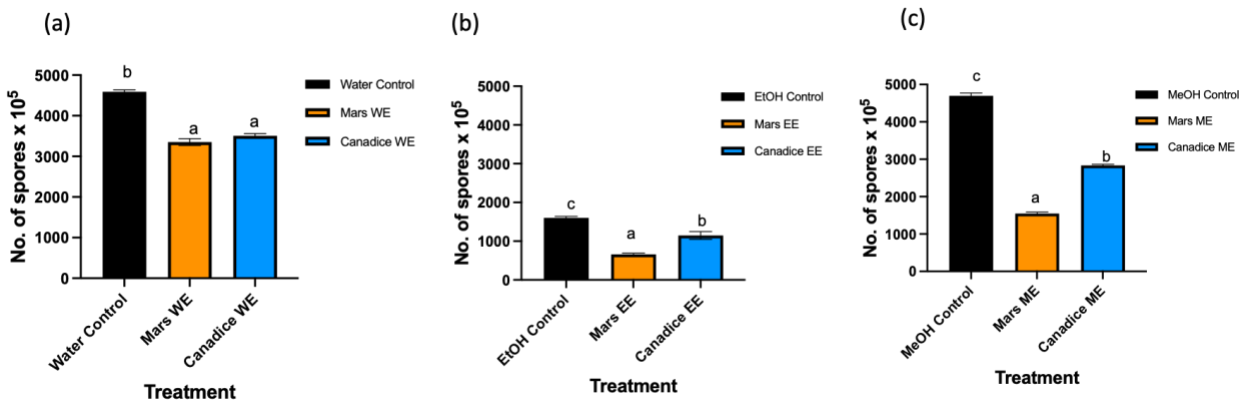

Figure 59. Bar graphs represent the number of spores produced on day 7 of *B. cinerea in vitro* for the treatment the antifungal activity of (a) Water extracts (b) Ethanolic and (c) Methanolic extracts of Mars and Canadice senescent leaves. Control (black bar), Mars extract (orange bar), and Canadice extract (blue bar). Values shown are mean ±SE (n=10). (one-way ANOVA, Tukey multiple comparison, $P < 0.05$). Different letters indicate significant differences. (WE represent water extract, EE represent ethanol extract, and ME represent methanol extract).

Senescent leaf extracts not only reduced fungal growth, but also reduced spore production for *B. cinerea.* I-plates treated with both Mars and Canadice leaf water extracts had significantly lower number of spores of *B. cinerea* compared to the water control (Fig. 59a; $P < 0.0001$). The I-plates treated with Mars leaf ethanolic and methanolic extracts had significantly lower number of spores of *B. cinerea* compared to the ethanol and methanol control, respectively (Fig. 59b and c; $P < 0.0001$). For both ethanolic and methanolic extracts (but not water), Mars leaf extracts had significantly lower number of spores of *B. cinerea* compared to the Canadice leaf extracts (Fig. 59a-c; $P < 0.0001$)

3.3.3 Effectiveness of cell suspension cultures in controlling *Botrytis cinerea* in berries

The Mars berries were treated with Mars and Canadice cell suspension cultures and the control and then challenged with *B. cinerea.* The lesion diameter was measured and calculated as area of fungal growth (AFG) and analyzed for main and simple effects using ANOVA.

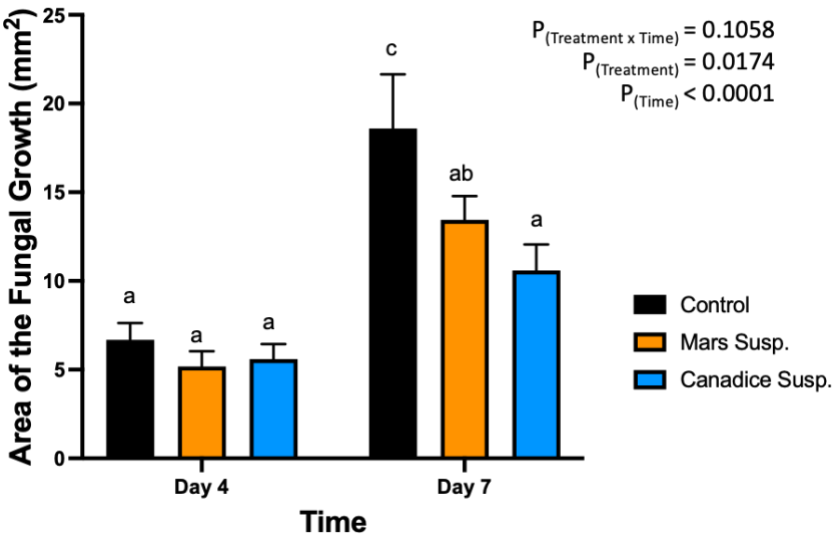

Figure 60. Bar graphs represent the effect of antifungal activity of Mars and Canadice cell suspension cultures on the area of the fungal growth (AFG) of *B. cinerea* in detached berries. Values shown are mean ± SE (n=10). Given significant effect of treatment (P = 0.0174) and time (P < 0.0001) simple effects ANOVAs and Tukey multiple comparison, P < 0.05 were performed separately for each day; different letters indicate significant differences. Black bar (control), orange bar (Mars suspension), and blue bar (Canadice suspension).

In Mars berries, there was significant effect of treatment (P = 0.0174) and time (P < 0.0001) (Fig. 60). The area of the fungal growth increased with time, and Mars and Canadice suspension culture treated berries had smaller AFG when compared to control after challenging with *B. cinerea*. Then simple effects were analyzed separately for day 4 and 7. On day 4, all three treatments (Mars and Canadice cell suspension, and control) had no significant effect on AFG of *B. cinerea.* On day 7, there was a significant effect of Canadice cell suspension culture on AFG of *B. cinerea* compared to control (P = 0.0269). The Mars suspension culture had no effect on AFG of *B. cinerea* compared to control and Canadice suspension culture.

No rotten berries were seen on day 4 or 7 when challenged with *B. cinerea* and thus rot % was not calculated. (data not shown).

3.3.4 Effectiveness of field-collected grapevine leaf extracts in controlling *Botrytis cinerea* in leaves and berries

After treated with water control, ethanol control, and Canadice ethanolic extracts greenhouse grown Canadice grapevines were challenged with *B. cinerea.* The number of lesions formed on the leaves were counted as represented in Fig. 61. The two-way ANOVA results showed a significant effect of treatment (Fig. 63a; P = 0.0006). Then simple effects were analyzed separately for day 7 and 14. For day 7, the three treatments had no significant effect on number of lesions of *B. cinerea* formed on the treated leaves. On day 14, Canadice ethanolic extract had reduced number of lesions compared to water and ethanol control. The Canadice leaf ethanolic extract had significant effect on number of lesions of *B. cinerea* compared to the ethanol control (P = 0.0034), but no effect compared to water control. Treatment of water control had a significantly reduced number of lesions *B. cinerea* compared to the ethanol control (P = 0.0261).

Figure 61. Representative Canadice grapevines treated with senescent leaf extracts (A) Water control (B) Ethanol control and (C) Canadice ethanolic extracts and challenged with *B. cinerea in planta* assay**.**

Mars detached leaves treated with water control, ethanol control, and Mars ethanolic extracts were challenged with *B. cinerea.* Then the number lesions formed were counted on day 7 and subjected to analyses to compare treatments shown in Fig. 62.

Figure 62. Representative Mars leaves challenged with B. cinerea in a detached leaf assay after having been pre-treated with (A) Water control (B) Ethanol control, and (C) Mars leaf ethanolic extracts and number of lesions counted on day 7.

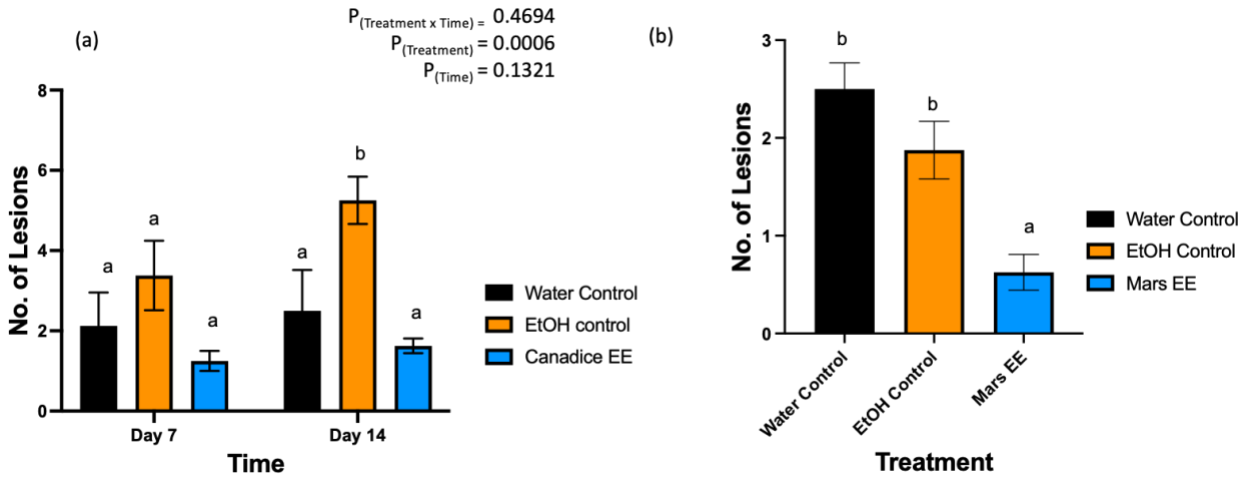

Figure 63. Bar graphs represent the effect of antifungal activity of Mars and Canadice senescent leaf extracts on the (a) number of lesions formed after being challenged with *B. cinerea* on Canadice leaves in an *in planta* assay. Water control (black bar), ethanol control (orange bar), and Canadice ethanolic extract (blue bar). Values shown are mean ± SE (n=8). Given significant treatment effect (P = 0.0006), simple effects were analyzed by one way ANOVA for each day (day 4 and 7) separately with Tukey multiple comparison, P < 0.05); different letters indicate significant differences. (b) number of lesions formed after challenged with *B. cinerea* on Mars leaves in detached leaf assay on day 7. Values shown are mean ± SE (n=8). (one-way ANOVA, Tukey multiple comparison, P < 0.05). Water control (black bar), ethanol control (orange bar), and Mars ethanolic extract (blue bar). Different letters indicate significant differences. EE is ethanolic extract.

Mars detached leaves treated with Mars ethanolic extracts had significantly reduced number of lesions of *B. cinerea* compared to both the water and the ethanol control (Fig. 63b; $P < 0.0001$and $P = 0.0059$, respectively). There was no significant effect of water control on number of lesions *B. cinerea* compared to ethanol control.

The detached store-bought green berries (variety unknown) were treated with both Mars and Canadice leaf extracts and then challenged with *B. cinerea.* The area of fungal growth was calculated and analyzed for difference between treatments. The green berries treated with grape leaf water extracts had a significant interaction effect of treatment x time ($P =0.0008$) (Fig. 64). Simple effects were analyzed for day 4 and 7 separately. For day 4, Mars and Canadice leaf water extracts had a significantly lower AFG of *B. cinerea* compared to water control ($P < 0.0001$). Mars leaf water extract had no significant effect on AFG of *B. cinerea* compared to the Canadice leaf water extract. On day 7, Mars leaf water extract had a significant effect on AFG of B. *cinerea* compared to water control and Canadice leaf water extract ($P < 0.0001$). There was no significant effect of Canadice leaf water extract on AFG of *B. cinerea* compared to water control.

Berries treated with leaf ethanolic extract had significant interaction effect of treatment x time ($P < 0.0001$) (Fig 65). The simple effects were analyzed for each day separately. On day 4, Mars and Canadice leaf ethanolic extract had significantly lower AFG of *B. cinerea* compared to ethanol control ($P < 0.0001$; $P = 0.0483$). There was a significant effect of Mars leaf ethanolic extract on AFG of *B. cinerea* compared to Canadice leaf ethanolic extract ($P = 0.001$). On day 7, Mars and Canadice leaf ethanolic extract had a significantly lower AFG of

B. cinerea compared to ethanol control ($P < 0.0001$). Mars leaf ethanolic extract had significantly lower AFG of *B. cinerea* compared to Canadice leaf ethanolic extract ($P < 0.0001$).

Berries treated with Mars and Canadice leaf methanolic extracts had significant interaction effect of treatment x time ($P < 0.0001$) (Fig 66). Simple effects were analyzed for each day separately to analyze the significance of each day between treatments. On day 4, Mars and Canadice leaf methanolic extract had significantly lower AFG of *B. cinerea* compared to the methanol control ($P = 0.0002$; $P = 0.0010$). There was no significant effect of Mars leaf methanolic extract on AFG of *B. cinerea* compared to Canadice leaf methanolic extract. On day 7, Mars leaf methanolic extract had significantly lower AFG of *B. cinerea* compared to Canadice leaf methanolic extract and methanol control ($P < 0.0001$). Canadice leaf methanolic extract had significantly lower AFG of *B. cinerea* compared to methanol control ($P < 0.0001$).

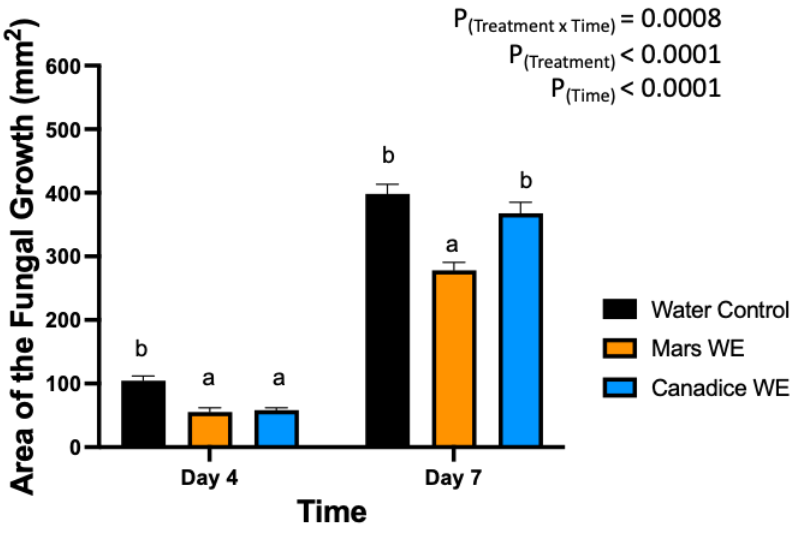

Figure 64. Bar graphs represent the antifungal activity of water extracts of Mars and Canadice leaves on area of the fungal growth (AFG) of *B. cinerea* on days 4 and 7 in detached berries. Bars show mean ± SE; (n=10). Given the significant interaction effect of treatment and time ($P = 0.0008$), simple effects ANOVAs were performed using one-way ANOVA, Tukey multiple comparison $P < 0.05$; different letters indicate significant differences. Black bars (water control), orange bars (Mars water extract (Mars WE)) and blue bar (Canadice water extract Canadice (WE)) respectively.

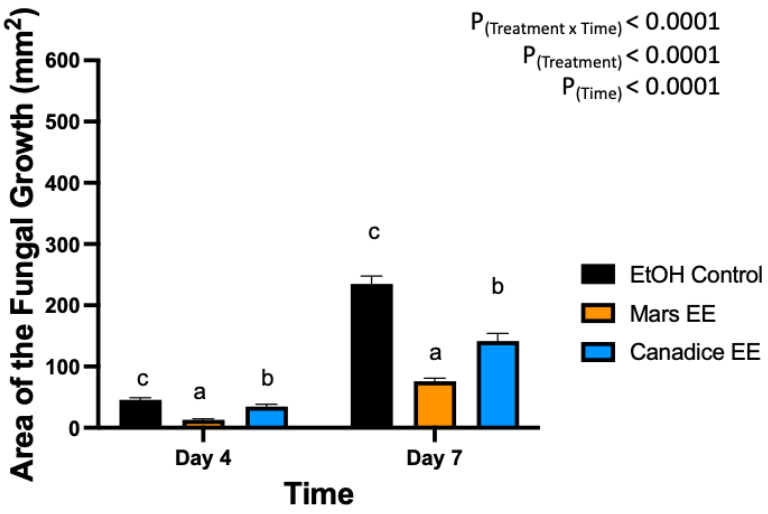

Figure 65. Bar graphs represent the antifungal activity of ethanolic extracts of Mars and Canadice leaves on area of the fungal growth (AFG) of *B. cinerea* on days 2, 3, 5, and 7 in detached berries. Bars show mean ± SE; (n=10). Given the significant interaction effect of treatment and time ($P < 0.0001$), simple effects ANOVAs were performed using one-way ANOVA, Tukey multiple comparison $P < 0.05$; different letters indicate significant differences. Black bars (ethanol control (EtOH)), orange bars (Mars ethanolic extract (Mars EE)) and blue bar (Canadice ethanolic extract (Canadice EE)) respectively.

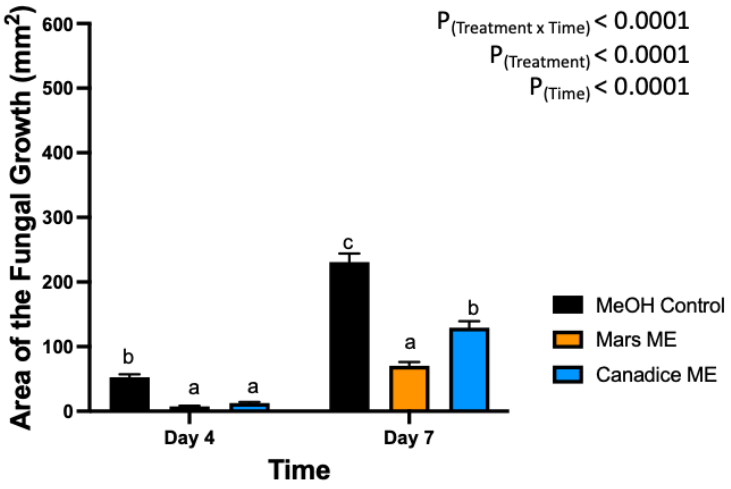

Figure 66. Bar graphs represent the antifungal activity of methanolic extracts of Mars and Canadice leaves on area of the fungal growth (AFG) of *B. cinerea* on days 4 and 7 in detached berries. Bars show mean ± SE; (n=10). Given the significant interaction effect of treatment and time ($P < 0.0001$), simple effects ANOVAs were performed using one-way ANOVA, Tukey multiple comparison $P < 0.05$; different letters indicate significant differences. Black bars (methanol control (MeOH)), orange bars (Mars methanolic extract (Mars ME)) and blue bar (Canadice methanolic extract (Canadice ME)) respectively.

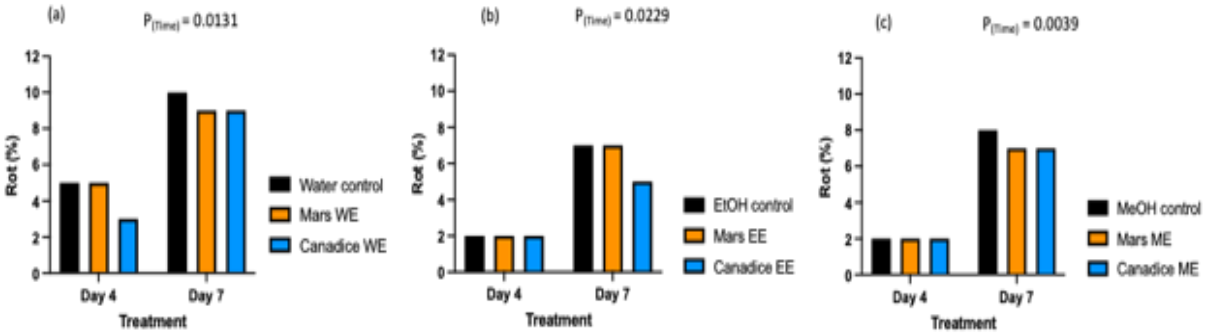

Figure 67. Bar graphs represent the effect of Mars and Canadice senescent leaf extracts on the rot (%) when challenged with *B. cinerea* on post-harvest green berries. Black bars represent control (water, ethanol, and methanol), orange bar represents Mars extracts, and blue bar represents Canadice extracts. Treatments are (a)Water extracts (b) Ethanolic extracts (C) Methanolic extracts. Values shown are mean ± SE (n=10). (Two-way ANOVA, Tukey multiple comparison, $P < 0.05$).

The rot percentage was higher for all the controls (water, ethanol, and methanol) when compared to the Mars and Canadice leaf extracts. The figure is representative of all treatments with respective controls, however the total rot percentage berries were calculated and used for statistical analysis. The analysis of two-way ANOVA shows that there was a significant effect of time on rot percentage for water extracts (Fig. 67a; P = 0.0131), ethanolic extracts (Fig. 67b; P = 0.0229), and methanolic extracts (Fig.67c; P = 0.0039).

3.3.5 Metabolic profiling of Mars and Canadice leaves and Cell Suspensions

The fold difference was calculated for metabolites that were identified using LC-MS analysis as described in methods section 3.2.2. The ten compounds with the greatest fold difference present in leaf versus cell suspension culture and vice versa for both grapevine varieties are listed in the Tables 7,8, 9, and 10.

Table 7. LC-MS data of the top 10 identified compounds that are higher in Mars leaves compared to cell suspension culture.

Name of the compound	Mars Leaf	Mars cell suspension	Fold difference (Leaf/Cell Susp.
Heptylbenzene	$1.69x10^3$	$8.24x10^7$	$4.87x10^4$
Dimethomorph	$8.42x10^2$	$3.98x10^7$	$4{,}73x10^4$
Indole-3-lactic acid	$1.27x10^3$	$4.95x10^7$	$3.89x10^4$
L- (+)-Tartaric acid	$1.39x10^4$	$3.76x10^8$	$2.71x10^4$
Esculin	$7.58x10^2$	$1.38x10^7$	$1.82x10^4$
(DSF) Diffusible signal factor (*cis*-11-methly-2-dodecenoic acid)	$1.79x10^3$	$2.99x10^7$	$1.67x10^4$
2-(2-phenylethoxy)-6-{[(3,4,5-trihydroxyoxan-2-yl)oxy]methyl}oxane-3,4,5-triol	$1.45x10^3$	$2.41x10^7$	$1.65x10^4$
L- (+)-Tartaric acid	$1.12x10^5$	$1.69x10^9$	$1.50x10^4$
1-[2-(3-Hydroxy-1-propen-2-yl)-2,3-dihydro-1-benzofuran-5-yl]ethanone	$1.5x10^3$	$2.16x10^7$	$1.40x10^4$
2-(2E)-2-Octen-1-ylcyclopentanone	$2.57x10^3$	$2.89x10^7$	$1.12x10^4$

Table 8. LC-MS data of the top 10 identified compounds that are higher in Mars cell suspension culture compared to leaves.

Name of the compound	Mars Leaf	Mars cell suspension	Fold difference (Cell Susp. /Leaf
Benzyladenine	$6.98x10^6$	$7.28x10^3$	$8.92x10^2$
N, N-Dimethylsphingosine	$4.43x10^6$	$1.32x10^3$	$3.33\ x10^2$
Cannabicitran	$8.16x10^5$	$2.74x10^3$	$2.97\ x10^2$
(2R)-1-(Octanoyloxy)-3-(phosphonooxy)-2-propanyl laurate	$2.89x10^5$	$1.36x10^3$	$2.12\ x10^2$
(2E,6E,10E)-13-[(2R)-6-Hydroxy-2,7,8-trimethyl-3,4-dihydro-2H-chromen-2-yl]-2,6,10-trimethyl-2,6,10-tridecatrienoic acid	3.52x105	$2.21x10^3$	$1.59\ x10^2$
2-[(1S,4S,5S)-5-Isopropyl-4-{[(isopropylcarbamoyl)amino]methyl}-2-methyl-2-cyclohexen-1-yl]-N-methyl-N-(3-pyridinylmethyl)acetamide	$7.77x10^5$	$5.57x10^3$	$1.39\ x10^2$
(22E)-Ergosta-5,7,22,24(28)-tetraen-3-ol	$4.61x10^5$	$3.55x10^3$	$1.29\ x10^2$
Tolcapone	$9.07x10^5$	$8.10x10^3$	$1.12\ x10^2$
Columbianetin	$1.61x10^6$	$1.51x10^3$	$1.07\ x10^2$
1-(1,8-dihydroxy-3,6-dimethyl-2-naphthyl) ethan-1-one	$6.37x10^5$	$6.16x10^3$	$1.03\ x10^2$

Table 9. LC-MS data of the top 10 identified compounds that are higher in Canadice leaves compared to cell suspension culture.

Name of the compound	Canadice Leaf	Canadice cell suspension	Fold difference (Leaf/Cell Susp)
Putaminoxin	$2.93x10^3$	$6.27x10^7$	$2.13x10^4$
1-Methyl-4-[(1E)-1-propen-1-yl]benzene	$4.40x10^3$	$9.19x10^8$	$2.08\ x10^4$
(1S,2S,3R,6S,1'S,2'S,3'R,6'S)-6,6'-Iminobis[4-(hydroxymethyl)-4-cyclohexene-1,2,3-triol]	$2.59x10^3$	$4.5\ x10^8$	$1.76x10^4$
1,1,6-Trimethyl-1,2-dihydronaphthalene	$3.22x10^3$	$5.4\ x10^7$	$1.64x10^4$
N-(4-Carbamimidamidobutyl)-5-{(1Z)-3-[(4-carbamimidamidobutyl)amino]-3-oxo-1-propen-1-yl}-7-hydroxy-2-(4-hydroxyphenyl)-2,3-dihydro-1-benzofuran-3-carboxamide	$7.42x10^2$	$8.18\ x10^6$	$1.10x10^4$
2-(3-phenylpropyl)oxolane	$8.60x10^3$	$9.36x10^7$	$1.08x10^4$
Piceol	$3.49x10^3$	$3.58x10^7$	$1.02x10^4$
3-(2-Oxopropyl)-2-pentylcyclopentanone	$5.48x10^3$	$5.3x10^7$	$9.83x10^3$
1,5-Anhydro-1-{2,4-dihydroxy-6-[(E)-2-(4-hydroxyphenyl)vinyl]phenyl}hexitol	$8.31x10^3$	$6.4x10^7$	$7.78x10^3$
Indole-3-lactic acid	$5.75x10^3$	$4.25x10^7$	$7.38x10^3$

Table 10. LC-MS data of the top 10 identified compounds that are higher in Canadice cell suspension culture compared to leaves.

Name of the compound	Canadice Leaf	Canadice cell suspension	Fold difference (Cell Susp /Leaf
3-O-(3-Methylbutanoyl)-beta-D-fructofuranosyl 2-O-acetyl-3-O-dodecanoyl-alpha-D-glucopyranoside	$7.00x10^5$	$1.11x10^3$	$6.26x10^2$
2,3,14,20-Tetrahydroxy-22,23-epoxyergost-7-en-6-one	$1.22x10^6$	$2.22x10^3$	$5.50x10^2$
16-Heptadecyne-1,2,4-triol	$2.93x10^6$	$1.08x10^4$	$2.71x10^2$
1,5-Dihydroxy-3,4-dimethoxy-10-methyl-9(10H)-acridinone	$1.56x10^6$	$7.35x10^3$	$2.13x10^2$
3-O-(3-Methylbutanoyl)-beta-D-fructofuranosyl 3-O-dodecanoyl-alpha-D-glucopyranoside	$2.94x10^5$	$1.52x10^3$	$1.93x10^2$
Benzyladenine	$1.31x10^6$	$7.49x10^3$	$1.75x10^2$
9(S)-HpOTrE	$4.18x10^5$	$2.84x10^3$	$1.47x10^2$
(2R)-1-(Octanoyloxy)-3-(phosphonooxy)-2-propanyl laurate	$6.57x10^4$	$4.69x10^2$	$1.40x10^2$
Ambruticin	$1.89x10^6$	$1.39x10^4$	$1.36x10^2$
Stearamide	$1.16x10^6$	$9.79x10^3$	$1.18x10^2$

3.4 Discussion

Results of this study suggest that grapevine derived products (both cell suspension cultures and senescent leaf extracts) could inhibit the growth of *B. cinerea* on grapevine foliage and post-harvest berries and be used in the viticulture as part of an IPM program to manage Botrytis. Use of grapevine-derived products as part of prevention of *B. cinerea* growth was demonstrated using greenhouse grown grapevines (Khawand *et al.*, 2021). Additional research is needed to evaluate the efficacy of grapevine-derived products compared with fungicides and to investigate the compatibility with other growing practices that are used in the vineyard. While other grapevine-derived products such as cane extracts, wood extracts, and berry skin extracts have been shown to suppress *B. cinerea* growth *in planta*, post-harvest berries, and *in vitro* studies (Guerrero *et al.*, 2016; Richard *et al.*, 2016; De Bona *et al.*, 2019), our study builds on this knowledge, by characterizing the suppression of Botrytis on greenhouse grown cold-hardy table grapevines. The results also indicate that antifungal activity differed among the grape varieties and different grapevine-derived products. Additionally, the efficacy of grapevine-derived products shown *in vitro* was not always confirmed by *in planta* and post-harvest berries.

3.4.1 The efficacy of cell suspensions differed between *in vitro, in planta* and detached berry assays

Our study utilized cell suspension cultures produced from Mars and Canadice and the results suggest that the cell suspension cultures have some antifungal activity on mycelial growth of *B. cinerea* when tested in Petri plate assay. A previous study was performed using *callus* produced from two American varieties (*V. riparia* and *V. rupestris),* two hybrids *(V. vinifera* and American species), and one *V. vinifera* to test their antifungal activity (Dai *et al.*,

1995*a*,*b*,*c*). According to Dai *et al.*, (1995) when *callus* from different resistant and susceptible grapevines were inoculated with the downy mildew causing organism, there was the development of short hyphae and necrosis on *callus* produced from resistant varieties and long hyphae with heavy sporulation on *callus* produced from susceptible varieties. Furthermore, this study showed that gallocatechin derivatives, induced flavonoids, and suberized cell walls played a major role in resisting the growth of *Plasmopara viticola* in the grapevine callus produced from resistant cultivars (Dai *et al.*, 1995*a*).

In our study, cell suspension cultures did not show an antifungal effect in the detached berry assay. Lesions were formed in both control and cell suspension culture treated berries, and the area of fungal growth (AFG) calculated for the extracts did not vary significantly. The Mars berries used were grown in the UNH vineyard and they have been suggested to be somewhat resistant varieties to many fungal pathogens (Sideman and Hamilton, 2016, 2019). The resistance capacity of Mars might have played a role in the development of lesion on the berries when challenged by *B. cinerea* as part of the detached berries assay. The results show that a lesion was formed and the size of the lesion increased from day 4 to day 7 in the inoculated area, but there were no rotten berries. The same assay was also conducted using UNH vineyard-grown Canadice (data not shown), which also had similar results on lesion size area which increased from day 4 to day 7 with no rotten berries. *In planta* assays using cell suspension treatments were not conducted due to unavailability of grapevines but should be conducted in the future.

The results of metabolic profiling of cell suspension cultures of both grape varieties and their fold difference when compared to leaf samples were identified and 10 compounds with the

greatest differences are in Table 8 and 10. In previous research few compounds from the list were reported to have antimicrobial activity, e.g., cannabicitran, columbianetin, 9(S)-HpOTrE, and other volatiles. Cannabicitran, a cannabinoid produced in *C. sativa* is reported to have antimicrobial against many bacteria in humans and popularly used in pharma industries (Bercht *et al.*, 1974; Karas *et al.*, 2020; Hong *et al.*, 2022). Columbianetin, is a furanocoumarin (phytoalexin) associated with celery resistance during storage against plant pathogens such as *B. cinerea, A. alternata,* and *S. sclerotiorum* (ED50 value of 25-48 µg/mL). ED50 is the dose of compound that produces effect in 50% of population that are treated with it (Afek *et al.*, 1995; Huang, 2001). 9(S)-HpOTrE, is a plant oxylipin, shown to be part of the lipid profile in Sauvignon Blanc (Podolyan, 1994). When oxidized to 9-Ox0OTrE, exhibits antimicrobial activity against plant pathogens including bacteria and fungi (Prost *et al.*, 2005; Tang *et al.*, 2020).

Cell suspension culture that presented some antifungal activity on the mycelial growth of *B. cinerea* in Petri plate experiments. However, the suspension culture did not show significant effect on detached berry assays. Both the assays were performed using aqueous extracts using 0.05mL/mL PDA for *in vitro* assay and 1 mL /berry for detached berry assay. At the same time, the metabolic profiling was performed using organic extracts (acetonitrile:isopropanol:water), and the compounds identified were previously reported to have antimicrobial activity. Moreover, cells recovered from 50 mL of cell suspension culture and 100 mg of cells were used for metabolic profiling. The antifungal activity of cell suspension cultures is yet to be confirmed *in planta* experiments. I hypothesize that different extraction solvents can influence both the results of antifungal activity *in vitro, in planta* and

detached berry assays and the compounds identified through metabolic profiling. Also, the volume of cells used to perform *in vitro* and berry experiments were different from the volume used for metabolic profiling. These two factors, extracts and volume might play a role in supporting the results and can only be confirmed by investigating using the organic extracts *in vitro, in planta* and detached berry assays.

3.4.2 The efficacy of senescent leaf extracts differed between *in vitro, in planta* and detached berry assays

The antifungal activity of water, ethanolic, and methanolic extracts of Mars and Canadice senescent leaves extracts were tested. There was a significant antifungal effect of all three treatments when tested *in vitro* for the antifungal activity, compared with the respective controls. The Mars extracts showed reduced area of fungal growth when compared to Canadice extracts. These results are in agreement with the results of a previous study showing that the methanolic and ethanolic extracts of grapevine canes have a better antifungal activity against *B. cinerea*, *P. viticola,* and *E. necator* when compared to aqueous extracts (Schnee *et al.*, 2013). In another report, grapevine ethanolic cane extracts had a direct antifungal activity against *B. cinerea* on nutrient agar medium, where the mycelial growth was halved when compared to the control (De Bona *et al.*, 2019). In our study, the number of spores formed on day 7 was counted. Though the number of spores were different between aqueous, methanolic and ethanolic extracts of Mars and Canadice, the statistical analysis showed that there was a significant effect of all leaf extract treatments on the *in vitro* spore formation.

Considering the observed leaf extract antifungal activity *in vitro* against *B. cinerea*, a reduced number of lesions was expected on grapevine leaves. In the detached leaf assay, treatment with Mars leaf ethanolic extracts led to lower number of lesions compared to the water and ethanol control treated leaves, when challenged with *B. cinerea*. Similar results were obtained in detached berry assays. Store-bought green berries (variety unknown) were treated with Canadice and Mars leaf water, ethanolic and methanolic extracts and then challenged with *B. cinerea*. All extracts were found to be effective against *B. cinerea* compared to their respective controls. This study builds on knowledge from previous investigation using pure phenolic compounds such as resveratrol, pterostilbene, and piceatannol treated berries challenged with *B. cinerea,* which showed reduced lesions on day 7 (Xu *et al.,* 2018*a,b*). From the LC-MS data obtained from this study it has been confirmed that the senescent leaves have distinct types of metabolites that includes different types of phenolic compounds. We hypothesize that these phenolic compounds may play a role in reducing the lesion diameter in the inoculated area. However, the *in vitro* results were not confirmed by *in planta* greenhouse experiments. The ethanolic extracts of Canadice did not show a significant effect *in planta.*

Our study utilizes the approach of testing the extracts of leaves that were senescing and were expected to have antifungal activity. In a previous study, extracts of leaves collected after harvest had more phenolic compounds than those collected early in the season (Katalinic *et al.,* 2009). Leaf extracts also showed a good antimicrobial activity against five different bacteria (Katalinić *et al.,* 2010). A previous study demonstrated that leaf extracts of red varieties *V. vinifera* L. cv Merlot and cv Vranac showed the presence of higher amounts of

flavonols, phenolic acids, and flavan-3-ols (Anđelković *et al.*, 2015). Further, the leaf extracts showed a stronger antimicrobial activity compared to methanol control against various types of bacteria and yeast and the study also suggested that the grapevine leaves can be used as additives in food and pharma industries (Anđelković *et al.*, 2015). In the present study, the results of *in vitro* experiments were not translated in the *in planta* experiments, similar to results obtained when Pinot noir cane extracts were compared *in vitro* with the *in planta* treatment (De Bona *et al.*, 2019).

The presence of fungicide residue on leaves is a limitation of using senescent leaves to test the antifungal activity in this study. Different types of protectant and systemic fungicides were applied to grapevines during the growing season for protecting them from fungal pathogens that can affect the vines at different stages of growth. Protectant fungicides remain outside the plant surface and kill fungal spores and other fungal products thereby preventing the infection, whereas systemic fungicides may move into the plant and sometimes throughout the plant. There are research reports that had demonstrated the persistence of fungicides such as captan and others being present for 7-14 days and reduced by more than 70% after 21 days (Frank *et al.*, 1985; Schilder, 2010; Gajbhiye *et al.*, 2011; Mohapatra and Ajithakumar, 2014). This study utilized field-collected grapevine leaves one month after harvest and two months after the last fungicide was applied (Table 1) believing that fungicide activity lasts for 21 days. The main reason behind using the field-collected ones instead of greenhouse leaves is that the grapevines growing in the vineyards are being faced by different types of abiotic and biotic stressors throughout the growing season. The natural mechanism is that vineyard grown grapevines, and all other plants produce several types of

secondary metabolites such as phenolics, flavonoids, and anthocyanins to protect themselves from distinct types of stressors (Petrova *et al.*, 2006; Batovska *et al.*, 2008; Katalinic *et al.*, 2013). In contrast, the greenhouse ones are grown in set experimental conditions and not being affected by stressors are believed to have limited produced compounds that can have antifungal activity. In future to overcome the limitation of fungicide residue interference with antifungal compounds present in grapevine leaves, metabolic profiling can be performed for both antifungal compounds and fungicides. This investigation will reveal the amount of fungicide residue present and also can help to differentiate between the natural antifungal compound's activity. Alternatively, leaves not treated with fungicides could be used.

The results of metabolic profiling of senescent leaves of both grape varieties were completely different when compared to their respective cell culture profiles. The list of compounds with greatest differences as listed previously in Table 7 and 9 have a different antimicrobial mechanism when compared to the cell culture compounds. Scientists demonstrated from the previous research that few compounds from the list were reported to have antimicrobial activity, e.g., Indole-3-lactic acid, esculin, DSF (diffusible signal factor), piceol, and other volatiles. Some of the compounds are part of coumarins and phenylpropanoid pathway metabolites having proven to have antifungal and antimicrobial activity as part of different research studies. Indole-3-lacticacid, part of phenylpropanoid pathway involved in synthesis of phenolic compounds that exhibit antifungal property (Fabre *et al.*, 2014). Esculin, natural dihydroxycoumarin present in *Fraxinus ornus* bark demonstrated antimicrobial activity against different microbes (Kostova *et al.*, 1993). Piceol, phenolic compound identified in resistant white spruce was actively produced when attacked by herbivory budworms (Delvas

et al., 2011). DSF, known as diffusible signal factor, is a monounsaturated fatty acid which is part of lipid profiles in different types of grapes (Matijasevic *et al.*, 2013; Lončarić *et al.*, 2022). Studies have reported that increasing DSF production by transformation in 'Freedom' grape have reduced Pierce's disease by reducing pathogen growth and mobility within the plant (Lindow *et al.*, 2014).

3.5 Conclusions

Our research has shown that grapevine-derived products such as cell suspension cultures and senescent leaf extracts may play a role in suppressing the effects of gray mold disease. The results also show differences in antifungal activity between *in vitro, in planta*, and detached berry assays. The cell suspension cultures and senescent leaf extracts have various kinds of phenolic compounds and secondary metabolites that can be involved in the inhibition of mycelial growth of *B. cinerea*. The cell suspension cultures have an advantage of not sacrificing whole plant and can be produced in enormous quantities using bioreactors. Resveratrol and other phenolics are expensive to purchase and use as an IPM alternative, instead grapevine-derived products, and wastes such as grape pomace, and pruning canes and leaves, which contain rich amounts of resveratrol and other phenolic compounds, may be a low-cost source that can be extracted and applied together with regular fungicides to control *Botrytis.* We hypothesize that the crude extracts of different parts of grapevine-derived products (*V. vinifera* based) were tested before and products from interspecific hybrids (*V. labrusca* and *V. vinifera)* appears to be effective at reducing the growth and spread of gray mold causing organism. This research suggests that there is still more to investigate and learn about interspecific cold-hardy grapevine-derived products and their role in performing antifungal activity against *B. cinerea*.

CHAPTER 4

CONCLUSION AND FUTURE PERSPECTIVES

Conclusion

The overarching goal of the research presented in this thesis was to determine how training systems influence the physiological and biochemical parameters of cold-hardy grapevines growing on two training systems and to investigate the putative antifungal activity of cold-hardy grapevine-derived products against *B. cinerea*, one of the most important grape pathogens. The research utilized interspecific hybrids Mars and Canadice, cold-hardy grapevines growing on vertical shoot positioning (VSP) and Munson (M) training systems. To the best of our knowledge, this study was the first to investigate the effect of training systems on the physiology and biochemistry of cold-hardy table grapevines. Mars and Canadice cell suspension cultures and senescent leaf extracts were used to test their putative antifungal activity against *B. cinerea*, as a way to obtain foundational knowledge on the impact of these cold-hardy grapevine-derived products on control of fungal diseases and add to the current understanding of botanical pesticides efficacy.

This study offers insight into some physiological aspects that differ concerning grapevine variety and are influenced by the training system. Grapevine metabolites differ in leaf and berries depending upon the phenological stages of grapevines growing on different training systems. In summary, our results showed that the physiological parameters such as SPAD, spectral indices, and gas exchange parameters were significantly different between grapevine varieties and training systems at some phenophases but could not infer which training system

is the best. The biochemical results of leaf metabolites showed that sucrose varied significantly between training systems during one growing season. The grape juice metabolites showed that amino acids such as alanine, threonine and valine, and small molecules such as 3-hydroxybutyrate and *myo*-Inositol were significantly different between training systems. Berry skin metabolites were also significantly different between training systems.

The results show that the aqueous, ethanolic, and methanolic extracts of senescent leaves showed antifungal activity against *B. cinerea*. These results were confirmed by performing *in vitro* and berry experiments, though the results were not translated *in planta* experiments. Later, the leaf ethanolic extracts were used to test the antifungal activity *in planta* in greenhouses. The aqueous extracts of cell suspension culture did show antifungal activity against *B. cinerea in vitro*, but not on detached berry experiments. These results suggests that the cell suspension culture has some antifungal activity, though it needs confirmation by performing *in planta* experiments in greenhouses. The metabolic profiling of senescent leaves and cell cultures was performed using organic extracts to identify metabolites responsible for antifungal activity. The results showed a list of compounds reported in different studies exhibiting antifungal activity.

Future Perspectives

This research provides Northeastern viticulturists with an insight into the performance of training systems translated to various physiological and biochemical parameters of cold-hardy table grapevines. A non-destructive method such as remote sensing could be utilized in

the future to monitor the overall productivity throughout the growing season. The sampling method for various assays can be performed differently, such as collecting leaves throughout entire plant canopy (for both training systems) to determine whether some additional differences exist that we were not able to capture with the sampling strategy that was used during our study. This study provides some preliminary evidence that plant-derived products might of some use to integrate with IPM approaches to control fungal pathogens. However, this is far from ready as a guidance to the growers. Botanical-derived products are increasingly becoming integral components of sustainable agriculture and botanical pesticides as part of IPM. Training systems regulate the microclimatic conditions of the grapevines and enhance the photosynthetic efficiency, which is translated to berry composition and productivity. The interaction of the training system, grapevine microclimate, photosynthetic efficiency, and leaf and berry metabolomic profiles are complex. Studies that focus on a few aspects of this complexity will provide essential pieces of information to improve our overall understanding of the grapevine metabolomes and provide growers with improved knowledge to choose the right training system that suits to grow grapevines in the geographical area of their interest. In recent decades, an explosion of different omic technologies has driven studies on the relationship between training systems and grapevine metabolites. Given that the various metabolomes of cold-hardy grapevines have been presented, future work should examine the transcriptomic and proteomic analysis of Mars and Canadice to explore the differences at the transcriptome level and various proteins that are translated and are involved in performing cold-hardy potential. Moreover, it would be interesting to explore how the profiles differ between training systems, and

document changes that occur during different grapevine phenological stages in the leaves and from veraison to harvest in berries.

The antifungal activity of grapevine-derived products against *B. cinerea* has been in their initial stages of research; future work should examine the changes of metabolites during the annual cycle of Mars and Canadice leaves. Future studies should also test the antifungal activity of ethanolic and methanolic extracts of grape cell suspension cultures against *B. cinerea.* Defense responses of Mars and Canadice cell suspensions can be elicited using pathogens, and subsequent metabolomic analysis could help clarify the various metabolites involved in the antifungal nature of the culture. The discrimination of profiles by eliciting and non-eliciting cell suspension cultures can be performed using the fast and easy approach of NMR spectroscopy. Moreover, the immense potential of NMR-based metabolomic studies can be demonstrated to accustom the sustainable approach of using botanical pesticides. This research used senescent leaves collected at harvest and fresh established *calli* to test antifungal activity. In the future, leaf samples at different phenophases can be used to investigate antifungal activity and simultaneously use the leaf extracts to profile metabolites. Grapevines are treated with various types of fungicides during the growing season and the fungicide residues may interfere with the performance of antifungal activity while using the leaves. To overcome this limitation, the leaves must be tested for quantification of fungicides with metabolic profiling to investigate their interference or use non-treated leaves which is more definitive. According to various research reports, the protectant fungicides such as captan, penncozeb, ziram and others are persistent in the leaves and grapes for 7-14 days depending upon the rate applied, and weather conditions (Frank *et al.*, 1985; Schilder, 2010; Gajbhiye *et al.*, 2011). The *calli* can be produced using different hormone combinations,

elicited using fungal pathogens, UV-irradiation, and chemicals to check the different secondary metabolites produced. Then they can be used to test antifungal activity and metabolic profiling to understand how cold-hardy grapevine metabolites differ from the *V. vinifera* cultivars. Mars and Canadice are among the interspecific hybrids (*V. labrusca* x *V. vinifera*) that can serve as models of other table grapes that were produced using similar parents.

LIST OF REFERENCES

Abdi AM, Boke-Olén N, Jin H, Eklundh L, Tagesson T, Lehstena V, Ardö J. 2019. First assessment of the plant phenology index (PPI) for estimating gross primary productivity in African semi-arid ecosystems. arXiv.

Adrian M, Jeandet P, Bessis R, Joubert JM. 1996. Induction of Phytoalexin (Resveratrol) Synthesis in Grapevine Leaves Treated with Aluminum Chloride ($AlCl_3$). Journal of Agricultural and Food Chemistry **44**, 1979–1981.

Adrian M, Jeandet P, Veneau J, Weston LA, Bessis R. 1997. Biological activity of resveratrol, a stilbenic compound from grapevines, against *Botrytis cinerea*, the causal agent for gray mold. Journal of Chemical Ecology **23**, 1689–1702.

Afek U, Carmeli S, Aharoni N. 1995. Columbianetin, a phytoalexin associated with celery resistance to pathogens during storage. Phytochemistry **39**, 1347–1350.

Aldayel MF. 2019. Biocontrol strategies of antibiotic-resistant, highly pathogenic bacteria and fungi with potential bioterrorism risks: Bacteriophage in focus. Journal of King Saud University - Science **31**, 1227–1234.

Ali K, Maltese F, Choi YH, Verpoorte R. 2010. Metabolic constituents of grapevine and grape-derived products. Phytochemistry Reviews **9**, 357–378.

Ali K, Maltese F, Figueiredo A, Rex M, Fortes AM, Zyprian E, Pais MS, Verpoorte R, Choi YH. 2012. Alterations in grapevine leaf metabolism upon inoculation with *Plasmopara viticola* in different time-points. Plant Science **191**–**192**, 100–107.

Ali K, Maltese F, Fortes AM, Pais MS, Choi YH, Verpoorte R. 2011*a*. Monitoring biochemical changes during grape berry development in Portuguese cultivars by NMR spectroscopy. Food Chemistry **124**, 1760–1769.

Ali K, Maltese F, Fortes AM, Pais MS, Verpoorte R, Choi YH. 2011*b*. Pre-analytical method for NMR-based grape metabolic fingerprinting and chemometrics. Analytica Chimica Acta **703**, 179–186.

Ali K, Maltese F, Zyprian E, Rex M, Choi HY, Verpoorte R. 2009. NMR metabolic fingerprinting based identification of grapevine metabolites associated with downy mildew resistance. Journal of Agricultural and Food Chemistry **57**, 9599–9606.

Aliaño-González MJ, Richard T, Cantos-villar E. 2020. Grapevine cane extracts: Raw plant material, extraction methods, quantification, and applications. Biomolecules **10**, 1–33.

Alves Filho EG, Silva LMA, Lima TO, Ribeiro PRV, Vidal CS, Carvalho ESS, Druzian JI, Marques ATB, Canuto KM. 2022. 1H NMR and UPLC-HRMS-based metabolomic approach

for evaluation of the grape maturity and maceration time of Touriga Nacional wines and their correlation with the chemical stability. Food Chemistry **382**, 132359.

Alzohairy SA, Gillett J, Saito S, Naegele RN, Xiao CL, Miles TD. 2021. Fungicide resistance profiles of *Botrytis cinerea* isolates from Michigan vineyards and development of a taqman assay for detection of fenhexamid resistance. Plant Disease **105**, 285–294.

Anđelković M, Radovanović B, Anđelković AM, Radovanović V. 2015. Phenolic Compounds and Bioactivity of Healthy and Infected Grapevine Leaf Extracts from Red Varieties Merlot and Vranac (Vitis vinifera L.). Plant Foods for Human Nutrition **70**, 317–323.

Andrews KP. 1984. Deep supercooling of dormant and deacclimating Vitis buds. American journal of enology and viticulture. **35**, 175–177.

Avenot HF, Morgan DP, Quattrini J, Michailides TJ. 2020. Resistance to Thiophanate-Methyl in *Botrytis cinerea* Isolates from Californian Vineyards and Pistachio and Pomegranate Orchards. Plant Disease **104**, 1069–1075.

Baigorri H, Antolin C, De Luis I, Geny L, Broquedis M, Aguirrezábal F, Sánchez-Díaz M. 2001. Influence of training system on the reproductive development and hormonal levels of *Vitis vinifera* L. cv. Tempranillo. American Journal of Enology and Viticulture **52**, 357–363.

Batovska DI, Todorova IT, Nedelcheva DV, Parushev SP, Atanassov AI, Hvarleva TD, Djakova GJ, Bankova VS, Popov SS. 2008. Preliminary study on biomarkers for the fungal resistance in Vitis vinifera leaves. Journal of Plant Physiology **165**, 791–795.

Bavaresco L, Petegolli D, Cantù E, Fregoni M, Chiusa G, Trevisan M. 1997. Elicitation and accumulation of stilbene phytoalexins in grapevine berries infected by *Botrytis cinerea*. Vitis **36**, 77–83.

Bavougian CM, Read PE, Schlegel VL, Hanford KJ. 2013. Canopy light effects in multiple training systems on yield, soluble solids, acidity, phenol and flavonoid concentration of 'Frontenac' grapes. HortTechnology **23**, 86–92.

de Bem BP, Bogo A, Everhart SE, Casa RT, Gonçalves MJ, Filho JLM, Rufato L, da Silva FN, Allebrandt R, da Cunha IC. 2016. Effect of four training systems on the temporal dynamics of downy mildew in two grapevine cultivars in southern Brazil. Tropical Plant Pathology **41**, 370–379.

Bercht CAL, Lousberg RJJC, Küppers FJEM, Salemink CA. 1974. Cannabicitran: A new naturally occurring tetracyclic diether from lebanese Cannabis sativa. Phytochemistry **13**, 619–621.

Bergqvist J, Dokoozlian N, Ebisuda N. 2001. Sunlight exposure and temperature effects on berry growth and composition of Cabernet Sauvignon and Grenache in the central San Joaquin Valley of California. American Journal of Enology and Viticulture **52**, 1–7.

Bertamini M, Nedunchezhian N. 2001. Effects of phytoplasma [stolbur-subgroup (Bois noir-BN)] on photosynthetic pigments, saccharides, ribulose 1,5-bisphosphate carboxylase, nitrate and nitrite reductases, and photosynthetic activities in field-grown grapevine (*Vitis vinifera* L. cv. Chardonn. Photosynthetica **39**, 119–122.

Bertamini M, Nedunchezhian N. 2005. Grapevine growth and physiological responses to iron deficiency. Journal of Plant Nutrition **28**, 737–749.

Billet K, Delanoue G, Arnault I, Besseau S, Oudin A, Courdavault V, Marchand PA, Giglioli-Guivarc'h N, Guérin L, Lanoue A. 2019. Vineyard evaluation of stilbenoid-rich grape cane extracts against downy mildew: a large-scale study. Pest Management Science **75**, 1252–1257.

De Bona GS, Adrian M, Negrel J, Chiltz A, Klinguer A, Poinssot B, Héloir MC, Angelini E, Vincenzi S, Bertazzon N. 2019. Dual Mode of Action of Grape Cane Extracts against *Botrytis cinerea*. Journal of Agricultural and Food Chemistry **67**, 5512–5520.

De Bona GS, Vincenzi S. 2020. Grapevine canes waste from Veneto region as a new source of stilbenoids content. Italian Journal of Food Science **32**, 310–320.

Bordelon BP, Skinkis PA, Howard PH. 2008. Impact of training system on vine performance and fruit composition of traminette. American Journal of Enology and Viticulture **59**, 39–46.

Bouderias S, Teszlák P, Jakab G, Kőrösi L. 2020. Age- and season-dependent pattern of flavonol glycosides in Cabernet Sauvignon grapevine leaves. Scientific Reports **10**, 1–9.

Bradshaw TL, Hazelrigg AL, Berkett LP. 2018*a*. Characteristics of the cold-climate winegrape industry in Vermont, USA. Acta Horticulturae, 469–476.

Bradshaw TL, Kingsley-Richards SL, Foster J, Berkett LP. 2018*b*. Horticultural performance and juice quality of cold-climate grapes in Vermont, USA. European Journal of Horticultural Science **83**, 42–48.

Brunetto G, Trentin G, Ceretta CA, Girotto E, Lorensini F, Miotto A, Moser GRZ, Melo GW de. 2012. Use of the SPAD-502 in Estimating Nitrogen Content in Leaves and Grape Yield in Grapevines in Soils with Different Texture. American Journal of Plant Sciences **03**, 1546–1561.

Burbidge CA, Ford CM, Melino VJ, *et al.* 2021. Biosynthesis and Cellular Functions of Tartaric Acid in Grapevines. Frontiers in Plant Science **12**, 1–22.

Candolfi-Vasconcelos MC, Koblet W, Howell GS, Zweifel W. 1994. Influence of defoliation, rootstock, training system, and leaf position on gas exchange of Pinot noir grapevines. American Journal of Enology and Viticulture **45**, 173–180.

Cappellini RA, Ceponis MJ, Lightner GW. 1986. Disorders in table grape shipments to the New York market, 1972-1984. Plant disease (USA).

Casanova-Gascón J, Martín-Ramos P, Martí-Dalmau C, Badía-Villas D. 2018. Nutrients assimilation and chlorophyll contents for different grapevine varieties in calcareous soils in the somontano do (Spain). Beverages **4**.

Çetin ES, Altinöz D, Tarçan E, Göktürk Baydar N. 2011. Chemical composition of grape canes. Industrial Crops and Products **34**, 994–998.

Choi YH, Kim HK, Linthorst HJM, Hollander JG, Lefeber AWM, Erkelens C, Nuzillard J-M, Verpoorte R. 2006. NMR Metabolomics to Revisit the Tobacco Mosaic Virus Infection in *Nicotiana tabacum* Leaves. Journal of Natural Products **69**, 742–748.

Clark JR. 2010. Eastern United States table grape breeding. Journal of the American Pomological Society **64**, 72–77.

Clark MD. 2019. Development of Cold Climate Grapes in the Upper Midwestern U.S. Plant Breeding Reviews **43**, 31–60.

Colcol JF, Baudoin AB. 2016. Sensitivity of Erysiphe necator and Plasmopara viticola in virginia to qoi fungicides, boscalid, quinoxyfen, thiophanate methyl, and mefenoxam. Plant Disease **100**, 337–344.

Coombe, Thornely JHM, Johnson IR, Casson S, Gray JE. 1992. Research on Development and Ripening of the Grape Berry. New Phytologist **43**, 669.

Costa RR da, Ferreira TO de, Lima MAC de. 2021. Training systems, rootstocks and climatic conditions influence quality and antioxidant activity of 'brs cora' grape. Acta Scientiarum - Agronomy **43**, 1–12.

Couvillon GA, Nakayama TOM. 1970. The effect of the Modified Munson training system on uneven ripening, soluble solids and yield of 'Concord' grapes. Journal of the American Society of Horticultural Science **95**, 158–162.

Creasy L, Coffee M. 1988. Phytoalexin production potential of grape berries. Journal of the American Society for Horticultural Science (USA) **113**, 230–234.

Creasy LG, Creasy LL. 2009. *Grapes : Crop production science in Horticulture*. (CABI, Wallingford, Oxfordshire, UK).

Dai GH, Andary C, Mondolot-Cosson L, Boubals D. 1995*a*. Involvement of phenolic compounds in the resistance of grapevine callus to downy mildew (Plasmopara viticola). European Journal of Plant Pathology **101**, 541–547.

Dai GH, Andary C, Mondolot-Cosson L, Boubals D. 1995*b*. Histochemical responses of

leaves of in vitro plantlets of Vitis spp. to infection with P*lasmopara viticola*. Phytopathology **85**, 149–154.

Dai GH, Andary C, Mondolot-Cosson L, Boubals D. 1995*c*. Histochemical studies on the interaction between three species of grapevine, *Vitis vinifera*, *V. rupestris* and *V. rotundifolia* and the downy mildew fungus, P*lasmopara viticola*. Physiological and Molecular Plant Pathology **46**, 177–188.

Davies CR, Wohlgemuth F, Young T, Violet J, Dickinson M, Sanders JW, Vallieres C, Avery S V. 2021. Evolving challenges and strategies for fungal control in the food supply chain. Fungal Biology Reviews **36**, 15–26.

Debnath T, Debnath S, Paul M. 2019. Detection of Age and Defect of Grapevine Leaves Using Hyper Spectral Imaging. Lecture Notes in Computer Science (including subseries Lecture Notes in Artificial Intelligence and Lecture Notes in Bioinformatics) **11854 LNCS**, 92–105.

Debnath S, Paul M, Motiur Rahaman DM, Debnath T, Zheng L, Baby T, Schmidtke LM, Rogiers SY. 2021. Identifying individual nutrient deficiencies of grapevine leaves using hyperspectral imaging. Remote Sensing **13**, 1–21.

DeLong AJ, Saito S, Xiao C-L, Rachel PN. 2020. Population Genetics and Fungicide Resistance of *Botrytis cinerea* on Vitis and Prunus spp.in California. Phytopathology **110**, 694–702.

Delvas N, Bauce É, Labbé C, Ollevier T, Bélanger R. 2011. Phenolic compounds that confer resistance to spruce budworm. Entomologia Experimentalis et Applicata **141**, 35–44.

Dercks W, Creasy LL. 1989. The significance of stilbene phytoalexins in the *Plasmopara viticola*-grapevine interaction. Physiological and Molecular Plant Pathology **34**, 189–202.

Dokoozlian NK, Kliewer WM. 1995. The light environment within grapevine canopies. II. Influence of leaf area density on fruit zone light environment and some canopy assessment parameters. American Journal of Enology and Viticulture **46**, 219–226.

Donnez D, Jeandet P, Clément C, Courot E. 2009. Bioproduction of resveratrol and stilbene derivatives by plant cells and microorganisms. Trends in Biotechnology **27**, 706–713.

Efferth T. 2019. Biotechnology Applications of Plant Callus Cultures. Engineering **5**, 50–59.
Eibach R, Töpfer R. 2015. *Traditional grapevine breeding techniques*. Elsevier Ltd.

El-kereamy A, Kurtural SK. 2022. Yield and Physiological Response of Autumn King and Scarlet Royal Table Grapes to Cane and Spur Pruning Systems. Horticulturae **8**, 1–13.

El-Khateeb YA, Elsherbiny AE, Tadros KL, Ali MS, Hamed BH. 2013. Phytochemical Analysis and Antifungal Activity of Fruit Leaves Extracts on the Mycelial Growth of Fungal Plant Pathogens. Journal of Plant Pathology & Microbiology **04**.

Elad Y, Melane V, Fillinger S. 2016. Botrytis - The fungus, the pathogen and its management in agricultural systems. Botrytis - The Fungus, the Pathogen and its Management in Agricultural Systems, 1–486.

Ellis MA, Erincik O. 2008. Anthracnose of Grape. , 1–3.

Ellis AM, Nita M. 2009. Organic Small Fruit Disease Management Guidelines Integrated Management of Grape Diseases. Agricultural Engineering.

Elolimy A, Alharthi A, Zeineldin M, Parys C, Helmbrecht A, Loor JJ. 2019. Supply of Methionine During Late-Pregnancy Alters Fecal Microbiota and Metabolome in Neonatal Dairy Calves Without Changes in Daily Feed Intake. Frontiers in Microbiology **10**, 1–20.

Etienne A, Génard M, Lobit P, Mbeguié-A-Mbéguié D, Bugaud C. 2013. What controls fleshy fruit acidity? A review of malate and citrate accumulation in fruit cells. Journal of Experimental Botany **64**, 1451–1469.

Fabre S, Absalon C, Pinaud N, Venencie C, Teissedre PL, Fouquet E, Pianet I. 2014. Isolation, characterization, and determination of a new compound in red wine. Analytical and Bioanalytical Chemistry **406**, 1201–1208.

Fan F, Hamada MS, Li N, Li GQ, Luo CX. 2017. Multiple fungicide resistance in *Botrytis cinerea* from greenhouse strawberries in Hubei Province, China. Plant Disease **101**, 601–606.

Favero AC, de Amorim DA, da Mota R V., de Souza CR, de Albuquerque Regina M. 2010. Resposta fisiológica e produção do vinhedo de 'Syrah' em funȧão dos sistemas de condução. Scientia Agricola **67**, 267–273.

Felicio JD, Santos RS, Gonçalez E. 2001. Chemical constituents from *Vitis vinifera* (Vitaceae). Arquivos do Instituto Biológico **68**, 47–50.

Fennell A. 2004. Freezing tolerance and injury in grapevines. Journal of Crop Improvement **10**, 201–235.

Fernandes F, Ramalhosa E, Pires P, Verdial J, Valentão P, Andrade P, Bento A, Pereira JA. 2013. Vitis vinifera leaves towards bioactivity. Industrial Crops and Products **43**, 434–440.

Filimon VR, Filimon R, Rotaru L. 2014. Characterization of some Vitis vinifera L. Indigenous Varieties by Analysis of Leaf Photosynthetic Pigments. Bulletin of University of Agricultural Sciences and Veterinary Medicine Cluj-Napoca. Horticulture **71**.

Filimon R V., Rotaru L, Filimon RM. 2016. Quantitative Investigation of Leaf Photosynthetic Pigments during Annual Biological Cycle of *Vitis vinifera* L. Table Grape Cultivars. South African Journal of Enology and Viticulture **37**, 1–14.

Findlay N, Oliver KJ, Nil N, Coombe BG. 1987. Solute accumulation by grape pericarp cells: IV. Perfusion of pericarp apoplast via the pedicel and evidence for xylem malfunction in ripening berries. Journal of Experimental Botany **38**, 668–679.

Frank R, Northover J, Braun HE. 1985. Persistence of Captan on Apples, Grapes, and Pears in Ontario, Canada, 1981–1983. Journal of Agricultural and Food Chemistry **33**, 514–518.

Gajbhiye VT, Gupta S, Mukherjee I, Singh SB, Singh N, Dureja P, Kumar Y. 2011. Persistence of azoxystrobin in/on grapes and soil in different grapes growing areas of India. Bulletin of Environmental Contamination and Toxicology **86**, 90–94.

Ghule SB, Sawant IS, Sawant SD, Saha S, Devarumath RM. 2018. Detection of G143A mutation in Erysiphe necator and its implications for powdery mildew management in grapes. Indian Journal of Horticulture **75**, 434–439.

Gill HK, Garg H. 2014. Pesticides: Environmental Impacts and Management Strategies. Pesticides toxic aspects.

Gladwin FE. 1919. A Test of Methods in Pruning the Concord Grape in the Chautauqua Grape Belt. Oxford University **464**, 60.

Goffinet MC. 2004. Anatomy of Grapevine Winter Injury and Recovery Living cells and freeze injury in grapevine cells and tissues.

Goufo P, Singh RK, Cortez I. 2020. A reference list of phenolic compounds (Including stilbenes) in grapevine (*Vitis vinifera* l.) roots, woods, canes, stems, and leaves. Antioxidants **9**, 398.

Gougeon L, da Costa G, Guyon F, Richard T. 2019. 1H NMR metabolomics applied to Bordeaux red wines. Food Chemistry **301**, 125257.

Grant S. 2019. Vertical shoot positioned trellis systems in warm regions. Lodi Wine Growers Blog.

Greer DH, Weedon MM. 2012. Modelling photosynthetic responses to temperature of grapevine (*Vitis vinifera* cv. Semillon) leaves on vines grown in a hot climate. Plant, Cell and Environment **35**, 1050–1064.

Guerrero RF, Biais B, Richard T, Puertas B, Waffo-Teguo P, Merillon JM, Cantos-Villar E. 2016. Grapevine cane's waste is a source of bioactive stilbenes. Industrial Crops and Products **94**, 884–892.

Guerrero RF, Cantos-Villar E, Ruiz-Moreno MJ, Puertas B, Cuevas FJ, Moreno-Rojas JM. 2019. Influence of vertical training systems on warm climate red winemaking: Wine parameters, polyphenols, volatile composition, and sensory analysis. Oeno One **53**, 471–486.

Hamzehzarghani H, Kushalappa AC, Dion Y, Rioux S, Comeau A, Yaylayan V, Marshall WD, Mather DE. 2005. Metabolic profiling and factor analysis to discriminate quantitative resistance in wheat cultivars against fusarium head blight. Physiological and Molecular Plant Pathology **66**, 119–133.

Hartman J, Beale J. 2008. Powdery Mildew and Drought. University of Kentucky Cooperative Extension Service.

Hazelrigg A, Kingsley-Richards LS. 2017. Pest Management Strategic Plan for Grapes in the Northeast.

Hebash K a H, Fadel HM, Soliman MM. 2012. Volatile components of grape leaves. J.Islamic Acad.Sci. **4**, 26–28.

Hemhill Jr DD, Sheets WA, Martin WL. 1992. Seedless Table Grapes for the Willamette Valley Seedless Table Grapes for the Willamette Valley.

Hendricks KE, Christman MC, Roberts PD. 2017. A statistical evaluation of methods of in-vitro growth assessment for *Phyllosticta citricarpa*: Average colony diameter vs. area. PLoS ONE **12**, 1–7.

Vanden Heuvel JE, Lerch SD, Lenerz CC, Meyers JM, Mansfield AK. 2013. Training system and vine spacing impact vine growth, yield, and fruit composition in a vigorous young 'Noiret' vineyard. HortTechnology **23**, 505–510.

Hildebrandt TM, Nunes Nesi A, Araújo WL, Braun HP. 2015. Amino Acid Catabolism in Plants. Molecular Plant **8**, 1563–1579.

HMDB. 2022. Human Metabolome Database.

Hong HJ, Sloan L, Saxena D, Scott DA. 2022. The Antimicrobial Properties of Cannabis and Cannabis-Derived Compounds and Relevance to CB2-Targeted Neurodegenerative Therapeutics. Biomedicines **10**.

Hoos G, Blaich R. 1990. Influence of Resveratrol on Germination of Conidia and Mycelial Growth of Botrytis cinerea and Phomopsis viticola. Journal of Phytopathology **129**, 102–110.

Horler DNH, Barber J. 1980. Effects of heavy metals on the absorbance and reflectance spectra of plants. **1**, 121–136.

Horler DNH, Dockray M, Barber J, Barringer AR. 1983. Red edge measurements for remotely sensing plant chlorophyll content. Advances in Space Research **3**, 273–277.

Howell GS. 2000. Grape Vine Cold Hardiness: Mechanisms of Cold Acclimation, Mid-Winter Hardiness Maintenance, and Spring Deacclimation

Howell GS, Miller DP, Edson CE, Striegler RK. 1991. Influence of Training System and Pruning Severity on Yield, Vine Size, and Fruit Composition of Vignoles Grapevines. American Journal of Enology and Viticulture **42**, 191–198.

Huang J-S. 2001. Accumulation of Phytoalexins as a Resistance Mechanism

Hunt ER, Rock BN. 1989. Detection of changes in leaf water content using Near- and Middle-Infrared reflectances. Remote Sensing of Environment **30**, 43–54.

Isaacs R, Schilder AMC, Zabadal TJ, Weigle T. 2003. A pocket guide for grape IPM scouting in the north central and eastern U.S.

Jeandet P, Bessis R, Gautheron B. 1991. The Production of Resveratrol (3,5,4'-trihydroxystilbene) by Grape Berries in Different Developmental Stages. American Journal of Enology and Viticulture **42**, 41–46.

Jeandet P, Bessis R, Sbaghi M, Meunier P. 1995. Production of the Phytoalexin Resveratrol by Grapes as a Response to Botrytis Attack Under Natural Conditions. Journal of Phytopathology **143**, 135–139.

Ji T, Dami IE. 2008. Characterization of free flavor compounds in traminette grape and their relationship to vineyard training system and location. Journal of Food Science **73**, 262–267.

Jogaiah S, Striegler KR, Bergmeier E, Harris J. 2012. Influence of Cluster Exposure to Sun on Fruit Composition of 'Norton' Grapes (*Vitis estivalis* Michx) in Missouri. International Journal of Fruit Science **12**, 410–426.

Jones DS, McManus PS. 2017. Susceptibility of cold-climate wine grape cultivars to downy mildew, powdery mildew, and black rot. Plant Disease **101**, 1077–1085.

Karas JA, Wong LJM, Paulin OKA, Mazeh AC, Hussein MH, Li J, Velkov T. 2020. The antimicrobial activity of cannabinoids. Antibiotics **9**, 1–10.

Karimi R. 2020. Cold Hardiness Evaluation of 20 Commercial Table Grape (*Vitis vinifera* L.) Cultivars. International Journal of Fruit Science **20**, 433–450.

Karkauskaite P, Tagesson T, Fensholt R. 2017. Evaluation of the plant phenology index (PPI), NDVI and EVI for start-of-season trend analysis of the Northern Hemisphere boreal zone. Remote Sensing **9**.

Kassemeyer HH, Berkelmann-Loehnertz B. 2009. *Fungi of grapes*.

Katalinic V, Generalic I, Skroza D, Ljubenkov I, Teskera A, Konta I, Boban M. 2009. Insight in the phenolic composition and antioxidative properties of *Vitis vinifera* leaves extracts. Croatian journal of food science and technology **1**, 7–15.

Katalinic V, Mozina SS, Generalic I, Skroza D, Ljubenkov I, Klancnik A. 2013. Phenolic profile, antioxidant capacity, and antimicrobial activity of leaf extracts from six *Vitis vinifera* L. Varieties. International Journal of Food Properties **16**, 45–60.

Katalinić V, Možina SS, Skroza D, *et al.* 2010. Polyphenolic profile, antioxidant properties and antimicrobial activity of grape skin extracts of 14 *Vitis vinifera* varieties grown in Dalmatia (Croatia). Food Chemistry **119**, 715–723.

KEGG. 2022. KEGG: Kyoto encyclopedia of genes and genomes. Nucleic Acids Research **27**.
Keller M. 2015. *The Science of Grapevines-Anatomy and Physiology*.

Khan T, Khan T, Hano C, Abbasi BH. 2019. Effects of chitosan and salicylic acid on the production of pharmacologically attractive secondary metabolites in callus cultures of Fagonia indica. Industrial Crops and Products **129**, 525–535.

Khanizadeh S, Rekika D, Levasseur A, Groleau Y, Richer C, Fisher H. 2004. Growing grapes in a cold climate with winter temperature below -25°C. Acta Horticulturae **663**, 931–936.

El Khawand T, Taillis D, Da Costa G, Pedrot E, Cluzet S, Decendit A, Valls Fonayet J, Richard T. 2021. Chemical process to improve natural grapevine-cane extract effectivity against powdery mildew and grey mould. OENO One **55**, 81–91.

Khawand T El, Taillis D, Da Costa G, Pedrot E, Cluzet S, Decendit A, Fonayet JV, Richard T. 2021. Chemical process to improve natural grapevine-cane extract effectivity against powdery mildew and grey mould. Oeno One **55**, 81–91.

Kliewer WM, Dokoozlian NK. 2005. Leaf area/crop weight ratios of grapevines: Influence on fruit composition and wine quality. American Journal of Enology and Viticulture **56**, 170–181.

Kostova IN, Nikolov NM, Chipilska LN. 1993. Antimicrobial properties of some hydroxycoumarins and Fraxinus ornus bark extracts. Journal of Ethnopharmacology **39**, 205–208.

Kramer J, Simnitt S, Calvin L. 2020. Fruit and Tree Nuts Outlook : September 2020 January through July Consumer Price Index Down from a Year Ago Price Outlook Fruit and Nut Grower Price Index Is Up.

Kraus C, Pennington T, Herzog K, Hecht A, Fischer M, Voegele RT, Hoffmann C, Töpfer R, Kicherer A. 2018. Effects of canopy architecture and microclimate on grapevine health in two training systems. Vitis - Journal of Grapevine Research **57**, 53–60.

Kulakiotu EK, Thanassoulopoulos CC, Sfakiotakis EM. 2004. Biological control of *Botrytis cinerea* by volatiles of ‘Isabella’ grapes. Phytopathology **94**, 924–931.

Ky I, Lorrain B, Jourdes M, Pasquier G, Fermaud M, Gény L, Rey P, Doneche B, Teissedre PL. 2012. Assessment of grey mould (Botrytis cinerea) impact on phenolic and

sensory quality of Bordeaux grapes, musts and wines for two consecutive vintages. Australian Journal of Grape and Wine Research **18**, 215–226.

Lago-Vanzela ES, Da-Silva R, Gomes E, García-Romero E, Hermosín-Gutiérrez I. 2011*a*. Phenolic composition of the edible parts (flesh and skin) of Bordô grape (*Vitis labrusca*) using HPLC-DAD-ESI-MS/MS. Journal of Agricultural and Food Chemistry **59**, 13136–13146.

Lago-Vanzela ES, Da-Silva R, Gomes E, García-Romero E, Hermosín-Gutiérrez I. 2011*b*. Phenolic composition of the Brazilian seedless table grape varieties BRS clara and BRS morena. Journal of Agricultural and Food Chemistry **59**, 8314–8323.

Langcake P. 1981. Disease resistance of Vitis spp. and the production of the stress metabolites resveratrol, ε-viniferin, α-viniferin and pterostilbene. Physiological Plant Pathology **18**, 213–226.

Langcake P, Pryce RJ. 1976. The production of resveratrol by *Vitis vinifera* and other members of the Vitaceae as a response to infection or injury. Physiological Plant Pathology **9**, 77–86.

Langcake P, Pryce RJ. 1977*a*. A new class of phytoalexins from grapevines. , 151–152.

Langcake P, Pryce RJ. 1977*b*. The production of resveratrol and the viniferins by grapevines in response to ultraviolet irradiation. Phytochemistry **16**, 1193–1196.

Lauten GN, Rock BN. 1992. Physiological and spectral analysis of the effects of sodium chloride on syringa vulgaris. International Geoscience and Remote Sensing Symposium (IGARSS) **1**, 236–238.

Li S, Zhang Z, Cain A, Wang B, Long M, Taylor J. 2005. Antifungal activity of camptothecin, trifolin, and hyperoside isolated from *Camptotheca acuminata*. Journal of Agricultural and Food Chemistry **53**, 32–37.

Lima MRM, Dias ACP. 2012. *Phaeomoniella chlamydospora*-induced Oxidative Burst in Vitis vinifera Cell Suspensions: Role of NADPH Oxidase and Ca 2+. Journal of Phytopathology **160**, 129–134.

Lima MRM, Felgueiras ML, Cunha A, Chicau G, Ferreres F, Dias ACP. 2017*a*. Differential phenolic production in leaves of *Vitis vinifera* cv. Alvarinho affected with esca disease. Plant Physiology and Biochemistry **112**, 45–52.

Lima MRM, Felgueiras ML, Graça G, Rodrigues JEA, Barros A, Gil AM, Dias ACP. 2010. NMR metabolomics of esca disease-affected *Vitis vinifera* cv. Alvarinho leaves. Journal of Experimental Botany **61**, 4033–4042.

Lima MRM, Ferreres F, Dias ACP. 2012. Response of *Vitis vinifera* cell cultures to *Phaeomoniella chlamydospora*: Changes in phenolic production, oxidative state and expression of defence-related genes. European Journal of Plant Pathology **132**, 133–146.

Lima MRM, MacHado AF, Gubler WD. 2017*b*. Metabolomic study of Chardonnay grapevines double stressed with esca-associated fungi and drought. Phytopathology **107**, 669–680.

Lindow S, Newman K, Chatterjee S, Baccari C, Lavarone AT, Ionescu M. 2014. Production of *Xylella fastidiosa* diffusible signal factor in transgenic grape causes pathogen confusion and reduction in severity of pierce's disease. Molecular Plant-Microbe Interactions **27**, 244–254.

Liswidowati, Melchior F, Hohmann F, Schwer B, Kindl H. 1991. Induction of stilbene synthase by *Botrytis cinerea* in cultured grapevine cells. Planta **183**, 307–314.

Liu S, Che Z, Chen G. 2016. Multiple-fungicide resistance to carbendazim, diethofencarb, procymidone, and pyrimethanil in field isolates of *Botrytis cinerea* from tomato in Henan Province, China. Crop Protection **84**, 56–61.

Liu MY, Chi M, Tang YH, Song CZ, Xi ZM, Zhang ZW. 2015*a*. Effect of three training systems on grapes in a wet region of China: Yield, incidence of disease and anthocyanin compositions of *Vitis vinifera* cv. Cabernet Sauvignon. Molecules **20**, 18967–18987.

Liu Y, Yan J, Li Q, Wang J, Shi Y. 2018. Effect of training systems on accumulation of flavan-3-ols in Cabernet Sauvignon grape seeds at the north foot of Mt. Tianshan. South African Journal of Enology and Viticulture **39**, 35–46.

Liu X, Zheng P, Zhao X, Zhang Y, Hu C, Li J, Zhao J, Zhou J, Xie P, Xu G. 2015*b*. Discovery and validation of plasma biomarkers for major depressive disorder classification based on liquid chromatography-mass spectrometry. Journal of Proteome Research **14**, 2322–2330.

Lodhi MA, Daly MJ, Ye GN, Weeden NF, Reisch BI. 1995. A molecular marker based linkage map of Vitis. Genome **38**, 786–794.

Lodhi MA, Weeden NF, Reisch BI. 1997. Characterization of RAPD markers in Vitis. Vitis **36**, 133–140.

Lončarić A, Patljak M, Blažević A, Jozinović A, Babić J, Šubarić D, Pichler A, Flanjak I, Kujundžić T, Miličević B. 2022. Changes in Volatile Compounds during Grape Brandy Production from 'Cabernet Sauvignon' and 'Syrah' Grape Varieties. Processes **10**.

Londo JP, Kovaleski AP. 2017. Characterization of wild North American grapevine cold hardiness using differential thermal analysis. American Journal of Enology and Viticulture **68**, 203–212.

Londo JP, Kovaleski AP. 2019. Deconstructing cold hardiness: variation in supercooling ability and chilling requirements in the wild grapevine *Vitis riparia*. Australian Journal of Grape and Wine Research **25**, 276–285.

Loupit G, Prigent S, Franc C, De Revel G, Richard T, Cookson SJ, Fonayet JV. 2020. Polyphenol Profiles of Just Pruned Grapevine Canes from Wild Vitis Accessions and *Vitis vinifera* Cultivars. Journal of agricultural and food chemistry **68**, 13397–13407.

Lovisolo C, Schubert A, Rcstagno M. 1996. Photosynthesis of grapevine leaves of different age at high and low light intensity. Acta Horticulturae **427**, 171–175.

Luby JJ. 1991. Breeding Cold-hardy Fruit Crops in Minnesota. HortScience **26**, 507–512.
Magnusson E, Cranfield JAL. 2005. Consumer demand for pesticide free food products in Canada: A probit analysis. Canadian Journal of Agricultural Economics **53**, 67–81.

Maia M, Ferreira AEN, Laureano G, Marques AP, Torres VM, Silva AB, Matos AR, Cordeiro C, Figueiredo A, Silva MS. 2019. *Vitis vinifera* 'Pinot noir' leaves as a source of bioactive nutraceutical compounds. Food and Function **10**, 3822–3827.

Martínez-Lüscher J, Sánchez-Díaz M, Delrot S, Aguirreolea J, Pascual I, Gomès E. 2016. Ultraviolet-B alleviates the uncoupling effect of elevated CO2and increased temperature on grape berry (*Vitis vinifera* cv. Tempranillo) anthocyanin and sugar accumulation. Australian Journal of Grape and Wine Research **22**, 87–95.

Matijasevic S, Todic S, Beslic Z, Rankovic Vasic Z, Zunic D, Atanackovic Z, Vukosavljevic V, Cirkovic B. 2013. Volatile components of grape brandies produced from Muscat table grapevine (*Vitis vinifera* L.) cultivars. Bulgarian Journal of Agricultural Science **19**, 783–791.

Mattivi F, Guzzon R, Vrhovsek U, Stefanini M, Velasco R. 2006. Metabolite profiling of grape: Flavonols and anthocyanins. Journal of Agricultural and Food Chemistry **54**, 7692–7702.

Miessner S, Mann W, Stammler G. 2011. Guignardia bidwellii, The causal agent of black rot on grapevine has a low risk for QoI resistance. Journal of Plant Diseases and Protection **118**, 51–53.

Millard LT. 2005. Effect of Training Systems on Viognier (*Vitis vinifera* L .) Grape and Wine Glycosides and Volatile Compounds.

Minnesota Grape Growers Association. 2016. Growing Grapes in Minnesota.

Mohapatra S, Ajithakumar R. 2014. Persistence of trifloxystrobin and tebuconazole in banana tissues and soil under the semi-arid climatic conditions of Karnataka, India. International Journal of Environmental Analytical Chemistry **94**, 506–518.

Monagas M, Hernández-Ledesma B, Gómez-Cordovés C, Bartolomé B. 2006. Commercial dietary ingredients from Vitis vinifera L. leaves and grape skins: Antioxidant and chemical characterization. Journal of Agricultural and Food Chemistry **54**, 319–327.
Moore NJ. 1986. United States Patent (19).

Moreira LS, Clark MD. 2021. Embryo rescue of cold-hardy table grapes. HortScience **59**,

1059–1065.

Moriondo M, Orlandini S, Giuntoli A, Bindi M. 2005. The effect of downy and powdery mildew on grapevine (*Vitis vinifera* L.) leaf gas exchange. Journal of Phytopathology **153**, 350–357.

Morris JR, Cawthon DL. 1980. Yield and Quality Response of ' Concord ' Grapes to Training Systems and Pruning Severity in Arkansas '. **105**, 307–310.

Morris J, Sims C, Bourque J, Oakes J. 1984. Influence of training system, pruning severity, and spur length on yield and quality of six french-american hybrid grape cultivars. American journal of enology and viticulture **35**, 23–27.

Mostert L, Denman S, Crous PW. 2017. In Vitro Screening of Fungicides Against *Phomopsis viticola* and *Diaporthe perjuncta*. South African Journal of Enology & Viticulture **21**.

Moyer M, Grove G. 2011. Botrytis bunch rot in commercial Washington grape production. , 1–5.

Munson T V. 1909. Foundations of American Grape culture.

Nadeem H, Ahmad F. 2019. Prospects for the Use of Plant Cell Culture as Alternatives to Produce Secondary Metabolites BT - Natural Bio-active Compounds: Volume 3: Biotechnology, Bioengineering, and Molecular Approaches. In: Akhtar MS,, In: Swamy MK, eds. Singapore: Springer Singapore, 153–182.

NASA. 2022. POWER Data Access Viewer. Nasa, 854.

Nascimento R, Maia M, Ferreira AEN, Silva AB, Freire AP, Cordeiro C, Silva MS, Figueiredo A. 2019. Early stage metabolic events associated with the establishment of *Vitis vinifera* – P*lasmopara viticola* compatible interaction. Plant Physiology and Biochemistry **137**, 1–13.

NCEI. 2022. Data Search | National Centers for Environmental Information (NCEI).

NEWA 2022. Network for Environment and Weather Applications (NEWA) in New Hampshire | Extension. https://extension.unh.edu/agriculture-gardens/pest-disease-growing-tools/network-environment-weather-applications-newa-new-hampshire, Accessed on 2022-08-25.

NOAA 2020. NOAA's Office of Legislative Affairs - NOAA In Your State and Territory. https://www.legislative.noaa.gov/NIYS/, Accessed on 2020-12-11.

Norberto PM, Regina MA, Chalfun NNJ, Soares AM. 2009. Effect of conduction system on some ecophysiological characteristics of the grapevine (*Vitis Labrusca* L.). Ciência e Agrotecnologia **33**, 721–726.

Northover J. 1986. Resistance of *Botrytis cinerea* to Benomyl and Iprodione in Vineyards and Greenhouses After Exposure to the Fungicides Alone or Mixed with Captan . Plant Disease **70**, 398.

Novello V, De Palma L, Bica D, Santovito A. 2001. Photosynthesis, leaf and stem water potentials, chlorophyll and macroelement leaf concentration as influenced by two root and training systems in Erbaluce wine grape. Advances in Horticultural Science **15**, 17–24.

Oerke EC, Herzog K, Toepfer R. 2016. Hyperspectral phenotyping of the reaction of grapevine genotypes to Plasmopara viticola. Journal of Experimental Botany **67**.

Pantazi XE, Moshou D, Tamouridou AA. 2019. Automated leaf disease detection in different crop species through image features analysis and One Class Classifiers. Computers and Electronics in Agriculture **156**, 96–104.

Pavela R, Waffo-Teguo P, Biais B, Richard T, Mérillon JM. 2017. *Vitis vinifera* canes, a source of stilbenoids against *Spodoptera littoralis* larvae. Journal of Pest Science **90**, 961–970.

Pereira GE, Gaudillere JP, Pieri P, Hilbert G, Maucourt M, Deborde C, Moing A, Rolin D. 2006. Microclimate influence on mineral and metabolic profiles of grape berries. Journal of Agricultural and Food Chemistry **54**, 6765–6775.

Petrie PR, Trought MCT, Howell GS. 2000. Influence of leaf ageing, leaf area and crop load on photosynthesis, stomatal conductance and senescence of grapevine (*Vitis vinifera* L. cv. Pinot noir) leaves. Vitis **39**, 31–36.

Petrova A, Popova M, Parushev S, Batovska D, Bankova V, Popov S, Review M. 2006. Chemical Composition and Biological Value of *Vitis Vinifera* L. Leaves. , 617–624.

Pierquet P, Stushnoff C. 1980. Relationship of Low Temperature Exotherms to Cold Injury in Vitis riparia Michx. American Journal of Enology and Viticulture **31**, 1–6.

Podolyan A. 1994. A Study of the Green Leaf Volatile Biochemical Pathway as a Source of Important Flavour and Aroma Precursors in Sauvignon Blanc Grape Berries. , 280.

Poni S, Casalini L, Bernizzoni F, Civardi S, Intrieri C. 2006. Effects of early defoliation on shoot photosynthesis, yield components, and grape composition. American Journal of Enology and Viticulture **57**, 397–407.

Pool R. 2000. Training Systems for New York Vineyards. Cornell University.

Pool RM, Watson JP, Kimball KH, Einset J. 1977. Canadice and Glenora Seedless Grapes Named. New York's Food and Life Scineces Bulletin **1977**, 1–2.

Porro D, Dorigatti C, Stefanini M, Ceschini A. 2001. Use of SPAD meter in diagnosis of nutritional status in apple and grapevine. Acta Horticulturae **564**, 243–252.

Possner DRE, Kliewer WM. 1985. The localisation of acids, sugars, potassium and calcium in developing grape berries. Vitis **24**, 229–240.

Prost I, Dhondt S, Rothe G, *et al.* 2005. Evaluation of the antimicrobial activities of plant oxylipins supports their involvement in defense against pathogens. Plant Physiology **139**, 1902–1913.

Ptak A, El Tahchy A, Skrzypek E, Wójtowicz T, Laurain-Mattar D. 2013. Influence of auxins on somatic embryogenesis and alkaloid accumulation in *Leucojum aestivum* callus. Central European Journal of Biology **8**, 591–599.

Rahmani M, Bakhshi D, Qolov M. 2015. *Impact of pruning severity and training systems on red and white seedless table grape (Vitis vinifera) qualitative indices*.

Rayne S, Karacabey E, Mazza G. 2008. Grape cane waste as a source of trans-resveratrol and trans-viniferin: High-value phytochemicals with medicinal and anti-phytopathogenic applications. Industrial Crops and Products **27**, 335–340.

Reisch BI. 1993. Seedless Table Grapes for Northeast. , 2–3.

Reisch BI, Peterson D V., Martens and M-H. 1979. Table grape varieties for cool climates. Cornell cooperative extension.

Ren R, Wan Z, Chen H, Zhang Z. 2022. The effect of inter-varietal variation in sugar hydrolysis and transport on sugar content and photosynthesis in *Vitis vinifera* L. leaves. Plant Physiology and Biochemistry **189**, 1–13.

Reyes J, Del Campillo M, Torrent J. 2006. Soil properties influencing iron chlorosis in grapevines grown in the Montilla-Moriles area, southern Spain. Communications in Soil Science and Plant Analysis **37**, 1723–1729.

Reynolds AG, Edwards CG, Wardle DA, Webster DR, Dever M. 1994. Shoot sensity affects 'Riesling' grapevines II. Wine composition and sensory response. Journal of the American Society of Horticultural Science **119**, 881–892.

Reynolds AG, Vanden Heuvel JE. 2009. Influence of grapevine training systems on vine growth and fruit composition: A review. American Journal of Enology and Viticulture **60**, 251–268.

Reynolds AG, Pool RM, Mattick LR. 1985. Effect of Training System on Growth, Yield, Fruit Composition, and Wine Quality of Seyval Blanc. American Journal of Enology and Viticulture **36**, 156–164.

Reynolds AG, Reisch BI. 2015. Grapevine breeding in the Eastern United States. Grapevine Breeding Programs for the Wine Industry, 345–358.

Reynolds AG, Wardle DA, Cliff MA, King M. 2004. Impact of training system and vine spacing on vine performance, berry composition, and wine sensory attributes of riesling. American Journal of Enology and Viticulture **55**, 96–103.

Reynolds AG, Wardle DA, Naylor AP. 1996. Impact of training system, vine spacing, and basal leaf removal on riesling. Vine performance, berry composition, canopy microclimate, and vineyard labor requirements. American Journal of Enology and Viticulture **47**, 63–76.

Ribeiro LF, Ribani RH, Francisco TMG, Soares AA, Pontarolo R, Haminiuk CWI. 2015. Profile of bioactive compounds from grape pomace (*Vitis vinifera* and *Vitis labrusca*) by spectrophotometric, chromatographic and spectral analyses. Journal of Chromatography B: Analytical Technologies in the Biomedical and Life Sciences **1007**, 72–80.

Ribéreau-Gayon J, Riberau-Gayon P, Seguin G. 1980. *Botrytis cinerea* in enology. Biology of Botrytis, edited by JR Coley-Smith, K. Verhoeff, WR Jarvis, 272–274.

Richard T, Abdelli-Belhadj A, Vitrac X, Waffo Teguo P, Mérillon JM. 2016. Vitis vinifera canes, a source of stilbenoids against downy mildew. Oeno One **50**, 137–143.

Rienth M, Vigneron N, Walker RP, Castellarin SD, Sweetman C, Burbidge CA, Bonghi C, Famiani F, Darriet P. 2021. Modifications of Grapevine Berry Composition Induced by Main Viral and Fungal Pathogens in a Climate Change Scenario. Frontiers in Plant Science **12**.

Rocha AD, Braga De Oliveira A, Dias De Souza Filho J, Lombardi JA, Braga FC. 2004. Antifungal constituents of *Clytostoma ramentaceum* and *Mansoa hirsuta*. Phytotherapy Research **18**, 463–467.

Rock BN, Hoshizaki T, Miller JR. 1988. Comparison of in situ and airborne spectral measurements of the blue shift associated with forest decline. Remote Sensing of Environment **24**, 109–127.

Rock BN, Lauten GN. 1996. K-12th grade students as active contributors to research investigations. Journal of Science Education and Technology **5**, 255–266.

Rock BN, Vogelmann JE, Williams DL, Vogelmann AF, Hoshizaki T. 1986. Remote Detection of Forest Damage. BioScience **36**, 439–445.

Rock BN, Williams DL, Moss DM, Lauten GN, Kim M. 1994. High-spectral resolution field and laboratory optical reflectance measurements of red spruce and eastern hemlock needles and branches. Remote Sensing of Environment **47**, 176–189.

Rock BN, Williams DL, Vogelmann JE. 1985. Field and Airborne Spectral Characterization of Suspected Acid Deposition Damage in Red Spruce (Picea Rubens) From Vermont. International Symposium - Machine Processing of Remotely Sensed Data, 71–81.

Romanazzi G, Feliziani E. 2014. *Botrytis cinerea (Gray Mold)*. Elsevier.

Romanazzi G, Murolo S, Pizzichini L, Nardi S. 2009. Esca in young and mature vineyards, and molecular diagnosis of the associated fungi. European Journal of Plant Pathology **125**, 277–290.

Romanazzi G, Sanzani SM, Bi Y, Tian S, Gutiérrez Martínez P, Alkan N. 2016. Induced resistance to control postharvest decay of fruit and vegetables. Postharvest Biology and Technology **122**, 82–94.

De Rosa V, Vizzotto G, Falchi R. 2021. Cold Hardiness Dynamics and Spring Phenology: Climate-Driven Changes and New Molecular Insights Into Grapevine Adaptive Potential. Frontiers in Plant Science **12**.

Ru C, Hu X, Wang W, Ran H, Song T, Guo Y. 2020. Evaluation of the crop water stress index as an indicator for the diagnosis of grapevine water deficiency in greenhouses. Horticulturae **6**, 1–19.

Rumpf T, Mahlein AK, Steiner U, Oerke EC, Dehne HW, Plümer L. 2010. Early detection and classification of plant diseases with Support Vector Machines based on hyperspectral reflectance. Computers and Electronics in Agriculture **74**, 91–99.

Salvi L, Cataldo E, Sbraci S, Paoli F, Fucile M, Nistor E, Mattii GB. 2021. Modeling carbon balance and sugar content of Vitis vinifera under two different trellis systems. Plants **10**, 1–13.

Sanchez-Rodriguez LA, Spósito MB. 2020. Influence of the trellis/training system on the physiology and production of *Vitis labrusca* cv. Niagara Rosada in Brazil. Scientia Horticulturae **261**, 109043.

Sbaghi M, Jeandet P, Bessis R, Leroux P. 1996. Degradation of stilbene-type phytoalexins in relation to the pathogenicity of Botrytis cinerea to grapevines. Plant Pathology **45**, 139–144.

Schilder A. 2010. Fungicide properties and weather conditions. MSU Extension.

Schilder AMC, Gillett JM, Sysak RW, Wise JC. 2002. Evaluation of environmentally friendly products for control of fungal diseases of grapes. 10th International Conference on Cultivation Technique and Phytopathological Problems in Organic Fruit-Growing and Viticulture, 163–167.

Schnee S, Queiroz EF, Voinesco F, Marcourt L, Dubuis PH, Wolfender JL, Gindro K. 2013. Vitis vinifera canes, a new source of antifungal compounds against *Plasmopara viticola*, *Erysiphe necator*, and *Botrytis cinerea*. Journal of Agricultural and Food Chemistry **61**, 5459–5467.

Schultz H. 1995. Grape canopy structure, light microclimate and photosynthesis. I: A two-dimensional model of the spatial distribution of surface area densities and leaf ages in two canopy systems. Vitis **34**, 211–215.

Sharma RR, Singh D, Singh R. 2009. Biological control of postharvest diseases of fruits and vegetables by microbial antagonists: A review. Biological Control **50**, 205–221.

Sideman B. 2021. Pruning and Training Grapes in the Home Vineyard. Extension, U N H Horticulture, Sustainable, 1–9.

Sideman B, Hamilton G. 2015. Research Report: Seedless Table Grape Variety & Training System Evaluation, 2015.

Sideman B, Hamilton G. 2016. Research Report: Seedless Table Grape Variety & Training System Evaluation, 2016. UNH Extension.

Sideman B, Hamilton G. 2019. Research Report: Seedless Table Grape Variety & Training System Evaluation, 2019. UNH Extension, 12–15.

Sims DA, Gamon JA. 2002. Relationships between leaf pigment content and spectral reflectance across a wide range of species, leaf structures and developmental stages. Remote Sensing of Environment **81**, 337–354.

Singh PN. 2017. Biocontrol of powdery mildew of grapes using culture filtrate and biomass of fungal isolates. Plant Pathology & Quarantine **7**, 181–189.

Slegers A, Angers P, Ouellet É, Truchon T, Pedneault K. 2015. Volatile compounds from grape skin, juice and wine from five interspecific hybrid grape cultivars grown in Québec (Canada) for wine production. Molecules **20**, 10980–11016.

Smart RE, Dick JK, Gravett IM, Fisher BM. 1990. Canopy Management to Improve Grape Yield and Wine Quality - Principles and Practices. South African Journal of Enology & Viticulture **11**, 3–17.

Smart R, Robinson M. 1992. *Sunlight into Wine: A Handbook for Winegrape Canopy Management*.

Smiley L, Cochran D. 2016. A Review of Cold Climate Grape Cultivars.

Souquet JM, Labarbe B, Le Guernevé C, Cheynier V, Moutounet M. 2000. Phenolic composition of grape stems. Journal of Agricultural and Food Chemistry **48**, 1076–1080.

Spayd SE, Tarara JM, Mee DL, Ferguson JC. 2002. Separation of sunlight and temperature effects on the composition of *Vitis vinifera* cv. Merlot berries. American Journal of Enology and Viticulture **53**, 171–182.

Steel CC, Blackman JW, Schmidtke LM. 2013. Grapevine bunch rots: Impacts on wine composition, quality, and potential procedures for the removal of wine faults. Journal of Agricultural and Food Chemistry **61**, 5189–5206.

Steele MR, Gitelson AA, Rundquist DC. 2008. A comparison of two techniques for nondestructive measurement of chlorophyll content in grapevine leaves. Agronomy Journal **100**, 779–782.

Steimetz E, Trouvelot S, Gindro K, Bordier A, Poinssot B, Adrian M, Daire X. 2012. Influence of leaf age on induced resistance in grapevine against *Plasmopara viticola*. Physiological and Molecular Plant Pathology **79**, 89–96.

Strik BC. 2011. Growing Table Grapes. Oregon State University Extension Service, 1–32.
Svyantek A, Köse B, Stenger J, Auwarter C, Hatterman-Valenti H. 2020. Cold-hardy grape cultivar winter injury and trunk re-establishment following severe weather events in North Dakota. Horticulturae **6**, 1–15.

Tang L, Shang J, Song C, Yang R, Shang X, Mao W, Bao D, Tan Q. 2020. Untargeted Metabolite Profiling of Antimicrobial Compounds in the Brown Film of Lentinula edodes Mycelium via LC-MS/MS Analysis. ACS Omega **5**, 7567–7575.

Taskos DG, Koundouras S, Stamatiadis S, Zioziou E, Nikolaou N, Karakioulakis K, Theodorou N. 2015. Using active canopy sensors and chlorophyll meters to estimate grapevine nitrogen status and productivity. Precision Agriculture **16**, 77–98.

Taware PB, Dhumal KN, Oulkar DP, Patil SH, Banerjee K. 2010. Phenolic alterations in grape leaves, berries and wines due to foliar and cluster powdery mildew infections. International Journal of Pharma and Bio Sciences **1**.

Tecchio MA, da Silva MJR, Callili D, Hernandes JL, Moura MF. 2020. Yield of white and red grapes, in terms of quality, from hybrids and *Vitis labrusca* grafted on different rootstocks. Scientia Horticulturae **259**, 108846.

Tucker CJ. 1979. Remote sensing of leaf water content in the near infrared. **32**.

U. S. Department of Agriculture. 2022. U.S. Department of Agriculture 2016 Official soil series descriptions: Charlton Series.

Uddling J, Gelang-Alfredsson J, Piikki K, Pleijel H. 2007. Evaluating the relationship between leaf chlorophyll concentration and SPAD-502 chlorophyll meter readings. Photosynthesis Research **91**, 37–46.

USDA. 2020. U.S. Department of Agriculture, National Agricultural Statistics Service, Noncitrus Fruits and Nuts 2019 Summary. Noncitrus Fruits and Nuts 2019 Summary, 12, 42.

Usha K, Singh B. 2013. Potential applications of remote sensing in horticulture-A review. Scientia Horticulturae **153**, 71–83.

Vannini A, Chilosi G. 2013. Botrytis Infection: Grey Mould and Noble Rot. Sweet, Reinforced

and Fortified Wines: Grape Biochemistry, Technology and Vinification, 159–169.

Vielba-Fernández A, Polonio Á, Ruiz-Jiménez L, de Vicente A, Pérez-García A, Fernández-Ortuño D. 2020. Fungicide resistance in powdery mildew fungi. Microorganisms **8**, 1–34.

Vijay P, Rakesh P, Madan P. 2017. Manual of ICAR Sponsored Training Programme for Technical Staff of ICAR Institutes on "Physiological Techniques to Analyze the Impact of Climate Change on Crop Plants". Division of Plant Physiology, ICAR-Indian Agricultural Research Institute (IARI), New Delhi, India, 130.

Vilanova M, Genisheva Z, Tubio M, Álvarez K, Lissarrague JR, Oliveira JM. 2017. Effect of Vertical Shoot-Positioned, Scott-Henry, Geneva Double-Curtain, Arch-Cane, and Parral Training Systems on the Volatile Composition of Albario Wines. Molecules **22**, 1500.
VitisGen. 2022. http://www.vitisgen.org.

Vogelmann JE, Rock BN, Moss DM. 1993. Red Edge Spectral Measurements from Sugar Maple Leaves. International Journal of Remote Sensing **14**, 1563–1575.

White R, Hickey C. 2020. Introdcution to Wine Grape Trellising, Training, and Pruning Terms. , 1–6.

Williamson B, Tudzynski B, Tudzynski P, Van Kan JAL. 2007. *Botrytis cinerea*: The cause of grey mould disease. Molecular Plant Pathology **8**, 561–580.

Wimmer M, Workmaster BA, Atucha A. 2018. Training systems for cold climate interspecific hybrid grape cultivars in northern climate regions. HortTechnology **28**, 202–211.

Wolf TK, Cook MK. 1994. Cold hardiness of dormant buds of grape cultivars: Comparison of thermal analysis and field survival. HortScience **29**, 1453–1455.

Wolf TK, Dry PR, Iland PG, Botting D, Dick J, Kennedy U, Ristic R. 2003. Response of Shiraz grapevines to five different training systems in the Barossa Valley, Australia. Australian Journal of Grape and Wine Research **9**, 82–95.

Wong FP, Wilcox WF. 2000. Distribution of baseline sensitivities to azoxystrobin among isolates of *Plasmopara viticola*. Plant Disease **84**, 275–281.

Wu BH, Liu HF, Guan L, Fan PGE, Li SH. 2011. Carbohydrate metabolism in grape cultivars that differ in sucrose accumulation. Vitis - Journal of Grapevine Research **50**, 51–57.

Xu XQ, Cheng G, Duan LL, Jiang R, Pan QH, Duan CQ, Wang J. 2015. Effect of training systems on fatty acids and their derived volatiles in Cabernet Sauvignon grapes and wines of the north foot of Mt. Tianshan. Food Chemistry **181**, 198–206.

Xu D, Deng Y, Han T, Jiang L, Xi P, Wang Q, Jiang Z, Gao L. 2018*a*. *In vitro* and *in vivo*

effectiveness of phenolic compounds for the control of postharvest gray mold of table grapes. Postharvest Biology and Technology **139**, 106–114.

Xu D, Yu G, Xi P, Kong X, Wang Q, Gao L, Jiang Z. 2018*b*. Synergistic effects of resveratrol and pyrimethanil against *Botrytis cinerea* on grape. Molecules **23**, 1–12.

Yamada N, Fujimura S. 1991. Nondestructive Measurement of Chlorophyll Pigment Content in Plant Leaves from three-color Reflectance and Transmittance. Applied optics **30**, 3964–3973.

Yang Z, Tian J, Feng K, Gong X, Liu J. 2021. Application of a Hyperspectral Imaging System to Quantify Leaf-scale Chlorophyll, Nitrogen and Chlorophyll Fluorescence Parameters in Grapevine. Plant Physiology and Biochemistry **166**, 723–737.

Yang J, Xiao YY. 2013. Grape Phytochemicals and Associated Health Benefits. Critical Reviews in Food Science and Nutrition **53**, 1202–1225.

Ye GN, Soylemezoglu G, Weeden NF, Lamboy WF, Pool RM, Reisch BI. 1998. Analysis of the Relationship Between Grapevine Cultivars, Sports and Clones via DNA fingerprinting. Vitis **37**, 33–38.

Yilmaz T, Alahakoon D, Fennell A. 2021. Freezing Tolerance and Chilling Fulfillment Differences in Cold Climate Grape Cultivars. Horticulturae **7**, 1–11.

Yin X, Liu RQ, Su H, *et al.* 2017. Pathogen Development and Host Responses to *Plasmopara viticola* in Resistant and Susceptible grapevines: An Ultrastructural Study. Horticulture Research **4**.

Yu R, Brillante L, Torres N, Kurtural SK. 2021. Proximal Sensing of Vineyard Soil and Canopy Vegetation for Determining Vineyard Spatial Variability in Plant Physiology and Berry Chemistry. Oeno One **55**, 315–333.

Zabadal TJ, Dami IE, Goffinet MC, Martinson TE, Chien ML. 2007. Winter Injury to Grapevines and Methods of Protection. Michigan State University Extension **E2930**, 1–44.

Zabadal TJ, Moore J, Swenson E, Baker W, Herman J, Tatter J, Lange A. 2002. Growing Table Grapes in a Temperate Climate.

Zahavi T, Reuveni M. 2012. Effect of Grapevine Training Systems on Susceptibility of Berries to Infection by *Erysiphe necator*. European Journal of Plant Pathology **133**, 511–515.

Zahavi T, Reuveni M, Scheglov D, Lavee S. 2001. Effect of Grapevine Training Systems on Development of Powdery Mildew. European Journal of Plant Pathology **107**, 495–501.

Zhang ZS, Li YT, Gao HY, Yang C, Meng QW. 2016. Characterization of Photosynthetic Gas Exchange in Leaves under Simulated Adaxial and Abaxial Surfaces Alternant Irradiation. Scientific Reports **6**, 1–11.

Zhang Z, Liu H, Sun J, Yu S, He W, Li T, Baolong Z. 2020. Nontarget Metabolomics of GrapeSeed Metabolites Produced by various Scion–Rootstock Combinations. Journal of the American Society for Horticultural Science **145**, 247–256.

Zoecklein BW, Wolf TK, Duncan SE, Marcy JE, Jasinski Y. 1998. Effect of Fruit Zone Leaf Removal on Total Glycoconjugates and Conjugate Fraction Concentration of Riesling and Chardonnay (*Vitis vinifera* L.) grapes. American Journal of Enology and Viticulture **49**, 259–265.

Zoecklein BW, Wolf TK, Pélanne L, Miller MK, Birkenmaier SS. 2008. Effect of Vertical Shoot-Positioned, Smart-Dyson, and Geneva Double-Curtain Training Systems on Viognier Grape and Wine Composition. Am. J. Enol. Vitic. **59**, 11–21.